PROTEIN PCS NMR SPECTROSCOPY UNDER PHYSIOLOGICAL CONDITIONS: DEVELOPMENT OF A NEW HIGH YIELD CYCLIZATION METHOD FOR RIGIDIFIED DOTA-BASED TAGS WITH SULFHYDRYL-REACTIVE ACTIVATORS FORMING A REDUCTIVELY STABLE LINKAGE

Inauguraldissertation
zur
Erlangung der Würde eines Doktors der Philosophie
vorgelegt der
Philosophisch-Naturwissenschaftlichen Fakultät
der Universität Basel

von

THOMAS MÜNTENER
aus Buchs (SG), Schweiz

Basel, 2019

Genehmigt von der Philosophisch-Naturwissenschaftlichen Fakultät:

auf Antrag von

Prof. Dr. Catherine E. Housecroft
PD. Dr. Daniel Häussinger
Prof. Dr. Oliver S. Wenger

Basel, den 26.06.2018

Prof. Dr. Martin Spiess

für meine Eltern

“Creativity Is Intelligence Having Fun.”

— Albert Einstein

ABSTRACT

This thesis focuses on the development of a new synthetic strategy towards twelve-membered tetraaza macrocycles and the synthesis of new sulfhydryl reactive linker moieties for the application in pseudocontact shift (PCS) NMR spectroscopy.

The first part addresses the development of a new robust synthetic procedure for the selective synthesis of twelve-membered tetraaza macrocycles using natural amino acids and derivatives as cheap chiral building blocks. Cyclization of linear tetrapeptides was attempted but due to the preferred *trans* configuration of the peptide bond only small amounts of the cyclic tetrapeptide were obtained. Tetraalanine was reduced to tetraalaninol and the cyclization of tetraalaninol in solution was attempted using a preorganized bisaminal approach. This approach was unsuccessful and no product could be isolated. A more flexible mixed amine / amide tetramer was synthesized and successfully cyclized under modest dilution conditions forming a C_2 symmetric twelve-membered bislactam. This reaction was highly efficient and afforded various bislactams based on alanine, alanine / valine and alanine / serine in good yields. From these bislactams various valuable intermediates for further tag synthesis are accessible as well as the final tetraaza macrocycles M4-cyclen, M2P2-cyclen and M3O1-cyclen. The newly developed approach allows the synthesis of a variety of differently substituted twelve-membered macrocycles.

The second part primarily focuses on the development of new sulfhydryl-reactive linker moieties for site-selective protein tagging. The widely used formation of a disulphide linkage has the inherent problem of being unstable under reductive conditions as they are found in living cells, limiting the range of application to buffered *in-vitro* applications. Pyridine phenyl sulfone based tags were synthesized and *in-cell* NMR experiments were conducted with the B1 domain of the streptococcal protein G (GB1). The structure of the protein was successfully calculated with the Rosetta approach using only pseudocontact shifts and residual dipolar couplings (RDCs) obtained from *in-cell* experiments in oocytes. We proved for the first time that accurate structures of proteins inside cells can be generated solely from experimental PCSs and RDCs within the Rosetta package. The conjugation speed was dramatically increased for the fluorine substituted pyridine phenyl sulfone analogue decreasing the reaction time from 24 h at 40 °C to six hours at 20-25 °C. Further enhancement was achieved using a pyridine thiazol allowing efficient tagging in less than one hour at 20-25 °C and pH 7.0.

The last part deals with various different applications of M8-DOTA in order to solve structural or biological problems. Gd-M8-DOTA was selectively coupled to the Pittsburgh compound B (PiB) for *in-vivo* magnetic resonance imaging experiments. PiB strongly interacts with the amyloid plaques found in Alzheimer's disease and thus PiB-Gd-M8-DOTA allows detecting amyloid plaques by MRI.

A second collaboration project addresses the problems found in the assignment of a hexa-polyproline. Due to the repetitive nature of this peptide the chemical shift dispersion was small. Increasing the chemical shift range found in hexa-polyproline was the goal of the attempted conjugation of M8-DOTA to the hexa-polyproline. We showed that M8-DOTA can not be coupled to the *N*-terminal aniline moiety and a less sterically demanding amine linker is required.

Prospective experiments were carried out on Eu-M8-DOTA and its closely related derivatives, Eu-M4-DOTA and Eu-DOTA, in order to check for possible applications in Förster resonance energy transfer (FRET) spectroscopy. All complexes were not luminescence under UV irradiation and a UV harvesting molecule was required. Eu-azaxanthon-M7-DOTA showed excellent luminescence properties required for potential applications in FRET spectroscopy. Preliminary experiments with Tb-M7PyThiazol-DOTA showed similar properties with a red shifted UV absorption maximum (from 250 nm to 300 nm) indicating great potential for FRET spectroscopy.

PUBLICATIONS

(*1*) Müntener, T., Thommen, F., Joss, D., Kottelat, J., Prescimone, A. and Häussinger, D. (submitted Jan 2019). Synthesis of chiral substituted nine and twelve-membered cyclic polyamines from natural building blocks. *Chemical Communications*.

(*2*) Zimmermann, K., Joss, D., Müntener, T., Nogueira, E., Knörr, L., Schäfer, M., Monnard, F. and Häussinger, D. (submitted Dec 2018). Localization of ligands within human carbonic anhydrase II using 19F pseudocontact shift analysis. *Chemical Science*.

(*3*) Müntener, T., Kottelat, J., Huber, A. and Häussinger, D. (2018). New Lanthanide Chelating Tags for PCS NMR Spectroscopy with Reduction Stable, Rigid Linkers for Fast and Irreversible Conjugation to Proteins. *Bioconjugate Chemistry 29*, 3344–3351.

(*4*) Bannwart, L. M., Jundt, L., Müntener, T., Neuburger, M., Häussinger, D. and Mayor, M. (2018). A Phenyl-Ethynyl-Macrocycle: A Model Compound for "Geländer"Oligomers Comprising Reactive Conjugated Banisters. *European Journal of Organic Chemistry 2018*, 3391–3402.

(*5*) Müntener, T., Häussinger, D., Selenko, P. and Theillet, F.-X. (2016). In-Cell Protein Structures from 2D NMR Experiments. *Journal of Physical Chemistry Letters 7*, 2821–2825.

(*6*) Delarue Bizzini, L., Müntener, T., Häussinger, D., Neuburger, M. and Mayor, M. (2017). Synthesis of trinorbornane. *Chemical Communications 53*, 11399–11402.

(*7*) Ris, D., Schneider, G., Ertl, C., Kohler, E., Müntener, T., Neuburger, M., Constable, E. and Housecroft, C. (2016). 4'-Functionalized 2,2':6',2"-terpyridines as the NˆN domain in [Ir(CˆN)2(NˆN)][PF6] complexes. *Journal of Organometallic Chemistry 812*, 272–279.

(*8*) Pannwitz, A., Rigo, S., Bannwart, L., Bizzini, L., Malzkuhn, S., Müntener, T. and Laupheimer, C. (2016). Basel chemistry christmas symposium 2015. *Chimia 70*.

Expect nothing. Appreciate everything.

— unknown

ACKNOWLEDGMENTS

During my thesis I had the chance to work and interact with so many great people that I cannot mention them all. It's my great pleasure to point those out who deserve special note.

I am very grateful to my supervisor PD. Dr. Daniel Häussinger. I really enjoyed working in your small group. I am very thankfull for all the theoretical and practical aspects of NMR spectroscopy you thought me. Your trust and confidence in my work as well as the freedom in how to achieve our goals was well appreciated. Thank you so much for all the past and future support.

Prof. Dr. Catherine E. Housecroft and Prof. Dr. Edwin C. Constable are thanked for all their support and helpful discussions. In addition Prof. Dr. Catherine E. Housecroft is thanked for being the Fakultätsverantwortliche.

I would like to thank Prof. Dr. Oliver S. Wenger for being the co-examiner of this thesis.

I would like to thank Prof. Dr. Christof Sparr for being the chairman of the PhD defence.

Special thanks goes to Dr. François-Xavier Theillet for the good and intense collaboration during our *in-cell* NMR project.

I also thank Prof. Dr. Marcel Mayor for the nice collaborations I had with many of his PhD students.

I also want to thank the former Häussinger group members and master students, Dr. Heiko Gsellinger, Dr. Kaspar Zimmermann, Dr. Roché Walliser, Florian Lüttin, Fabienne Thommen and Raphael Vogel.

Being a one PhD student and one supervisor group throughout most of the thesis is a very lonely thing would it not be for the friendly and welcoming nature of other groups and their members. I shared many good hours with the Gademann and Sparr groups as well as the Constable, Mayor and Wenger groups. Thank you guys it was a pleasure. I deliberately did not mention you by name, because the chance is high that I would miss one.

Special thanks goes to Dr. Andrea Pannwitz for her friendship, our weekly lunch dates and all other outside the university activities.

A big thank you goes to Linda Bannwart for her great effort in proof reading my experimental part.

I would also like to thank Lorenzo Bizzini and Patrick Zwick for the great discussions we had and the good time we spent off the lab.

During the progress of the thesis I had the chance to supervise two master students during their master thesis in our group. Fabienne Thommen and Raphael Vogel thank you for the great work and the excellent working atmosphere.

Jérémy Kottelat, I thank you for all the work you have done as a trainee in our group.

Many students visited the Häussinger group for a Wahlpraktikum, however, those selected ones who joined my lab for some hard work are noted here. I thank Julia Hildesheim, Murat Alkan, Fabiennen Thommen, Annika Huber and Raphael Vogel for their support and motivated work.

I also want to thank our newly joined PhD student Daniel Joss, for his help during the writing of this thesis.

I thank the whole technical and administrative staff of the chemistry department for their hard work and support. Special thanks goes to Dr. Heinz Nadig for measuring countless HRMS samples.

Without financial support unfortunately nothing happens in science, therefore, Fondation Claude et Giuliana and the department of chemistry is acknowledged for financial support.

Marco Rogowski is acknowledged for providing us with ubiquitin mutants.

I thank Jonas Schätti for his introduction into the field of solid phase peptide synthesis.

The university high performance computing facility sciCORE is acknowledged for their support.

Dr. Alessandro Prescimone is acknowledged for measuring X-ray structures.

Last but definitely not least I am very very grateful to my family without their support this would not have been possible. Thank you so much, Mum and Dad.

In the end there is not much more to say. If I have forgotten anyone please consider finding yourself in the last statement. Thank you, thank you so much!

CONTENTS

ACRONYMS

AIBN	Azobisisobutyronitrile
Bn	Benzyl
BnBr	Benzyl bromide
Cbz	Carboxybenzyl
Cbz-Cl	Benzyl chloroformate
COSY	Correlation spectroscopy
CRINEPT	Cross relaxation-enhanced polarization transfer
DCC	*N*, *N*′-Dicyclohexylcarbodiimide
DCM	Dichloromethane
DD	Dipole-dipole
DIC	*N*, *N*′-Diisopropylcarbodiimide
DIPEA	*N*, *N*-Diisopropylethylamine
DMF	*N*, *N*-Dimethylformamide
DMP	Dess–Martin periodinane
DMSO	Dimethyl sulfoxide
DOTA	1,4,7,10-Tetraazacyclododecane-1,4,7,10-tetraacetic acid
DSA	Dipolar shift anisotropy
DTPA	Pentetic acid
EDTA	Ethylenediaminetetraacetic acid
ee	enantiomeric excess
FBn	4-Fluorobenzyl
FBnBr	4-Fluorobenzyl bromide
FRET	Förster Resonance Energy Transfer
HATU	1-[Bis(dimethylamino)methylene]-1H-1,2,3-triazolo-[4,5-b]pyridinium 3-oxid hexafluorophosphate
HMBC	Heteronuclear multiple-bond correlation
HMQC	Heteronuclear multiple-quantum coherence
HSQC	Heteronuclear single-quantum correlation
IBX	2-Iodoxybenzoic acid
LacOtBu	Lactic acid *tert*-butyl ester
LBP	Lanthanide binding peptides
LCT	Lanthanide Chelating Tag

mCPBA	meta-Chloroperoxybenzoic acid
Mes-Cl	Methanesulfonyl chloride
MRI	Magnetic Resonance Imaging
MTSL	*S*-(1-Oxyl-2,2,5,5-tetramethyl-2,5-dihydro-1H-pyrrol-3-yl)methyl methanesulfonothioate
NBS	*N*-Bromosuccinimide
NMR	Nuclear Magnetic Resonance
NOE	Nuclear Overhauser effect
NOESY	Nuclear Overhauser effect spectroscopy
Ns	4-Nitrobenzene-1-sulfonyl
NsCl	4-Nitrobenzene-1-sulfonyl chloride
PCS	Pseudocontact Shift
PDB	Protein Data Bank
PiB	Pittsburgh compound B
PRE	Paramagnetic Relaxation Enhancement
RACS	Residual anisotropic chemical shift
RDC	Residual Dipolar Coupling
RNA	Ribonucleic acid
SAP	Square antiprism
T3P	Propylphosphonic anhydride
TAHA	Triaminohexaacetate
TBAF	Tetrabutylammonium fluoride
TCEP	Tris(2-carboxyethyl)phosphine
TCP	2,4,6-Trichlorophenol
TFA	Trifluoroacetic acid
THF	Tetrahydrofuran
TMS-Cl	Trimethylsilyl chloride
TOCSY	Total correlated spectroscopy
TROSY	Transverse relaxation optimized spectroscopy
Ts-Cl	4-Toluenesulfonyl chloride
TSAP	Twisted square antiprism
UTR	Unique tensor representation

1

INTRODUCTION

1.1 METHODS IN STRUCTURAL BIOLOGY.

Understanding of biological process inside living organisms ultimately breaks down to the understanding and accurate description of the molecules involved and their interactions. Biological processes are based on highly specific interactions between several biomolecules. In the field of structural biology, a whole variety of different techniques is used to study interactions and to solve structures of biomacromolecules like proteins and DNA/RNA. In the early 1900s little to nothing was known about proteins and their structures.[1] Technological advancement in mass spectrometry and the development of Edman degradation[2] allowed the determination of the protein sequence as a first key step in understanding protein structures and functions. Nowadays mass spectrometry can also provide valuable insights into the stoichiometry and composition of proteins and their complexes, and the presence of small molecules.[3] Modern techniques like multiangle light scattering[4] and small angle scattering are used to provide information about the absolute molar mass and the average size and shape of molecules in aqueous solutions. The first breakthrough in achieving atomic resolution was already made in 1958 by Kendrew *et al*.[5] with the determination of the first protein structure by X-ray to a resolution of 6 Å. Since then the vast majority of protein structures deposited in the Protein Data Bank (PDB) were determined using X-ray crystallography. Although the principles of nuclear magnetic resonance (NMR) were discovered already in the 1930's by Rabi *et al*.,[6] it was not until 1982 when Wüthrich *et al*. showed that NMR spectroscopy can be used to determine protein structures in solution.[7] It was only due to the fast development in the field of NMR and the discovery of the Fourier transformation and multidimensional NMR methods that such an undertaking was possible. Wüthrich *et al*.[7] used nuclear Overhauser enhancements,[8] scalar couplings and amide proton exchange rates to calculate the structure.[9] In the early days NMR spectroscopy and X-ray crystallography were the only methods to obtain atomic resolution structures of biomolecules. At the time of this writing (May 2018) around 117'000 X-ray and 11'000 NMR protein structures were deposited in the PDB database. Making X-ray still de facto the most convenient tool to obtain accurate 3D structures of proteins. Nevertheless, NMR has proven very useful in the many cases were the protein could not be crystallized or highly dynamic regions were present. Due to the solid nature of X-ray crystal-

lography, limits are reached if dynamics are involved and NMR spectroscopy has been tremendously valuable to overcome these limits. Nowadays many protein structures are solved using both X-ray and NMR methods. Structural information in solids can also be obtained by means of electron microscopy. This technique was developed roughly two decades later than X-ray crystallography and by the 1960s electron microscopy had made significant improvements in terms of resolution. De Rosier and Klug[10] obtained the first three dimensional electron microscopy structure of the T4 bacteriophage tail with a resolution of 35 Å, which was then further refined to 20 Å.[11] Although this resolution was relatively low, Henderson and Unwin[12] determined in 1975 the structure of bacteriorhodopsin to 7 Å matching the resolution achieved by the first X-ray structure of a protein. One drawback of both X-ray and electron microscopy lies in the susceptibility of biomolecules towards strong radiation.[13] Damage-induced disorder leads to missing diffraction spots at high resolutions. Cooling of protein crystals not only allowed the usage of high energy synchrotron X-rays but also lied the foundation for cryo electron microscopy.[14] Electron microscopy started as a crystallographic tool but nowadays it is a single particle method that does not rely on crystals. Traditionally, cryo electron microscopy was limited to large macromolecules but very recently it could be shown by Khoshouei[15] and co-workers that high resolutions of 3.2 Å can be achieved on smaller proteins like haemoglobin (64 kDa) which is anticipated to drop even further to proteins smaller than 10 kDa. Cryo electron microscopy has been a revolution in the field of structural biology and allows not only the study of structures but also the observation of dynamic processes.[16,17] The whole conformational space accessible by the protein can be present in a thermodynamic equilibrium prior to flash freezing and are therefore measurable. This provides valuable information about flexible regions within the protein structure. Dynamical processes is the area where NMR spectroscopy can provide the most detailed information about conformational changes and dynamics.[18,19] However, NMR spectroscopy is limited to relatively small proteins or parts thereof. Studying huge biomolecules with NMR is extremely challenging[20] and cryo electron microscopy is the way to go for such systems. Nevertheless X-ray crystallography, cryo electron microscopy and most standard NMR spectroscopy methods require samples and experimental conditions vastly different to those found inside living cells. The crowded intracellular environments in which proteins usually fulfil their functions are not well represented. Huge efforts are made to develop new biophysical methods that allow the study of biomolecules inside living cells. High resolution methods like cryo electron microscopy and X-ray crystallography are therefore simply excluded due to the requirement of vitrified or crystalline samples and the usage of high-energy radiation. On the other hand NMR spectroscopy can provide non-destructive atomic resolution information of isotope-enriched NMR-active protein samples inside living cells.[21,22] This offers the unique opportunity to study proteins under physiological conditions, something which is up to now not possible with the other atomic resolution methods. Newer methods like Förster resonance energy transfer

spectroscopy[23,24] and electron paramagnetic resonance spectroscopy[25] have proven to provide valuable information about relative distances.

1.2 PROTEIN NMR SPECTROSCOPY

1.2.1 *Historical Background*

Since the first protein structure has been solved by Wüthrich *et al.*,[7,26,27] many more were solved and added to the PDB. Nowadays 8 % of all protein structures deposited in the PDB are solved by NMR spectroscopy. It can also be seen that the number of published structures solved by NMR has stagnated. This is a direct consequence of the fact that once crystals are obtained a structure can be solved quickly, while NMR structures usually require a lot more effort. Nevertheless, NMR can provide unique information that can hardly be obtained by other means. Compared with the other two major contributors to three-dimensional structures (X-ray crystallography and cryo electron microscopy) NMR spectroscopy requires larger amounts of samples especially in the early days of NMR spectroscopy given the low sensitivity of past devices. Initially protein structures were solved relying entirely on two-dimensional homonuclear correlation experiments. Information was extracted from correlations caused by scalar coupling or from the through space distance-dependent nuclear Overhauser effect.[28] It is clear that such strategies could only be applied to relatively small proteins as larger proteins gave overly crowded proton spectra which were extremely difficult to interpret. The introduction of heteronuclear experiments significantly simplified the problem due to the increased chemical shift dispersion and the resulting reduced signal overlap. Unfortunately the natural abundance of ^{13}C and ^{15}N is small with 1.1 % and 0.37 %, respectively.[29] Various isotope labelling schemes were developed and are now routinely applied in protein NMR spectroscopy. However, the development of triple resonance experiments has pushed the field tremendously forward and with the steady increase of magnetic field strength the range of proteins accessible by NMR increased. Efficient backbone and sidechain assignments became possible and allowed the assignments of proteins up to 30 kDa.[30] The increased size of larger proteins causes the proteins to tumble more slowly which leads to larger linewidths and, therefore, a lower signal-to-noise ratio. In severe cases the signal is broadened beyond detection disallowing the measurement of large proteins by NMR spectroscopy. Deuterium labelling[31] was used to increase relaxation times and to minimize spin-diffusion which leads to smaller linewidths therefore making proteins accessible well beyond 30 kDa. Improvements in NMR pulse sequence programming namely the invention of transverse relaxation optimized spectroscopy (TROSY)[32] and cross relaxation-enhanced polarization transfer (CRINEPT)[33] enabled the community to study very large proteins. Today, new superconducting magnets with field strength beyond 1 GHz are available and the introduction of cryogenic probeheads as well as sophisticated statistical approaches allow the efficient and fast measurement of large

proteins and their complexes.[34] Proteins in the one MDa range are nowadays accessible by NMR spectroscopy.[35] Knowledge of three-dimensional structures, binding modes, dynamics and interactions can be provided by NMR spectroscopy and are extremely valuable for drug discovery. NMR allows the detection of weak interactions which sometimes are to weak to be detected by other biological assays like FRET.[36,37]

1.2.2 *Resonance assignment*

First thing needed for the determination of any three-dimensional structure or any dynamics is the knowledge of the chemical shift of a particular spin. Therefore, before any information can be obtained about relative orientations, distances or angles, an assignment needs to be done. For well-behaved small proteins with less than 80-100 amino acids, a homonuclear strategy can be applied. Using TOCSY and COSY spectra for intra-residue correlation and NOESY spectra for inter-residue correlation. NOESY experiments are generally optimized to detect only short distances at the cost of sensitivity as due to the overall protein fold several protons can be quite close in space even if they are largely separated in the protein sequence itself. For larger proteins this approach is not sufficient any more as signal overlap and spectral crowding increases with size. For larger proteins, the standard procedure for the resonance backbone assignment involves recording HNCACB and HN(CO)CACB spectra. These spectra correlate each NH group with the C_α and the C_β shifts of the corresponding amino acid while providing a correlation with weaker intensity to the preceding amino acid. Most triple resonance experiments use ^1J and ^2J couplings to establish connectivities between adjacent amino acids. These experiments are often used in pairs like HNCO and HN(CA)CO which help to correlate each NH group with the carbonyl group of the corresponding and preceding amino acids. Similar results are obtained for the HNCA and HN(CO)CA experiments which link the NH group with the C_α shifts (see Figure 1.1). In optimal cases those experiments allow a complete walk through the peptide chain that only stops at prolines due to the missing NH. Nevertheless, many more three-dimensional as well as two-dimensional experiments exist which allow the assignment of the complete backbone as well as the side chains.[19,38] For a complete assignment of all ^{1}H, ^{13}C, and ^{15}N shifts in a protein using magnetization transfers through internuclear J couplings, a total of at least six NMR spectra is required. HNCACB, CBCA(CO)NH, (H)CCH-TOCSY (aliphatic and aromatic regions) and H(C)CH-TOCSY (aliphatic and aromatic regions). However, ^{13}C- and ^{15}N-edited NOESY-HSQC spectra are extremely useful for the generation of ^{1}H-^{1}H distance restraints, providing valuable input data for future structure calculations.[38] Nowadays many software tools exist that focus on automating the assignment as well as the recording of the required experimental data such that resonance assignments of small to medium sized proteins are routinely performed.[39]

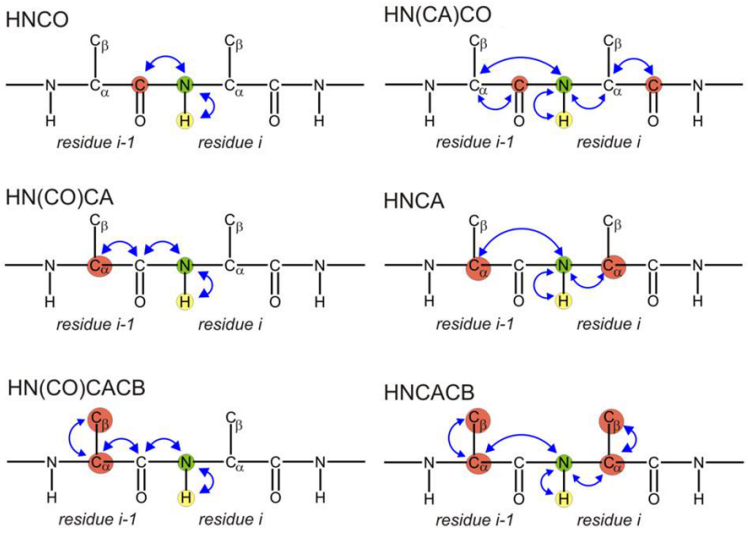

Figure 1.1: Backbone assignment using multidimensional NMR experiments. Figure adapted from http://chem.rutgers.edu.

1.2.3 *Protein structure determination*

For protein structure determination usually a set of different geometrical restraints is used. While distance restraints offer information about intermolecular distances, angle restraints are used to define relative orientation between small units. On the other hand orientation restraints can be used to calculate the relative orientation of large subunits with respect to one another.

Distance restraints

Distance restraints are most often obtained from ^{1}H-^{1}H NOE signals. The NOE effect is the transfer of spin polarization from one set of spins to another set of spins through a mechanism called cross-relaxation. In simple cases were the molecule is considered a rigid body were only one rotational correlation time exists for the whole molecule this effect is simply proportional to r^{-6}.[40] Unfortunately, a protein is not rigid nor does it necessarily have only one correlation time. Local mobility can cause part of the proteins to have considerable different correlation times and thus introducing large errors into the distance calibration. This is however not a big problem since NOEs are usually classified into three categories weak/medium/strong only. For structure calculations these categories are simply transferred to 1.8-2.7 Å, 1.8-3.3 Å, and 1.8-5.0 Å, where 1.8 Å corresponds to two times the van der Waals radius of a hydrogen atom. The sloppy classification of NOE can be attributed to the difficulty of accurately correlate an intensity to a distance because of various competing and influencing mechanisms. The intensity does not only depend on the interatomic distance but also on factors like spin diffusion and local structural fluctuations due to conformational averaging. Because of this, generally a large set of NOEs (10-20 per residues) is required and in particular

long-range NOE information is crucial for a successful structure calculation by NOEs. Automated NOE assignment is usually performed in an iterative fashion were an ambiguous NOE assignment is followed by a structure calculation which guides further NOE assignments.[41] The recent development of exact NOEs[42] offers a new method to accurately convert NOE data to internuclear distances with average errors of around 0.07 Å. Nevertheless, exact NOEs and normal NOEs can routinely only be observed up to a distance of 5-6 Å. The extremely valuable long-range information can only be obtained by other methods like paramagnetic relaxation enhancement (PRE) and pseudocontact shift (PCS).[19,43]

Angle restraints

Backbone dihedral angles ϕ(N-Cα), ψ(Cα-C'), ω(C'-N) and side-chain χ(n) can be determined by a variety of multi-dimensional NMR experiments. The angles ϕ, ψ and ω define the secondary structure and the conformation of the side-chain is defined by the χ angles.[43] According to Karplus equation,[44] the angle can be estimated from the corresponding ^3J coupling, some of them can be directly determined using three-dimensional experiments.[43] The torsion angles ϕ and ψ are usually obtained using coupling constants while most side-chain angles and the *cis/trans* peptide bond angles (ω) are determined by NOEs. Recording coupling constant experiments with sufficient precision and intensity is difficult, because long evolution and refocusing periods are needed. Fortunately apart from coupling constants and relaxation rates, also chemical shifts are sensitive to torsion angles. It turned out that ^{1}H, ^{13}C and ^{15}N chemical shifts are also susceptible to changes in dihedral angles especially H_α, C_α and CO shifts are strongly affected by the backbone angles ϕ and ψ. On the other hand ^{15}N shifts are sensitive to the side-chain angles of the preceding amino acids. It is relatively straight forward to measure most chemical shifts and, therefore, various software package have been developed that allowed the prediction of torsion angles from chemical shifts and sequence homology.[45,46]

Orientation restraints

Due to the relatively short ranged information obtained by NOEs it sometimes still remains an unsolved question what the orientation of two secondary elements relative to each other is. In such cases additional information is required which can be provided by the measurement of residual dipolar couplings. The orientation of a bond vector in a protein can be determined relative to the principal axis of the molecular alignment tensor. RDCs usually have large errors but given a large data set the structure can also be solved using entirely RDCs. Knowing how certain bonds are orientated relative to each other helps to solve the overall orientation of flexible loops or secondary structure elements.[47–49]

Structure calculation using Rosetta

The three-dimensional structure of a protein is directly related to its amino acid sequences. Therefore it should be possible to calculate the structure of a protein solely from its sequence. The Rosetta protein modelling suite is a unified software package that allows protein structure prediction without any additional experimental data relying solely on the statistics of the PDB.[50,51] Nevertheless, experimental data can be added that drive the algorithm towards a structure that best represents the experimentally obtained data. The Rosetta approach uses short fragments of three and nine amino acids. For each of these small segments Rosetta selects a few hundred fragments from the crystallographic structural database that are similar in their sequence to represent the conformational space that this segment is most likely to be found in during folding. Rosetta then applies a Monte Carlo strategy to yield native-like protein conformations with typical accuracies of 3-6 Å (see Figure 1.2).

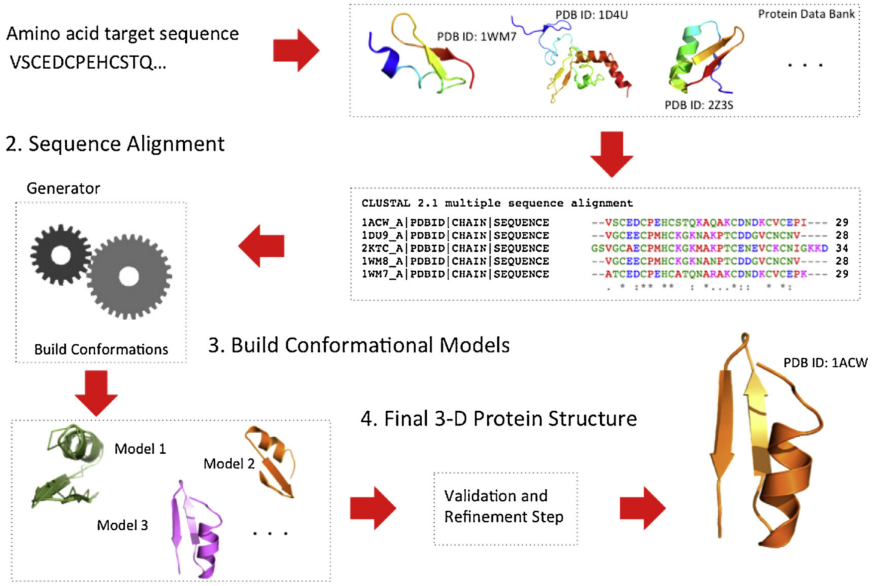

Figure 1.2: "Schematic representation of a typical process of comparative modeling by homology. Initially, template proteins are identified. Then the sequence of the target protein is aligned against the sequence of the protein templates, and then a model is built and validated, obtaining in the end, the 3-D structure of the target protein. If necessary, the final structure may undergo a refinement process." Figure taken from (*52*).

Adding structural information from experimental NMR data can significantly improve the quality of the final models. Protein NMR chemical shifts are highly sensitive to the surrounding local structure. An extension to Rosetta, CS-Rosetta was developed which uses chemical shifts obtained from backbone assignments to optimize the selection of protein fragments from the Protein Data Bank.[53] In contrast to the previously selected fragments, these fragments are not only similar in their sequence they are also more closely

related to the native state as their chemical shifts match better. Extremely valuable long-range pseudocontact shift informations obtained from a single metal binding site were successfully incorporated in the Rosetta approach. PCS-Rosetta can automatically calculate the anisotropy of the magnetic susceptibility tensor and the metal position from the experimental data during structure calculations.[54] It could be shown that proteins of up to 150 residues could be accurately calculated from exclusively PCS data. The program successfully discriminates correctly folded states from incorrectly folded ones. While PCS-Rosetta allowed only the usage of one single paramagnetic center, this approach was quickly extended to multiple paramagnetic centres. The GPS-Rosetta approach uses multiple paramagnetic centres thus in a way operates like GPS satellites to pinpoint the location of spins.[55] All components of the anisotropy of the magnetic susceptibility tensors are simultaneously fitted during the low-resolution backbone-only annealing of the Rosetta program.

1.3 *in-cell* PROTEIN NMR SPECTROSCOPY

With the huge variety of possible experiments and computation approaches, structure determination of small to medium sized proteins has become straightforward. The introduction of structural restraints obtained from NMR spectroscopy has proven extremely useful. Nevertheless, most protein samples are recorded in buffered aqueous solution that only poorly mimic the natural environment of the protein. A completely different approach is needed if one wants to study proteins and their interactions at their native, intracellular location. *In-vitro* studies have increased our three-dimensional knowledge of these proteins. Nevertheless they do not necessarily represent the state of proteins inside a living cell.[56] Various specific and non-specific interactions with the crowded cellular environment can be crucial for the proteins structure and function. *In-cell* NMR can address these changes as well as post-translational protein modifications. The first *in-cell* NMR has been described by Serber *et al.*.[57] Since then the term *in-cell* NMR has been used for measurements inside living cells while *in-vivo* refers to measurements in living organisms. Most of today's *in-cell* NMR approaches exploit the fact that most atomic nuclei (with the exception of hydrogen) are not NMR active in their most abundant isotope. Isotope labelling is used as a selective filter that renders the whole cellular background invisible to the spectrometer due to the very low natural abundance. In essence the protein of interest is expressed in growth media with isotopically enriched precursors. If bacteria are grown in unlabelled medium first and only switched to labelled material before the induction of recombinant protein expression the selective isotope labelling is generally restricted to the protein of interest. This allows the direct measurement of intact bacteria cells without further purification. On the other hand, proteins can also be purified from bacteria cells and then transferred to eukaryotic cells. For measurements in *Xenopus laevis* oocytes the labelled proteins can be deposited by microinjection due to the conveniently large size of the cell. These cells are collected and can then be measured

using established protein NMR experiments.[21,56,58] Alternatively, the protein can also be brought into cells by means of other methods like electroporation, cell penetrating peptides[59] and osmotic shock.

1.4 PARAMAGNETIC PROTEIN NMR SPECTROSCOPY

In paramagnetic systems, many different effects can be observed that provide long-range structural information. Paramagnetic relaxation enhancement (PRE), residual dipolar couplings (RDC) and pseudocontact shifts (PCS) are commonly used for structural information (see Figure 1.3). Contact shifts (CS), dipolar shift anisotropy (DSA), correlation between Dipole-Dipole (DD) interactions and DSA (DD-DSA) and residual chemical shift anisotropy (RACS) are not commonly used for structure determinations.[60]

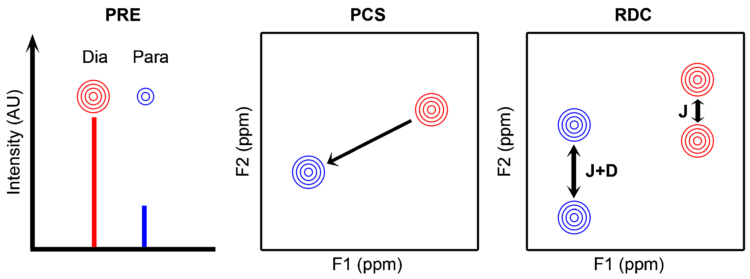

Figure 1.3: "Restraints observed from paramagnetic NMR. Left panel: Reduction in the peak intensity is observed for the resonances that are close to paramagnetic centres due to paramagnetic relaxation (PRE). With anisotropic paramagnetic centres, both PCS (middle panel) and RDCs (right panel) are observed. Peaks with red and blue represent resonances in diamagnetic and paramagnetic conditions, respectively." Figure taken from (*61*).

1.4.1 *Paramagnetic relaxation enhancement*

Every paramagnetic center causes line broadening to the NMR spectrum due to the paramagnetic enhancement of the transverse relaxation rates. The PRE effect arises due to a dipole-dipole interaction and decreases similarly to the NOE effect with a r^{-6} dependency.[62–64] However, replacing one of the nuclear spins by an electron spin the relaxation can be enhanced by a factor of 658 boosting the observable range up to 30-40 Å. Although paramagnetic relaxation enhancements can be observed with every paramagnetic center, nitroxide radicals, Mn^{2+} and Gd^{3+} are preferred. These paramagnetic centres have an isotropic electron g-factor and thus do not give rise to any pseudocontact shift. The PRE is measured by taking the difference in nuclear relaxation rates between a paramagnetic and a diamagnetic sample. In practice most PRE studies use a simplistic approach by taking the ratio of peak intensities in the paramagnetic and diamagnetic sample. PREs are in general far less accurate than NOEs nevertheless they have proven to be of great use in structure

determination especially also in the context of the determination of sparsely populated states of proteins and their complexes.[63] Due to conformational changes, a spin in a minor populated state can come relatively close to the paramagnetic center and thus influences the PRE in such a way that a closer apparent distance is obtained, which can be mathematically decomposed into an ensemble of structures thus providing unique information especially about sparsely populated states.[63]

1.4.2 *Residual dipolar couplings*

In NMR spectroscopy, dipolar couplings are useful for the characterizations of protein structures as they depend on distance and orientation between two spins as well as dynamics. The dipolar coupling is a through space effect which arises from the interaction of any two magnetically active nuclei. However, Brownian motion averages dipolar couplings to zero under isotropic conditions. It is only under anisotropic conditions that these dipolar couplings are not averaged to zero and are thus observable as residual dipolar couplings. The partial alignment of the proteins (roughly one in thousand) causes the dipolar couplings which are generally in the range of kHz to be observable as residual dipolar couplings of a few Hz. The RDC D_{AK} between two spins A and K depends on their distance and orientation,[64]

$$D_{AK} = -(hB_0^2\gamma_A\gamma_K/(240r_{AK}^3k_bT\pi^3)* \\ [\Delta_{\chi_{ax}}(3cos^2\Theta-1)+1.5\Delta_{\chi_{rh}}sin^2\Theta cos2\Phi] \quad (1.1)$$

where γ_A and γ_K are the gyromagnetic ratios of spin A and K, respectively, r_{AK} is the internuclear distance and, h is Planck's constant, T the temperature, k_b the Boltzmann constant and Θ and Φ are the polar angles. This equation clearly reveals that RDCs do not depend on the distance from the spin to the paramagnetic center.[64] RDCs can only be recorded if the molecules Brownian motion is not averaged over all three principle room directions. For this purpose liquid crystals were introduce in 1963 by Saupe and Englert.[65] However, multiple dipolar couplings made the spectra extremely difficult to interpret. In the early 1990s, bicells were introduced[66] and since then extensively used for the partial alignment of proteins in solution. Besides bicells also various other alignment media like phage particles[67] and strain-induced gels[68] have been developed. Most of this methods rely on steric hindrance to enforce a preferential orientation and require the addition of some sort of alignment media.[69] On the other hand metal ions with an anisotropic χ tensor cause a weak alignment in the direction of the magnetic B_0 field. However, the introduction of a paramagnetic metal often requires paramagnetic tagging of the protein with a suitable tag.[70]

1.4.3 *Contact shift*

The contact shift is an effect that arises through direct spin delocalization and/or spin polarization. The contact shift can be described by the simplified equation 1.2,

$$\delta^c = \frac{A}{\hbar}\frac{g_e\mu_b S(S+1)}{3\gamma_I k_b T} \tag{1.2}$$

where $A/\hbar$ is the contact coupling constant, μ_b is the Bohr magneton, k_b the Boltzmann constant, T the temperature, S the total spin quantum number and g_e is the electron g-factor. This equation only holds true for a single electron in an orbital which is well separated from excited states and has an isotropic electron g-factor. Most other cases are difficult to describe especially in complexes with low symmetry. Due to the contact shift being mostly a through bond effect it is often neglected for atoms more than four bond away from the paramagnetic center. In fact, contact shifts are rich of structural information and conformational arrangements. Nevertheless, this information can hardly be derived into useful restraints for structure determination.[71]

1.4.4 *Pseudocontact shift*

The pseudocontact shift is an effect that arises due to a through-space dipole-dipole interaction. The effect manifests itself in a chemical shift change originating from the interaction of the spin with a paramagnetic center with an anisotropic electron g-factor. For the point-dipole approximation and a rigid molecule the PCS can be described by equation 1.3,

$$\Delta\delta^{PCS} = \frac{1}{12\pi r^3}[\Delta\chi_{ax}(3cos^2\Theta - 1) + 1.5\Delta\chi_{rh}sin^2\Theta cos2\Phi] \tag{1.3}$$

where $\Delta\delta^{PCS}$ is the PCS usually reported in ppm, r is the distance of the nuclear spin to the paramagnetic center, $\Delta\chi_{ax}$ and $\Delta\chi_{rh}$ are the axial and rhombic components of the anisotropy of the magnetic susceptibility tensor χ, and Θ and Φ are the polar angles describing the relative position of the nuclear spin.[72] The magnetic susceptibility tensor χ can be decomposed in an isotropic χ_{iso} and and anisotropic component $\Delta\chi$. Only the anisotropic part is of interest in terms of pseudocontact shifts. The anisotropy can be decomposed into an axial ($\Delta\chi_{ax}$) and a rhombic ($\Delta\chi_{rh}$) component according to the equations 1.4 and 1.5.[73]

$$\Delta\chi_{ax} = \chi_{zz} - \frac{\chi_{xx} + \chi_{yy}}{2} \tag{1.4}$$

$$\Delta\chi_{rh} = \chi_{xx} - \chi_{yy} \tag{1.5}$$

For future comparison of different χ tensors, a convention was introduced. The unique tensor representation (UTR) was established by Schmitz *et*

al..[74] The χ tensor axes were labelled according to the following scheme: $|\chi_z| > |\chi_y| > |\chi_x|$. This convention ensures that the axial and rhombic component will always have the same sign and that the rhombic component is at most 2/3 of the axial component. Equation 1.3 can only be applied if the coordinate frame of the molecule is aligned with the coordinate frame of the tensor and the metal position is at the origin. In order to achieve this, tensor parameters are usually reported with the metal coordinates in the molecular frame and the three euler angles (α, β, γ) describing the required rotations to align both coordinate frames. The Euler angles in the UTR representation adhere to the ZYZ' convention and are reported between 0-180°. However, special care needs to be taken if one compares tensors in the UTR, because due to the symmetric nature of the tensor a rotation around 170° can be equivalent to a rotation around 10°. It is also possible due to the definition of the axial and rhombic components that two tensors have the same sign but completely different euler angles resulting in an overall shift to the opposite direction.[72] Determination of the $\Delta\chi_{ax}$ and $\Delta\chi_{rh}$ can be accomplished by fitting pseudocontact shifts to a known structure. In total there are eight parameters that need to be determined $\Delta\chi_{ax}$ and $\Delta\chi_{rh}$, the three metal coordinates x,y,z (for the translation of the structure coordinate frame to the tensor frame) and the three Euler angles α, β, γ (for the rotation of the structure coordinate frame to align with the tensor frame). If at least eight shifts are known the equation can be solved and the tensor can be determined. In practice many more shift are required to get an accurate representation of the tensor due to experimental errors. If the metal position is known the problem reduces to five variables, which can be solved using five shifts. Pseudocontact shifts can be observed over a very long range of up to 70 Å. Large pseudocontact shifts are only observed in close proximity to the metal center and can therefore be loosely correlated to a distance, because the errors introduced by the angular dependency are small. However, small to medium sized PCS can not be directly correlated to a distance as it would be the case for NOEs or PREs due to the angular dependency. The experimentally observable shift is the sum of the diamagnetic shift, contact shift and the pseudocontact shift. In order to calculate the pseudocontact shift a diamagnetic reference must be measured to obtain the diamagnetic reference shift. Unfortunately contact shifts are not easily separated from pseudocontact shifts and, therefore, only shifts from nuclei significantly faraway (i.e. more than 4-5 bounds), where the contact shift is negligibly small, are used. Pseudocontact shifts can be measured more precisely than for example PREs and NOEs as the only relevant information is the chemical shift difference and not the linewidths or intensities. Shift differences can be measured very accurately to a precision of better than 0.01 ppm. Commonly used for performing PCS NMR spectroscopy is the ^{1}H-^{15}N HSQC experiment. From a completely assigned diamagnetic reference spectrum the shifted peaks can be identified in the paramagnetic ^{1}H-^{15}N HSQC due to their characteristic shift on a 45° angle. Assigning a few easily recognizable shifts allows the estimation of the tensor and thus finding new additional shifts and their correct assignments. In principle, if three different

magnetic susceptibility tensors of three metals were known (provided their main directions differ by at least 10°) each individual nucleus can be located. In practice, however, the uncertainties are too large such that usually four different tensors are needed for a precise location, if no other restraints are used.[71,72]

1.5 LANTHANIDE CHELATING TAGS

A prerequisite for paramagnetic protein NMR spectroscopy is the introduction of a paramagnetic center. Most often paramagnetic lanthanides are used in their plus three oxidation state. Some proteins contain a metal binding pocket where the lanthanide can replace the naturally occurring metal. Nevertheless most proteins do not contain such binding sites and artificial methods are required for selective protein labelling.

1.5.1 *Lanthanide binding proteins*

Many proteins have metal binding pockets, however, lanthanides have no relevant function in nature and, therefore, no natural highly selective lanthanide binding motifs have evolved. In contrast, the natural occurring Ca^{2+} Mg^{2+} and Mn^{2+} ions have highly selective binding motifs in proteins. In some cases these metals can be substituted by a lanthanide.[72] Ca is particularly well suited as it is most similar to lanthanides in terms of ionic radius and complexation chemistry. Metalloproteins containing the EF-hand motif have been successfully substituted with Ln^{3+} to generate pseudocontact shifts. Calbindin D_{9K} selectively binds two Ca^{2+} ions. Bertini *et al*. replaced one calcium ion with paramagnetic lanthanides and determined the $\Delta\chi$ values (see Figure 1.4). Up to date this is the most complete series of $\Delta\chi$ values for the whole lanthanide series except promethium which is radioactive.[75] Although replacing a naturally occurring metal with a lanthanide is convenient, its binding is not very tight, structural changes may occur and the observable pseudocontact shifts are small. Also this approach is only viable for proteins containing a suitable metal binding motif which is roughly a third of all natural proteins.[76]

1.5.2 *Lanthanide binding peptides*

Inspired by nature's EF-hand motif several lanthanide binding peptides (LBP) were developed for the site-specific attachment of Ln^{3+} ions to the protein. In principle this limits the application of this LBP to the N or C terminus of the protein. Nevertheless it could also be shown that such LBP can be engineered with a cysteine residue such that disulphide conjugation becomes possible. If prior knowledge of the proteins three dimensional structure is available the LBP can also be engineered into a flexible loop of the protein. Peptide fusion offers in contrast to chemical reactions, a quantitative yield.

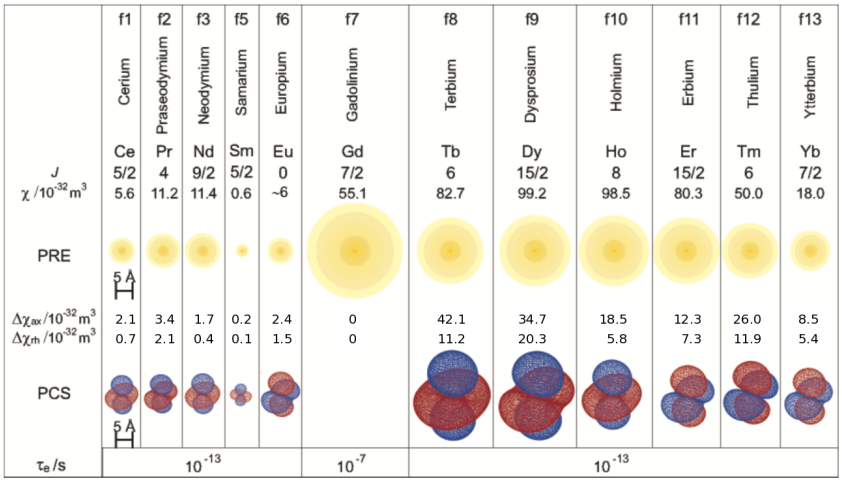

Figure 1.4: "Paramagnetic properties of Ln^{3+} ions. Only paramagnetic and non radioactive lanthanides are included. Representative isosurfaces are plotted for PCSs by $\pm$ 5 ppm using tensors reported by Bertini et al.Bertini *et al*. The radius of the yellow sphere indicates the distance from the metal ion at which 1H NMR signals of macromolecules with a rotational correlation time of 15 ns broaden by 80 Hz due to paramagnetic relaxation enhancement (PRE) at a magnetic field strength of 18.8 T. For Eu^{3+}, the estimate of the relaxation enhancement includes a contribution from excited J manifolds." Tensor parameters were converted to UTR. Figure adapted from (*77*).

However, isotopic labelling of the protein also labels the LBP and can thus complicate the NMR spectra. It could be shown that 16-residue LBP are sufficient to tightly bind the lanthanide ion with affinities reaching 50 nM.[78] LBP synthesized with cysteines at different locations within the 16-residue sequence allow fine tuning of the resulting χ tensor relative to the protein.[79] This feature is not easily accessible with most other lanthanide chelating tags as their tagging mode can not be altered easily. Increased rigidity of the LBP can be achieved by N- or C-terminal fusion and one carefully engineered cysteines disulphide bridge between the LBP and the protein. Unfortunately finding an optimal linkage to the target protein is challenging both on the C- and N-terminus. Conjugation on a highly solvent exposed cysteine residue is likely to yield a very flexible and mobile tag which results in very small observable pseudocontact shifts.[72]

1.6 NON-PEPTIDIC SYNTHETIC LANTHANIDE CHELATING TAGS

Most lanthanide chelating tags are conjugated to proteins taking advantage of the nucleophilicity of sulphur. Targeting free cysteines with sulfhydryl reactive probes has become the method of choice for selective couplings. Few example also involve click-chemistry.[72]

1.6.1 *Sulfhydryl reactive functional groups used for tagging*

The vast majority of the tags reported in literature are using disulphides, pyridine-disulphides or thiosulfonate (see Scheme 1). All of these sulfhydryl-reactive motifs form a mixed disulphide between the tag and the protein and are therefore not stable under strongly reducing conditions as they are found for example in living cells.[72] Maleimides are regularly used in biological assays for the fast and selective labelling of cysteines forming a very stable thioether bond.[80] However, in terms of PCS NMR spectroscopy, this linkage is not preferred due to the formation of two diastereomers upon conjugation with the protein. More recent approaches involve the usage of vinyl pyridines[81,82] or pyridine phenyl sulfones[83–85] to form a stable non-reducible linkage. It could be shown that such conjugates are highly stable under physiological conditions, nevertheless, the limited reactivity of these tags enforced using a high pH and/or high temperature. Tagging under such harsh conditions is not a problem for small and very stable proteins like ubqiuitin or GB1. Most other proteins would suffer degradation under conditions largely deviating from physiological values. Iodoacetamide and bromoacetamide are used for the formation of thioether bonds between proteins and linkers under much milder conditions.[86,87] Nevertheless, tagging was relatively slow if compared to standard disulphide bond formation and required generally higher amounts of tag. Introducing non-natural amino acids into the protein allows the usage of a copper catalysed azide-alkyne cycloaddition.[88] Unfortunately, the formed linkage is also rather long and it could be shown that many proteins are sensitive to the presence of copper and precipitate out of solution. Approaches dealing with the formation of thioether suffer from low reactivity and/or increased linker size.[72]

1.6.2 *Open chain molecules*

EDTA-based tags

Initially lanthanide chelating tags were based on the EDTA scaffold. EDTA is a universal high affinity hexadentate metal chelator.[89] Protein conjugation was achieved using pyridine-disulphides or thiosulfonate as activator (see Scheme 2). Although EDTA itself is not chiral, metal complexes formed with EDTA are chiral and two enantiomers are obtained.[89] Conjugation with the already chiral protein leads to two diastereoisomers which consequently results in peak doubling giving rise to two sets of signals in the NMR spectra. This is clearly seen by PCS NMR spectroscopy as the two different tag enantiomers also have two different χ tensors. It could be shown that the introduction of a single stereogenic center to the EDTA tags can lead to only one observable set of peaks.[72,89]

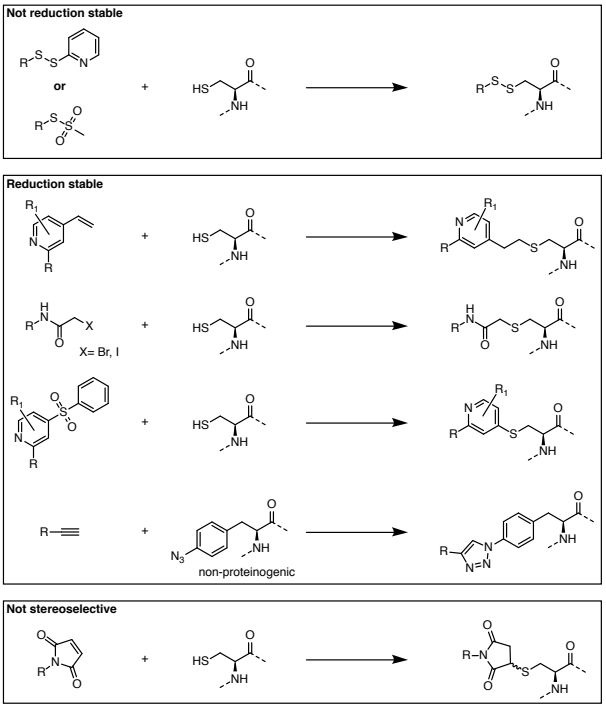

Scheme 1: General reaction scheme for the covalent attachment of lanthanide chelating tags to proteins. The Lanthanide chelating tag is represented as R and no further reaction conditions are stated.

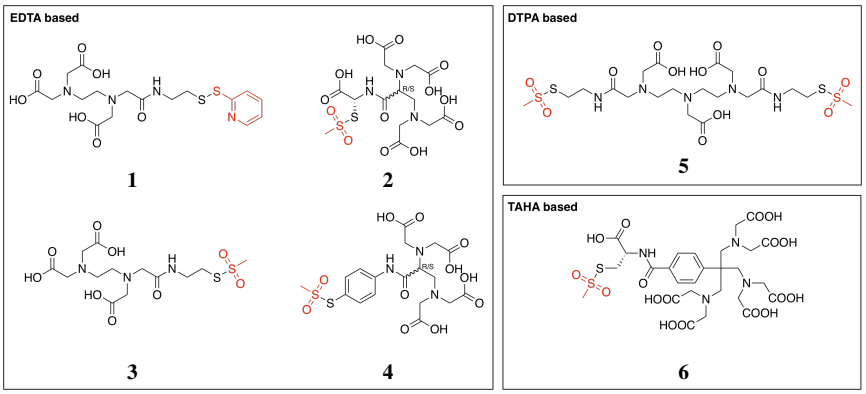

Scheme 2: Selection of thiol reactive open chain ligands for lanthanide chelating tags. Thiol reactive part is highlighted in red. Tags based on EDTA form hexadentate complexes whereas DTPA forms octadentate and TAHA nonadentate complexes.

DTPA-based tags

Consequently by going from hexadentate to octadentate the binding affinity for lanthanide(III) ions increased. Unfortunately the number of possible diastereoisomers increased to eight. Double attachment to the protein surface was tried to increase the tags probability to adapt only a single conformation (see Scheme 2). This approach was unsuccessful as up to five different set of signals were observed, however, shifts up to a distance of 40 Å could be obtained. On small proteins, decomposition of multiple sets of signals might be possible, however, on medium to large sized proteins this becomes infeasible.[72,90]

TAHA-based tags

A nonadentate TAHA-based tag was conjugated to cysteine mutants of ubiquitin and pseudocontact shifts were recorded for Tm^{3+} and Tb^{3+} loaded tags (see Scheme 2). Only one set of signals was obtained for each sample indicating the presence of only one diastereoisomer.[91]

1.6.3 *DOTA-type ligand*

DOTA in MRI applications

In magnetic resonance imaging (MRI) a variety of gadolinium based contrast agents are used as the quality of a MR image depends amongst other factors on the increased relaxation rates caused by the PRE effect. Due to the seven unpaired electrons Gd is strongly paramagnetic and has a very slow electronic relaxation rate. However, free gadolinium is extremely toxic, because the ionic radius of Gd^{3+} (107.8 pm) is close to that of Ca^{2+} (114 pm). Gadolinium blocks many voltage-gated calcium channels at nano- to micromolar concentrations. For potential application in humans, gadolinium must be chelated in highly stable complexes to avoid intoxication of the patient. Many MRI contrast agents are based on DTPA which has also been applied for PCS NMR spectroscopy (see Figure 1.5). The development of Gd-DOTA for MRI application showed the high stability of DOTA based gadolinium tags. Gd-DOTA (Dotarem®) showed the highest Kd (25.6) of all marketed MRI contrast agents.[92,93] This property is highly favourable not only for MRI application but also for PCS NMR spectroscopy. Recent studies have shown that gadolinium based contrast agents are retained in the brain and especially the linear contrast agents leak gadolinium which in some rare cases presumably even harmed the patients.[94]

DOTA isomers

Tags based on the DOTA scaffold form highly stable and inert complexes with lanthanide(III) ions. This is the result of the good match between the size of the cavity formed by DOTA and the ionic radii of lanthanide(III)

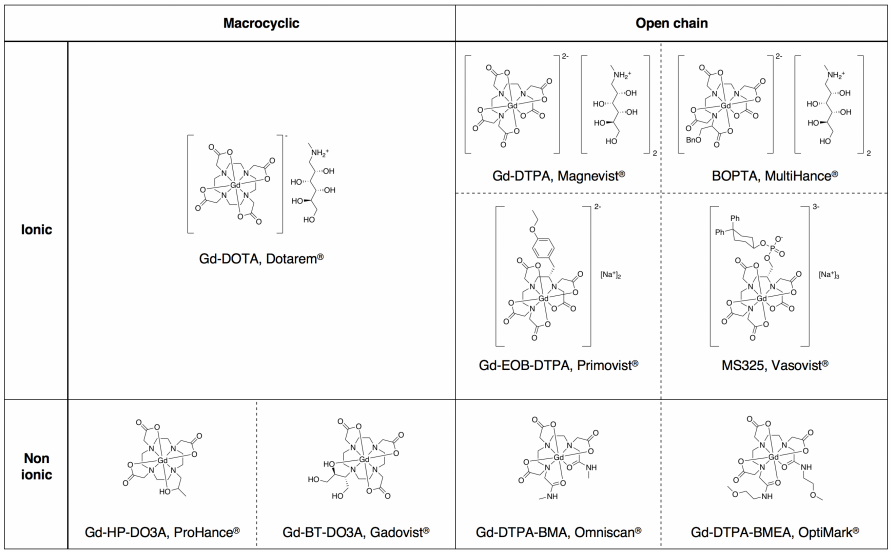

Figure 1.5: Structures of marketed gadolinium chelates used for magnetic resonance imaging. Figure adapted from (*92*).

ions. Usually a lanthanide ion has eight to nine coordination sites and eight are provided by the DOTA-ligand. The ninth coordination site can either be empty or occupied by a small ligand like water. This largely depends on the ionic radii of the lanthanide as DOTA complexes with small lanthanides prefer eight coordination sites while the complexes with larger lanthanides have enough space to accommodate a ninth coordination site. The lanthanide(III) ion is sandwiched between two square planes. One plane is formed by the four nitrogens of the cyclen base and one is formed by the four oxygens of the carboxylic acid sidechains. Lanthanide DOTA complexes form two isomers in solution, referred to as square antiprism (SAP) and twisted square antiprism (TSAP) (see Figure 1.6). Each of these isomeric forms is present as an enantiomeric pair giving rise to four different isomers. The interconversion between isomers may occur by pendant arm rotation resulting in a clockwise (Λ) or anticlockwise (Δ) conformation or by a ring flip from $\lambda\lambda\lambda\lambda$ to $\delta\delta\delta\delta$. The SAP isomers are displayed by $\Delta(\lambda\lambda\lambda\lambda)$ and $\Lambda(\delta\delta\delta\delta)$ while the opposite configurations ($\Delta(\delta\delta\delta\delta)$ and $\Lambda(\lambda\lambda\lambda\lambda)$) form the TSAP isomers. The interconversion between different isomers causes no problems for isotropic paramagnetic effects, however, the measurement of pseudocontact shift relies on the anisotropic component of the magnetic susceptibility and thus is largely affected by motional averaging.[95]

DOTA in PCS NMR spectroscopy

DOTA-SSPy **7** was tested on calcium dependent cell adhesion protein ECAD12 S87C and small PCS and a weak alignment was observed.[96] The motional averaging caused by the flexibility significantly reduced the PCSs as well as the RDCs. A modified DOTA based tag (CLaNP-3 **8**) with two

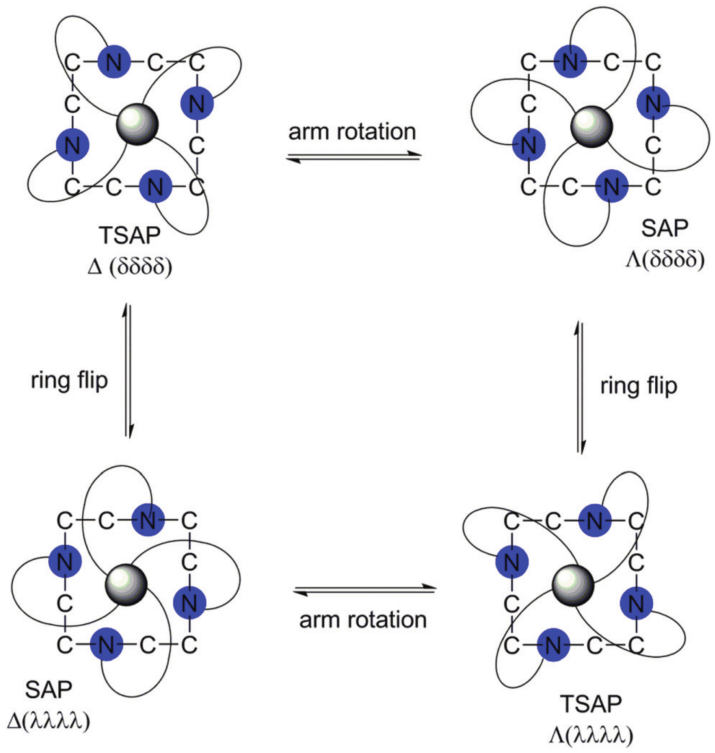

Figure 1.6: "Schematic representation of SAP and TSAP isomer conformations for Ln-DOTA-type complexes." Figure taken from (*95*).

attachment sites was tested to reduce flexibility (see Scheme 3).[97] However, in this case two attachment sites were not sufficient to select only one of the four possible DOTA conformations and the observed PCS were small and peak doubling was observed. Using two attachments sites instead of one significantly reduces the tags mobility with respect to the protein surface. However, it does not necessarily reduce the mobility inside the tag caused by ring flipping motions or side arm rotations. The problem of peak doubling was solved by the introduction of sterically more demanding side arms and for tag **9** no evidence was found for peak doubling and larger $\Delta\chi$ values were obtained.[98] This tag has an overall +3 charge as all donors are neutral. The net charge of the tag was reduced to +1 by the installation of two nitro phenolic groups instead of the pyridine *N*-oxides (tag **10**).[99] CLaNP-5 (tag **9**) has become one of the most successful double-arm cyclen based tags and is clearly superior to its single-arm pendant were one pyridine *N*-oxide is replaced by an acetate.[100] Favouring one conformer can also be induced by chiral sidearms. Tag **11** is a close analogue of CLaNP-3 **8** were the acetates are substituted by isopropanol moieties and the thiosulfonate was replaced by pyridine-disulphide.[101] A more recent version of CLaNP-5 **9**, CLaNP-9 **12**, addresses the reduction stable problem by using alpha bromo acetamides as sulfhydryl-reactive probes.[86] The measured PCS are generally lower than for CLaNP-5 **9** which was mostly attributed to the increased linker size. Unfortunately, the tags reactivity causes problems in synthesis, handling as

well as tagging. All of these double-arm cyclen-based tags require two single cysteine mutations separate by a specific distance that must be carefully engineered. Nevertheless, if carefully planned very large PCS and a strong alignment can be observed with these tags.

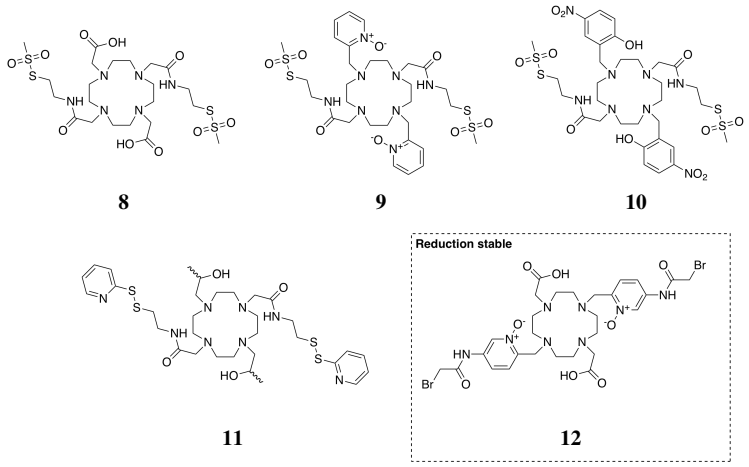

Scheme 3: Selection of double-arm- cyclen-based tags. The lanthanide is omitted.

Initial results obtained for the single arm analogue of CLaNP-5 revealed that the conformational and translational freedom is to large. Häussinger *et al*. developed a single-arm cyclen-based tag with eight stereospecific methyl groups (see Scheme 4).[102] Using a four times methyl substituted cyclen (4*S*-M4-cyclen) and lactic acid, a sterically more crowded and highly rigid tag was obtained. This tag exists in two different forms (4*R*4*S*) and (8*S*)-DOTA-M8. First experiments were reported using the 8*S* variant. It was shown that the introduction of the eight methyl groups dramatically reduced the conformational flexibility. Comparison with the non substituted DOTA showed significantly larger χ tensors. Initial experiments performed with Dy^{3+} loaded (8*S*)-DOTA-M8 showed the presence of a second species. Opina *et al*. showed that the second species arises from the slow conformational equilibrium between a TSAP and SAP geometry.[95] The ratio strongly correlates with the size of the lanthanide. For lanthanum a ratio of 98:2 ($\Lambda(\delta\delta\delta\delta)$: $\Delta(\delta\delta\delta\delta)$) was found while for lutetium the opposite 3:97 was found. In terms of DOTA conformers this corresponds to a SAP to TSAP switch although strictly speaking this is not true for DOTA-M8 as both conformers are twisted square antiprisms. The only major difference is the sense of ration of the pendant arms. For intermediate lanthanides the ratio approaches in extreme cases (holmium) almost 50:50. Surprisingly the (4R4S) variant of DOTA-M8 was not studied by Opina *et al*. However, recent work performed in our research group involving DFT calculations suggest a $\Lambda(\delta\delta\delta\delta$ (SAP) geometry for the whole lanthanide series.

If averaging motions are fast enough on the NMR time scale the PCS are small but still only one set of signals is observed. The presence of a second species can be avoided by introducing large chiral substituents to the side arms. Tag **13**, synthesized in both enantimoeric forms ((*S*,*S*,*S*) and (*R*,*R*,*R*)) showed large tensor parameters and only a single set of paramagnetic peaks.[103] Single arm variants of **11**, **14** and **15**, showed also only one set of paramagnetically shifted peaks. Introducing chiral and/or large chiral side arms to cyclen based-tags suppresses slow conformational changes, which would lead to peak doubling. However, fast averaging processes are not necessarily removed. Ring flip motions are completely suppressed in the DOTA-M8 tag as the methyl groups would need to adopt a very unfavourable axial position.[95]

A reduction stable derivative of DOTA-M8, M8-CAM-I, was developed, where the activator was replaced by a propyliodoacetamide. Tensor parameters obtained for these derivative were generally worse than for DOTA-M8 which was attributed to the increased linker length.[87] In order to reduce the linker length M7-Py-DOTA was developed.[83] M7-Py-DOTA features the same scaffold as DOTA-M8 with one pendant arm replaced by a sulfhydryl reactive pyridine phenyl sulfone moiety. Two closely related analogues of M7-Py-DOTA were published shortly after, featuring the opposite chirality on the pendant arms and cyclen as core.[104] These tags offer a non-reducible covalent linkage with the protein and are therefore suited for *in-cell* measurements. All of these tags suffer from a relative low reactivity thus requiring harsh conditions like increased pH or elevated temperatures. The M7-Py-DOTA tag was developed in the (3*R*4*S*) configuration and displayed no second set of peaks for thulium and terbium, although terbium showed a ration of 80:20 ($\Lambda(\delta\delta\delta\delta) : \Delta(\delta\delta\delta\delta)$) for the (8*S*)-DOTA-M8 tag.[95]

The vast majority of tags relies on one or two cysteines on the protein surface. Introduction of unnatural amino acids allows the usage of chemistry not relying on the high nucleophilicity of thiols. *Para* azido-*L*-phenylalanine can selectively be introduced into the protein sequence and requires an alkyne installed on the tag for a copper catalysed azide-alkyne cycloaddition. Tags, **16** and **17**, were specifically designed for this propose, but showed smaller PCS than tag **13** due to the increased tether size.[105] Also some proteins are sensitive to copper and precipitate out of solution. Designing a short and highly reactive reduction stable tag remains challenging and further development is needed.

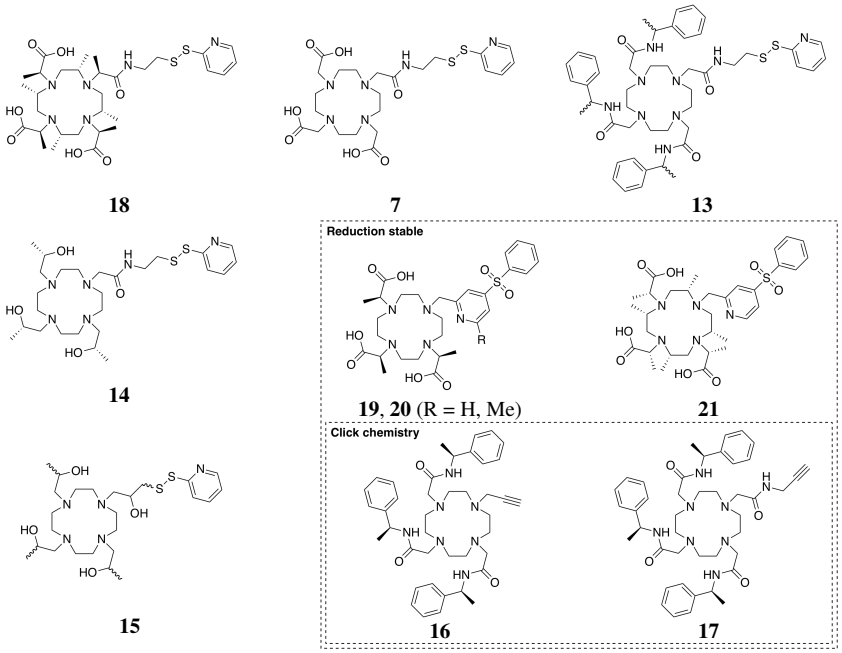

Scheme 4: Selection of single-arm- cyclen-based tags. The lanthanide is omitted.

2

RESEARCH GOAL

Pseudocontact shift protein NMR spectroscopy relies on the principle of attaching a paramagnetic source on the surface of the protein or inside. A very convenient source of paramagnetism are lanthanide $^{3+}$ ions. Today most PCS NMR experiments were carried out using a lanthanide chelating tag which is site-selectively conjugated to the protein surface. The most promising lanthanide chelating tags are based on the DOTA framework. The DOTA framework as well as the linkage are under constant development in order to push the range of applications even further.

The Häussinger group focuses its research mainly on the development of new high performing lanthanide chelating tags mostly based on M4-cyclen. The literature known procedure for the synthesis of M4-cyclen[106] has proven to be extremely challenging to up-scale in industry and academia. Therefore, a up-scalable and robust synthetic procedure to obtain M4-cyclen was needed. The first aim of this thesis involved the development of a robust procedure for the synthesis of M4-cyclen which should be highly flexible. The procedure should allow the synthesis of selectively labelled compounds as well as the synthesis of differently substituted twelve-membered tetraaza macrocycles. The procedure should also allow the introduction of substituents with functional groups on the macrocycle such that the installation of a sulfhydryl reactive moiety on the base ring becomes possible.

The second part of the thesis aims to extend the applicability of pseudocontact shift NMR spectroscopy to *in-cell* applications. Most PCS experiments published in literature are conducted in buffered solution that mimic biological environments. Under the reductive environments found inside living cells the commonly used disulphide bridge is quickly cleaved. Therefore, the second aim of the thesis was to develop a reduction stable linker moiety which allows the determination of protein structures inside living cells using PCS NMR spectroscopy.

Thirdly, not only proteins but also RNAs are important biological molecules and targeting these by PCS NMR spectroscopy is desirable but challenging. Therefore, we aimed for the development of a suitable tag for RNA PCS NMR spectroscopy.

Part I

SYNTHESIS OF SUBSTITUTED TWELVE-MEMBERED TETRAAZA MACROCYCLES

This part of the thesis focuses on the development and exploration of new synthetic routes towards substituted twelve-membered tetraaza macrocycles suitable as core building blocks for DOTA based lanthanide chelating tags.

3

DEVELOPMENT OF A MULTIGRAM SCALE SYNTHESIS FOR 4(*S*)M4-CYCLEN

3.1 RETROSYNTHETIC ANALYSIS AND CONSIDERATIONS

The literature known procedure for the synthesis of 4(*S*)M4-cyclen utilizes nucelophilic ring opening of the corresponding alanine-based aziridine.[106] This method could so far not been up scaled. 4(*S*)M4-cyclen could be obtained by simply reducing its cyclic tetraalanine precursor. Many cyclic tetrapeptides have biological activity and are therefore of great interest for both academia and industry. Nevertheless a high yielding general approach to synthesize cyclic tetrapeptides has not been reported so far.[107] Many procedures involve proline[108] or unnaturally configured amino acids as turn inducing amino acid. Some approaches apply click chemistry to form a triazol which mimics a carboxylic amide.[109] For our synthesis of 4(*S*)M4-cyclen we envisioned three different approaches starting from enantiomerically pure alanine derivatives. Method A in Scheme 5 utilizes a Head-to-Tail cyclization of an alanine-based tetramer in solution or on solid phase support. Method B and C (see Scheme 5) involve the formation of a preorganized open chain intermediate. Either one or two sequential ring closing reactions close the preorganized structure forming the twelve-membered macrocycle.

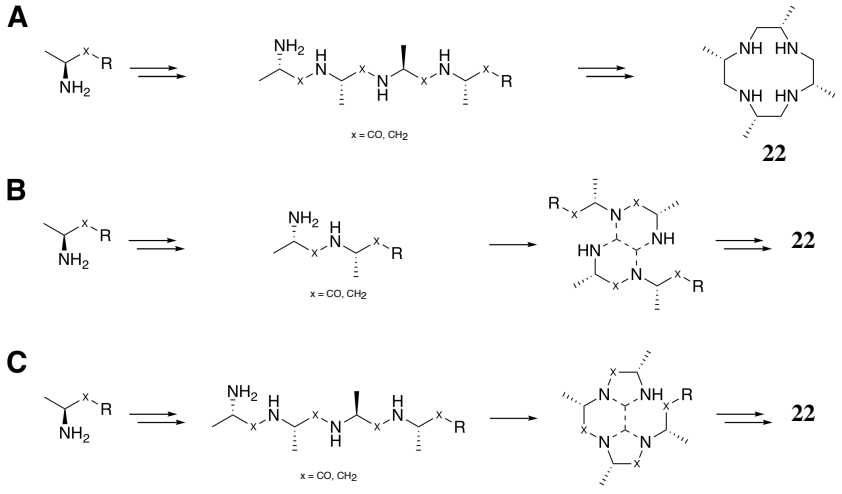

Scheme 5: General strategies to synthesis 4(*S*)-M4 cyclen.

3.2 HEAD-TO-TAIL SOLID PHASE CYCLIZATION (METHODE A)

Cyclic tetrapeptides were synthesised using an polymer based approach.[110] Cyclic tetraalanine was successfully synthesised in small scales (mg) by Florian Lüttin during his master thesis within our group. He showed that a polymer assisted Head-to-Tail cyclization is possible on an functionalized polymer support (see Scheme 6).[111] His findings were the starting point for further investigations during this thesis. We investigated if this process could be extended to larger quantities of up to multigram scale.

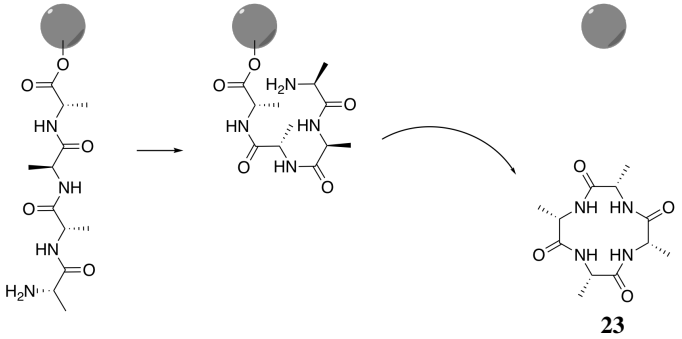

23

Scheme 6: Polymer based approach to facilitate Head-to-Tail cyclization. For clarity the polymer is shown as a grey sphere.

3.2.1 *Synthesis of N-Cbz-protected tetraalanine **30***

The synthesis of *N*-Cbz-protected tetraalanine was adapted from the procedure described by Florian Lüttin (see Scheme 7).

Starting from commercially available *tert*-butyl alanine **25** and *N*-Cbz-alanine the dimer **24** was synthesised in high yields using HATU and DIPEA in acetonitrile. On large scale this process was very time consuming as the final product required purification by flash column chromatography. In order to avoid purification by flash column chromatography HATU could be exchanged to T3P offering an easier work-up due to the water soluble by-products with, however, lower yields. Subsequent deprotection forming the free amine **28** and the free acid **27** were carried out in excellent yields. A second peptide coupling with HATU and DIPEA in acetonitrile formed the fully protected tetramer **29**. The product crystallized out of solution during the reaction and was isolated by filtration in medium yield. The lower yield was attributed to the high solubility of the product in acetonitrile. Nevertheless, the time consuming purification step was avoided and this method was preferred on large scales. A solvent with a lower solubility for tetraalanine **29** could increase the yield. However, material cost are low and the reaction was not further optimized. Final deprotection with trifluoroacetic acid yielded the

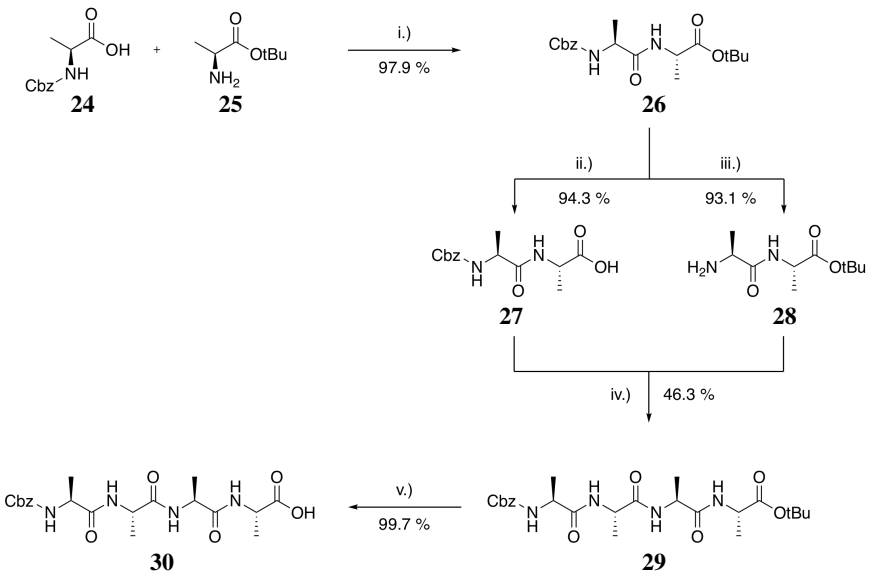

Scheme 7: Synthesis of compound **30**. Reaction conditions: i.) HATU, DIPEA, MeCN, 20-25 °C, 3.5 h; ii.) TFA / H_2O, 20-25 °C, 2 h; iii.) Pd/C, MeOH, 20-25 °C, 2 h; iv.) HATU, DIPEA, MeCN, 20-25 °C, 2 h; v.) TFA / H_2O, 20-25 °C, 30 min.

desired *N*-Cbz-protected tetramer **30** in quantitative yield.

3.2.2 *Polystyrene functionalization*

The first successful cyclization of tetraalanine on a small scale in our group was performed using a nitrophenol functionalized polystyrene by Florian Lüttin. During up scaling experiments we tested three different functionalized polymers (see Scheme 8). Loading capacity as well as cost and reusability were critical criteria. Each polymer consisted of a nitrophenol analogue covalently bound to polystyrene.

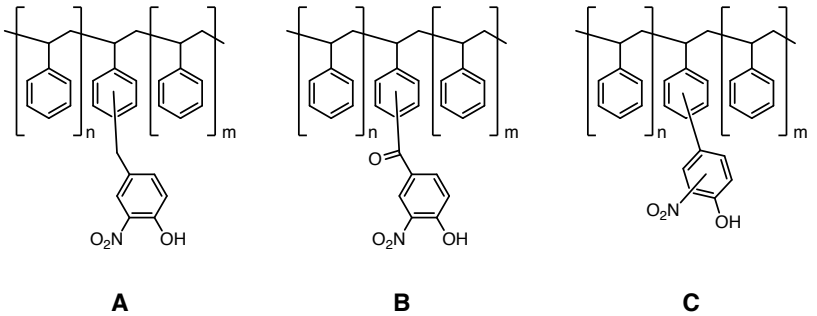

Scheme 8: Nitrophenol-based polymers **A**, **B** and **C**

*Polymer **A***

We synthesised 4-(chloromethyl)-2-nitrophenol (**31**) by hydroxymethylation of 2-nitrophenol followed by converting the hydroxyl group to chlorine using hydrogen chloride gas in chloroform. Hydroxymethylation of 2-nitrophenol had a very low yield and an alternative was searched. Using commercially available 4-hydroxy-3-nitrobenzoic acid (**32**) and the procedure described by Chen *et al.*[112] we obtained 4-(hydroxymethyl)-2-nitrophenol (**33**) in better yield by reducing the acid with borane tetrahydrofuran complex and boron trifluoride diethyl etherate in tetrahydrofuran (see Scheme 9). The conversion strongly depended on the amount of BH_3 and BF_3 used. We found that best results were obtained using 4 eq. of $BH_3 \cdot THF$ and 1 eq. $BF_3 \cdot OEt_2$ (see entry 5 in Table 3.1) instead of 2 and 1.5 as described.

Table 3.1: Reaction condition screening for the reduction of 4-hydroxy-3-nitrobenzoic acid with borane tetrahydrofuran complex and boron trifluoride diethyl etherate.

Entry	eq. $BH_3 \cdot THF$	eq. $BF_3 \cdot OEt_2$	Conversion [%]
1	2	1	23
2	2	1	25
3	2	0	22 (solid precipitate)
4	3	1	71
5	4	1	100

All reactions were carried out in tetrahydrofuran at 20-25 °C. Conversion was determined by ^{1}H-NMR.

Our first synthesis of 4-(chloromethyl)-2-nitrophenol (**31**) used an HCl generator (H_2SO_4 and NaCl). However, during up scaling HCl gas from a gas cylinder was used. Surprisingly the reaction did not take place. We found that little traces of sulphuric acid and water present in the gas synthesised with the HCl generator were responsible for catalysing the reaction. After the intentional addition of sulphuric acid and water the reaction performed equally well with HCl gas from a gas cylinder. Polystyrene was functionalized by Friedel-Crafts alkylation using aluminium trichloride with a low yield of 7.3 %. The functionalization efficiency dropped significantly if less precursor was used and we were not able to recycle the precursor. During the reaction the unreacted precursor decomposed. The polymer functionalization was determined by elemental analysis. A loading of 2.08 mmol N/g polymer was achieved. This indicated the presence of 2.08 mmol of available coupling sites per gram polymer. The steps needed to synthesise the precursor **31** and the low yield during functionalization made this polymer very expensive for up scaling.

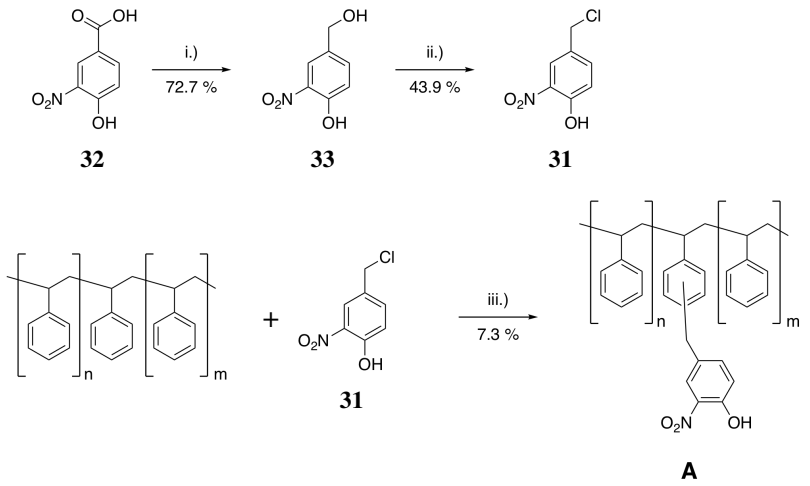

Scheme 9: Reaction conditions for the functionalization of polymer **A**: i.) BH_3 / $BF_3 \cdot Et_2O$, THF, 20-25 °C, 18 h; ii.) HCl (g), CH_3Cl, 20-25 °C, 18 h; iii.) $AlCl_3$, nitrobenzene, 65 °C, 48 h.

*Polymer **B***

Polymer **B** was developed to reduce up scaling costs. 4-(Hydroxymethyl)-2-nitrophenol (**32**) was acetylated to protect the hydroxyl group during the *in-situ* generation of the carboxylic acid chloride. In a one pot synthesis **34** was converted to the corresponding acyl chloride and subsequently reacted with polystyrene and aluminium trichloride in nitrobenzene (see Scheme 10). The acetyl group was cleaved off under basic conditions.

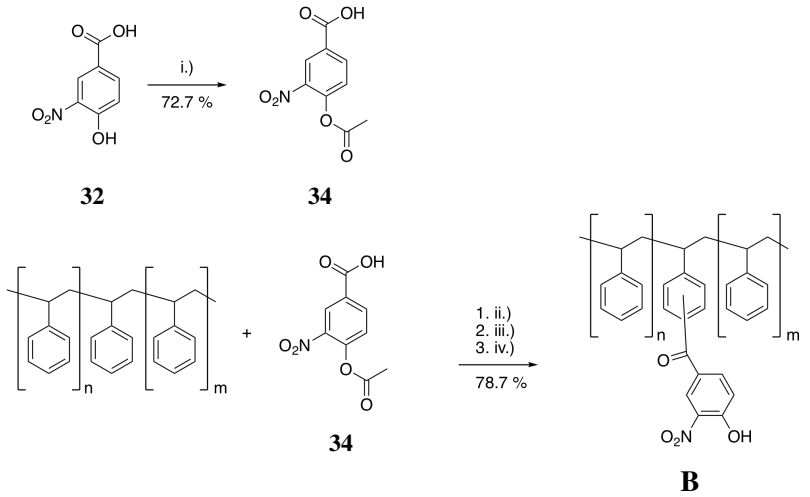

Scheme 10: Synthesis of polymer **B**. Reaction conditions: i.) acetyl chloride, THF, 0-5 °C - 20-25 °C, 18 h; ii.) oxalyl chloride cat. DMF, nitrobenzene, 20-25 °C, 45 min; iii.) $AlCl_3$, nitrobenzene, 40 °C, 18 h; iv.) aq. NaOH, 40 °C, 4 h.

A polymer loading of 1.06 mmol N/g polymer was obtained. In comparison to polymer **A** the functionalization extent is only 50 %. However the overall functionalization yield with respect to the nitro compound was increased by a factor of ten. This polymer can be more easily scaled up due to its lower cost and fewer reaction steps involved.

*Polymer **C***

As a third approach, not involving the synthesis of any nitrophenol precursor, direct nitration of commercially available phenol polymer-bound was tested. The polymer was nitrated in nitric acid at 20-25 °C without sulphuric acid to avoid over nitration (see Scheme 11). The achieved polymer nitration was 0.75 mmol N/g polymer. This labelling was lower than for polymer A and B. The commercially available phenol polymer-bound has a functionalization ranging between of 0.5-1.5 mmol /g. Roughly 50 % of the polymer was nitrated. The high cost of this polymer and the low yields during functionalization made this polymer unpractical to use for a large scale synthesis.

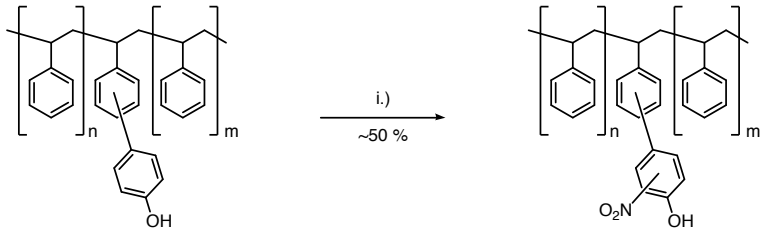

C

Scheme 11: Synthesis of Polymer **C**. Reaction conditions: i.) nitric acid 68 %, 20-25 °C, 5 h.

3.2.3 *Functionalized polystyrene induced cyclization*

Polymer **A** was used to screen for optimal polymer loading conditions. The *N*-Cbz-protected tetramer **30** was coupled to the polymer using DCC, DIC and HATU as coupling reagent. We found that HATU offered by far the best coupling efficiency based on the weight increase of the polymer. DCC was not suitable for this type of reaction as its by product were difficult to separate from the polymer. DIC offers soluble by-products but coupling performance was lower than for HATU. All three polymers were loaded with *N*-Cbz-protected tetraalanine **30** using HATU and DIPEA in dimethylformamide. Polymer **A** and **B** performed equally well. Both polymers allowed the loading of roughly half the available active sites (entry 1 and 2 Table 3.2). Polymer **C** showed a very low loading probably due to the unspecific nitration. Polymer **C** was, therefore, skipped from further investigations.

Table 3.2: Loading efficiency for the three different polymers using HATU and DIPEA in dimethylformamide.

Entry	Poly.	Polymer functionalization [g^{-1}]	Polymer loading [g^{-1}]
1	A	2.08 mmol	0.91 mmol 44 %
2	B	1.06 mmol	0.51 mmol 48 %
3	C	0.75 mmol	0.03 mmol 4 %

All reactions were carried out at 20-25 °C for 18 h.

Polymers **A** and **B** were treated with hydrogen bromide solution in acetic acid. This procedure was used to remove the N-terminal protecting group and afforded the free tetraalanine polymer bound as a hydrobromide salt. Extensive washing of the polymer was required to remove impurities and acetic acid from the polymer. The pH was increased to >9 with DIPEA in dimethylformamide to induce cyclization. The polymer was stirred at 20-25 °C for 24 h. Although we detected the formation of the desired compound by ESI-MS it was not possible to isolate cyclic tetraalanine **23** in pure form after the cyclization. Reduction of the crude material with lithium aluminium hydride yielded 4(*S*)M4-cyclen in very low yields after purification by preparative HPLC.

3.3 HEAD-TO-TAIL IN SOLUTION CYCLIZATION

3.3.1 *Cyclization of tetraalanine*

It has been shown by Titlestad[113] that activated tetrapeptide esters cyclize in solution. Using TCP to form an active ester was already tested by Florian Lüttin during his master thesis with little success. The yield was considerably smaller than the one reported. During this study HATU was used to form the active ester *in-situ* from tetraalanine **35**. Tetraalanine **35** was obtained by catalytic hydrogenation of the *N*-Cbz-protected tetraalanine in methanol (see Scheme 12).

Cyclization was performed in dimethylformamide under moderate dilution conditions (1 g L^{-1}) and under pseudo dilution conditions with HATU and DIPEA at 60 °C. Small amounts of the cyclic tetrapeptide **23** were detected in the crude material. Using HATU instead of TCP as active ester resulted in an lower yield. The lower stability of the active ester at high temperature presumably caused decomposition prior to cyclization. The highly rigid structure of the tetrapeptide **35** is unfavourable for a cyclization. For further up scaling purposes this cyclization method was not considered.

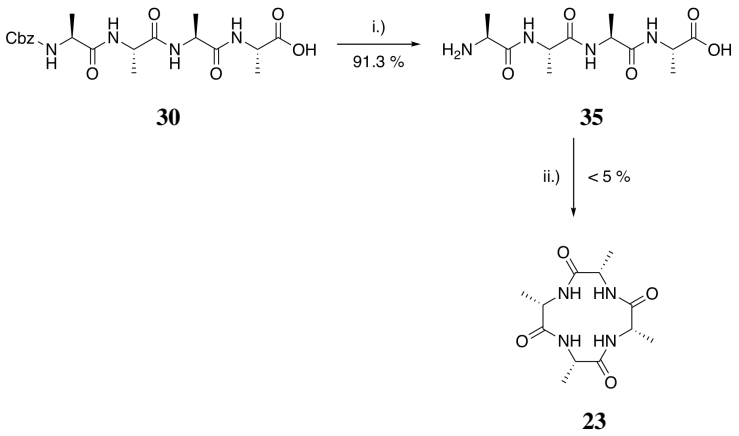

Scheme 12: Synthesis of compound **23**. Reaction conditions: i.) Pd/C, H_2, methanol, 20-25 °C, 2 h; ii.) HATU, DIPEA, DMF, 60 °C, 24 h.

3.3.2 *Cyclization of tetraalaninol (Method C)*

In order to reduce the rigidity of the open chain tetramer, tetraalanine was reduced to tetraalaninol. To force tetraalaninol into a conformation suitable for cyclization it was treated with a 1,2-dicarbonyl compound forming a pre-organized bisaminal (see Scheme 13). This step was necessary to block all the amines within the chain from performing side reactions. Upon bisaminal formation several different regio and diastereoisomers are possible. Some of them are probably less favoured due to steric effects induced by the four methyl groups.

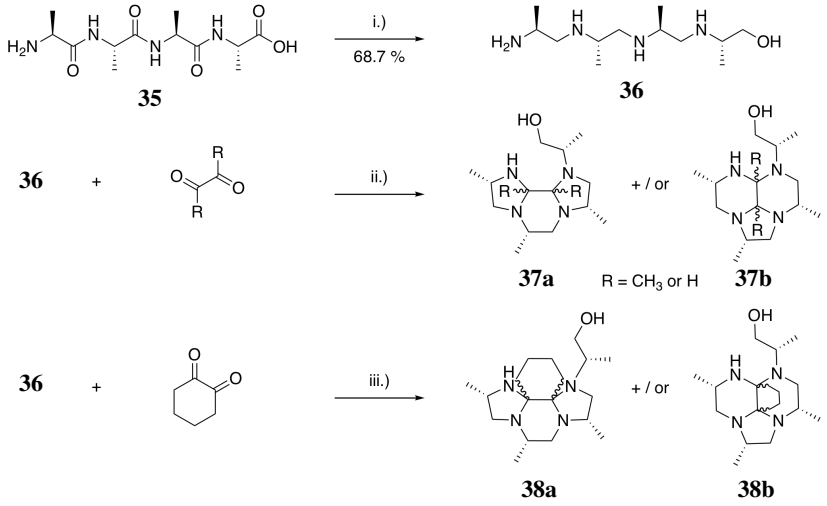

Scheme 13: Formation of bisaminal **37a**, **37b** and **38a**, **38b**. Reaction conditions: i.) $LiAlH_4$ in THF, reflux, 16 h; ii.) DCM, 20-25 °C; iii.) DCM, 20-25 °C.

Among the tested 1,2-dicarbonyl compounds glyoxal, 1,2-butandion and 1,2-cyclohexadion, only glyoxal formed an intermediate that was detected by

ESI-MS. For the other 1,2-dicarbonyl compounds the steric hindrance was to large or the intermediate stability was to low prohibiting the formation of any bisaminal species. NMR analysis of the glyoxal intermediate showed the presence of multiple different species. The protons of the aldehyde did not favour the formation of a single species as their size is to small to cause any significant steric repulsion with the methyl groups. To close the bisaminal intermediate two strategies were tried. A Mitsunobu-type ring closing and the transformation of the hydroxy group to a bromide leaving group by Appel reaction. Both reaction could not be performed successfully. We found no evidence for the presence of a closed bisaminal species by ESI-MS. This strategy was infeasible because the bisaminal key intermediates could not be purified and decomposed upon further reaction. Any attempts with two dimeric subunits (Method B) resulted in a complex mixture and were not further investigated.

3.4 HEAD-TO-TAIL IN SOLUTION CYCLIZATION OF FLEXIBLE ALANINE-BASED TETRAMERS

3.4.1 *Retrosynthetic analysis and considerations*

The results previously obtained clearly revealed that a highly rigid tetramer like tetraalanine (**35**) is not suitable for the large scale synthesis of 4(*S*)M4-cyclen **22**. However a highly flexible molecule like tetraalaninol (**36**) is also not suitable due to the lack of a functional group to close the ring. We concluded that for the successful cyclization of a linear tetramer it would be best to use an amide coupling. The reaction velocities obtained by HATU mediated peptide bond formations are remarkably high. On the other hand the linear precursor needs to be flexible enough to allow the formation of an intermediate conformer with both ends in close proximity. Therefore, we investigated the cyclization properties of compound **39**, that can be closed by peptide coupling (see Figure 3.1).

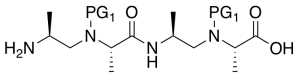

39

Figure 3.1: Proposed flexible tetramer cyclization.

Compound **39** contains only one rigid peptide bond in contrast to the three present in tetraalanine **35**. Protecting groups are required for the non-terminal amine groups to avoid the formation of smaller sized cycles during the final peptide coupling step. Scheme 14 shows a retrosynthetic analysis for the 4(*S*)M4-cyclen synthesis based on a flexible alanine-based tetramer.

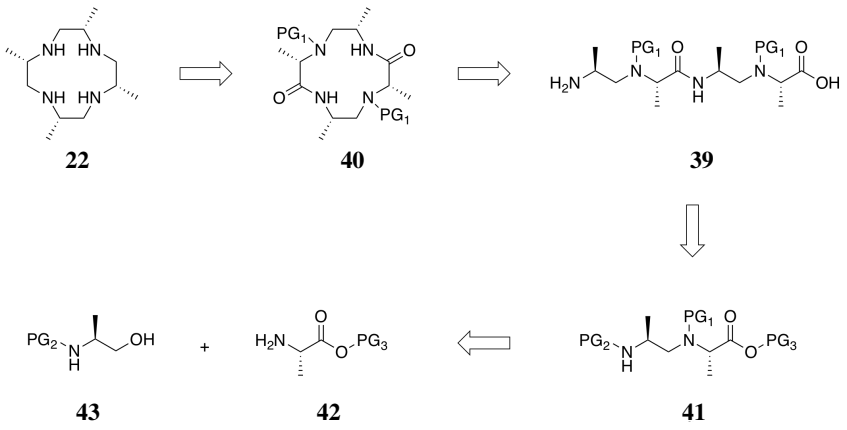

Scheme 14: Retrosynthetic analysis for the synthesis of 4(*S*)M4-cyclen using a flexible tetramer **39**.

We envisioned that the desired target compound **22** can be obtained by reduction and deprotection of the bislactam **40**. The bislactam **40** could be synthesised by an intramolecular peptide bond formation under diluted conditions. The synthesis of the required alanine-based tetramer **39** could be accomplished in a convergent fashion starting from the alanine-based dimer **44** which itself could by prepared from commercially available alanine derivatives **43** and **42**.

3.4.2 *Synthesis of alanine-based tetramers*

We planned to synthesise the dimer **45** by nucleophilic substitution of an activated *N*-terminal protected alaninol derivative (see Scheme 15). Although the installation of a tosyl and mesyl leaving group on *N*-Boc-protected alaninol **46** was possible, the subsequent nucleophilic substitution with *tert*-butyl-protected alanine **25** resulted in very low yields and mostly decomposed starting materials. It turned out that nucleophilic substitutions with protected alanine derivatives require high temperature and long reaction times. This conditions decomposed the reactive tosyl **47** and mesyl **48** *N*-Boc-protected alaninol. The synthesis of the more reactive triflate **49** was not possible.

Considering these findings, we proposed a new strategy to synthesise a suitable alanine-based dimer by nucleophilic ring opening of nosyl-protected methyl aziridine. Although initially we wanted to avoid the usage of highly toxic aziridines this strategy produced the required alanine-based dimer (**52**) in medium yield. A benzyl moiety was chosen as protecting group for the secondary amine (**52**) as it does not severely restrict the flexibility. This protection step was required to prevent side reactions from occurring during further chain elongation steps. The proposed fully protected alanine-based dimer (**53**) was synthesised in three steps in an overall yield of 30 %. The overall yield was low, however, all the required steps were scalable and in-

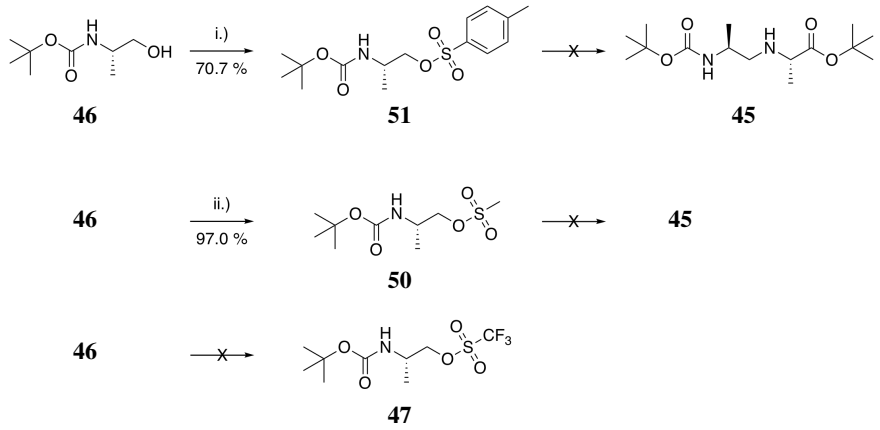

Scheme 15: Synthesis of compound **45**. Reaction conditions: i.) Ts-Cl, DCM, 20-25 °C, 18 h; ii.) Mes-Cl, DCM, 0-5 °C, 3 h.

volved relative inexpensive starting materials.

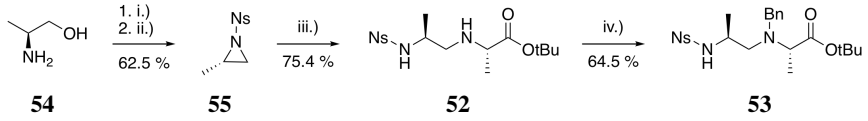

Scheme 16: Synthesis of compound **53**. Reaction conditions: i.) NsCl, MeCN, 0-5 °C, 2 h; ii.) DIPEA, 20-25 °C, 30 min; iii.) *tert*-butyl alanine **25**, THF, 60 °C, 18 h; iv.) BnBr, K_2CO_3, MeCN, 50 °C, 18 h.

For further chain elongation two independent deprotection steps were developed (see Scheme 17). Under aqueous acidic conditions the *tert*-butyl ester was hydrolysed in excellent yield. The deprotection of the nosyl protecting group was carried out using either thiophenol or dodecanethiol. Dodecanthiol was preferred as it is far less malodorous and toxic which was essential especially considering further large scale experiments. Deprotection was completed overnight, however, work-up was difficult, because the dodecanethiol adduct and the free amine **56** could only be separated by an acid-base extraction. Different acids (formic acids, hydrochloric acid) as well as different acid concentrations were tested. Nevertheless, the yields remained moderate and best results were obtained by performing a quick extraction with 1 M hydrochloric acid. We were surprised to find that further peptide coupling of the free amine **56** and the free acid **57** did not yield the expected alanine-based tetramer **58**. We found that upon reaction of HATU with the free acid **57** an intramolecular reaction forming the six membered ring **59** took place. This finding was unexpected and in combination with the generally rather moderate yields obtained for the synthesis of the precursors we were forced to search for an alternative way.

We realized that nucleophilic substitution of an activated alaninol derivative with alanine derivatives generally resulted in low yields. Therefore, we

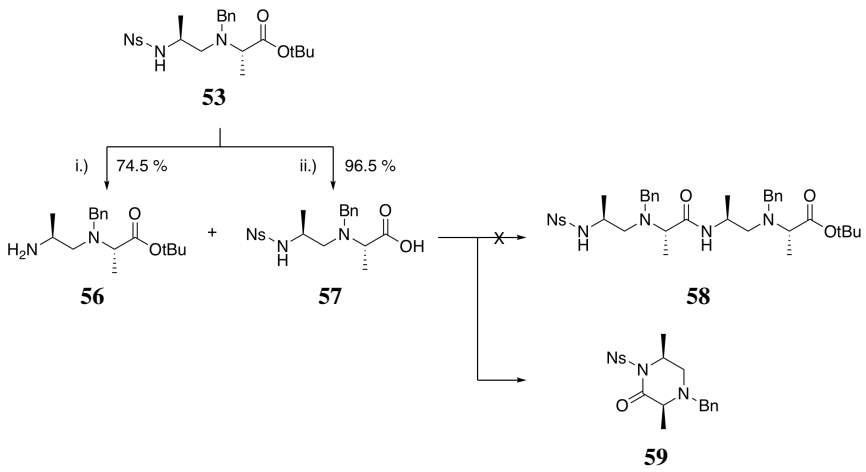

Scheme 17: Attempted synthesis of compound **58**. Reaction conditions: i.) Dodecanthiol, K_2CO_3, MeCN, 50 °C, 18 h; ii.) aq. 4 M HCl, MeCN, 50 °C, 6 h.

envisioned to synthesise the alanine-based dimer by reductive amination of *N*-Cbz-protected alanine aldehyde **60** with *tert*-butyl-protected alanine **25**. Reductive aminations are known to be very fast and high yielding. Although there are various methods available to selectively reduce a carboxylic ester to an aldehyde we thought it would be easier to selectively oxidise the corresponding amino alcohol (see Scheme 18).

Starting from commercially available *L*-alaninol (**54**), Cbz protection was carried out in high yields using a biphasic system. Purification of the product was done by crystallization. Several oxidation conditions, including DMP, Swern-oxidation and IBX were tested. It was found that best results were obtained using IBX as oxidizing agent. Initial reactions were carried out in DMSO at 20-25 °C, however, final separation of the aldehyde **60** from DMSO and the IBX by-products was difficult. Inspired by the results obtained by More and Finney,[114] ethyl acetate as solvent was used at reflux. The yield was low and decomposition occurred due to the long reaction time needed for full conversion. We found that the addition of 2 eq. of DMSO per equivalent IBX dramatically increased the reaction rate. This might be due to the increased solubility of IBX in DMSO compared to ethyl acetate. Reductive amination of aldehyde **60** with *tert*-butyl alanine **25** was carried out in dichloromethane. The much milder reducing agent, sodium triacetoxyborohydride, was superior to sodium borohydride. Using sodium borohydride partially deprotected the *tert*-butyl ester. Benzyl protection of **62** was achieved using benzylbromide in acetonitrile with potassium carbonate in good yields. The desired alanine-based dimer **63** was synthesised in four steps with an excellent overall yield of 72 %. *tert*-Butyl deprotection was carried out in hydrochloric acid and yielded the free acid **64** in quantitative yield. Hydrochloric acid deprotection was preferred over trifluoroacetic acid due to the undesired formation of a trifluoroacetate salt which caused lower yields on the subsequent peptide coupling reaction. Cbz deprotection was difficult. Experiments performed with Pd/C and

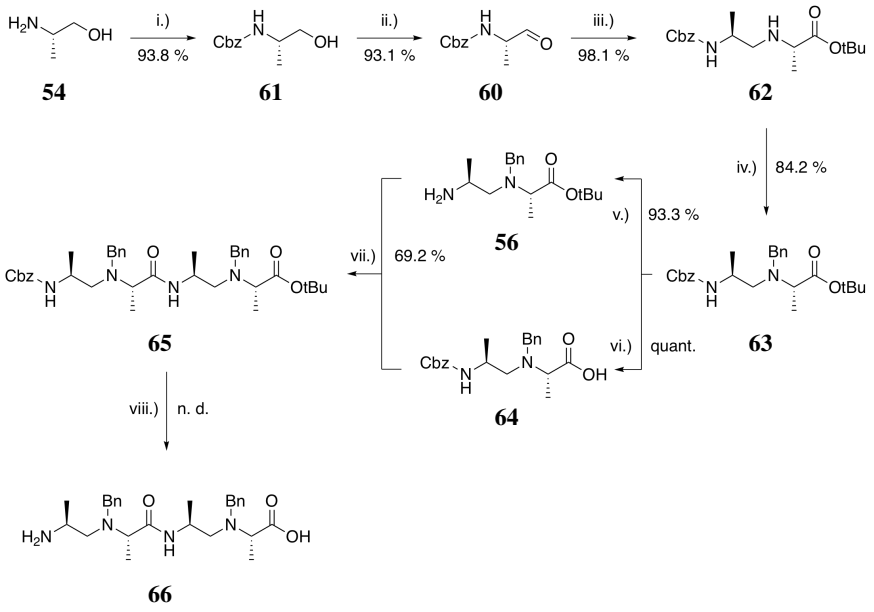

Scheme 18: Synthesis of compound **66**. Reaction conditions: i.) Cbz-Cl, Na_2CO_3, H_2O / EtOAc, 20-25 °C, 1 h; ii.) IBX, DMSO, EtOAc, reflux, 3.5 h; iii.) *tert*-butyl alanine **25**, $NaBH(OAc)_3$, DCM, 16 h; iv.) BnBr, K_2CO_3, MeCN, 50 °C, 16 h; v.) $Pd/BaSO_2$, H_2, 1 bar, MeOH, 20-25 °C, 2 h; vi.) conc. HCl in 1,4-dioxane, 40 °C, 18 h; vii.) HATU, DIPEA, MeCN, 20-25 °C, 40 min; viii.) HBr in acetic acid, 40 °C, 30 min.

H_2 in methanol revealed that the Cbz protecting group as well as the benzyl protecting group got cleaved off. Screening of different solvents (methanol, ethanol, isopropanol, ethyl acetate and tetrahydrofuran) resulted in longer reaction times but no improvements in selectivity. Therefore, different deactivated catalysts were tested. Lindlar's catalyst showed no reactivity. We were pleased to see that Rosenmund's catalyst did deprotect the Cbz protecting group within 2 h in methanol while keeping the benzyl group mostly unaffected. Subsequent peptide bond formation between the free acid **64** and the free amine **56** afforded the linear fully protected alanine-based tetramer **65** in 69 % yield. In order to form the bislactam **67** both terminal protecting groups need to be cleaved off. Due to the low acidic stability of the *tert*-butyl group as well as the low stability of the Cbz protecting group towards strong acids both protecting groups were simultaneously removed using hydrogen bromide solution in acetic acid. Although these procedure was highly convenient and avoided a second hydrogenation, special care had to be taken in order to remove acetic acid from the final product **66**. Acetic acid was removed by a repeated sequence of dissolving the product in a mixture of acetonitrile and hydrochloric acid and evaporation to dryness. In addition extensive drying for several days under vacuum at 40 °C was required.

3.4.3 *Synthesis of alanine-based twelve-membered macrocycles*

Formation of the bislactam was performed under moderate dilution (1 g L^{-1}) in acetonitrile and DIPEA using HATU as coupling reagent (see Scheme 19). We were very surprised to find that this reaction is extremely fast and completion was achieved within five minutes. We found no evidence for the formation of a 32-membered macrocycle or other polymers. The only by-product detected was the *N*-acetylated alanine-based tetramer arising from an insufficient acetic acid removal. Starting from the fully protected alanine-based tetramer **65**, the deprotection and cyclization was done in an astonishing yield of 81 %. The final two steps, deprotection and reduction, could be performed in any order. However, we observed that reduction prior to deprotection is favourable. Isolation of dibenzyl-protected cyclen **68** after the reduction was more efficient and required less solvent. We found that 4(*S*)M4-cyclen **22** adsorbs exceptionally strong to the lithium and aluminium salts arising from the quenching of the reduction forming sparingly soluble aluminium cyclen salts. Quantitative extraction of 4(*S*)M4-cyclen **22** from these salts required extensive washing and was not always succesfull. Applying standard reduction conditions (lithium aluminium hydride in tetrahydrofuran) to reduce the bislactam resulted in low yields and partial debenzylation was observed. Using a trimethylsilyl mediated reduction with lithium aluminium hydride in dichloromethane at 20-25 °C afforded the dibenzyl protected 4(*S*)M4-cyclen **22** in high yields. This compound itself is a highly useful intermediated for further lanthanide chelating tag synthesis because selective trans protection is difficult to achieve starting from 4(*S*)M4-cyclen **22**. Final deprotection of the benzyl groups was achieved using the procedure described by Ranganathan *et al.*[106] for the tetrabenzylated 4(*S*)M4-cyclen or by catalytic hydrogenation under high pressure. Although this reaction sequence was preferred due to the above mentioned issues with the isolation of 4(*S*)M4-cyclen **22** from the reduction and the formation of the valuable trans benzyl-protected 4(*S*)M4-cyclen **68**, performing the debenzylation first followed by the reduction was possible and sometimes even higher overall yields were achieved. However, the reduction of bislactam **67** to 4(*S*)M4-cyclen **22** was poorly reproducible. Although the conversion was always comparable the isolated yield varied between 25-90 %. This poor reproducibility was not encounter in the reduction - debenzlyation sequence and, therefore, this sequence was considered for up scaling. Overall the target compound **22** could be synthesised in 27 % overall yield. We also grew crystals of 4(*S*)M4-cyclen **22** suitable for X-ray analysis (see Figure 3.2).

3.4.4 *Development of a large scale synthesis for alanine-based tetramers*

Up scaling of the first four steps (see Scheme 18) resulting in the fully protected dimer **63** was possible on multigram scales. The acidic deprotection forming the free acid **70** could also be achieved in high yields on large scales.

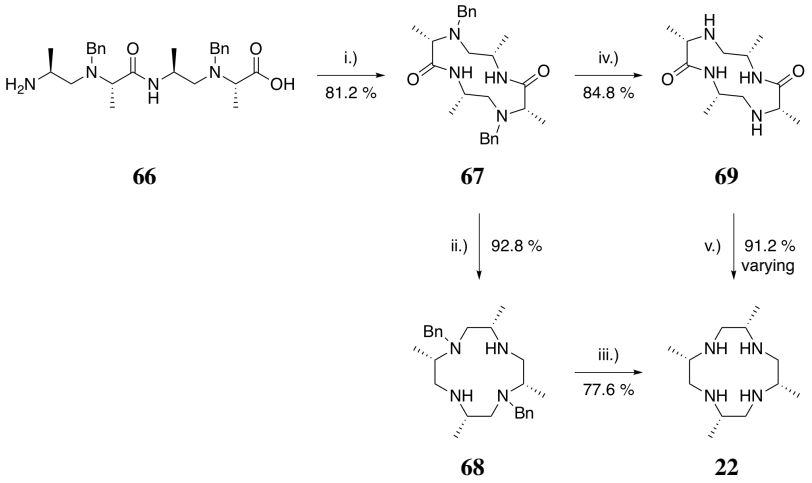

Scheme 19: Synthesis of compound **22**. Reaction conditions: i.) HATU, DIPEA, MeCN, 20-25 °C, 20 min; ii.) TMS-Cl, $LiAlH_4$, DCM, 0-5 °C to 20-25 °C, 3 h; iii.) ammonium formate, $Pd(OH)_2$/C, EtOH, reflux, 16 h; iv.) Pd/C, H_2, 45 bar, acetic acid, 20-25 °C, 16 h; v.) TMS-Cl, $LiAlH_4$, DCM, 0-5 °C to 20-25 °C, 3 h.

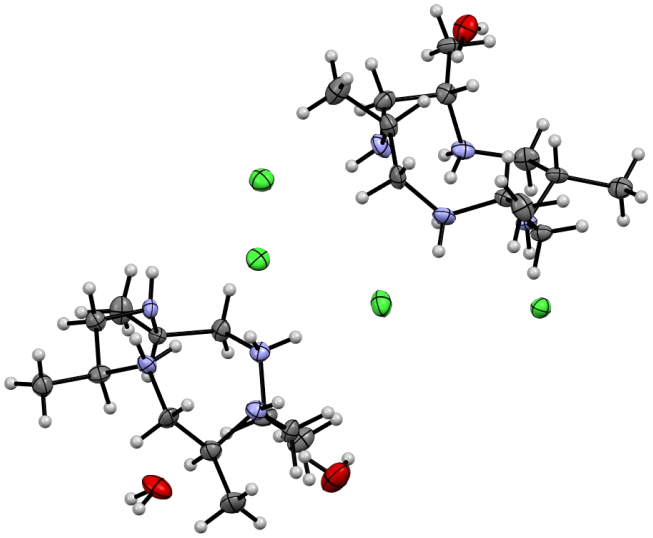

Figure 3.2: X-Ray structure of compound **22**$*2H_2O*2$HCl, the ellipsoids represent the 50 % probability level. The bond lengths and angles are within normal ranges.

However, the deprotection of the Cbz protecting group using Rosenmund's catalyst was not scalable. Several small scale reactions showed a poor reproducibility. We observed that only slight deviations from the optimal reaction time lead to a large over deprotection. Several different solvents and temperatures were screened and the reaction progress monitored by ESI-MS and NMR. It was not possible using an identical setup to obtain an identical reaction time. This might be attributed to the inhomogeneous inactive catalyst used. It was observed that the time required for the catalyst to turn active (brown to black color change) was always slightly different varying a few minutes. Addition of the substrate after catalyst activation was tried but no reproducibility was observed. After extensive screening we found no conditions for a selective hydrogenation on large scale. Therefore, an alternative synthetic route towards the alanine-based tetramer **66** was needed. Nevertheless, the achieved high yields, during cyclization of the alanine-based tetramer **66** was remarkable an proved our initial strategy to be correct.

3.4.5 *Alternative synthesis for alanine-based tetramers*

Retrosynthetic analysis and considerations

Trying to avoid the Cbz deprotection step in the previous synthesis (see Scheme 18). We envisioned the synthesis of the alanine-based tetramer **66** could be accomplished by two selective reductive aminations and a final benzyl protection step (see Scheme 20). This alternative approach lacks the convergent nature of the previous one. The synthesis of *N*-Cbz-alaninal (**60**) as well as all reductive amination steps could be carried out accordingly. This approach is based on the synthesis of the middle part **71** followed by the extension on the *C*-terminus and the *N*-terminus. The introduction of the benzyl group could be done on the late alanine-based tetramer stage. The middle block of the alanine-based tetramer could be obtained by coupling *N*-Cbz-alanine (**72**) with *L*-alaninol (**54**) followed by an oxidation of the alcohol **73**. A second alternative would be the introduction of the protected aldehyde **74** followed by a selective deprotection.

Synthesis of alanine-based tetramer

Cbz-protected alaninal **60** was treated with trimethyl orthoformate forming the dimethyl acetal **77** in high yield (see Scheme 21). The Cbz deprotection was carried out using Pd/C and H_2 in methanol with moderate yield. The volatile nature of the free amine **74** caused the loss of product during work-up. The final peptide coupling was successfully performed using T3P. The liberation of the aldehyde **71** by acidic hydrolysis of the dimethyl acetal **78** was not possible. The acteal **78** was highly stable under most acidic conditions and only got cleaved in pure trifluoroacetic acid forming the enol **79**.

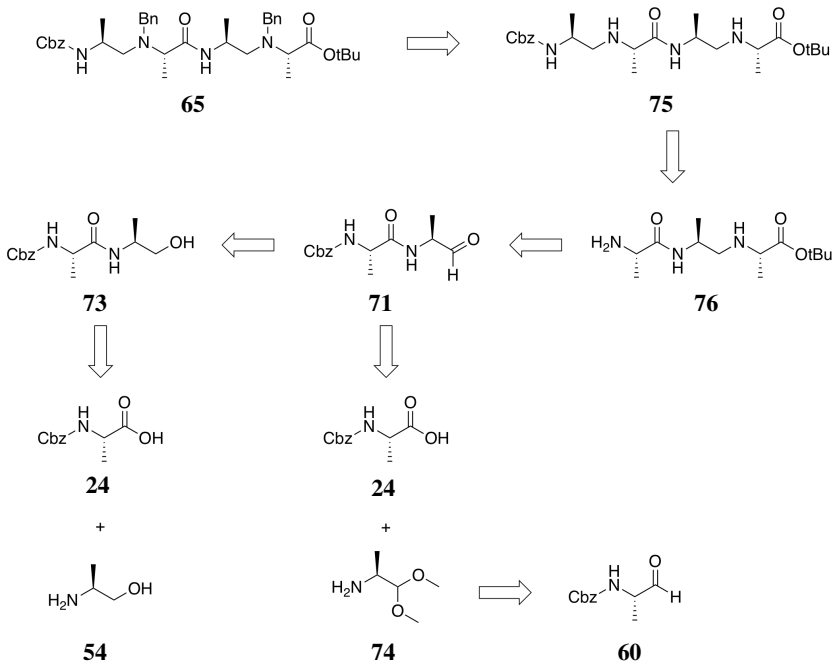

Scheme 20: Retrosynthetic analysis for the alternative synthesis of the flexible tetramer **66**.

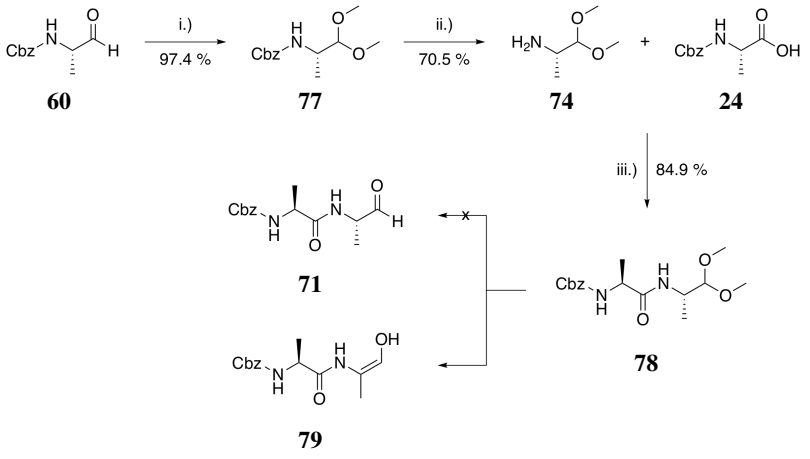

Scheme 21: Attempted synthesis of **71**. Reaction conditions: i.) trimethyl orthoformate, MeOH, 20-25 °C, 18 h; ii.) Pd/C, H_2, 1 bar, MeOH, 20-25 °C, 6 h; iii.) T3P, DIPEA, EtOAc, 20-25 °C, 18 h.

Unable to deprotect the dimethyl acetal **78** under milder conditions, the required aldehyde **71** was synthesised by oxidation of the corresponding amino alcohol **73** (see Scheme 22). Direct coupling of *N*-Cbz-alanine (**72**) with *L*-alaninol (**54**) was possible using HATU and DIPEA in acetonitrile. However, purification was very difficult and resulted in low yields. Using T3P did not result in the formation of amino alcohol **73**. A very convenient way, using sodium borohydride in tetrahydrofuran, methanol and water, to reduce dialanine methylester **80** to the coresponding alcohol **73** was described by Heidelberg and Martin.[115] Dialanine methylester **80** was synthesised by a HATU mediated peptide coupling in excellent yields but the cumbersome purification on large scale rendered this reagent unattractive. On the other hand using T3P resulted in lower yields but isolation of the pure product was achieved without flash column chromatography using solely aqueous extractions to remove any by-products. The dipetide **80** was reduced using the procedure described by Heidelberg and Martin[115] in 84 %. Further oxidation was achieved in 92 % using an adapted procedure of the *N*-Cbz-alaninal (**60**) oxidation. Due to the low solubility of the starting material in ethyl acetate, acetonitrile was used instead. In acetonitrile the reaction could be performed without the addition of DMSO. The procedure developed for the reductive amination was applied for the formation of the Cbz-protected alanine-based trimer **81**. Further deprotection resulted in the alanine-based trimer **76** and reductive amination yielded the protected alanine-based tetramer **82** in good yields. Final benzyl protection was achieved using the same conditions already developed for the fully protected alanine-based dimer **63**. Using this second approach yielded the fully protected alanine-based tetramer in 36 % overall yield which was slightly lower than the yield obtained for the first approach (40 %). Nevertheless, no catalytic hydrogenation was needed.

Development of a large scale synthesis for alanine-based tetramers

The T3P mediated peptide coupling and the sodium borohydride reduction were easily scaled up to multigram scales. The IBX oxidation performed comparable to the large scale synthesis of *N*-Cbz-alaninal (**60**) and so did the subsequent reductive amination. The Cbz deprotection, however, was incomplete even after several hours under a hydrogen atmosphere. Additional Pd/C as well as applying high hydrogen pressure did not significantly increase the conversion. Presumably small contaminations carried through from the IBX oxidation deactivated the catalyst after a short period of time. This impurity were most likely less pronounced in the small scale. In order to use this procedure on larger scales the intermediate aldehyde **84** should be purified by flash column chromatography prior to reductive amination. This procedure was not suitable for large scale synthesis. Nevertheless, it allows interesting opportunities for the synthesis of selectively labelled ^{13}C marked compounds. The formation of an alanine-based trimer followed by the last reductive amination allows the introduction of a labelled compound at the latest state possible. Purifying the alanine-based trimer **81** would ensure that losses of expensive labelled material can be minimized. This strategy was

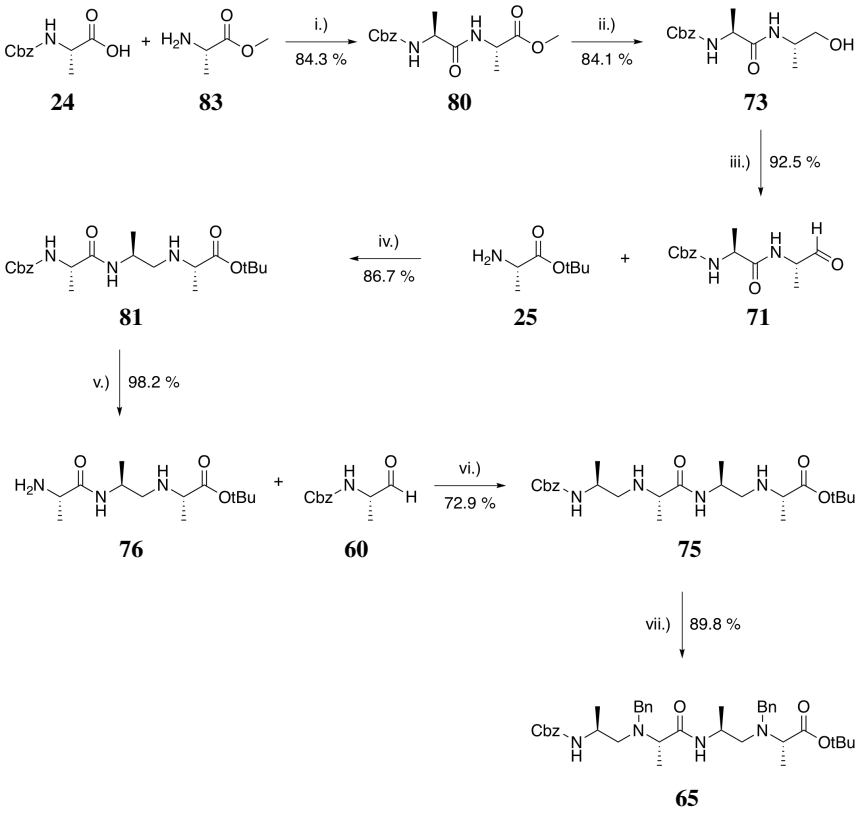

Scheme 22: Synthesis of compound **65**. Reaction conditions: i.) T3P, DIPEA, EtOAc, 20-25 °C, 18 h; ii.) $NaBH_4$, H_2O, MeOH, THF, 20-25 °C, 18 h; iii.) IBX, MeCN, 80 °C, 4 h; iv.) $NaBH(OAc)_3$, DCM, 20-25 °C, 4 h; v.) Pd/C, H_2, 1 bar, MeOH, 20-25 °C, 6 h; vi.) $NaBH(OAc)_3$, DCM, 20-25 °C, 16 h; vii.) BnBr, K_2CO_3, MeCN, 40 °C, 18 h.

successfully applied by Raphael Vogel during his master thesis within our group to synthesise 4(*S*)M4-cyclen with one methyl group selectively ^{13}C labelled.[116]

3.4.6 *Alternative protecting groups*

Retrosynthetic analysis and considerations

Inspired by the findings presented by Kanai *et al.*[117] we envisioned that replacing the benzyl group with a fluoro benzyl group would increase the stability and therefore a selective hydrogenation would be possible. The rest of the synthesis could then be performed accordingly to the procedures already developed for the benzyl derivatives.

Synthesis of alanine-based tetramers

Starting from the alanine-based dimer **62** which was obtained as described previously the introduction of the fluorobenzyl group was achieved in comparable yields using fluorobenzyl bromide instead of benzyl bromide (see Scheme 23). The *tert*-butyl deprotection of **85** was performed as for its benzyl analogue. The Cbz deprotection was surprisingly still time sensitive. Deprotection reactions using Rosenmund's catalyst were also badly reproducible. In search for a better reproducible method transferhydrogenation with ammonium formate, cyclohexene and 1,4-cyclohexadiene were tested. This method allowed for a more specific control over the amount of reducing agent. Various reaction screenings were performed and best conditions were found using Pd/C and ammonium formate in ethanol at 50 °C. Cyclohexene and 1,4-cyclohexadiene did not react. We found that heating the reaction for 15 min before the addition of substrate ensures the activation of the catalyst and thus creating a more reproducible setting. It was key to slow down the reaction to such a rate that careful monitoring by HPLC was possible. This required the overreaction to be slow enough such that 10 min prolonged reaction time does not deprotect a significant amount of the desired product. To minimize the risk of product loss due to overreaction the deprotection was carried out in small batches of 7.5 g maximum. The peptide coupling forming the alanine-based tetramer **86** was performed in moderate yield. The free acid **87** and the free amine **88** could not be purified by flash column chromatography or crystallization and were used without further purification. This and small amounts of overdeprotection caused the yield to drop to 55 % after flash column chromatography of the alanine-based fully protected tetramer **86**. Final deprotection was carried out analogously to the deprotection of the fully benzyl protected tetramer **89**. Although the Cbz deprotection of the alanine-based dimer **85** remained critical it was possible to synthesise large quantities of the alanine-based tetramer **90**.

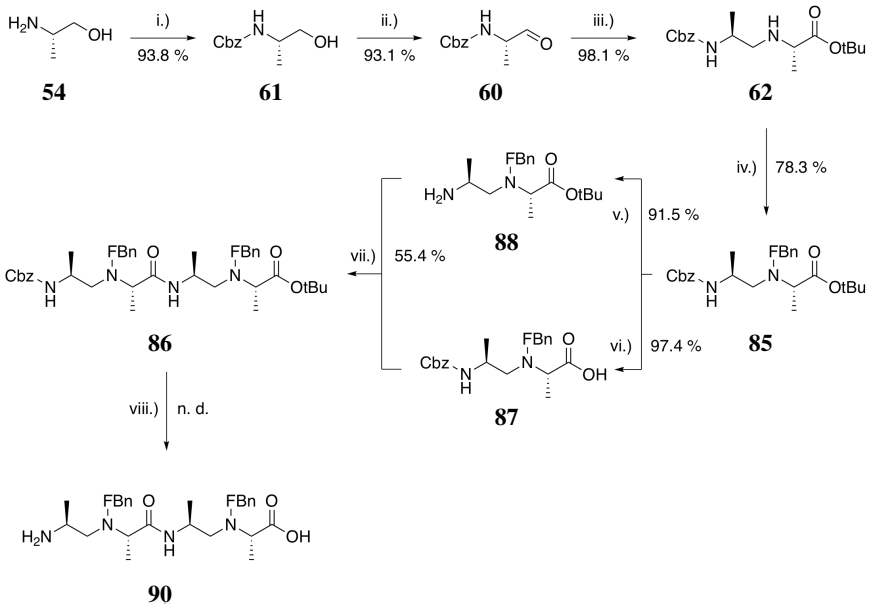

Scheme 23: Synthesis of compound **90**. Reaction conditions: i.) Cbz-Cl, Na_2CO_3, H_2O / EtOAc, 20-25 °C, 1 h; ii.) IBX, DMSO, EtOAc, reflux, 3.5 h; iii.) *tert*-butyl alanine **25**, $NaBH(OAc)_3$, DCM, 16 h; iv.) FBnBr, K_2CO_3, MeCN, 45 °C, 16 h; v.) Pd/C, ammonium formate, EtOH, 50 °C, 1 h; vi.) conc. HCl in 1,4-dioxane, 20-25 °C, 2 h; vii.) HATU, DIPEA, 20-25 °C, 16 h; viii.) HBr in acetic acid, 40 °C, 30 min.

Synthesis of alanine-based twelve-membered macrocycles

For the cyclization the same conditions were applied as for the benzyl analogue (see Scheme 24). We found that above a two litre scale reaction, meaning two gram of the alanine-based tetramer in two litre of acetonitrile the cyclization efficiency dropped significantly. This finding is most like attributed to the lower stirring efficiency in larger flasks. It turned out to be highly critical that the alanine-based tetramer **90** was completely dissolved and homogeneously distributed before the addition of the coupling reagent. We also found that slow addition of the coupling reagent is not favourable. Best results were obtained by dissolving the alanine-based tetramer **90** in acetonitirile and DIPEA followed by the addition of HATU in one portion. The same procedure as for the reduction and the debenzylation of the dibenzylated bislactam **67** was applied. Surprisingly we found that the difluorobenzyl-protected 4(*S*)M4-cyclen **91** could not be deprotected by transferhydrogenation. Even under high pressure using Pd/C and H_2 in acetic acid at elevated temperatures the protecting group could not be removed. However, it was possible to remove the fluorobenzyl protecting groups from the difluorobenzylated bislactam **92**. This lead to the same inconveniences as described above for the isolation of 4(*S*)M4-cyclen **22** after the reduction. The unavailability of a *trans* protected 4(*S*)M4-cyclen derivative could be tolerated as it was not the primary goal of this study. Nevertheless, we found that the benzyl protecting group could be reinstalled after the deprotection allowing the usage of

the already developed reduction - deprotection sequence. The slightly lower yields during peptide coupling and the fluorobenzyl protecting reaction as well as the additional two steps dropped the overall yield to 11 %.

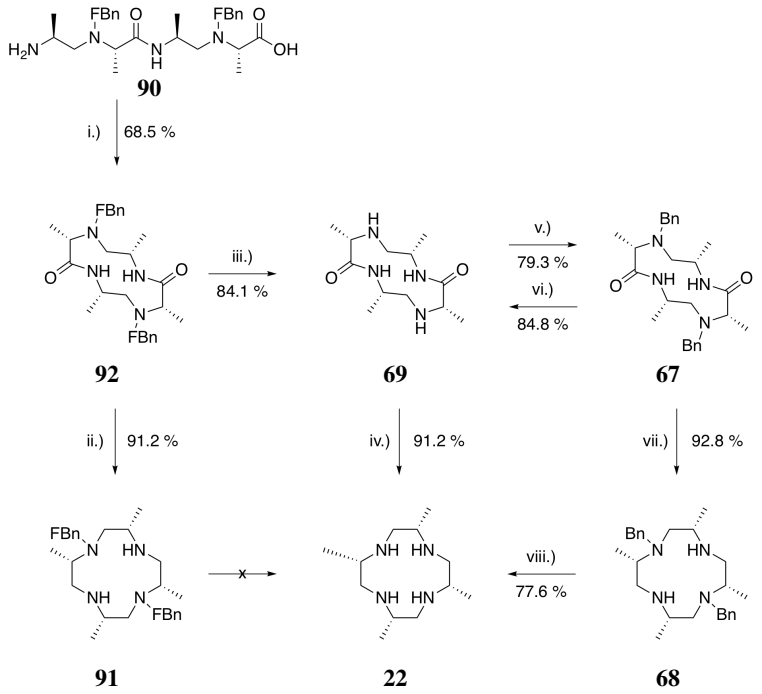

Scheme 24: Synthesis of compound **22**. Reaction conditions: i.) HATU, DIPEA, MeCN, 20-25 °C, 20 min; ii.) TMS-Cl, $LiAlH_4$, DCM, 0-5 °C to 20-25 °C, 3 h; iii.) Pd/C, H_2, 45 bar, acetic acid, 20-25 °C, 16 h; iv.) TMS-Cl, $LiAlH_4$, DCM, 0-5 °C to 20-25 °C, 3 h; v.) BnBr, K_2CO_3, MeCN, 55 °C, 16 h; vi.) Pd/C, H_2, 45 bar, acetic acid, 20-25 °C, 16 h; vii.) TMS-Cl, $LiAlH_4$, DCM, 0-5 °C to 20-25 °C, 3 h; viii.) ammonium formate, $Pd(OH)_2$/C, EtOH, reflux, 16 h.

Synthesis of mixed alanine-based twelve-membered macrocycles

Unfortunately the synthesis of the alanine-based tetramer **65** was not possible on large scale due to the problems encountered in deprotecting the Cbz protecting group. However, large quantities of the alanine-based dimer **63** were already prepared. Using the free amine **88** from the fluorobenzyl route and the free acid **64** from the benzyl route the mixed fully protected alanine-based tetramer **93** was synthesised (see Scheme 25). Following the same procedures as for the other alanine-based tetramers **66** and **90** the mixed protected bislactam **94** was synthesised. We found that the benzyl protecting group can be selectively removed in the presence of the fluorobenzyl protecting group using milder hydrogenation conditions. Replacing acetic acid with methanol and using a hydrogen pressure of one bar the benzyl protecting group was selectively removed. This could potentially be used for further selective modifications. However, during this study there was no need for such an additional functionalization. Therefore, complete deprotection was performed in acetic

acid with Pd/C under high hydrogen pressure. After the deprotection of both protecting groups the bislactam **69** was obtained which was further used as described previously.

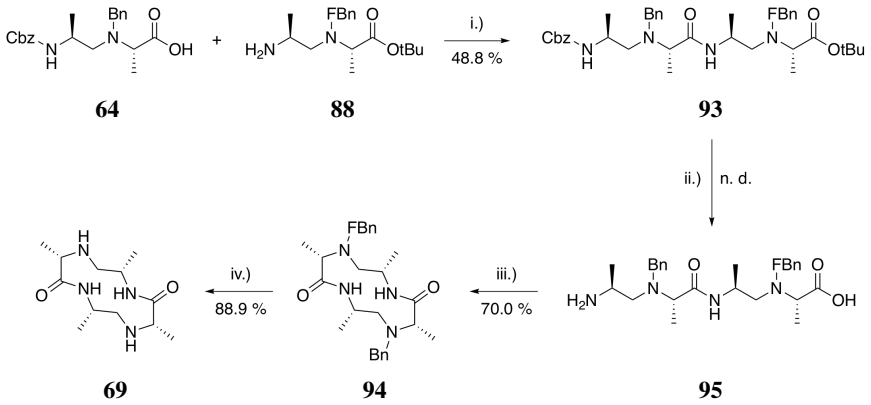

Scheme 25: Synthesis of compound **69**. Reaction conditions: i.) HATU, DIPEA, MeCN, 20-25 °C, 16 h; ii.) HBr in acetic acid, 40 °C, 30 min, 30 min; iii.) HATU, DIPEA, MeCN, 20-25 °C, 20 min; Pd/C, H_2, 45 bar, acetic acid, 20-25 °C, 16 h.

4

SYNTHESIS OF NEW SUBSTITUTED CYCLEN DERIVATIVES

Work described in this chapter has been partially performed in collaboration with Fabienne Thommen during her master thesis within our group and is also described in her master thesis.[118] We investigated the scope and applicability of the synthetic strategies developed for 4(*S*)M4-cyclen **22** in order to synthesize a more rigid cyclen derivative. The larger substituents could have an influence not only on the Δ / Λ ratio but also on the observed tensor parameters. The coordination geometry becomes more asymmetric and thus could improve the observed PCSs.

4.1 SYNTHESIS OF 4(*S*)M2P2-CYCLEN

4.1.1 *Retrosynthetic analysis and considerations*

Using the same procedure as described for the synthesis of 4(*S*)M4-cyclen **22** we envisioned that 4(*S*)M2P2-cyclen **96** could be made out of the bislactam **97** (see Scheme 26). The bislactam **97** could be synthesised from the linear alanine / valine-based tetramer **98**. Reductive amination of *N*-Cbz-alaninal **60** and *tert*-butyl valine **99** followed by a benzyl protection step would yield the alanine / valine-based dimer **100**. We encountered no problems during *tert*-butyl deprotection steps in the 4(*S*)M4-cyclen synthesis. Similar conditions could be applicable for the alanine / valine-based dimer **100**. We proposed that Cbz deprotection of the alanine / valine-based dimer **100** results in a higher selectivity due to the higher steric hindrance caused by the isopropyl group. This would avoid the introduction of the more stable fluorobenzyl protecting group. In principle it would also be possible to synthesise the amino aldehyde of Cbz-valinol and performing a reductive amination with *tert*-butyl alanine **25**. However this would result in a dimer having the Cbz protecting group close to the isopropyl group and the labile benzyl group would be next to the alanine methyl group. We thought this configuration is potentially even more problematic as the Cbz group is sterically more shielded and thus less reactive.

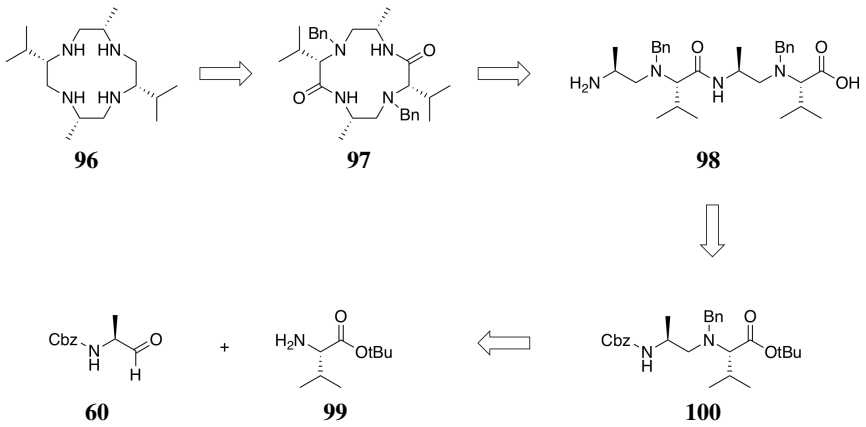

Scheme 26: Retrosynthetic analysis for the synthesis of 4(*S*)M2P2-cyclen **96**.

4.1.2 *Synthesis of alanine / valine -based tetramers*

Starting from *N*-Cbz-alaninal **60** a reductive amination with *tert*-butyl valine was performed in good yield (see Scheme 27). Subsequent benzyl protection was slower and longer reaction times were needed to achieve a comparable conversion. We attributed this to the larger steric hindrance induced by the isopropyl substituent. We found that the selective *tert*-butyl deprotection could be carried out analogously with comparable yield. We were delighted to find that the Cbz deprotection could be carried out using Pd/$BaSO_4$ and H_2 at 20-25 °C. The benzyl protecting group was much more stable towards catalytic hydrogenolysis and was mostly unaffected. Presumably the size difference between methyl and isopropyl caused the higher selectivity. The coupling of the free amine **101** and the free acid **102** was achieved using HATU and DIPEA in acetonitrile. The final deprotection step was carried out using hydrogen bromide solution in acetic acid. Although the findings obtained for the Cbz deprotection of the alanine / valine based dimer **100** suggested that it would be possible to do this final deprotection in two steps the one step procedure was preferred.

4.1.3 *Synthesis of alanine / valine -based twelve-membered macrocycles*

We were pleased to find that although the steric crowding of the alanine / valine-based tetramer **105** is increased a cyclization took place (see Scheme 28). The HATU mediated cyclization of the alanine / valine-based tetramer **105** formed the bislactam **97** in good yields of up to 59 % starting from the fully protected alanine / valine-based tetramer **106**. The yields were lower than those obtained for the methyl analogue. The reduction of the protected bislactam **97** to the *trans* dibenzylated 4(*S*)M2P2-cyclen **107** showed no significant influence of the two isopropyl groups. The final transferhydrogenation afforded 4(*S*)M2P2-cyclen **96** in excellent yields. The target compound

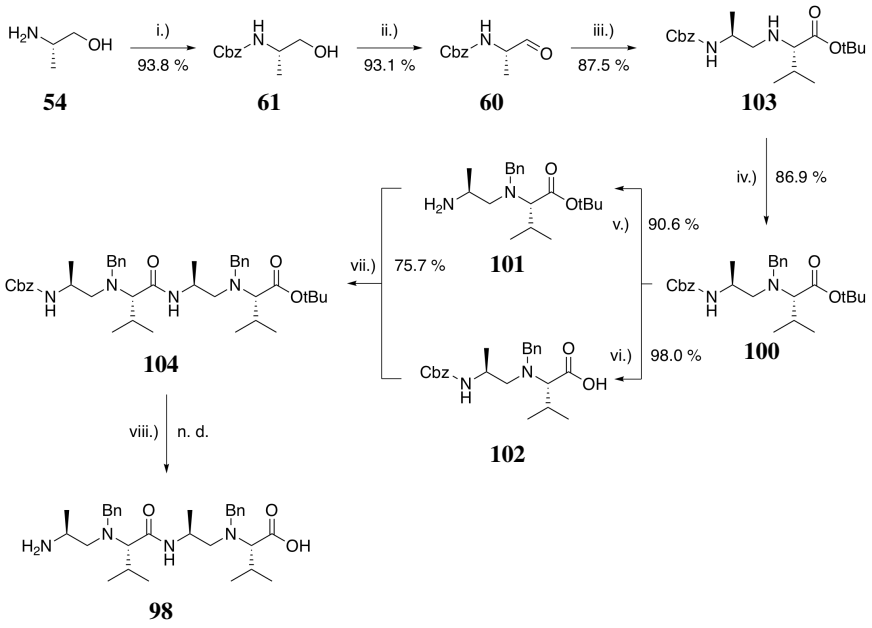

Scheme 27: Synthesis of compound **98**. Reaction conditions: i.) Cbz-Cl, Na_2CO_3, H_2O / EtOAc, 20-25 °C, 1 h; ii.) IBX, DMSO, EtOAc, reflux, 3.5 h; iii.) *tert*-butyl alanine **25**, $NaBH(OAc)_3$, DCM, 16 h; iv.) BnBr, K_2CO_3, MeCN, 65 °C, 2 d; v.) $Pd/BaSO_4$, H_2, 1 bar, MeOH, 20-25 °C, 2 h; vi.) conc. HCl in 1,4-dioxane, 40 °C, 16 h; vii.) HATU, DIPEA, MeCN, 20-25 °C, 20 min; viii.) HBr in acetic acid, 40 °C, 30 min.

could be synthesised in an overall yield of 23 %. This is slightly less than the yield we observed for the initial synthesis of 4(*S*)M4-cyclen **22** on small scales, however, still larger than the overall yield obtained for the fluorobenzyl based route. The lower yield predominantly originated from the lower yields achieved during the cyclization. We also grew crystals of 4(*S*)M2P2-cyclen **96** suitable for X-ray analysis (see Figure 3.2).

4.2 SYNTHESIS OF 3(*S*)1(*R*)M301-CYCLEN

Driven by the success in synthesising 4(*S*)M2P2-cyclen **96** and 4(*S*)M4-cyclen **22** we extended the scope of the methodology to an amino acid containing a functional group on the side chain. Introducing a functional group to one of the substituents would offer interesting possibilities for further functionalization. It would allow the installation of a cysteine-reactive linker moiety on the cyclen core which could offer a different tagging geometry. There is so far no cyclen based lanthanide chelating tag known in literature with a linker installed on the base cyclen ring.

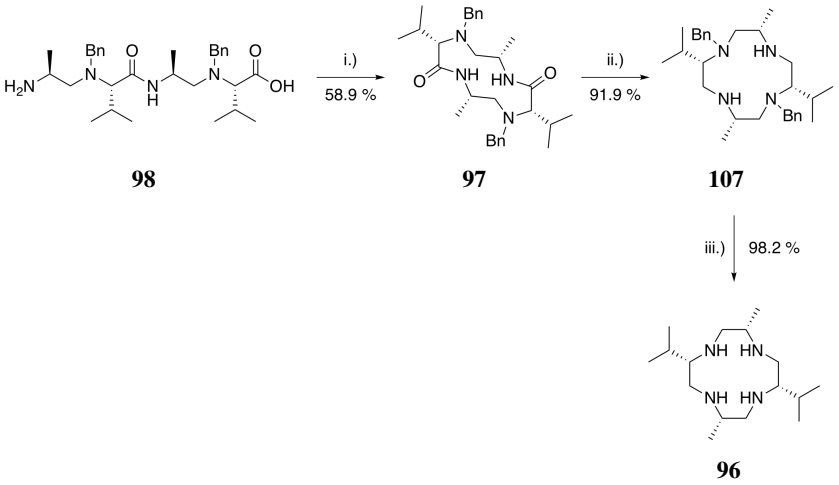

98 **97** **107** **96**

Scheme 28: Synthesis of compound **96**. Reaction conditions: i.) HATU, DIPEA, MeCN, 20-25 °C, 20 min; ii.) TMS-Cl, $LiAlH_4$, DCM, 0-5 °C to 20-25 °C, 3 h; iii.) ammonium formate, Pd/C, EtOH, reflux, 16 h.

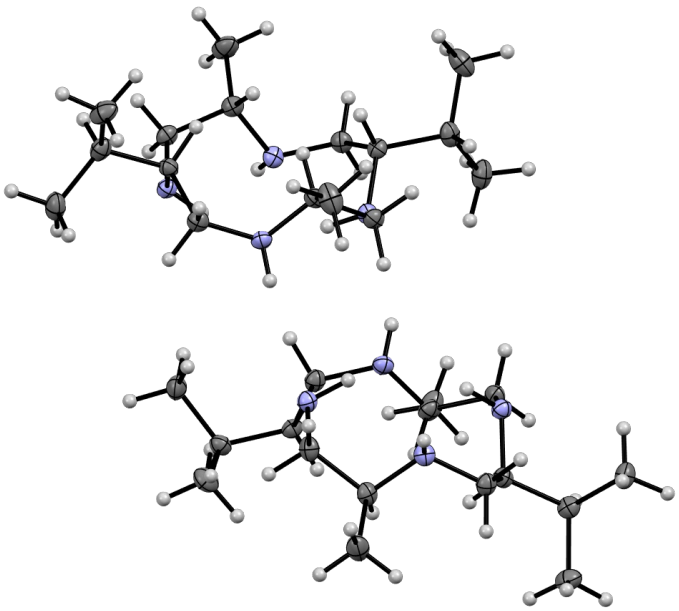

Figure 4.1: X-Ray structure of compound **96**, the ellipsoids represent the 50 % probability level. The bond lengths and angles are within normal ranges.

4.2.1 *Retrosynthetic analysis and considerations*

In order to ensure that all substituents direct in the same direction we planned to synthesise 3(*S*)1(*R*)M301-cyclen **108**. Although on of the configurations is (*R*) in the final product, topologically the starting materials can still be based on the natural amino acids. The priority of the different substituents changes during the course of the synthesis causing an initially (*S*) configured substituent to be (*R*) configured in the final product.

The synthesis of the C_2 symmetric 4(*S*)M2P2-cyclen **96** had lower yields than the original 4(*S*)M4-cyclen **22** synthesis. We envisioned that one methyl group could be replaced by a hydroxy methyl group if a protected serine derivative is used (see Scheme 29). The synthesis of the alanine / serine-based tetramer **109** could start from the already developed free acid **64** and the free amine **110**. For the synthesis of the free amine **110** the same procedure should be applicable as for the free amine **101** used for the synthesis of 4(*S*)M2P2-cyclen **96**. We proposed that the large steric bulkiness of the hydroxy *tert*-butyl group has the same influence than the isopropyl group on the selectivity of the hydrogenation. Deprotection of the hydroxy *tert*-butyl group was anticipated during the final hydrogen bromide deprotection step. However, acetylation of the free hydroxy group might occur under strongly acidic conditions in acetic acid. Reduction of the protected bislactam **111** would also reduce the acetyl protecting group to the corresponding alcohol. Final deprotection could be achieved using transferhydrogenation conditions.

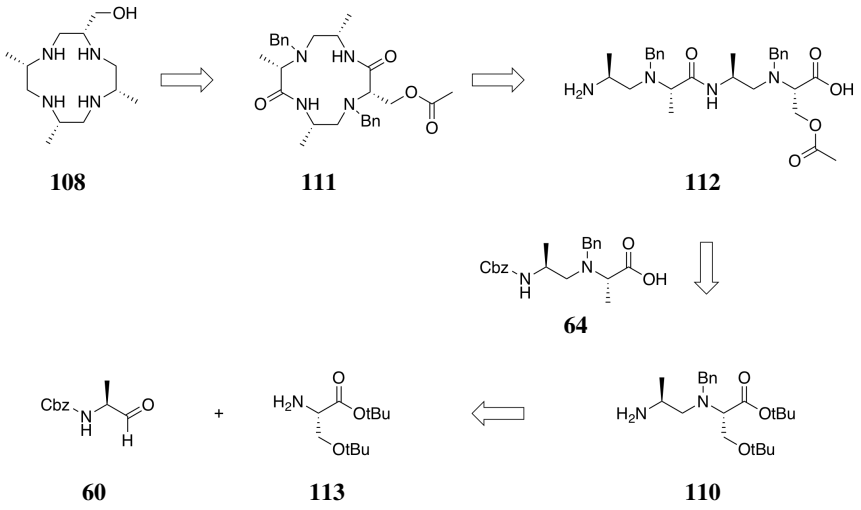

Scheme 29: Retrosynthetic analysis for the synthesis of 3(*S*)1(*R*)M301-cyclen **108**.

4.2.2 *Synthesis of alanine / serine -based tetramers*

The synthesis of *N*-Cbz-alaninal **60** was performed as described previously. The aldehyde **60** was further reacted with *tert*-butyl-protected serine **113** yielding the dimer **114** in excellent yield. The installation of the benzyl protecting group was more challenging due to the increased steric hindrance and required longer reaction times. The subsequent Cbz deprotection worked well showing that the increased size difference between the methyl group and the hydroxy *tert*-butyl group is responsible for the better selectivity achieved during hydrogenation. The free amine **110** and the free acid **115** were coupled in high yields resulting in the fully protected alanine / serine-based tetramer **116**. Final acidic deprotection with hydrogen bromide in acetic acid afforded the free alanine / serine-based tetramer **117**. To our delight we observed that the hydroxy *tert*-butyl group indeed got cleaved off and *in-situ* replaced by an acetyl protecting group. This protecting group is less bulky and protects the alcohol functionality from side reactions during the cyclization.

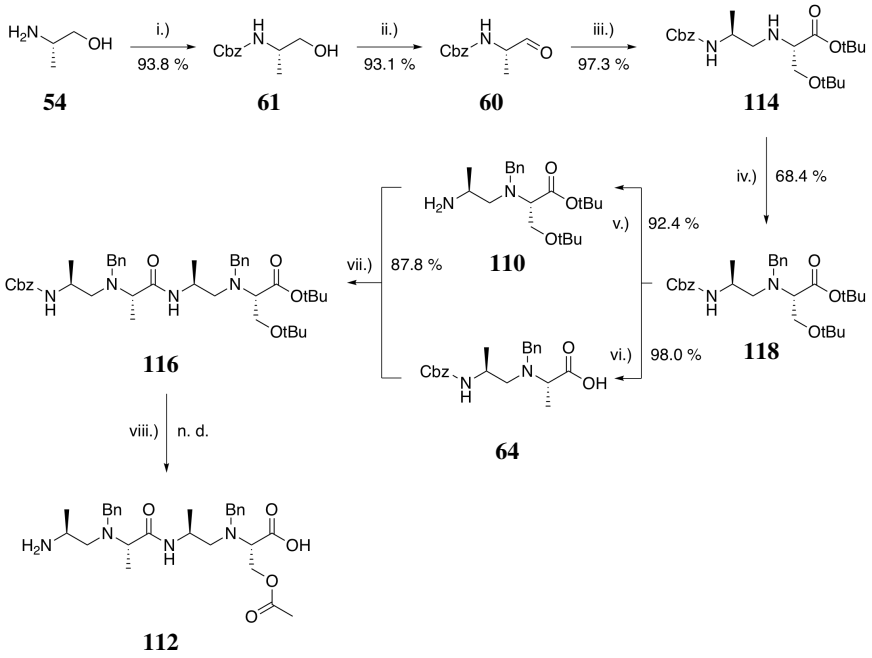

Scheme 30: Synthesis of compound **112**. Reaction conditions: i.) Cbz-Cl, Na_2CO_3, H_2O / EtOAc, 20-25 °C, 1 h; ii.) IBX, DMSO, EtOAc, reflux, 3.5 h; iii.) *tert*-butyl O-*tert*-butyl serine **113**, $NaBH(OAc)_3$, DCM, 16 h; iv.) BnBr, K_2CO_3, MeCN, 65 °C, 2 d; v.) $Pd/BaSO_4$, H_2, 1 bar, MeOH, 20-25 °C, 24 h; vi.) conc. HCl in 1,4-dioxane, 40 °C, 16 h; vii.) HATU, DIPEA, MeCN, 20-25 °C, 2 h; viii.) HBr in acetic acid, 40 °C, 30 min.

4.2.3 *Synthesis of alanine / serine -based twelve-membered macrocycles*

The cyclization of the free alanine / serine-based tetramer **117** was accomplished analogously to the already established protocol. We found that the yields were lower than those observed for the other cyclizations. However, after purification of the protected bislactam **111** the final reduction and deprotection step proceeded with comparable yields. As a convenient side effect during the reduction of the protected bislactam **111** the acetyl protecting group was removed as well. The desired macrocycle could be obtained in an overall yield of 17 %. The lower yield can be mostly attributed to the less efficient cyclization compared to 4(*S*)M4-cyclen **22** and 4(*S*)M2P2-cyclen **96**. We also grew crystals of 3(*S*)1(*R*)M301-cyclen **108** suitable for X-ray analysis (see Figure 4.2).

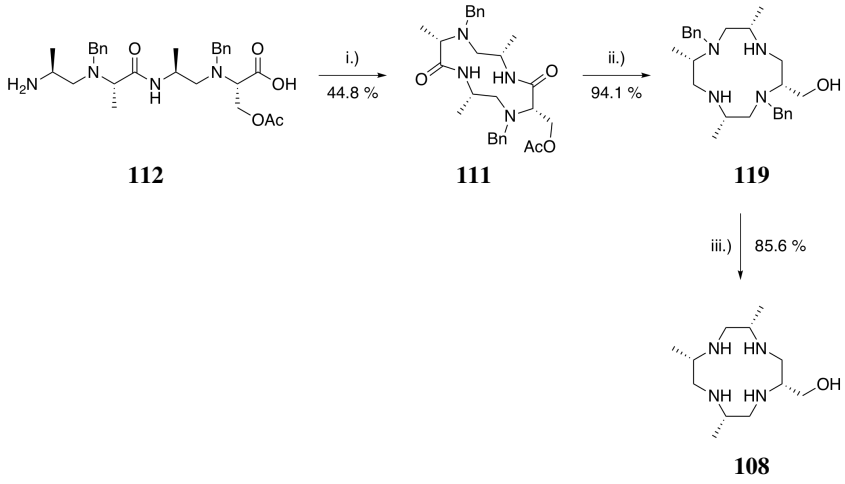

Scheme 31: Synthesis of compound **108**. Reaction conditions: i.) HATU, DIPEA, MeCN, 20-25 °C, 1 h; ii.) TMS-Cl, $LiAlH_4$, DCM, 0-5 °C to 20-25 °C, 24 h; iii.) Pd/C, H_2, 90 bar, 20-25 °C, 17 h.

4.3 RACEMIZATION STUDY OF *N*-CBZ-ALANINAL

During the synthesis of 4(*S*)M2P2-cyclen **96** we observed the presence of multiple species in the proton NMR spectra of most linear precursors (e. g. **100** and **104**) which were less pronounced for the 4(*S*)M4-cyclen **22** synthesis. Initially we attributed these signals to the presence of different conformers. Those signals were most clearly visible in the proton spectrum of the alanine / valine-based dimer **100**. We assumed conformational dynamics as well as *cis-trans* isomerization of the amide bond to be the reason for these signals. We performed variable temperature NMR analysis of the fully protected alanine / valine-based dimer **100** and we found evidence for a dynamical process arising from the isomerization of the carbamate (see Figure 4.3).

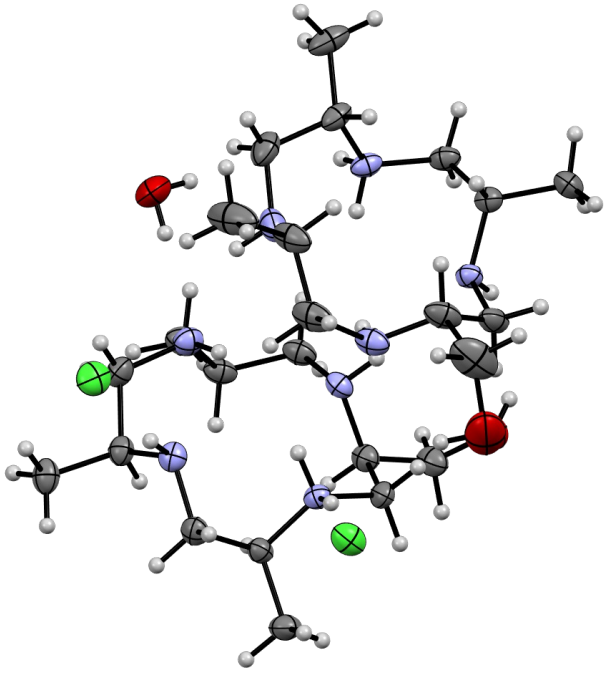

Figure 4.2: X-Ray structure of compound **108** $*H_2O$ *HCl, the ellipsoids represent the 50 % probability level. The bond lengths and angles are within normal ranges.

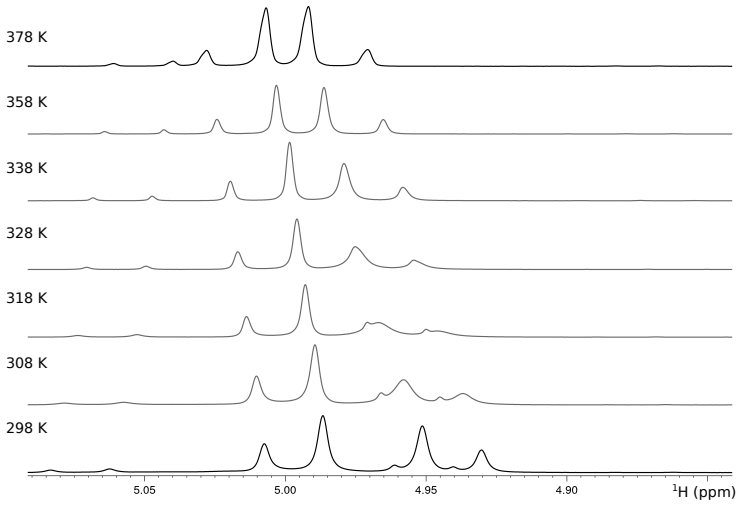

Figure 4.3: Variable temperature ^{1}H-NMR spectroscopy for **100**: Spectra were recorded in DMSO$-d_6$ from 298-378 K. The region of the benzylic Cbz protons is shown.

Nevertheless, not all signals present in the room temperature proton NMR spectrum could be explained by this dynamics. Therefore, we suspected the other signals might arise from undesired diastereoisomers. The most likely source of racemization was the oxidation of *N*-Cbz-alaninol **61** to *N*-Cbz-alaninal **60**. Amino aldehydes are known to be susceptible to racemization.[119] For further clarification we synthesised the undesired diastereoisomer **120** from commercially available *N*-(D)-Cbz-protected alaninol **121** (see Scheme 32).

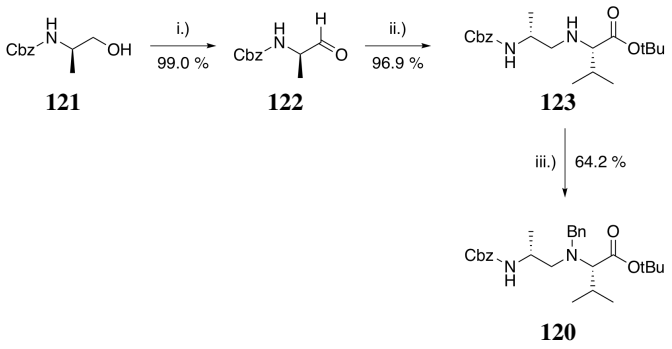

121 **122** **123** **120**

Scheme 32: Synthesis of compound **120**. Reaction conditions: i.) IBX, DMSO, EtOAc, reflux, 3.5 h; ii.) *tert*-butyl alanine **25**, $NaBH(OAc)_3$, DCM, 16 h; iii.) BnBr, K_2CO_3, MeCN, 65 °C, 18 h

Comparison of the proton NMR shifts for the non-benzylated alanine / valine-based dimers **103** and **123** showed little to no difference. However for the benzylated alanine / valine-based dimers **100** and **120** the difference was clearly visible (see Figure 4.4). We found that during the IBX oxidation of *N*-Cbz-alaninol **61** to *N*-Cbz-alaninal **60** racemization occurred. We further investigated this issue and found that racemization occurs during the oxidation step and not during the following work up. We determined the extend of racemization to be around 10-15 % in all experiments performed using the IBX oxidation in ethyl acetate.

Close inspection of the NMR data obtained for the alanine-based dimers and the alanine-based tetramers synthesised during the 4(*S*)M4-cyclen **22** synthesis also suggested the presence of undesired diastereoisomers. Although, racemization occurred during the first oxidation step we found that the percentage of undesired diastereoisomers gradually decreases. We found that after the cyclization the undesired diastereoisomers were reduced to less than 5 % in the case of the 4(*S*)M4-cyclen **22** and 4(*S*)M2P2-cyclen **96** syntheses. We hypothesized that the ability to cyclize is decreased for a compound having the wrong overall stereochemistry. The final products were obtained with less than 2 % of the undesired diastereoisomers. In the case of 3(*S*)1(*R*)M301-cyclen **124** the undesired diastereoisomers were not sufficiently removed during the subsequent reaction steps. Due to the lack of a purification method for 3(*S*)1(*R*)M301-cyclen the final product contained

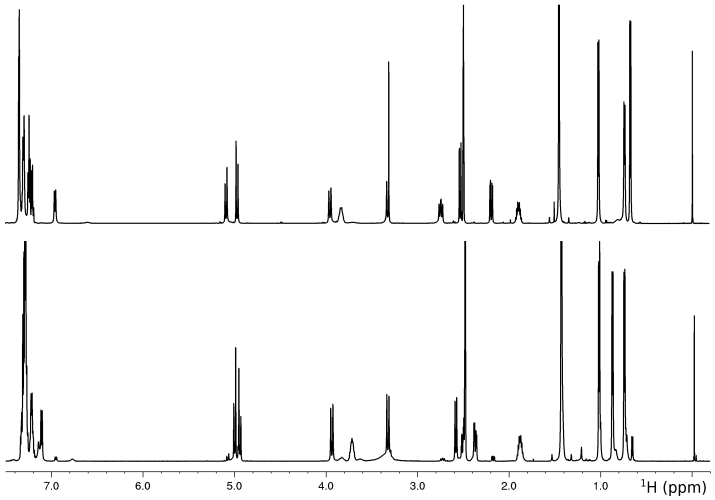

Figure 4.4: Comparison between the proton NMR spectrum for **120** (top) and **100** (bottom) in DMSO$-d_6$ at 298 K.

roughly 5-10 % of other diastereoisomers.

Surprisingly, we found that the (*R*)(*S*)alanine / valine-based dimer **120** was a highly crystalline solid which could be easily crystallized exceeding an ee of 99 %. On the other hand we did not find a crystallization method for the desired (*S*)(*S*)alanine / valine-based dimer **100**. The compound was always obtained as an oil. We suspect that this behaviour is likely true for most closely related dimers. This offers the possibility to enrich enantiomeric excess after the fourth step using simple crystallization techniques. Using a (*R*)(*S*)dimer would ultimately end in the formation of a macrocycle with alternating stereochemistry. If such a compound could be cyclized and further used to synthesise a functional tag was beyond the scope of this thesis.

5

CONCLUSION & OUTLOOK

5.1 CONCLUSION

A new synthesis for 4(*S*)M4-cyclen **22** was successfully developed starting from commercially available alanine-based precursors. Inducing cyclization on solid phase with tetraalanine was challenging and only successful in small scales up to 20 mg. Cyclization of tetraalanine in solution resulted in even lower yields. The steric hindrance and the preferred *trans* configuration of the peptide were the key reasons for the low obtained yields. This process was not scalable to multigram scales due to the high cost of materials and the low cyclization yield. Using the much more flexible tetraalaninol analogue was unsuccessful as no method could be developed to selectively close the ring. The three secondary amines needed protection and the *C*-terminal hydroxy group could not be converted into a good leaving group that would allow intramolecular ring closure. This findings were the key to the development of a mixed alanine / alaninol tetramer which allowed an intramolecular peptide bond formation in high yields under diluted conditions. The benzyl protected alanine-based tetramer was the key intermediate that allowed high cyclization yields.

The synthesis of this key intermediate proved to be challenging as two different approaches developed on small scales failed in up scaling. The low selectivity obtained during the Cbz deprotection of the alanine-based dimer **63** forced us to replace the benzyl group with the much more stable fluorobenzyl group. However, this introduced deprotection problems on the later stages. The fluorobenzyl group offered higher stability towards the Cbz-deprotection conditions, nevertheless, it was not completely inert and up scaling remained challenging. Over the course of the development of the synthesis more than two grams of the desired 4(*S*)M4-cyclen **22** were synthesised. The synthesis of 4(*S*)M4-cyclen **22** initially developed by Ranganathan *et al.*[106] is much shorter and remains an alternative. The new developed approaches on the other hand do not rely on a random cyclization and can therefore be used for the rational synthesis of various differently substituted twelve-membered tetraaza macrocycles. The synthesis was successfully adopted to synthesise 4(*S*)M2P2-cyclen **96** and 3(*S*)1(*R*)M301-cyclen **124**. The larger substituents reduced the yield obtained during the formation of the bislactam. In principal most natural amino acids could be used, however, special attention has to be

paid on the stability of the intermediate amino aldehyde especially towards racemization. Also the strongly acidic conditions used to deprotect the fully protected tetramers are problematic for acid labile substituents. Due to the general strategy of forming a bislactam any substituent carrying a reducible functional group (carboxylic acid, carboxylic amide, etc.) will suffer transformation during the reduction step.

5.2 OUTLOOK

One critical step during the synthesis of 4(*S*)M4-cyclen **22** is the formation of the free amine **56**. Further investigation towards an alternative protecting scheme should be taken. Although the fluorobenzyl protecting group dramatically reduces the problem, avoiding it is preferred. The introduction of a third orthogonal protecting group would be advisable. The synthesis for the free acid **64** could still be done using the Cbz protected alanine-based dimer **63**. The convergent nature of the first approach would be lost, however, the obtained fully protected alanine-based tetramer would be identical. Further optimization should also address the oxidation of the amino alcohol **61** to the amino aldehyde **60**. A oxidation procedure without racemization is definitely desirable. Although, the undesired diastereomers were removed during the later steps they significantly reduce the overall yield. Optimization of the reaction conditions are still desirable as most of the linear precursor turned out to be non crystalline and therefore no crystallization can be performed. Flash column chromatography on large scale is expensive and time consuming and thus should be avoided as much as possible.

Part II

SYNTHESIS OF REDUCTIVLY STABLE LINKERS FOR PCS NMR SPECTROSCOPY

This chapter deals with the development and application of new reductivly stable lanthanide chelating tags for PCS NMR spectroscopy.

6

SYNTHESIS AND APPLICATION OF M7PY-DOTA

Part of this work was conducted in collaboration with Dr. Francois-Xavier Theillet and Dr. Philipp Selenko and has been published.[83]

6.1 RETROSYNTHETIC ANALYSIS AND CONSIDERATIONS

To address the inherent problem of the instability of the disulfide bond towards strongly reductive environments as they are encountered in cells we suggested the formation of a thioether linkage. Results published by Yang *et al.*[84] showed that the formation of a thioether is possible via a nucleophilic aromatic substitution on a pyridine phenyl sulfone moiety. Work previously conducted in our group by Dr. Heiko Gsellinger, published in his doctoral thesis,[120] showed that introducing an aliphatic cysteine reactive functional group like an alpha bromo keton or an alpha beta unsaturated keton is very difficult. We envisioned that introducing a pyridine phenyl sulfone could solve several problems encountered during the synthesis of alpha bromo ketons due to the higher stability towards acidic hydrolysis and simpler reaction steps. We proposed that one of the coordinating lactic acid side arms in the original M8-SSPy-DOTA[102] tag could be replaced by the pyridine moiety (see Scheme 33). Taking advantage of not only forming a shorter linker but also of introducing a different donor atom. The proposed synthesis for the new linker starts from bromo methyl pyridine **125** and thiophenol **126** followed by an oxidation to the sulfone **127**. Free radical bromination should deliver the desired alpha bromo methyl pyridine **128** which could undergo nucleophilic substitution with three times lactic acid *tert*-butyl ester (LacOtBu) alkylated M4-cyclen **129**. Final acidic hydrolysis and metallations could form the desired tags **130**.

6.2 SYNTHESIS OF LN-M7PYSO$_2$PH-DOTA

Three times LacOtBu alkylated M4-cyclen **129** was synthesized using three equivalents of the triflate of LacOtBu in a mixture of acetonitrile / dichloromethane (1:1) as solvent. We found that using pure dichloromethane results in incomplete alkylation and the majority of the product was two times alkylated. Using pure acetonitrile on the other hand resulted in a mixture with significant overalkylation. We found that starting the reaction with di-

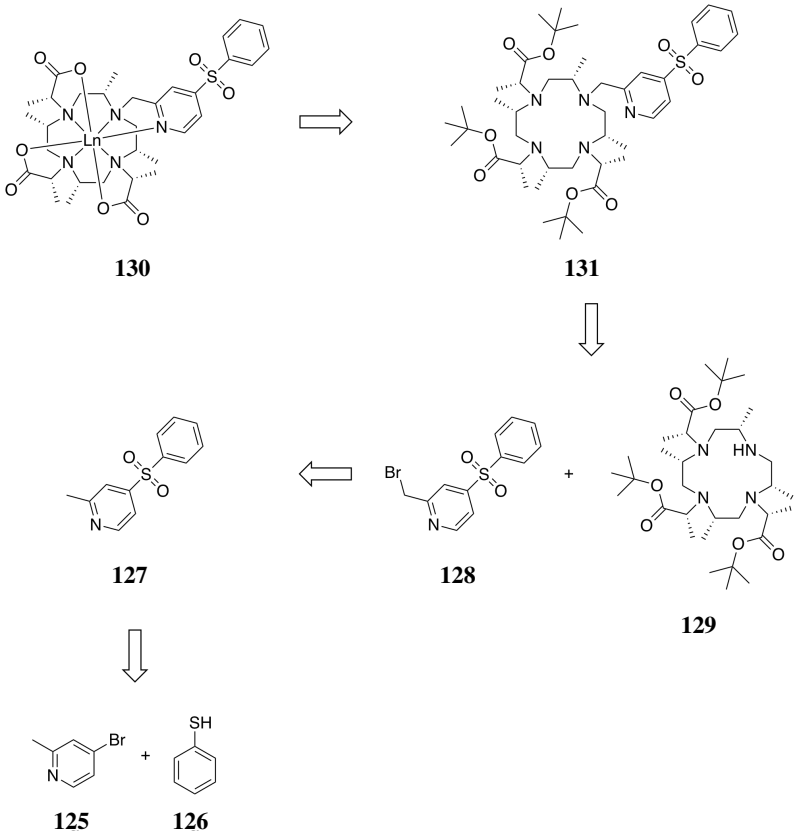

Scheme 33: Retrosynthetic analysis for the synthesis of Ln-M7PySO2Phe-DOTA **130**.

chloromethane and adding acetonitrile after two to three hours is optimal and minimizes the formation of the fourfold alkylated product. Separation of the formed products was achieved using preparative HPLC. To reduce expensive material losses the one and two times alkylated products were reused in future reactions. Methyl pyridine phenyl sulfone **127** was synthesized from methyl bromo pyridine **125** and thiophenol **126** immediately followed by an oxidation of the thioether to the sulfone **127** (see Scheme 34). Free radical bromination was performed using NBS and AIBN in tetrachloromethane. We found that using less toxic solvents like acetonitrile and dichloromethane resulted in low yields and complex mixtures. The monobrominated product **128** was separated from the dibrominated product by flash column chromatography and was immediately used afterwards. We were delighted to find that the alpha bromo pyridine **128** was highly reactive towards nucleophilic substitution on the already sterically very crowded three times alkylated M4-cyclen **129**. Subsequent acidic hydrolysis was achieved using aqueous hydrochloric acid and final metallation was performed using four equivalents of the corresponding lanthanide $^{3+}$ salt.

6.3 TAGGING OF GB1 MUTANTS

We prepared diamagnetic Lu-M7Py-DOTA **132**, and paramagnetic Tm-M7Py-DOTA **133** and Tb-M7Py-DOTA **134** complexes, which we coupled to the streptococcal protein G B1 domain (GB1) via cysteine residues. We used site-directed mutagenesis to prepare three different mutants of GB1, E19C, K28C and E42C. Initial tagging reactions at 20-25 °C in 50 mM phosphate buffer, 0.5 mM TCEP at pH 7.0 showed no conversion. Adjusting the pH to 7.6 increased reaction rates but no full conversion was observed within 24 h. Due to the high thermal stability of the GB1 protein tagging was performed at 45 °C and was >95 % completed after 24 h. GB1 concentrations were adjusted to 300 µM and a four-fold excess of M7Py-DOTA loaded with Lu, Tm, or Tb was used. Although tagging was possible for all mutants of GB1 the high temperatures required for tagging are not suitable for more labile proteins. Nevertheless, tagging in presence of TCEP clearly demonstrated the stability of the thioether bond towards reduction. TCEP is a much strong reducing agent than glutathione which is present in cells and, therefore, no cleavage of the tag should occur inside a cell. Tagging in the presence of TCEP offered two major advantages over the standard procedure applied for tagging with M8-SSPy-DOTA. First, protein dimerization was hindered in the presence of TCEP and second, the removal of TCEP prior to tagging was not required as it would be for M8-SSPy-DOTA. A simple buffer exchange from high TCEP concentrations to minimal TCEP concentrations was sufficient.

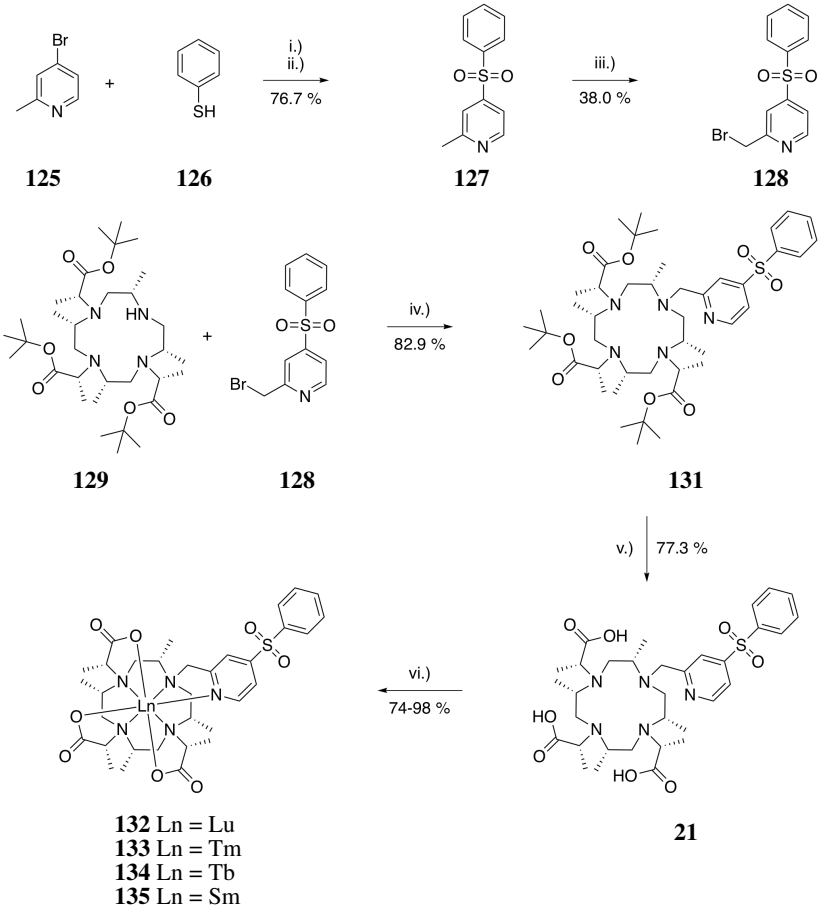

Scheme 34: Synthesis of tags **132**-**135**. Reaction Conditions: i.) K_2CO_3, DMF, 90 °C, 22 h; ii.) NaOCl, acetic acid, 20-25 °C, 16 h; iii.) NBS, AIBN, CCl_4, reflux, 10 h; iv.) K_2CO_3, MeCN, 20-25 °C, 18 h; v.) MeCN, aq. HCl 1 M, 80 °C, 4 h; vi.) Ln^{3+}, aq. NH_4OAc 100 mM, 80 °C, 18 h.

6.4 IN-VITRO AND IN-CELL NMR ANALYSIS

For GB1 samples we recorded 2D ^{1}H-^{15}N HSQC spectra at 600 MHz which showed large pseudocontact shifts of up to 6 ppm (see Figures 6.1, 6.2 and 6.3). We also detected strong cross peak splitting in 2D ^{1}H-^{15}N IPAP-HSQC spectra due to the partial alignment of the GB1 within the magnetic field. This resulted in residual dipolar couplings reaching 25 Hz. We found that samples tagged with Tm-M7Py-DOTA showed the largest pseudocontact shifts.

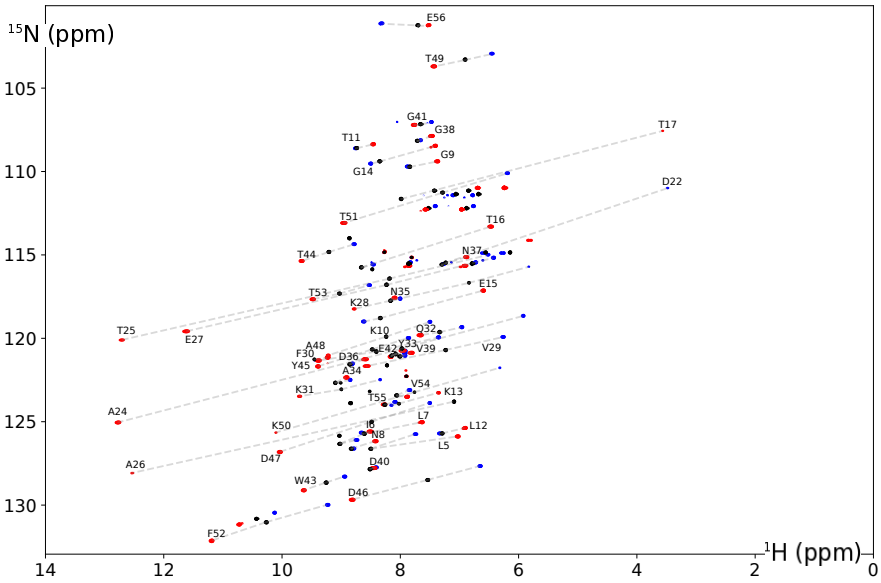

Figure 6.1: *In-vitro* PCS by metal-loaded DOTA-M7Py. Superposition of full 2D ^{1}H-^{15}N HSQC spectra of GB1-E19C coupled to diamagnetic Lu-M7Py-DOTA (black) and paramagnetic Tm-M7Py-DOTA (red/blue) at 600 MHz and 293 K. Water signal removed for clarity.

For further *in-cell* NMR experiments only the Tm and Lu loaded proteins were used. Using microinjection we injected GB1 carrying either paramagnetic (Tm) or diamagentic (Lu) M7Py-DOTA into *Xenopus laevis* oocytes for *in-cell* NMR measurements. We recorded 2D 1H-15N HSQC spectra at effective NMR concentrations of ~25 µM (intracellular GB1 concentrations ~50 µM). The PCSs we obtained were virtually indistinguishable from the respective *in-vitro* samples with an overall RMSD of 0.04 ppm, indicating that the structure of the protein is *in-cell* similar to the structure of the protein *in-vitro*. This was expected as GB1 is known to be a very stable protein that does not change conformation inside cells.[121] The measured RDCs were also comparable to the one obtained *in-vitro*. Because the intracellular viscosity is higher than the viscosity *in-vitro*, a faster T2 relaxation was observed. This lead to overall broader lines and larger errors especially for the RDC measurements. Free lanthanide ions are highly toxic and we did not detect any sample degradation or leakage of the metal for up to 24 h. This clearly showed the excellent stability of this tag inside living *Xenopus laevis* oocytes.

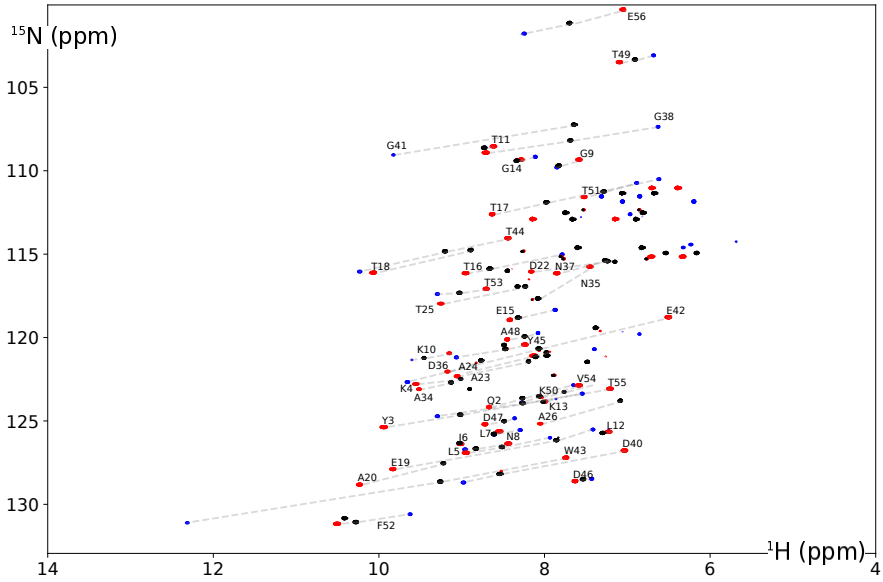

Figure 6.2: *In-vitro* PCS by metal-loaded M7Py-DOTA. Superposition of full 2D ^{1}H-^{15}N HSQC spectra of GB1-K28C coupled to diamagnetic Lu-M7Py-DOTA (black) and paramagnetic Tm-M7Py-DOTA (red/blue) at 600 MHz and 293 K. Water signal removed for clarity.

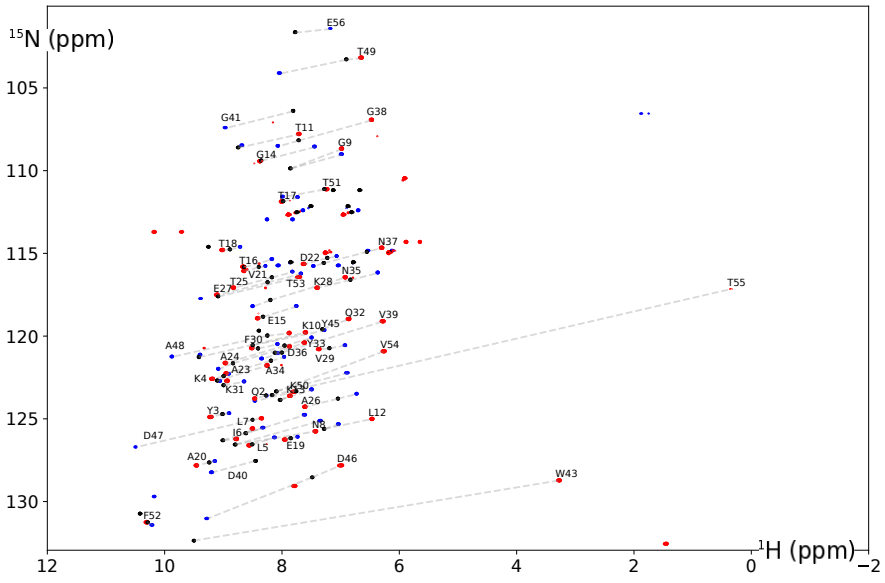

Figure 6.3: *In-vitro* PCS by metal-loaded DOTA-M7Py. Superposition of full 2D ^{1}H-^{15}N HSQC spectra of GB1-E42C coupled to diamagnetic Lu-M7Py-DOTA (black) and paramagnetic Tm-M7Py-DOTA (red/blue) at 600 MHz and 293 K. Water signal removed for clarity.

We determined magnetic susceptibility tensor parameters for both *in-cell* and *in-vitro* measurements using the program Numbat.[74] We chose the atomic coordinates of the C_β of the corresponding cysteine residue as starting coordinates for the metal position in the minimization. The position was then further refined in an iterative fashion. Table 6.1, 6.2 and 6.3 show the calculated magnetic susceptibility tensor parameters. We found that Tm and Tb have opposite signs in their magnetic susceptibility tensor parameters which results in an overall trend of shifting towards the opposite direction. This can be best seen in Figure 6.4 where all tensor isosurfaces have opposite colors going from Tb to Tm.

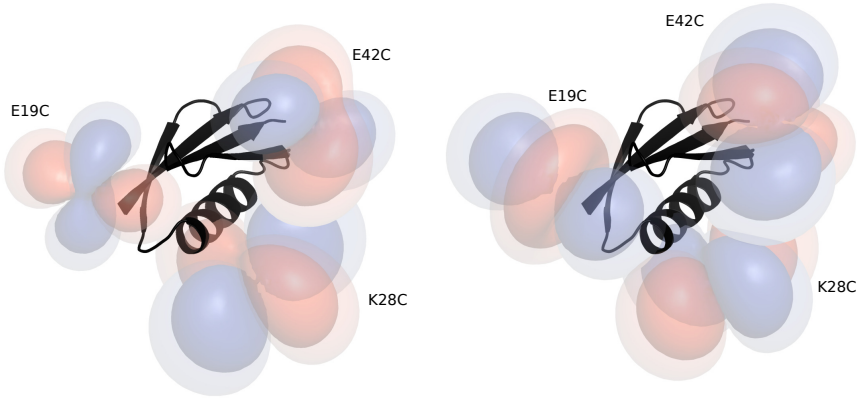

Figure 6.4: Tensor isosurfaces of the three GB1 mutants E19C, K28C and E42C. Tb-M7Py-DOTA left and Tm- M7Py-DOTA right. The red isosurfaces indicate a shift of -8 ppm (inner) and -4 ppm (outer). The blue isosurfaces indicate the corresponding positive shift.

Table 6.1: *In-vitro* and *in-cell* PCS tensor parameters for GB1 K28C fitted against the GB1 X-ray structure (PDB code: 2QMT).

	in-vitro		***in-cell***
	Tb, 50 PCS	Tm, 62 PCS	Tm, 62 PCS
$\Delta\chi_{ax}$ / $10^{-32}m^3$	38.5 (1.3)	-31.9 (0.8)	-32.9 (0.9)
$\Delta\chi_{rh}$ / $10^{-32}m^3$	22.8 (0.9)	-18.2 (0.5)	-17.8 (0.6)
x / Å	9.8 (0.2)	9.8 (0.2)	9.8 (0.2)
y / Å	12.3 (0.1)	12.3 (0.1)	12.1 (0.1)
z / Å	31.5 (0.1)	31.5 (0.1)	31.6 (0.1)
α / °	108.1 (0.8)	96.3 (0.5)	96.9 (0.5)
β / °	41.4 (0.7)	48.4 (0.5)	46.9 (0.4)
γ / °	156.09 (1.4)	172.6 (0.9)	171.3 (0.9)

Tensor parameters (errors) were calculated in Numbat[74] from the indicated number of selected PCS. All tensor parameters are reported in the UTR. The following amino acids were excluded from the fit because of too close proximity (<15 Å) to the final lanthanide position: K10, T11, L12, E19, V21, A23, A24, T25, A26, Q32, G38, D40, T53.

Table 6.2: *In-vitro* and *in-cell* PCS tensor parameters for GB1 E19C fitted against the GB1 X-ray structure (PDB code: 2QMT).

	in-vitro		***in-cell***
	Tb, 76 PCS	Tm, 74 PCS	Tm, 60 PCS
$\Delta\chi_{ax}$ / $10^{-32}m^3$	-13.9 (1.7)	31.4 (2.2)	27.3 (2.1)
$\Delta\chi_{rh}$ / $10^{-32}m^3$	-7.0 (0.8)	7.1 (2.8)	3.6 (0.9)
x / Å	-3.5 (0.3)	-3.5 (0.8)	-4.8 (0.3)
y / Å	30.5 (0.3)	30.5 (0.6)	30.5 (0.3)
z / Å	21.7 (0.3)	21.7 (0.9)	22.0 (0.3)
α / °	148.3 (1.9)	148.6 (6.2)	155.1 (1.8)
β / °	103.4 (1.1)	115.9 (6.0)	106.3 (1.1)
γ / °	65.5 (10.0)	5.6 (5.3)	126.3 (9.9)

Tensor parameters (errors) were calculated in Numbat[74] from the indicated number of selected PCS. All tensor parameters are reported in the UTR. The following amino acids were excluded from the fit because of too close proximity (<15 Å) to the final lanthanide position: L5, T16, D22, A48, T49, T51, F52.

Table 6.3: *In-vitro* and *in-cell* PCS tensor parameters for GB1 E42C fitted against the GB1 X-ray structure (PDB code: 2QMT).

	in-vitro		***in-cell***
	Tb, 76 PCS	Tm, 74 PCS	Tm, 60 PCS
$\Delta\chi_{ax}$ / $10^{-32}m^3$	25.5 (1.6)	-34.8 (2.0)	-32.9 (4.6)
$\Delta\chi_{rh}$ / $10^{-32}m^3$	10.9 (0.8)	-22.5 (1.4)	-21.9 (3.1)
x / Å	16.5 (0.2)	16.5 (0.3)	16.0 (0.3)
y / Å	12.8 (0.1)	12.8 (0.1)	12.8 (0.1)
z / Å	10.7 (0.2)	10.7 (0.2)	10.4 (0.1)
α / °	80.4 (0.3)	62.0 (0.3)	63.1 (2.6)
β / °	96.4 (0.3)	104.1 (0.4)	105.5 (6.7)
γ / °	120.2 (0.1)	100.4 (0.1)	101.7 (1.7)

Tensor parameters (errors) were calculated in Numbat[74] from the indicated number of selected PCS. All tensor parameters are reported in the UTR. The following amino acids were excluded from the fit because of too close proximity (<15 Å) to the final lanthanide position: N8, N35, D36, G41, Y45, D46, D47, A48, F52, T53, V54, T55.

6.5 ROSETTA STRUCTURE CALCULATION

We used our *in-cell* PCS and RDC data as input for a structure calculation within GPS-Rosetta. GPS-Rosetta includes PCS restraints from multiple paramagnetic centers and uses them as distance and angle restraints in its calculation routines. We generated the 3- and 9-residue fragments of known protein structures with the Robetta protein sequence server. We excluded all homologous of the GB1 sequences. Using these fragments, we generated 10000 GB1 structures, out of which we collected the 100 lowest-energy structures and compared their conformations to experimentally determined GB1 structures from X-ray crystallography (PDB code: 2QMT) and solution NMR (PDB code: 1GB1, 2PLP). Using Rosetta's ab-initio approach without any additional experimental data we found poor convergence of individual structures, with a median backbone Cα RMSD of 1.85 Å (see Figure 6.5). We added a PCS-based weighting function and recalculated 10000 GB1 structures. We used 72, 86, and 96 PCS constraints from the E19C, K28C, and E42C GB1 mutants, respectively. The convergence of GB1 structures was substantially improved. For this PCS-based approach we found an average Cα RMSD of the 100 lowest-energy models was 0.98 Å and 0.64 Å between the closest model and the crystal structure (PDB code: 2QMT) (see Figure 6.6). We calculated another 10000 GB1 structures using PCS and RDC data. The convergence we obtained was similar to the one without RDC data. We found an average Cα RMSD of 1.04 Å for the 100 lowest-energy structures, 0.64 Å for the closest model and the X-ray structure (PDB code: 2QMT) (see Figure 6.7).

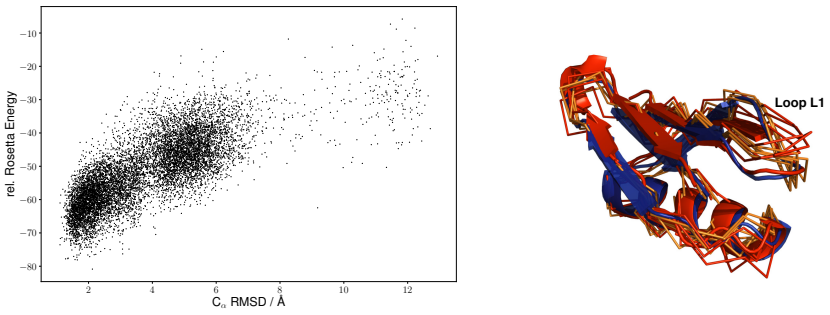

(a) (b)

Figure 6.5: Ab initio GB1 structures without using experimental restraints. (a) Scatter plots depict Rosetta energy scores and C_α RMSDs of 10'000 GB1 structures compared to the GB1 X-ray structure (2QMT). (b) A superposition of the ten lowest energy structures. GB1 models with L1 conformations corresponding to the one of the GB1 X-ray structure are shown in red, deviating L1 conformers are coloured orange.

We inspected the 10 lowest energy structures of each set and found a remarkable difference between the structures obtained with PCS data and

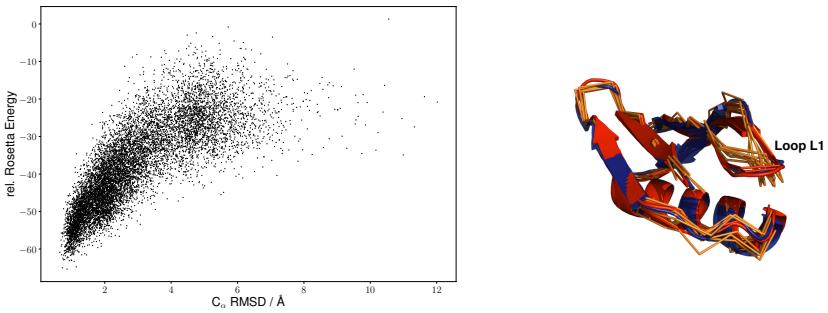

(a) (b)

Figure 6.6: GB1 structures with PCS input data. (a) Scatter plots depict Rosetta energy scores and C_α RMSDs of 10'000 GB1 structures compared to the GB1 X-ray structure (2QMT). (b) A superposition of the ten lowest energy structures. GB1 models with L1 conformations corresponding to the one of the GB1 X-ray structure are shown in red, deviating L1 conformers are coloured orange.

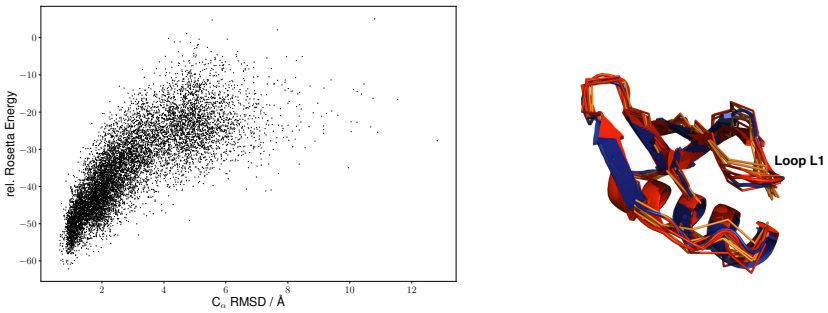

(a) (b)

Figure 6.7: GB1 structures with PCS and RDC input data. (a) Scatter plots depict Rosetta energy scores and C_α RMSDs of 10'000 GB1 structures compared to the GB1 X-ray structure (2QMT). (b) A superposition of the ten lowest energy structures. GB1 models with L1 conformations corresponding to the one of the GB1 X-ray structure are shown in red, deviating L1 conformers are coloured orange.

the ones we obtained with PCS and RDC data. In both ensembles loop L1 (residues N8 to E15), which connects strands $\beta 1$ and $\beta 2$ of GB1, displayed two distinct conformations. One conformation was identical to the X-ray structure with an average C_α RMSD of 1.1 Å, and the other conformation had a kink and a larger C_α deviation and average RMSD of 1.6 Å. We found only 3 out of ten structures adopted the X-ray loop L1 conformation in PCS alone generated structures. In the case of PCS and RDC data five out of ten adopted the X-ray conformation. Previous solution NMR data indicated that loop L1 is highly flexible and the *in-vitro* solution conformation is similar to the conformation obtained in X-ray crystallography. Although it was expected that GB1 adopts the same conformation *in-cell* and *in-vitro* we were delighted to see that PCS and RDC data from single 2D *in-cell* NMR experiments are sufficient to determine protein structures within GPS-Rosetta.

6.6 FLUORINATED LEAVING GROUPS

6.6.1 *Retrosynthetic analysis and considerations*

To counteract the low reactivity exhibited by our M7PySO$_2$Phe-DOTA complexes we envisioned to synthesize complexes with fluorinated leaving groups (see Scheme 35). Although the nature of the leaving group only plays a minor role in nucleophilic aromatic substitution reactions its nature is not entirely irrelevant. An increased acidity of the leaving group could enhance the reactivity. We proposed three different leaving groups based on fluorinated thiophenols **136**, **137** and **138**. Upon nucleophilic substitution, oxidation and bromination the alpha bromo pyridines **139**, **140** and **141** could be obtained. The procedures already developed for the synthesis of M7PySO$_2$Phe-DOTA could be adapted for the synthesis of the corresponding complexes.

6.6.2 *Synthesis of fluorinated derivatives of DOTA-M7PySO2Ph*

The synthesis of the mono-CF_3 substituted analogue of M7PySO$_2$Phe-DOTA started from bromo methyl pyridine **125** (see Scheme 36). A nucleophilc aromatic substitution with thiophenol **136** in acetonitrile and potassium carbonate yielded the intermediate thioether after 18 h at 65 °C. The immediate oxidation of the thioether with bleach was unsuccessful as only the formation of the intermediate sulfoxide was detected. The increased electronegativity resulted in an lower oxidation tendency. We isolated the crude intermediate and oxidized it with sodium tungstate and hydrogen peroxide in methanol at 20-25 °C. We found that this oxidizing conditions are superior and no formation of the *N*-oxide was detected. Using stronger oxidizing agents like hydrogen peroxide in acetone resulted in the formation of the sulfone *N*-oxide. Finally a free radical bromination of the sulfone **142** yielded the alpha bromo pyridine **139**. Subsequent alkylation of triply alkylated M4-

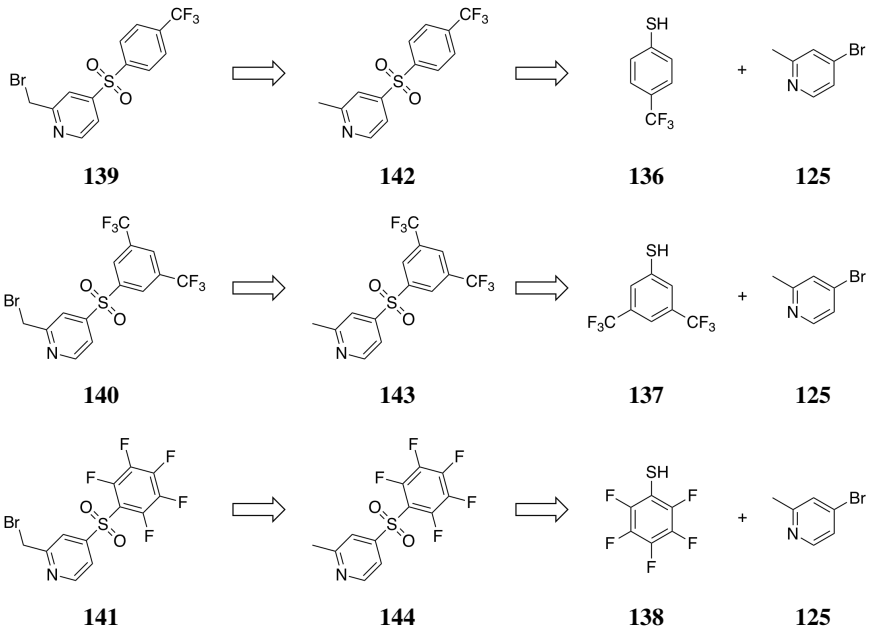

Scheme 35: Retrosynthetic analysis for three fluorine substituted analogues (**139**, **140**, **141**) of **128**.

cyclen **129**, deprotection and metallation yielded Tm and Lu complexes of M7PySO$_2$-para-CF$_3$-Ph-DOTA **145** and **146**.

Similar conditions were applied for the synthesis of 3,5-bis-CF$_3$ substituted analogue of M7PySO$_2$Ph-DOTA . The nucleophilc substitution of bromo methyl pyridine **125** with thiophenol **137** yielded the intermediate thioether which was oxidized using the optimized conditions described previously. Free radical bromination of the sulfone **143** yielded the alpha bromo pyridine **140**. Subsequent alkylation of three times alkylated M4-cyclen **129**, deprotection and metallation yielded Tm and Lu complexes of M7PySO$_2$-bis-CF$_3$-Ph-DOTA **149** and **150**.

The synthesis of a penta fluoro substituted pyridine sulfone **144** was not possible. We tried several oxidizing conditions including bleach, hydrogen peroxide / acetone and sodium tungstate / hydrogen peroxide. It was only possible to oxidize the sulphur once forming the sulfoxide. Harsher conditions yielded the sulfoxide *N*-oxide. We found that the increased electronegativity of the thiophenols influence both the aromatic substitution and the oxidation leading to lower yields in the case of para-CF$_3$ and 3,5-bis-CF$_3$ substitution.

6.6.3 *Tagging of GB1 E42C*

We applied the same conditions as for our initial tagging experiments for Tm and Lu loaded M7PySO$_2$Ph-DOTA. Tagging was performed using GB1 E42C

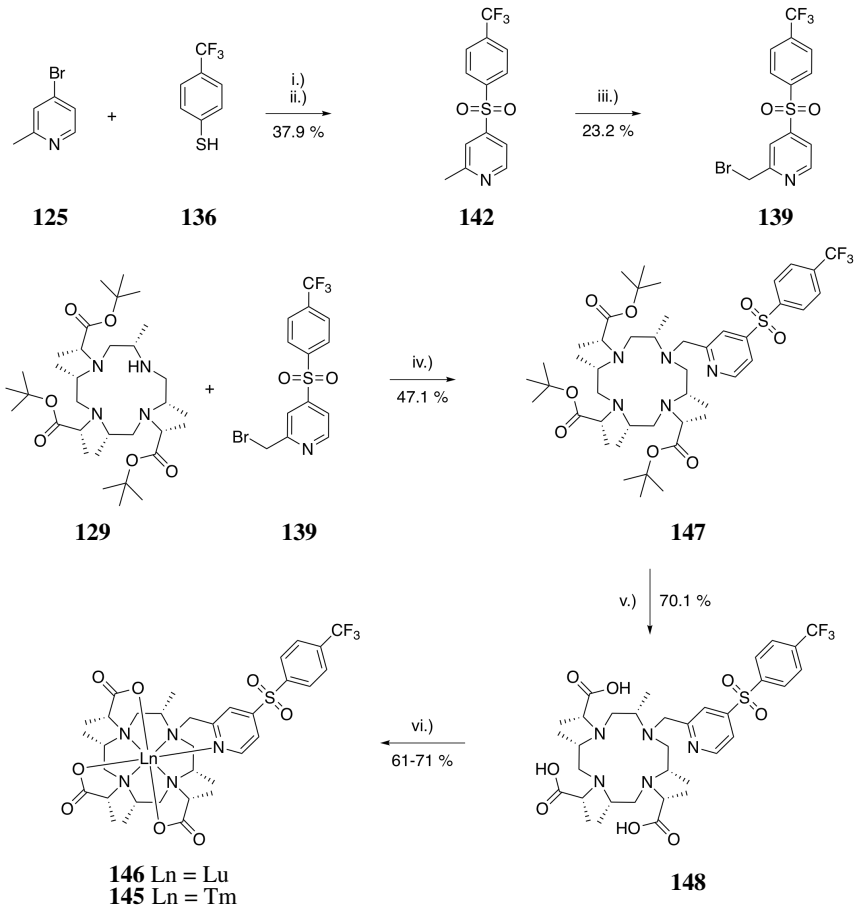

Scheme 36: Synthesis of tags **146** and **145**. Reaction Conditions: i.) K_2CO_3, DMF, 65 °C, 18 h; ii.) Na_2WO_4, H_2O_2, 20-25 °C, 18 h; iii.) NBS, AIBN, CCl_4, reflux, 18 h; iv.) K_2CO_3, MeCN, 20-25 °C, 18 h; v.) MeCN, aq. HCl 1 M, 80 °C, 4 h; vi.) Ln^{3+}, aq. NH_4OAc 100 mM, 80 °C, 18 h.

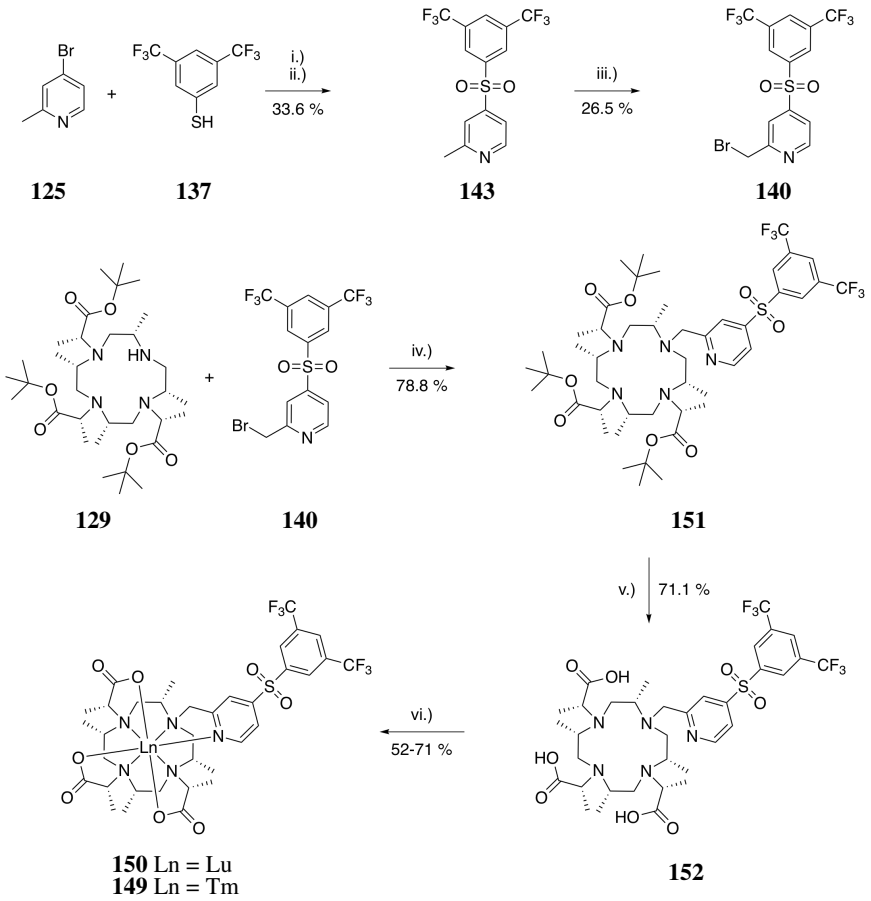

125 **137** **143** **140**

129 **140** **151**

150 Ln = Lu
149 Ln = Tm

152

Scheme 37: Synthesis of tags **150** and **149**. Reaction Conditions: i.) K_2CO_3, DMF, 80 °C, 18 h; ii.) Na_2WO_4, H_2O_2, 20-25 °C, 18 h; iii.) NBS, AIBN, CCl_4, reflux, 18 h; iv.) K_2CO_3, MeCN, 20-25 °C, 18 h; v.) MeCN, aq. HCl 1 M, 80 °C, 4 h; vi.) Ln^{3+}, aq. NH_4OAc 100 mM, 80 °C, 18 h.

at 20-25 °C in 50 mM phosphate buffer, 0.5 mM TCEP at pH 7.0. The protein concentration was adjusted to 300 µM and a fourfold excess of Tm-M7PySO_2-para-CF_3-Ph-DOTA **145** and Tm-M7PySO_2-3,5-bis-CF_3-Ph-DOTA **149** was used. We observed no changes in reaction rates for these two fluorinated tags in comparison to the non fluorinated tag indicating that the stronger acidity of the leaving group has only a minor or no influence on the overall reaction rate.

7

SYNTHESIS AND APPLICATION OF M7PY-DOTA DERIVATIVES

7.1 RETROSYNTHETIC ANALYSIS AND CONSIDERATIONS

Driven by the finding for the fluorinated leaving groups we envisioned that a significant gain in reaction rate should be obtained by stabilizing the intermediate Meisenheimer complex.[122] Nucleophilc aromatic substitution largely depend on the stability of the intermediate Meisenheimer complex (see Scheme 38).

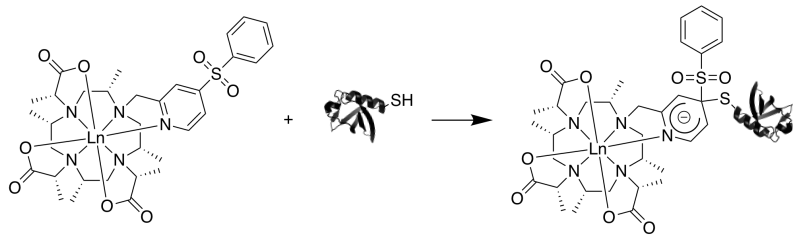

130 **153**

Scheme 38: Formation of the intermediate Meisenheimer complex **153**.

The incoming nucleophile brings in a negative charge. Thus, stabilizing this negative charge within the aromatic system is favourable and enhances reactivity. In nucleophilic aromatic substitution with pyridines the 2 and 4 position are susceptible to substitution due to their ability to delocalize the electron pair towards the nitrogen. In order to increase the tendency to undergo nucleophilic aromatic substitutions the electron density of the pyridine has to be reduced. This causes the pyridine ring to more likely accept an incoming electron pair. We envisioned that substituting a hydrogen in the 5 position with a fluorine would significantly increase the reactivity. The desired alpha bromo pyridine sulfone **154** could be synthesized from the commercially available 5-fluoro-4-bromo-2-methyl pyridine **155** (see Scheme 39).

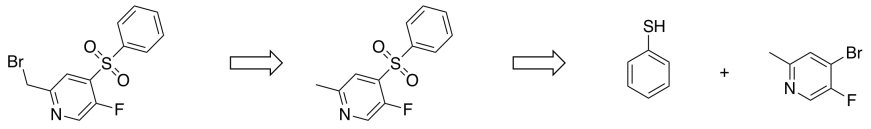

154 **156** **126** **155**

Scheme 39: Retrosynthetic analysis for the synthesis of the fluorinated alpha bromo pyridine **154**.

7.2 SYNTHESIS OF M7FPYSO$_2$PH

The fluoro pyridine phenyl sulfone **156** was synthesized by nucleophilic aromatic substitution of fluoro bromo methyl pyridine **155** and thiophenol (**126**) followed by the oxidation of the intermediate thioether (see Scheme 40). The rate of the nucleophilic aromatic substitution was enhanced due to the increased electrophilicity of the fluorinated pyridine. Compound **156** was found to be not stable at 20-25 °C. After several days the compound turned blue. The blue minor impurities could be easily separated by flash column chromatography. A free radical bromination of the fluoro pyridine phenyl sulfone **156** yielded the alpha bromo compound **154** in low yields. Due to the costly starting material **157** the reaction was stopped early in order to reduce the amount of dibrominated by-products. The starting material could be recovered using flash column chromatography. Further nucleophilic substitution, deprotection and metallation showed no significant differences in terms of yields in comparison to the previously shown complexes. We synthesized Tm-M7FPySO$_2$Ph-DOTA **158** and Lu-M7FPySO$_2$Ph-DOTA **159**. Most of the time we observed lower yields for the Tm metallation in comparison to Lu^{3+}. We attributed this behaviour to the presumably stronger catalytic activity of Tm^{3+}. The excess of lanthanide ions in solution was reduced from 4 equivalents to 1.2. Although this reduction did slightly increase the overall yield, the yield for Tm was still lower than for Lu and sometimes incomplete conversion was detected. We also studied the temperature required for metallation and we found that at 20-25 °C and below 50 °C no formation of the complex is detected. Therefore, we decided to reduce the excess to two-fold in order to ensure complete conversion and we kept the temperature at 80 °C for 18 h as described by Häussinger *et al.*.[102]

7.3 TAGGING OF UBIQUITIN S57C

The protein ubiquitin S57C was expressed by PD Dr. Daniel Häussinger according to the procedure reported by Sass *et al.*.[123] We tagged ubiquitin S57C at 20-25 °C in 10 mM phosphate buffer, 2.0 mM TCEP at pH 7.0. Ubiquitin S57C concentrations were adjusted to 150 µM and a four-fold excess of M7FPy-DOTA loaded with Lu and Tm was used. The reaction progress was monitored using LC-ESI-MS. We found that 80 % of the protein was tagged

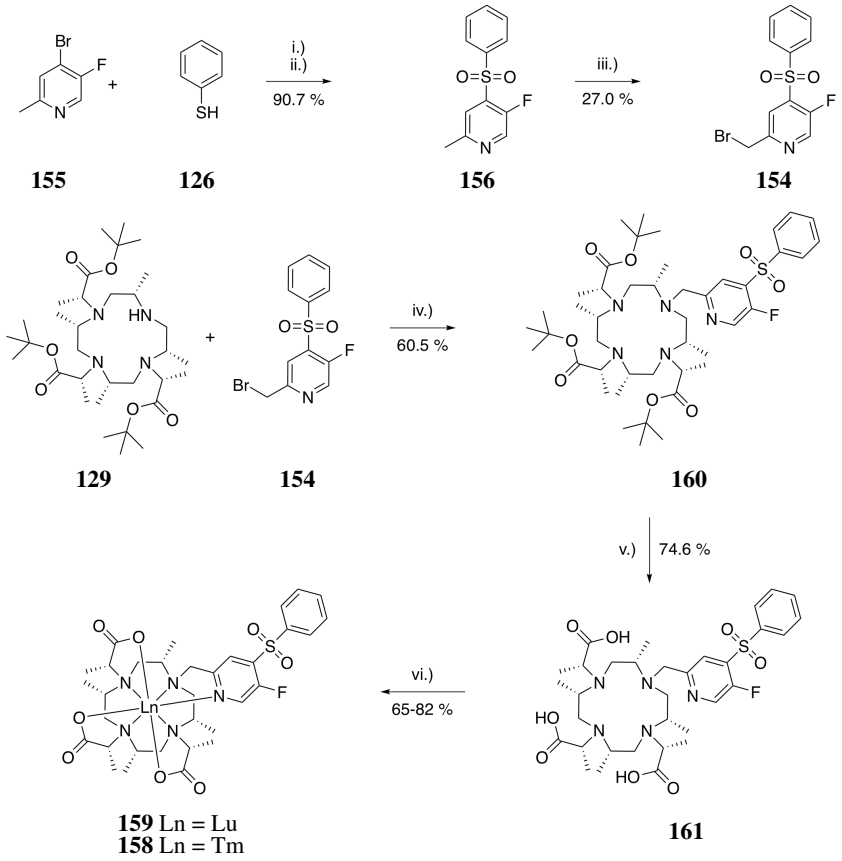

Scheme 40: Synthesis of tags **159** and **158**. Reaction Conditions: i.) K_2CO_3, DMF, 70 °C, 1 h; ii.) Na_2WO_4, H_2O_2, 20-25 °C, 48 h; iii.) NBS, AIBN, CCl_4, reflux, 6 h; iv.) K_2CO_3, MeCN, 20-25 °C, 18 h; v.) MeCN, aq. HCl 1 M, 65 °C, 2 h; vi.) Ln^{3+}, aq. NH_4OAc 100 mM, 80 °C, 18 h.

within 3 h. To ensure compleation of the tagging reaction the tagging was prolonged for additional 16 h until ESI-MS showed full conversion. Upon closer inspection of the ESI-MS spectra we found that the tag slowely decomposes due to the reaction with TCEP. Therefore, we performed the same tagging reactions without TCEP. Finally, we recorded ^{1}H-^{15}N HSQC spectra and found in the paramagentic Tm spectrum two sets of signals. One set belonged to the desired paramagnetically shifted species while the other set has almost identical shifts as the untagged protein. If tagging was performed without TCEP the second species was around 30 %, in the presence of TCEP the second species was only around 15 %. We concluded that the untagged species is most likely dimerized protein. However, the exact percentage could not be estimated well, since the tagged protein experienced strong PRE effects due to paramagnetic metal. On the other hand the untagged species did not experience this effect and therefore could be overestimated. Nevertheless from this experiments it was clear that tagging without TCEP results in a larger amount of apparently untagged protein. It has been reported in literature that benzenesulfinic acid can induce the formation of thiolsulphonate derivatives which are susceptible towards nucleophilic substitution forming disulfides.[124] Upon successful tagging one equivalent of benzenesulfinic acid is released for each tagged protein, but also one equivalent of benzenesulfinic acid is released per molecule of tag destroyed by TCEP. This self induced protein dimerization could explain the special reaction kinetics observed for the tagging reaction. This could explain why we observed 80 % conversion after 3 h but still needed an additional 16 h in order to not dectect any monomeric ubiquitin by ESI-MS. For future tagging reactions we reduced the amount of TCEP from 2.0 mM to 450 µM and increased the amount of tag from a four-fold excess to a six-fold excess. This conditions reduced the amount of untagged species from 15 % to less then 10 %.

7.4 IN-VITRO NMR ANALYSIS

For ubiquitin S57C samples we recorded 2D ^{1}H-^{15}N HSQC spectra at 600 MHz which showed large pseudocontact shifts of up to -10 ppm. We found that samples tagged with Tm-M7FPy-DOTA **158** showed predominantly negative PCS shifts and only a few positive PCS shifts (see Figure 7.1). We determined magnetic susceptibility tensor parameters using the program Numbat[74] (see Table 7.1 see Figure 7.2). We chose the atomic coordinates of the C_β of the corresponding cysteine residue as starting values for the minimizations. The position was then further refined in an iterative fashion. Figure 7.2 shows the tensors orientation with respect to the protein. Inspection of the relative orientation revealed that mostly the "belt" of the tensor is pointing towards the protein and the axial component is pointing away from the protein. This arrangement is less favourable because the tensor's axial component is in general larger.

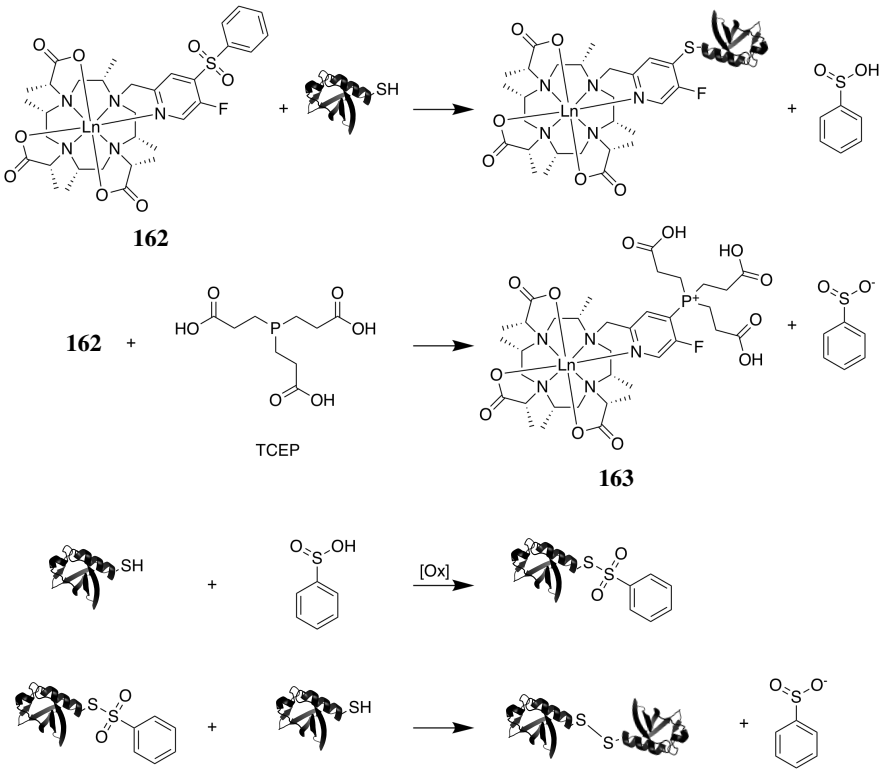

Scheme 41: Tagging reaction, formation of TCEP adduct **163** and dimerization of ubiqutin catalysed by benzensulfinic acid.

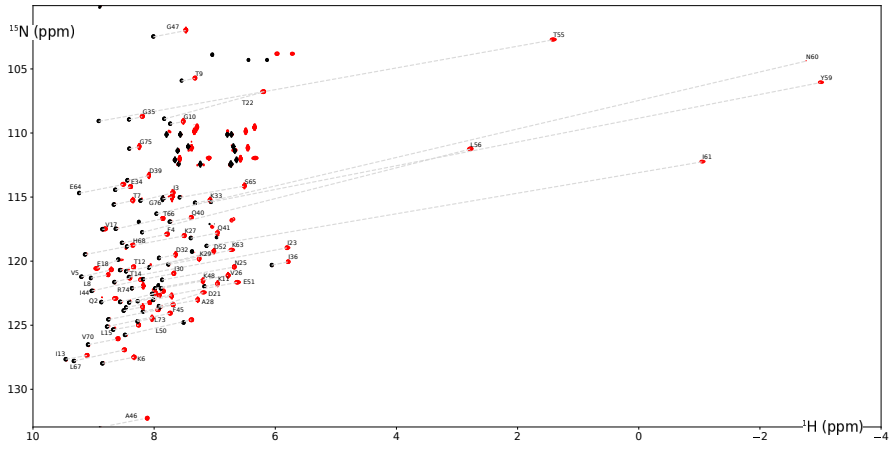

Figure 7.1: *In-vitro* PCS by metal-loaded MF7Py-DOTA. Superposition of full 2D ^{1}H-^{15}N HSQC spectra of ubiquitin S57C coupled to diamagnetic Lu-M7FPy-DOTA (black) and paramagnetic Tm-M7FPy-DOTA (red) at 600 MHz and 298 K. Water signal removed for clarity.

Table 7.1: *In-vitro* PCS tensor parameters for ubiquitin S57C fitted against the ubiquitin X-ray structure (PDB code: 1UBI).

	Tm, 80 PCS
$\Delta\chi_{ax}$ / $10^{-32}m^3$	17.8 (1.5)
$\Delta\chi_{rh}$ / $10^{-32}m^3$	9.8 (1.0)
x / Å	20.7 (0.5)
y / Å	11.4 (0.4)
z / Å	12.7 (0.5)
α / °	2.8 (8.3)
β / °	154.3 (7.0)
γ / °	27.0 (6.4)

Tensor parameters (errors) were calculated in Numbat[74] from the indicated number of selected PCS. All tensors are represented in the UTR. Only amino acids residing in a stable secondary structure (2-7, 12-16, 23-34, 38-40, 41-45, 48-49, 56-59 and 66-71) were used if present in the spectra.

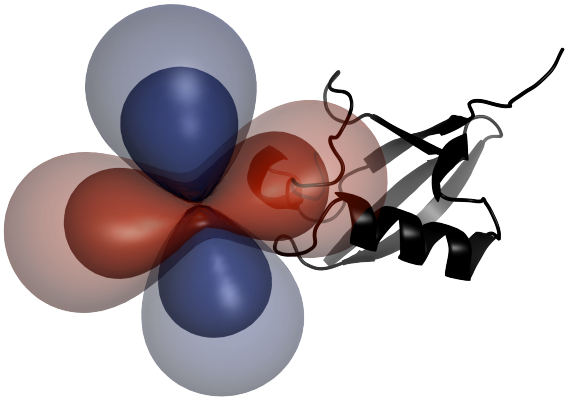

Figure 7.2: Tensor representation of Tm-M7FPy-DOTA tagged to ubiquitin S57C. The red isosurfaces indicate a shift of -3 ppm (inner) and -1 ppm (outer). The blue isosurfaces indicate the corresponding positive shift.

7.5 NON AROMATIC SULFINIC ACIDS AS LEAVING GROUPS

7.5.1 *Retrosynthetic analysis and considerations*

To address the major problems arising from the release of benzenesulfinic acid we envisioned the synthesis of non aromatic leaving groups. The comercially available spin label tag MTSL releases methylsulfinic acid upon conjugation and is widly applied and no product dimerization has been reported due to the release of methylsulfinic acid.[125] The introduction of a sulfonamide (compound **164**) would produce SO_2 and NH_3 upon successful nucleophilic aromatic substitution. On the other hand the introduction of a methylsulfone (compound **165**) would release methylsulfinic acid which quickly hydrolyses to SO_2 and methanol. Both compounds would avoid the formation of benzenesulfinic acid and most likely avoid dimerization. Due to the harsh conditions required for the free radical bromination of the methyl pyridine precursors we proposed modification of the final phenyl sulfone tag **162**. Primary sulfonamides can be easily prepared under aqueous conditions using hydroxylamine-*O*-sulfonic acid.[126] The methylsulfone could be introduced by alkylation of the free thiol **166** with methyliodid followed by an oxidation. For further testing reaction we planned to prepare only Tm-based complexes and no Lu-based complexes as only Tm offers measurable PCS shifts.

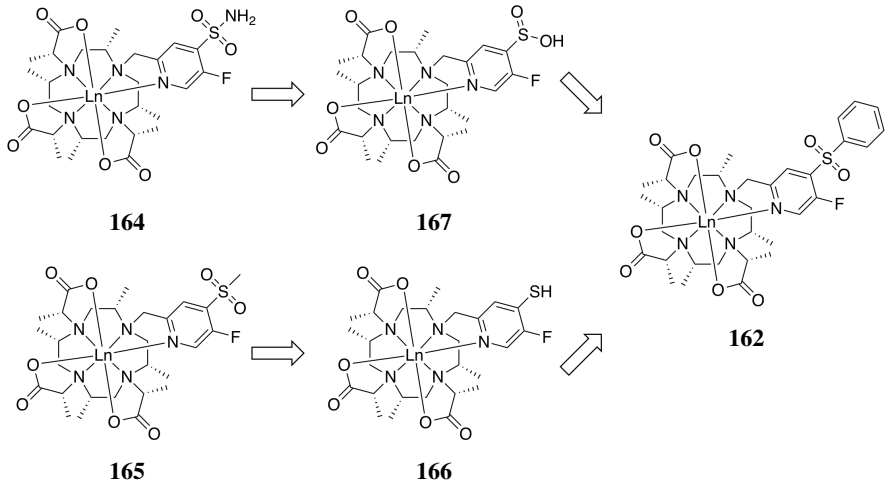

Scheme 42: Retrosynthetic analysis for the synthesis of sulfonamide-based tags **164** or methylsulfone-based tags **165**.

7.5.2 *Synthesis of M7FPySO2NH2 DOTA and M7FPySO2Me DOTA*

We tried the direct substitution of Tm-M7FPySO_2Ph-DOTA **158** with sodium sulfide. The result we obtained was unsatisfying as most of the starting material decomposed and only little product was produced. We obtained similar results for the direct substitution with sodium sulfite. Neither the free thiol nor the sulfinic acid could be produced directly. However, we were very pleased

to find that 2-(trimethylsilyl)ethanethiol quantitatively reacts at 20-25 °C in the presence of K_2CO_3 in acetonitrile (see Scheme 43). This rather special protecting group for a thiol can be selectively cleaved in the presence of tetrabutylammonium fluoride. It was also possible to oxidize the thioether **168** forming the sulfoxide **169**. Treatment of the sulfoxide **169** with tetrabutylammonium fluoride released the sulfinic acid which was *in-situ* transformed to the sulfonamide **170**. The alkylation of the free thiol **171** with methyliodide was performed quantitatively and the following oxidation was achieved in moderate yield (see Scheme 44). We could prepare two close analogues of Tm-M7FPySO_2Phe-DOTA bearing a sulfonamide and a methyl sulfone. We found that once a metal is introduced into the tag its stability greatly increases and various modifications could be performed under mild conditions. This strategy requires a few more steps but is definitely preferable due to the stability of the pyridine phenyl sulfone **156** under acidic and free radical conditions.

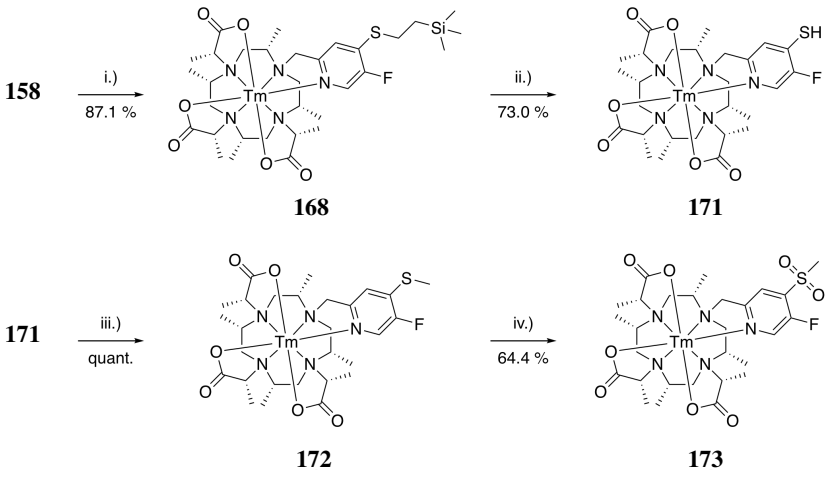

Scheme 43: Synthesis of tag **168**. Reaction Conditions: i.) $HSC_2H_4Si(CH_3)_3$, K_2CO_3, MeCN, 20-25 °C, 2 h; ii.) TBAF 1 M in THF, MeCN, 20-25 °C, 30 min; iii.) CH_3I, K_2CO_3, MeCN, 20-25 °C, 2 h; iv.) Na_2WO_4, H_2O_2, MeOH, 20-25 °C, 18 h.

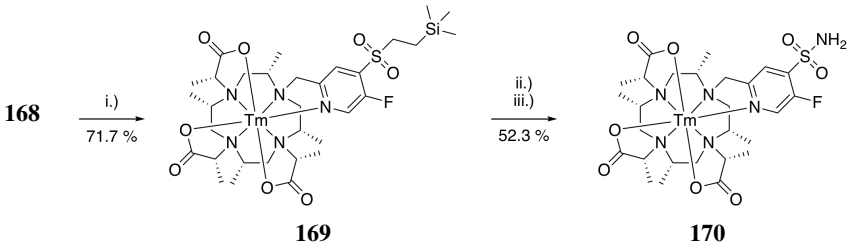

Scheme 44: Synthesis of tag **170**. Reaction Conditions: i.) Na_2WO_4, H_2O_2, MeOH, 20-25 °C, 18 h; ii.) TBAF 1 M in THF, MeCN, 20-25 °C, 30 min; iii.) NaOAc, hydroxylamine-*O*-sulfonic acid, H_2O, 20-25 °C, 6 h

7.5.3 *Tagging of ubiquitin S57C*

We tagged ubiquitin S57C at 20-25 °C in 10 mM phosphate buffer, 0.45 mM TCEP at pH 7.0. Ubiquitin S57C concentrations were adjusted to 150 µM and a six-fold excess of Tm-M7FPySO_2NH_2-DOTA **170** and Tm-M7FPySO_2Me-DOTA **173** was used. We found that Tm-M7FPySO_2NH_2-DOTA **170** did not react within 24 h and a conversion of approximately 10 % was achieved within 24 h for Tm-M7FPySO_2Me-DOTA **173**. Although our experiments with the fluorinated leaving groups indicated that the leaving group plays a minor role in the overall reaction kinetics we found that only phenyl sulfone pyridines offer a high enough reactivity for useful protein tagging reactions.

7.6 DETERMINATION OF INTRINSIC MAGNETIC SUSCEPTIBILITY TENSORS

This section of the thesis summarizes the key findings of the study of the intrinsic magnetic susceptibility tensors of Ln-M7FPySO_2Phe-DOTA tags. The results presented here are obtained in collaboration with Raphael Vogel during his master thesis in our group and are described in more detail in his thesis.[116]

7.6.1 *Pseudocontact shift tensor fitting*

For a full determination of magnetic susceptibility tensor parameters a detailed knowledge of the position and the corresponding shift is required. Due to the large PRE effect exhibited by paramagnetic lanthanides the measurement of 2D NMR spectra is severely limited and in some cases impossible. Therefore, a precise assignment of a shift to a position becomes impossible in severe cases. We used a selectively ^{13}C methyl labelled M4-cyclen to synthesize Ln-M7FPySO_2Phe-DOTA tags. The synthesis of singly labelled M4-cyclen was performed using the dimer to trimer to tetramer strategy described previously. In the target lanthanide complexes all cyclen methyl groups are 25 % labelled. This is due to the statistical distribution obtained by the alkylation of the singly labelled M4-cyclen. This allowed the identification of the corresponding methyl proton shift in the 1D proton spectrum of the early lanthanide from Ce-Eu and Yb due to their characteristic $^1J_{CH}$ splitting. However, for the late lanthanide the linewidths were too broad to observe any doublet splitting. Measuring 1D carbon spectra allowed us to identify the four methyl carbon shifts. However, we found that those carbon shifts as well as the fluorine shift from the linker are heavily influenced by the contact shifts and therefore could not be used for the tensor determination. The carbon shifts were broadened due to the PRE and the coupling to the protons. Decoupling became very inefficient for most shifted signals due to the small decoupling bandwidth. For example if the proton chemical shift range is 1400 ppm we would require a decoupling bandwidth of 840 kHz on a 600 MHz spectrometer (1400 ppm x 600 MHz). Even using a very broad decoupling

scheme like GARP with a figure of merit of 4.8 this would still correspond to a decoupler field strength of 175 kHz. At this field strength the 90° pulse would be around 1 µs. Typical high power proton pulse lengths are in the order of 10 µs. A shorter pulse would require more power and thus damage the probehead. Therefore it is not possible to decouple the whole proton chemical shift range in strongly paramagnetic samples (see Figure 7.3).

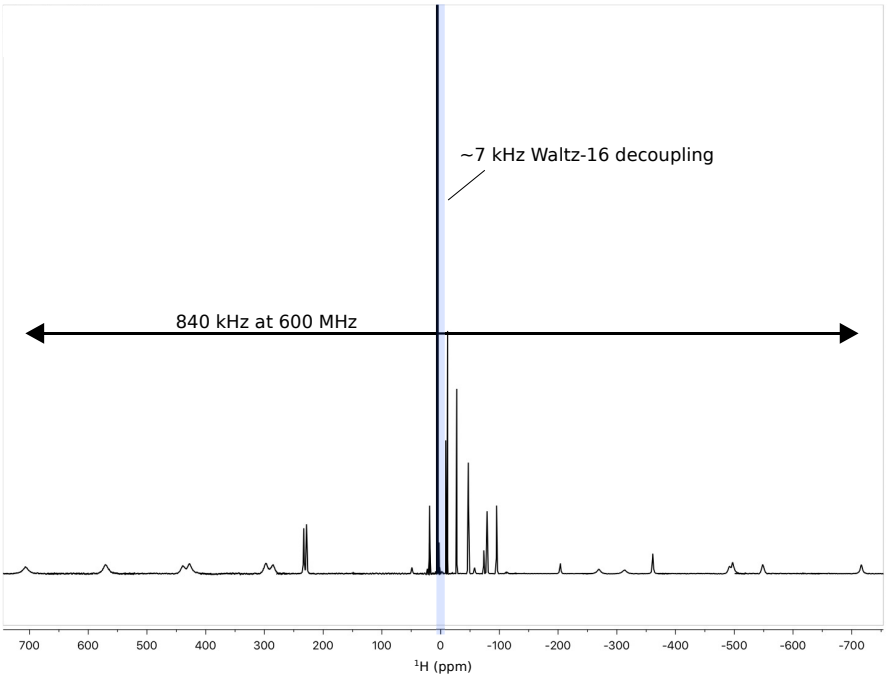

Figure 7.3: Proton spectrum of Dy-M7FPy-DOTA[116] and decoupling bandwidth at 600 MHz for the routinely applied Waltz-16 decoupling sequence.

However, this circumstance could be used to our advantage as a series of selectively ^{1}H decoupled 1D carbon spectra allowed us to identify pairs of carbon and proton shifts. If the decoupler offset matches the frequency of the connected protons the signal becomes sharper as the signal is only broadened by PRE and not broadened by the coupling with the protons (see Figure 7.4). Therefore, four proton signals could be assigned to four possible positions. Furthermore, for the early lanthanides it was possible to record 2D COSY spectra which allowed the assignment of individual spin systems. In the case of the weakly paramagnetic lanthanides Sm and Eu we were able to record in addition 2D HSQC HMBC and ROESY spectra. In this cases the tensors could be determined precisely because all proton shifts could be assigned. The atomic coordinates were taken from a DFT optimized structure of the corresponding lanthanide tag. For Ce to Nd it was only possible to record COSY spectra. In this case we could only assign different spin systems but no exact positions.

In the cases were only individual spin systems could be assigned but no exact assignment, a combinatorial approach was used to find the best solution. For, however, the late lanthanides no individual spin systems could be

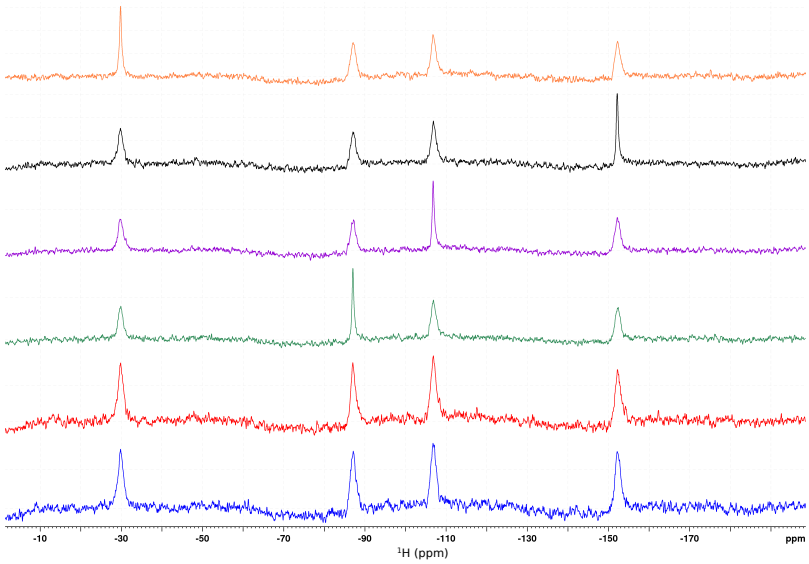

Figure 7.4: Selectively decoupled ^{13}C spectra of Tb-DOTA-M7FPy.[116] The ^{1}H decoupler offset has been set to the following proton frequencies: 8.3 ppm (orange), -68.5 ppm (black), -45.3 ppm (violet), -29.6 ppm (green) and - 25.6 ppm (red). The blue spectra with no decoupling was taken as a reference. The red spectra shows the effect of decoupling at a wrong frequency.

identified as it was not possible to measure COSY spectra. For these difficult cases information gained from the early lanthanides could be used. It was found that certain group of protons always shifted in the same direction and are always found on either the low or high field end of the spectrum. Using this information and the proton shifts from the cyclen methyl protons a combinatorial approach was applied to find the assignment with the best fit. We found several possible solutions with an r^2 value of >0.999. Therefore, the correct assignment could not be deduced. However, the distribution of the fitted tensor parameters allowed us to obtain an estimate of the true size of the tensor (see Table 7.2 and 7.3). We found that this numbers are much larger than the tensor parameters we obtained for both GB1 and ubiquitin S57C samples. To further confirm this finding we investigated the tags performance on the protein ubiquitin S57C and we found that approximately 80 % of the tensors potential is lost. This percentage is roughly constant for all lanthanide complexes of M7FPy-DOTA.

These findings clearly showed that although our previously developed tags have very large intrinsic tensors most of the PCS effect is lost and not transferred onto the protein. The reason for this extreme loss of performance is the relative movement of the tag with respect to the protein surface. Our pyridine-based tags have already a very short and rigid linker and it is highly doubtable whether this could actually be shortened further. These tags offer only one rotatable bond formed between the protein and the pyridine ring. There-

Table 7.2: Tensor parameters calculated for the early lanthanide Ln-M7FPySO_2Phe-DOTA tags (top) and conjugated to ubiquitin S58C (bottom).

	Ce	Pr	Nd	Sm	Eu
$\Delta\chi_{ax}$	3.5	10.4	4.6	-0.83	4.5
$\Delta\chi_{rh}$	2.1	2.7	2.1	-0.27	2.6
$\Delta\chi_{ax}$	-0.99	2.4	1.1	-0.76	-1
$\Delta\chi_{rh}$	-0.65	1.5	0.59	-0.46	-0.66

All tensor parameters are reported in the UTR. Axial and rhombic components are given in $10^{-32}m^3$.

Table 7.3: Tensor parameters calculated for the late lanthanide Ln-M7FPySO_2Phe-DOTA tags (top) and conjugated to ubiquitin S58C (bottom).

	Tb	Dy	Ho	Er	Tm	Yb
$\Delta\chi_{ax}$	58 (-7.4)	93 (10)	38 (4.6)	29 (2.2)	83 (0.8)	23 (1.9)
$\Delta\chi_{rh}$	32 (9.0)	32 (16)	19 (6.4)	14 (2.9)	22 (4.6)	8.7 (1.6)
$\Delta\chi_{ax}$	-12	-21	6.6	5.1	-16	-2.7
$\Delta\chi_{rh}$	-7.5	-12	4.2	0.52	-9	-1.7

All tensor parameters are reported in the UTR. Axial and rhombic components are given in $10^{-32}m^3$.

fore, the rotation around this bond is presumably responsible for the great loss of performance. Translational motions are far less likely to cause large averaging effects as most often no crossing of the tensors node planes occurs. On the other hand rotation around the linkage can cause crossing of node planes going from positive to negative values thus having a large influence on the observed shifts. Inside the tag the four base nitrogens and the metal form a square pyramid. The tensors z-axis is only slightly tilted away from the axis created by the center of the base square and the tip. Therefore, rotation around the protein pyridine thioether bond caused a significant reduction of especially the axial component of the tensor. On the other hand if a tensor could be created where the z-axis of the tensor and the thioether bond are perfectly aligned then a rotation around this bond would only average the rhombic component of the tensor. Future study should focus on restricting the tensors mobility and reducing the losses caused by rotational motions. Increasing the tags intrinsic tensor parameters is still desirable but considering the loss of almost 80 % of the potential makes this approach less efficient.

7.7 DECREASING ELECTRON DENSITY OF THE COORDINATING PYRIDINE RING BY NITRO SUBSTITUTION

7.7.1 *Retrosynthetic analysis and considerations*

We thought one alternative way to circumvent the protein dimerization would be to enhance the tagging reaction rate. Changing the leaving group was unsuccessful therefore a change of the pyridine ring was needed. One way the reduce the electron density of the pyridine ring even further would be to replace the fluorine group with a nitro group. Unfortunately, the required nitro bromo methyl pyridine was not readily commercially accessible. Therefore, we envisioned to synthesize the compound **174** by nitration of hydroxy methyl pyridine **175** and a subsequent hydroxy to bromine transformation (see Scheme 45). This would install the nitro group on the 3 position and not on the 5 position of the coordinating pyridine ring. However, as long as the electron withdrawing group is ortho to the leaving group the stabilizing effect should take place. With the nitro bromo methyl pyridine **174** in hand we could apply the same procedure as for all previously shown pyridine phenyl sulfones.

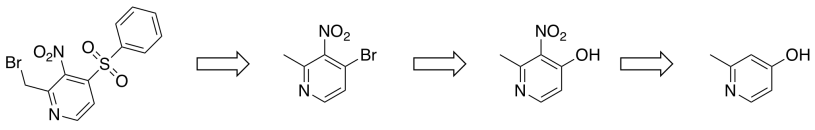

176 **174** **177** **175**

Scheme 45: Retrosynthetic analysis for the synthesis of the nitrated alpha bromo pyridine phenyl sulfone **176**.

7.7.2 *Synthesis of NO_2PySO_2Phe*

The nitration of hydroxy methyl pyridine **175** was challenging and did only proceed if fuming nitric acid was used. We were surprised that upon heating of the reaction mixture not only the desired mononitrated species was formed. We also observed significant formation of the dinitro compound which is rather unusual for a deactivated pyridine ring. Surprisingly upon prolonged heating also the methyl group got oxidized and decarboxylated yielding 3, 5-dinitropyridin-4-ol as the only product. Finally, best results were obtained by nitrating methyl hydroxy pyridine **175** at 0-5 °C to 20-25 °C for 3 h. The product precipitated out of solution after the reaction mixture was poured on ice. The hydroxy nitro methyl pyridine **177** was then further reacted with phosphoroxy bromide forming the nitro bromo methyl pyridine **174** in very low yield after purification by flash column chromatography. The nucelophilic aromatic substitution with thiophenol was accomplished in quantitative yield. We already noticed during the oxidation of the fluorinated leaving groups that removing electron density from both rings severely hinders the oxidation of the thioether to the sulfone. First, we oxidized the thioether **178** with sodium tungstate and hydrogen peroxide at 20-25 °C for 24 h and found conversions of only 20 %. However, upon heating of the reaction mixture significant amount of the overoxidized by-product (*N*-oxide sulfoxide) was detected. We found that best results were obtained by oxidizing the starting material at 20-25 °C for an extended period of time. After conversion of 50-60 % was reached the reaction started to slow down dramatically and the product was recovered by preparative HPLC. With the compound **179** in hand we tested its reactivity and benchmarked it against the fluoro analogue **156**. We were delighted to see that the nitro compound **179** reacts several order of magnitude faster with our model compound (*N*-acetyl cysteine) than the fluoro compound **156**. Unfortunately we were not able to perform a free radical bromination with the compound **179**. It was, therfore, not possible to synthesize the alpha bromo 3-nitro pyridine 4-phenyl sulfone **176**. However, it was possible to synthesize the methyl thioether **180** and perform a free radical bromination to yield the alpha bromo nitro pyridine methyl sulfide **181**. We chose to perform the free radical bromination before the oxidation to avoid having a too deactivated aromatic system. Compound **181** was then further reacted with three times *tert*-butyllactic acid alkylated M4-cyclen **129**. To our great surprise we found that a nucleophilic substitution did occur on the nitro position and not on the bromo position. It turned out that the nitro position is more reactive. Although, the initial results were promising we were not able to synthesize a nitro analogue of Ln-M7FPySO_2Ph-DOTA.

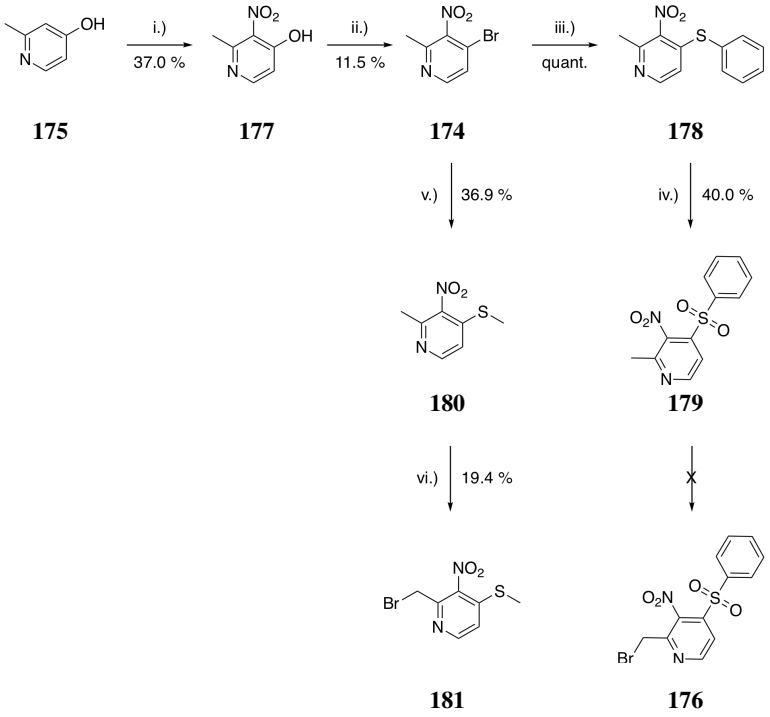

Scheme 46: Synthesis of nitro based linkers **179** and **181**. Reaction Conditions: i.) HNO_3 90 %, H_2SO_4, 0-5 °C - 20-25 °C, 3 h; ii.) $POBr_3$, toluene, reflux, 18 h; iii.) thiophenol, K_2CO_3, DMF, 80 °C, 70 min; iv.) Na_2WO_4, H_2O_2, MeOH, 20-25 °C, 72 °C; v.) $NaSCH_3$, K_2CO_3, DMF, 70 °C, 18 h, NBS, AIBN, CCl_4, reflux, 6 h

8

SYNTHESIS AND APPLICATION OF M7PYTHIAZOL-DOTA

8.1 RETROSYNTHETIC ANALYSIS AND CONSIDERATIONS

Toda *et al*. showed that certain activated hetroaromatic systems like tetrazole, oxadiazole, triazole and benzothiazole are suceptible towards nucleophilic substitutions.[127] Some derivatives achieved similar kinetics than maleimides for the conjugation to cysteines. For our tag design we envisioned to synthesize a methyl substituted benzothiazol analogue, because this molecule is relatively short and rigid. However, for coordination with the lanthanide a coordinating atom is required. Therefore, we planned to replace carbon seven by a nitrogen atom generating a pyridinethiazol (see Scheme 47). A pyridinethiazol should be even more reactive than their corresponding benzothiazol counterparts due to the enhanced delocalization of electron density towards the nitrogen. The target molecule, alpha bromo pyridinethiazol **182**, could be synthesized by forming the intermediate pyridinethiazol via a nucleophilic aromatic substitution of 6-methyl 3-amino 2-bromo pyridine **183** and potassium ethylxanthate (**184**). A subsequent alkylation and oxidation followed by a free radical bromination would produce the required alpha bromo pyridinethiazol **182**.

8.2 SYNTHESIS OF M7PYTHIAZOL-DOTA

Starting from commercially available amino bromo methyl pyridine **183** we synthesized the pyridinethiazol **186** in excellent yield. Nucleophilic substitution with iodomethane was high yielding and after purification by flash column chromatography the methylated intermediate **187** was obtained. We found that our standard oxidizing procedure (sodium tungstate and hydrogen peroxide) offered a very low conversion. We applied mCPBA in dichloromethane instead and obtained full conversion within one hour. This finding was remarkable and might have also been applicable to the more difficult cases obtained earlier. Free radical bromination was carried out and similar yields were obtained. The alkylation with threefold alkylated M4-cyclen **129** progressed similarly and the yields were comparable. However upon aqueous acidic deprotection we found that hydrolysis of the methyl sulfone took place. Therefore, the yield dropped dramatically to 41 % for the deprotection step.

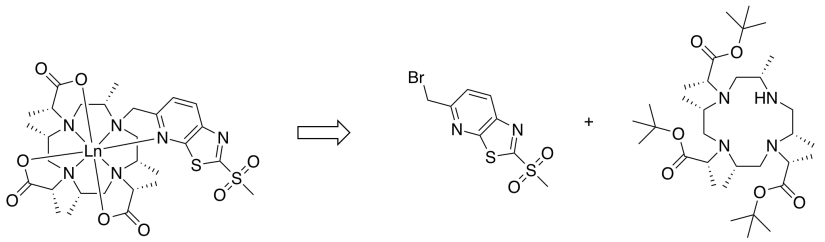

185 **182** **129**

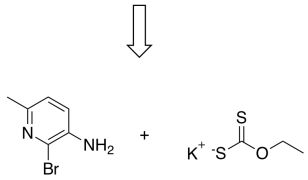

183 **184**

Scheme 47: Retrosynthetic analysis for the synthesis of Ln-M7PyThiazol-DOTA **185**.

The metallation with Ln^{3+} in aqueous ammonium acetate at 80 °C was especially low yielding for Tm whereas Lu performed only slightly worse than for the pyridine based analogues. In this case we also observed hydrolysis during the metallation step. Further study revealed that the target compounds **188** and **189** are not stable in pure water at elevated temperatures. However the thioether compound **187** was very stable and did not hydrolyse under these conditions. Therefore for future synthesis of different lanthanide tags an adopted procedure was used.

In order to avoid the large losses caused by the hydrolysis we performed a free radical bromination on the thioether **187**. The yield for this reaction was significantly lower, however, due to the availability of the inexpensive starting materials this route was further used. Alkylation of the three times alkylated M4-cyclen **129** was performed with similar yields. We found that the yield for the deprotection step was increased by a factor of two. We were delighted to see that metallations with Tb, Dy and Sm were higher yielding and the final oxidation worked smoothly in good yields. This approach offered an increased overall yield and was therefore definitely preferred although an additional reaction step was required.

8.3 TAGGING OF UBIQUITIN S57C AND K48C

Two different ubiqutin mutants S57C and K48C were tagged at 20-25 °C in 10 mM phosphate buffer, 0.45 mM TCEP at pH 7.0. We adjusted the protein concentrations to 150 µM and a fourfold excess of M7FPy-DOTA loaded with Lu, Tm, Dy, and Tb was used. The tagging progress was monitored by

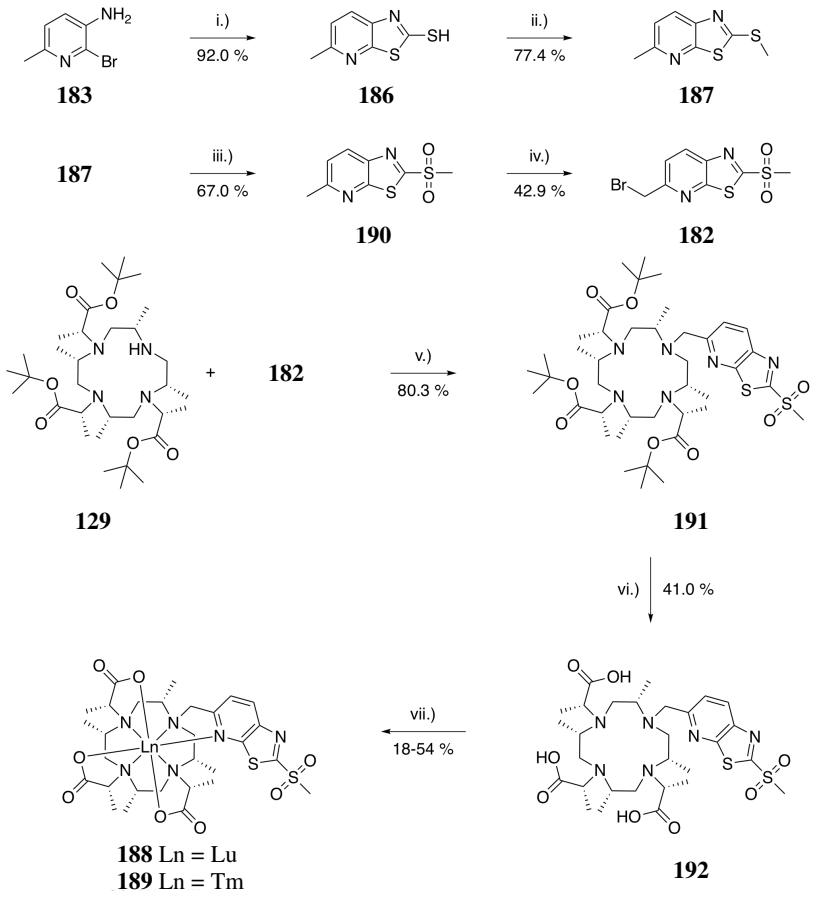

Scheme 48: Synthesis of tags **188** and **189**. Reaction Conditions: i.) potassium ethyl xanthogenate, DMF, 130 °C, 18 h; ii.) CH_3I, K_2CO_3, MeCN, acetone, 20-25 °C, 2 h; iii.) mCPBA, DCM, 0-5 °C - 20-25 °C, 1 h; iv.) NBS, AIBN, CCl_4, reflux, 2.4 h; v.) K_2CO_3, MeCN, 20-25 °C, 18 h; vi.) MeCN, aq. HCl 1 M, 65 °C, 2 h; vii.) Ln^{3+}, aq. NH_4OAc 100 mM, 80 °C, 18 h.

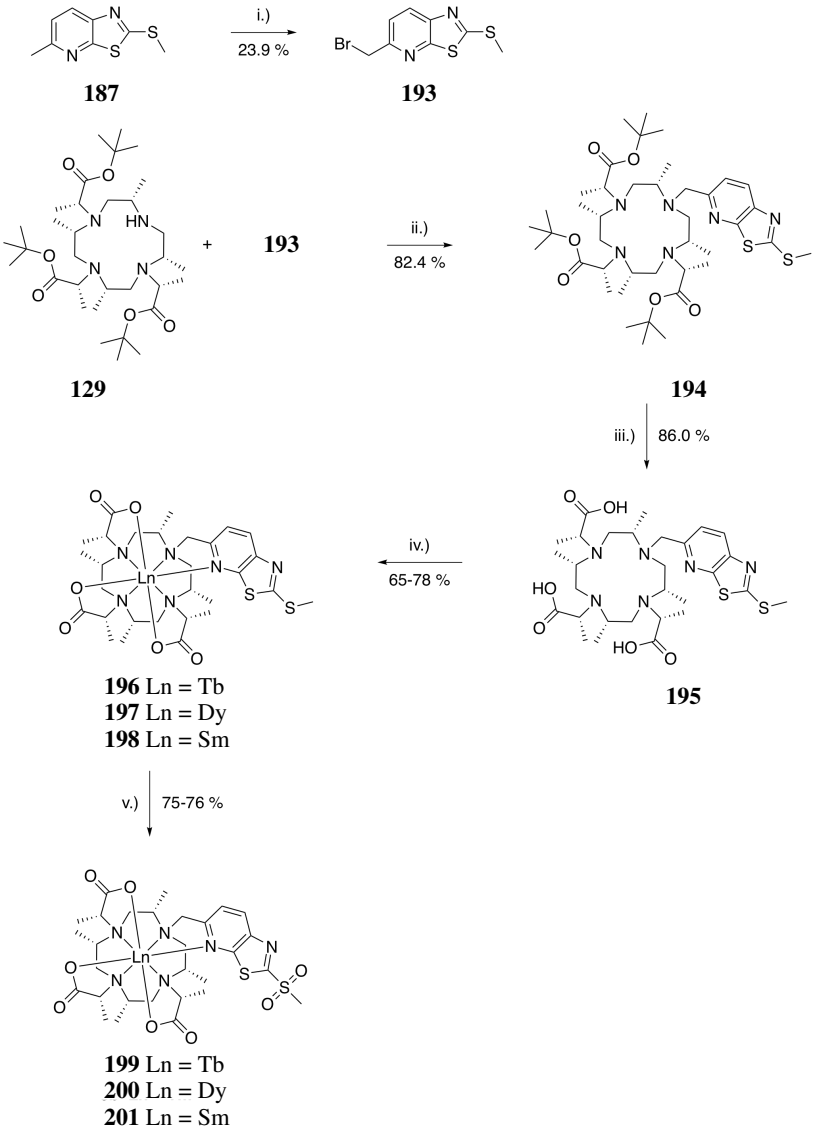

Scheme 49: Synthesis of tags **199** - **201**. Reaction Conditions: i.) NBS, AIBN, CCl_4, reflux, 4 h; ii.) K_2CO_3, MeCN, 20-25 °C, 18 h; iii.) MeCN, aq. HCl 1 M, 65 °C, 2 h; iv.) Ln^{3+}, aq. NH_4OAc 100 mM, 80 °C, 18 h; v.) mCPBA, DCM, 0-5 °C - 20-25 °C, 18 h.

LC-ESI-MS. We were delighted to find that upon addition of the tag within less than five minutes a conversion of more than 80 % and within 15 minutes greater than 95 % was reached (see Figure 8.1).

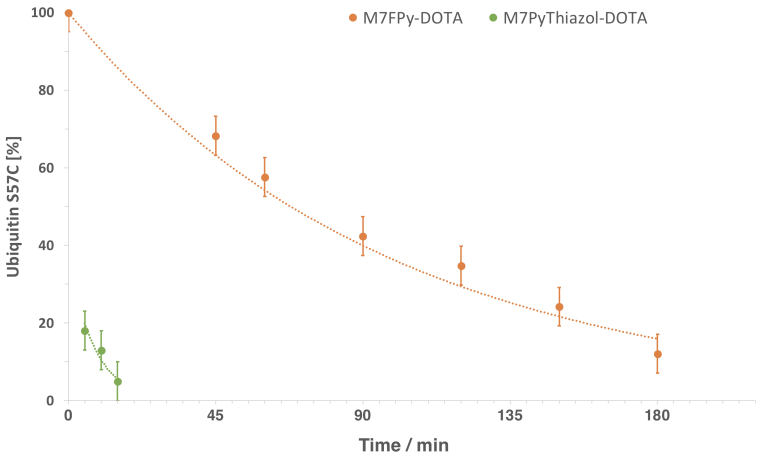

Figure 8.1: Reaction kinetics measured by LC-ESI-MS for M7FPySO_2Phe-DOTA and M7PySO_2MeThiazol-DOTA in 10 mM phosphate buffer pH 7.0 at 20-25 °C. Protein concentrations were adjusted to 150 µM.

To ensure completion of tagging the reaction was prolonged for additional four hours. We knew from the synthesis of the tag that hydrolysis of the tag might occur in aqueous conditions. We found no evidence for the hydrolysed tag, however, we detected the degradation product formed by the tag upon reaction with TCEP. The M7PyThiazol-DOTA as well as the M7FPy-DOTA type tags are more reactive than M7Py-DOTA type tags and thus do react with TCEP. We also incubated ubiquitin S57C samples with M7Pythiazol-DOTA for two days and found that under the applied conditions only cysteines are reactive enough to conjugate to the tag. For example lysine or serine residues did not react with the tag. M7PyThiazol-type tags do release methylsulfinic acid upon conjugation which quickly hydrolyses to SO_2 and methanol. Therefore, no dimerization due to the formation of benzenesulfinic acid should occur. Upon close inspection of the paramagnetic ^{1}H-^{15}N HSQC spectra we found a second unshifted species. We compared the integrals in the 2D HSQC spectra and found that the amount of this species varied between (10-20 %) going from Tm to Dy. This difference in intensity could be attributed to the difference in PRE strength. In order to get a better estimate of the percentage of untagged protein we tagged ubiquitin S57C with Sm-M7PyThiazol-DOTA. Sm has only a weak PRE and therefore the intensity should be affect to a lower extent. Unfortunately most signals also did not shift because Sm has in general only a very small tensor. We found three shifted signals and compared their intensities and found that greater 95 % of the protein was tagged which is in agreement with the LC-ESI-MS measurement. We tried to push the reaction to 100 % by retagging an already tagged sample. We found no significant difference in comparison to the only once tagged samples. The nature of the

untagged species remains unclear. We speculate that to a small degree the cysteine free thiol gets chemically modified (i.e. oxidation or methylation) and is no longer capable of performing a nucleophilic aromatic substitution. Nevertheless tagging efficiencies of greater 95 % are perfectly acceptable for PCS NMR spectroscopy. We could only detect the second species due to the relative small size of ubiquitin. In NMR data obtained from larger proteins this second species will most likely disappear in the noise due to the limited signal-to-noise.

8.4 IN-VITRO NMR ANALYSIS

We recorded 2D ^{1}H-^{15}N HSQC spectra at 600 MHz for both mutants tagged with Lu, Tm, Dy and Tb loaded M7PyThiazol-DOTA. In the case of ubiquitin S57C we found that Tm-M7PyThiazol-DOTA **189** almost exclusively offers positive shifts while Dy-M7PyThiazol-DOTA **200** and Tb-M7PyThiazol-DOTA **199** offer predominately negative shifts. On the other hand for the K48C mutant we observed mixed positive and negative shifts for all three paramagnetic lanthanides. In general we found that terbium and dysprosium both shift in the same direction with dysprosium being stronger while thulium shifts to the opposite. For both mutants we obtained large measurable pseudo-contact shifts reaching up to ten ppm (see Figure 8.2, 8.3, 8.4 and 8.5). We also detected strong cross-peak splitting in 2D ^{1}H-^{15}N IPAP-HSQC spectra due to paramagnetic alignment of ubiquitin and resulting RDC effects (amplitudes reaching 30 Hz at 298 K, 600 MHz).

We determined magnetic susceptibility tensor parameters for both mutants using the program Numbat[74] (see Table 8.1 and 8.2). The tensor are represented in Figure 8.6 and 8.7. The alignment of the tensors main axes with the protein remains constant. The observed tensor for thulium is tilted by 90° in comparison to terbium and dysprosium resulting in shifts going the opposite direction. We found that tensor parameters for terbium are smaller than for dysprosium however their overall shape looks similar. The ratio between the axial and rhombic component of the magnetic susceptibility tensor describes the overall shape of the tensor. In the case of thulium the ratio is very large resulting in an tensor with an overall shape similar to a d_{z^2} orbital whereas the ratio is small for terbium resulting in an overall shape similar to a d_{xy} orbital. We found that the tensor parameters for the Tm-M7PyThiazol-DOTA are twice as large as for Tm-M7FPy-DOTA. This fact shows the great potential of the pyridine thiazol based tags as they only loose roughly 50 % of their intrinsic tensor if measured on the protein if compared to tensor parameters obtained for the free Tm-M7FPySO_2Phe-DOTA **158**.

Upon closer inspection of the two coordination geometries for M7FPy-DOTA and M7PyThiazol-DOTA type tags we concluded that the gain in performance can not simply be explained by the rigidity or the absolute dis-

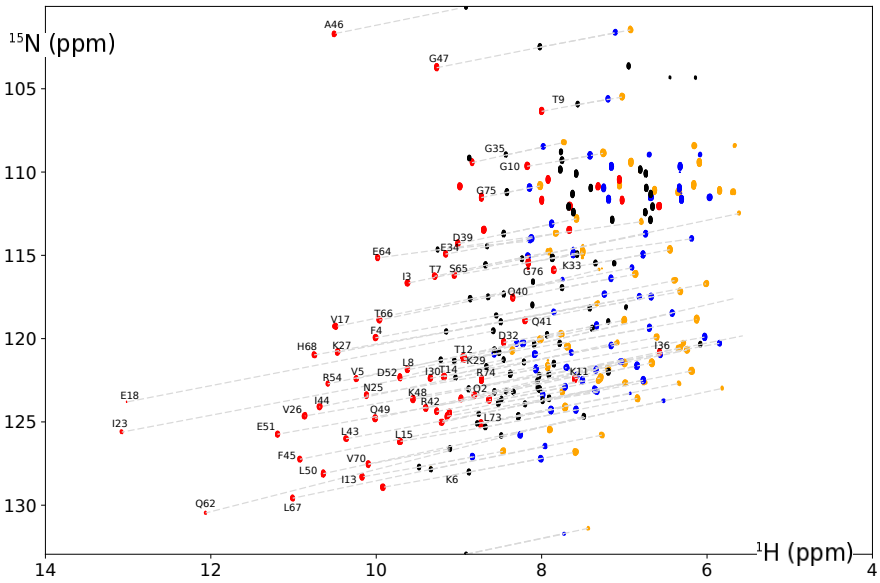

Figure 8.2: *In-vitro* PCS effects by metal-loaded M7PyThiazol-DOTA. Superposition of full 2D ^{1}H-^{15}N HSQC spectra of ubiquitin S57C coupled to diamagnetic Lu-M7PyThiazol-DOTA (black) and paramagnetic Tm-M7PyThiazol-DOTA (red), Tb-M7PyThiazol-DOTA (blue) and Dy-M7PyThiazol-DOTA (orange) at 600 MHz and 298 K. Water signal removed for clarity.

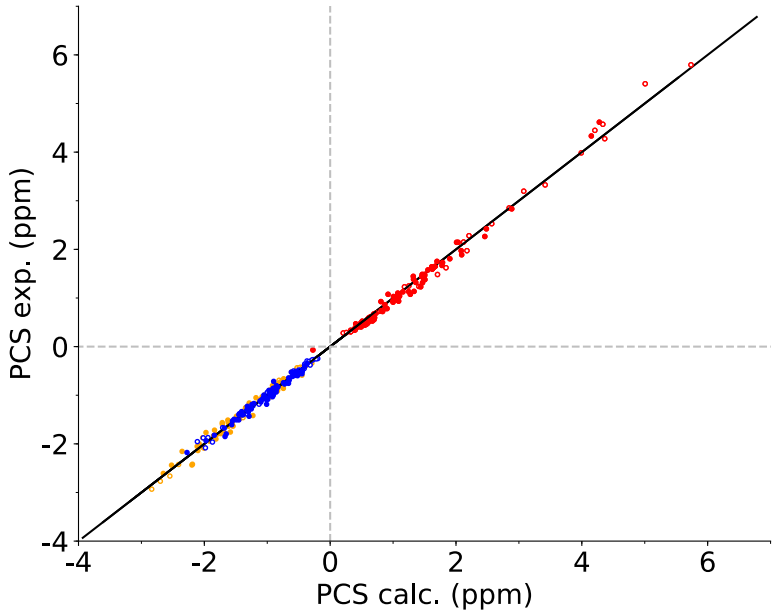

Figure 8.3: Correlation graphs between PCSs calculated from the X-ray structure 1UBI and the experimental *in-vitro* PCSs obtained for Tm-M7PyThiazol-DOTA (red), Tb-M7PyThiazol-DOTA (blue) and Dy-M7PyThiazol-DOTA (orange) at 600 MHz and 298 K on ubiquitin S57C. Hollow markers indicate PCSs not used during the fit displayed in Table 8.1.

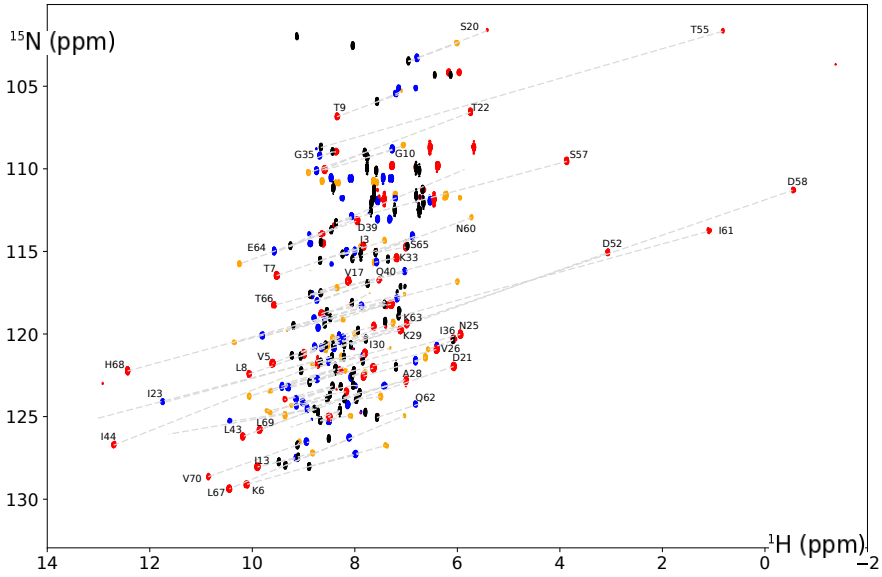

Figure 8.4: *In-vitro* PCS effects by metal-loaded M7PyThiazol-DOTA. Superposition of full 2D ^{1}H-^{15}N HSQC spectra of ubiquitin K48C coupled to diamagnetic Lu-M7PyThiazol-DOTA (black) and paramagnetic Tm-M7PyThiazol-DOTA (red), Tb-M7PyThiazol-DOTA (blue) and Dy-M7PyThiazol-DOTA (orange) at 600 MHz and 298 K. Water signal removed for clarity.

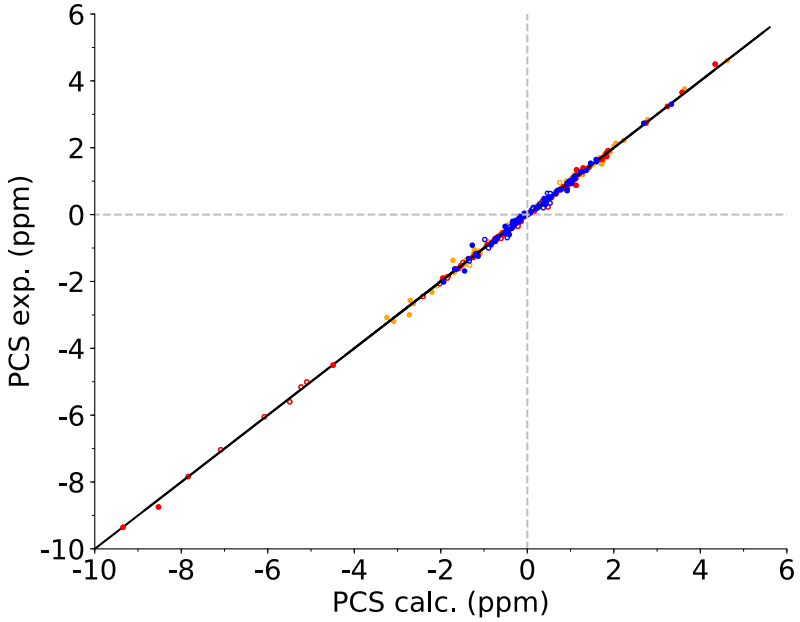

Figure 8.5: Correlation graphs between PCSs calculated from the X-ray structure 1UBI and the experimental *in-vitro* PCSs obtained for Tm-M7PyThiazol-DOTA (red), Tb-M7PyThiazol-DOTA (blue) and Dy-M7PyThiazol-DOTA (orange) at 600 MHz and 298 K on ubiquitin K48C. Hollow markers indicate PCSs not used during the fit displayed in Table 8.2.

Table 8.1: *In-vitro* PCS tensor parameters for ubiquitin S57C fitted against the ubiquitin X-ray structure (PDB code: 1UBI).

	Tm, 74 PCS	Dy, 66 PCS	Tb, 72 PCS
$\Delta\chi_{ax}$ / $10^{-32}m^3$	35.4 (0.6)	41.9 (0.8)	30.8 (1.1)
$\Delta\chi_{rh}$ / $10^{-32}m^3$	11.3 (0.7)	26.1 (0.5)	19.6 (0.7)
x / Å	20.5 (0.2)	20.5 (0.2)	20.5 (0.2)
y / Å	15.1 (0.1)	15.1 (0.1)	15.1 (0.1)
z / Å	6.3 (0.2)	6.3 (0.2)	6.3 (0.2)
α / °	50.3 (1.6)	145.9 (1.3)	146.5 (0.9)
β / °	44.0 (0.9)	84.3 (1.1)	84.5 (1.3)
γ / °	17.9 (3.0)	138.4 (2.6)	132.0 (4.1)

Tensor parameters (errors) were calculated in Numbat[74] from the indicated number of selected PCS. All tensors are represented in the unique tensor representation UTR. Only amino acids residing in a stable secondary structure (2-7, 12-16, 23-34, 38-40, 41-45, 48-49, 56-59 and 66-71) were used if present in the spectra.

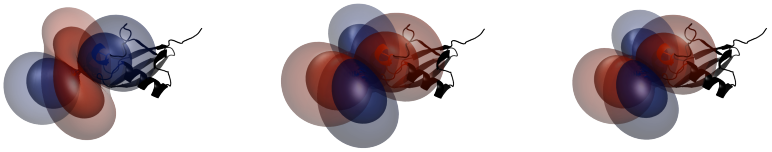

(a) Tm (b) Dy (c) Tb

Figure 8.6: Tensor representation of Tm, Dy and Tb-M7PyThiazol-DOTA tagged to ubiquitin S57C. The red isosurfaces indicate a shift of -3 ppm (inner) and -1 ppm (outer). The blue isosurfaces indicate the corresponding positive shift.

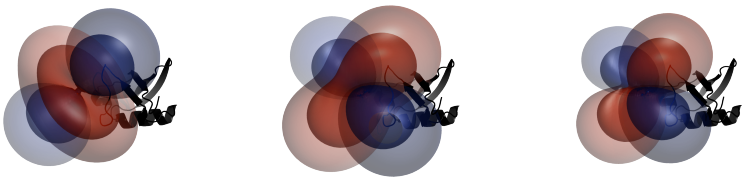

(a) Tm (b) Dy (c) Tb

Figure 8.7: Tensor representation of Tm, Dy and Tb-M7PyThiazol-DOTA tagged to ubiquitin K48C. The red isosurfaces indicate a shift of -3 ppm (inner) and -1 ppm (outer). The blue isosurfaces indicate the corresponding positive shift.

Table 8.2: *In-vitro* PCS tensor parameters for ubiqutin K48C fitted against the ubiqutin X-ray structure (PDB code: 1UBI).

	Tm, 70 PCS	Dy, 70 PCS	Tb, 72 PCS
$\Delta\chi_{ax}$ / $10^{-32}m^3$	47.4 (1.7)	58.0 (2.0)	36.0 (1.3)
$\Delta\chi_{rh}$ / $10^{-32}m^3$	8.3 (1.3)	24.6 (1.0)	21.8 (0.9)
x / Å	19.0 (0.2)	19.0 (0.1)	19.0 (0.1)
y / Å	18.6 (0.2)	18.6 (0.1)	18.6 (0.1)
z / Å	22.8 (0.1)	22.8 (0.1)	22.8 (0.1)
α / °	88.3 (0.5)	8.5 (0.5)	7.1 (0.4)
β / °	81.5 (1.1)	71.2 (0.8)	70.7 (1.1)
γ / °	143.9 (2.1)	178.2 (2.5)	5.0 (1.1)

Tensor parameters (errors) were calculated in Numbat[74] from the indicated number of selected PCS. All tensors are represented in the unique tensor representation UTR. Only amino acids residing in a stable secondary structure (2-7, 12-16, 23-34, 38-40, 41-45, 48-49, 56-59 and 66-71) were used if present in the spectra.

tance from the metal to the protein. The rigidity is in both cases very similar as there is only on rotatable bond between the tag and the cysteine. In addition the relative distance from the metal center to the attachment point is almost identical (5.4 Å to 5.6 Å). Therefore we hypothesize that the difference most likely originates from the different axis of rotation with respect to the protein (see Figure 8.8). The alignment of the tensors principle z-axis with the rotatable bond axis is much better for M7PyThiazol-DOTA than for M7FPy-DOTA. This presumably causes smaller averaging effects of the tensors anisotropy especially for the axial component. A rotation around the linkage cases larger averaging effects for M7FPy-DOTA than for M7PyThiazol-DOTA due to the higher probability of crossing a node plane of the tensor. In ideal cases the rotation occurs around the tensors principle z-axis causing only averaging effects to the rhombic component of the anisotropy tensor.

8.4.1 *Determination of the absolute configuration for M7PyThiazol*

The configuration of the basal 4(*S*)-M4-cyclen is locked in ($\delta\delta\delta\delta$) configuration as there is no possibility to form a ($\lambda\lambda\lambda\lambda$) tag because the four methyl group on the base ring would need to adopt a sterically very unfavourable axial position. However, for the side arms two configurations are possible: Δ counter-clockwise and Λ clockwise. Both configurations are possible for (8*S*)-M8-DOTA tags and their relative percentage varies with the size of the lanthanide having a 27/73 ratio for Dy.[95] During our tagging experiments we observed no second set of shifted signals for Dy-M7PyThiazol-DOTA. Further investigations of the Lu-M7PyThiazol-DOTA and Sm-M7PyThiazol by

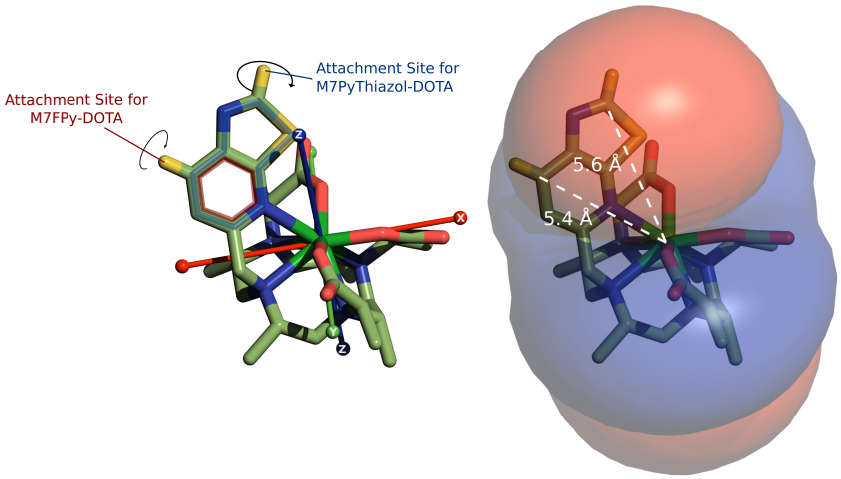

Figure 8.8: Different attachments sites for M7FPy-DOTA and M7PyThiazol-DOTA.

NMR clearly showed that both complexes adopt the Λ configuration. Therefore we concluded that all complexes between Sm and Lu and most likely the whole lanthanide series adopts a Λ configuration with the M7PyThiazol-DOTA ligand. In addition we fitted the magnetic susceptibility tensor for the Sm-M7PyThiazol-SO_2Me-DOTA and found a correlation coefficient of 0.905 for the Δ and 0.987 for the Λ configuration. In addition in NOESY spectra we only observe NOEs between the side arm methyls and one of the methyls from the base ring (see Figure 8.9). If the structure would be Δ configured we would expect to either observe none or two NOEs between the side arm methyls and the base ring methyls, because both distances are almost identical, whereas in the Λ case one group of methyls is significantly closer than the other resulting in one observed NOE.

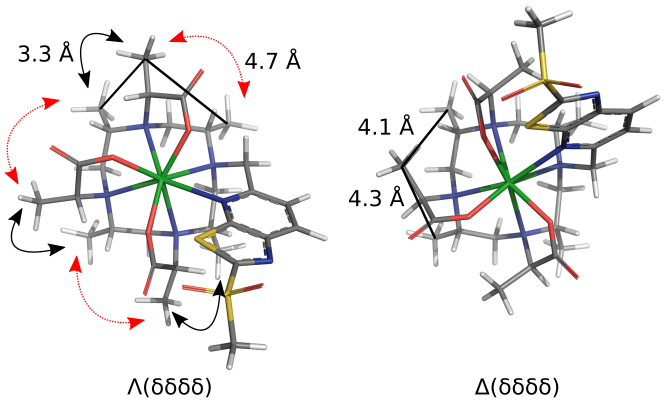

Figure 8.9: Possible conformations for M7PyThiazol-DOTA calculated using DFT.

9

CONCLUSION AND OUTLOOK

9.1 CONCLUSION

It could be shown that nucleophilic aromatic substitution is suitable for protein tagging reactions. Our first attempt, the pyridine phenyl sulfone based tag, was successfully applied to tag GB1 and recording *in-cell* pseudocontact shifts. The structure of GB1 could be calculated using the Rosetta approach with the addition of pseudocontact shifts and residual dipolar couplings. The initial reaction rate was slow and tagging required high temperature for prolonged time. We demonstrated that increasing the acidity of the leaving group has a negligible influence on the overall reaction rate. However, the introduction of an electron withdrawing group on the coordinating pyridine ring, nitro or fluorine, increased the reactivity of the linker towards nucleophilic displacement by thiols significantly. The fluoropyridine phenyl sulfone could be successfully installed on the DOTA framework forming the M7-FPy-DOTA tag. The reactivity of this tag was significantly improved, and the conjugation proceeded at room temperature within six hour. The complex kinetics we observed were primarily due to the formation of benzenesulfinc acid which catalysed protein dimerization. A sulfonamide as well as aliphatic sulfones were tested as leaving groups but they showed significantly lower reaction rates. Although our initial experiments with the fluorine substituted phenyls as leaving groups clearly demonstrated that an increase in acidity does not speed up the reaction it was still crucial for the leaving group to be of aromatic nature. The problem could be avoided using the much more reactive pyridine thiazol which is highly reactive towards nucleophilic aromatic substitution especially in the two position. The pyridine thiazol allowed us to use methylsulfinic acid as leaving group, which relatively quickly hydrolyses in aqueous solution. The tagging reaction with M7-PyThiazol-DOTA is extremely fast at room temperature under physiological conditions offering a complete tagging (>95 %) within less than one hour. M7FPy-DOTA and M7PyThiazol-DOTA were both tested on ubiquitin mutants and it could be shown that pyridine thiazol based tags are far superior to the relatively similar fluoro pyridine tags not only in reaction speed but also with respect to the size of observable pseudocontact shifts.

9.2 OUTLOOK

Future experiments should focus on the development of pyridine thiazol based tags as they are highly reactive and provide large tensor parameters. In future experiments it should be investigated what the nature of the second species present in all ubiquitin samples is. Applications to larger proteins should show whether this is a significant issue or not, as small concentrations of untagged protein usually disappear in the background noise. Up to now it remains an open question if tagging would also be possible at lower temperatures (5 °C). In general, we showed that tagging at pH 7.00 does not cause tagging of unwanted residues like serine or lysine, however, the highest pH possible without tagging unwanted amino acid residues has not been determined. Our prospective experiments with the M7-azaxanthon-DOTA (see Part III) showed that DOTA based tags potentially could be used for FRET experiments, if a UV harvesting antenna is installed. Future experiments could reveal if pyridine thiazol or fluoro pyridine -based DOTA tags are suitable for FRET, as some of the complexes (especially Tb and Eu) are highly luminescent under UV light irradiation at 366 nm (see Appendix for UV/VIS absorption and emission spectra of Tb-M7PyThiazol-DOTA).

Part III

MISCELLANEOUS

This part of the thesis focuses on smaller side-projects involving the usage of lanthanide chelating tags.

10

MISCELLANEOUS

10.1 PROSPECTIVE INVESTIGATIONS OF DOTA-TYPE COMPLEXES FOR FRET ANALYSIS.

Apart from being excellent shift reagents, lanthanide complexes can also serve as valuable probes for FRET spectroscopy. Luminescent lanthanide complexes have unique spectroscopic properties. They are a result of transitions within the 4f-orbitals. These transitions are symmetry forbidden electronically induced dipole transitions. This leads to very narrow and well separated emissions bands and extremely long excited-state lifetimes of up to milliseconds. Most lanthanide ions have a very low extinction coefficient in aqueous solutions due to the very efficient quenching with coordinating water molecules. However many chelating ligands have been developed to shield the lanthanide ion from solvent influences. The emission bands for terbium and europium lie in the visible range and therefore, they are used most often. Nevertheless, dysprosium, samarium and thulium also emit in the visible range but with lower intensity. Considering the strength of the measurable pseudocontact shifts terbium should be preferred for a combination tag, i.e. suitable for both applications simultaneously.[128,129] However our initial experiments focused on europium which is more common for FRET applications than terbium. Europium also exhibits smaller PREs and thus is better suited for NMR analysis.

10.1.1 *Synthesis and photoluminescence study of Eu-DOTA, Eu-M4-DOTA and Eu-DOTA*

In order to test the photophysical properties of our M8-SSPy-DOTA tag we synthesized the model compound **202** and its lesser rigidified analogues **203** and **204** (see Scheme 50). The synthesis of Eu-M8-DOTA **202** started from M4-cyclen **22** while the other two ligands **205** and **206** were commercially available and used as obtained. We performed metallation using europium triflate in aqueous ammonium acetate at 80 °C for 18 h. The yields were significantly higher for the less substituted ligands presumably due to the lower steric hindrance during the metallation step. We studied the photophysical properties of these three complexes and found no visible luminescence on irradiation with UV light at 254 nm and 366 nm. All these complexes lack a

functional group which could act as UV-light harvesting antenna.

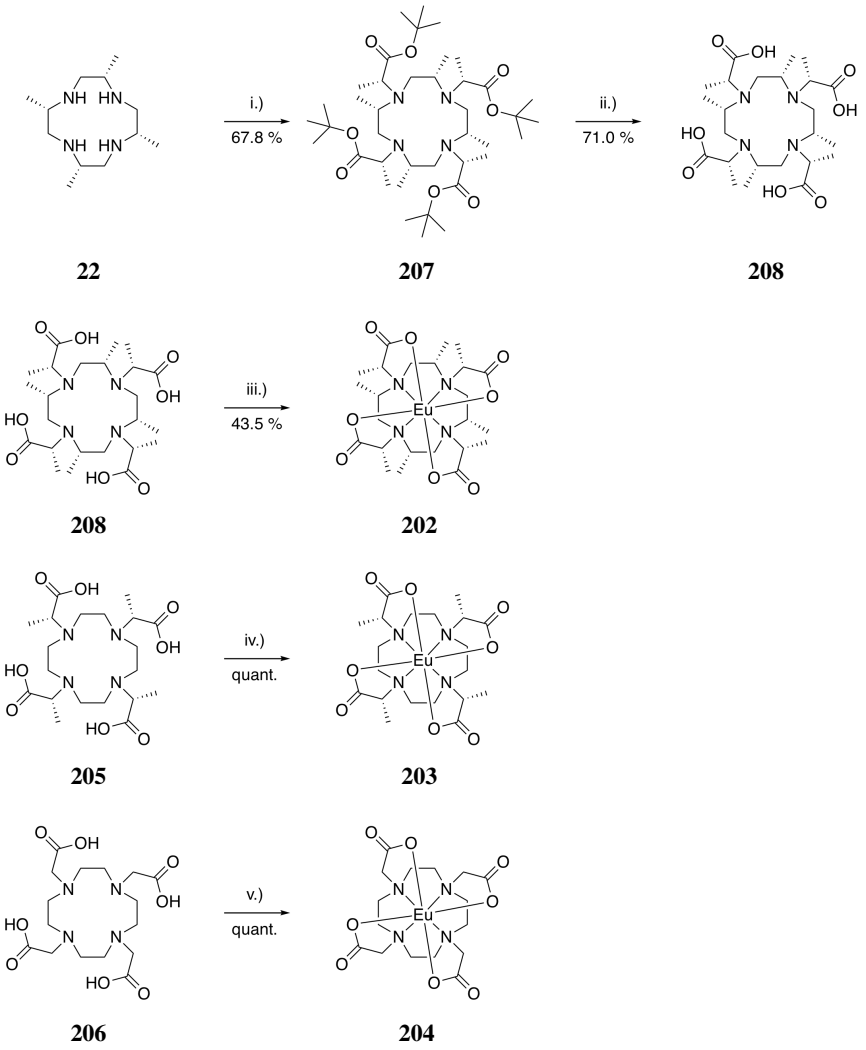

Scheme 50: Synthesis of Eu-complexes **202**, **203** and **204**. Reaction Conditions: i.) K_2CO_3, MeCN, 20-25 °C, 6 h; ii.) TFA, water, MW: 120 °C, 30 min; iii.) / iv.) / v.) Eu^{3+}, aq. NH_4OAc 100 mM, 80 °C, 18 h

10.1.2 *Synthesis and photoluminescence study of Eu-Azaxanthon-M7-DOTA*

It has been shown on DOTA-based tags that the installation of an azaxanthon leads to emissive lanthanide complexes.[130,131] We synthesized Eu-M7-azaxanthon-DOTA **209** for further photophysical studies. The azaxanthon **210** was prepared from commercially available 6-methyl-2-chloronicotinic acid (**211**) and methyl-4-hydroxybenzoate (**212**) followed by an intramolecular condensation (see Scheme 51). The free radical bromination of compound **210** was very slow and a reaction time of four days was required to achieve

a conversion of 70 %. The desired monobromide **213** was isolated by flash column chromatography and reacted with the three times alkylated M4-cyclen **129**. Subsequent deprotection and metallation yielded the desired europium complex **209**.

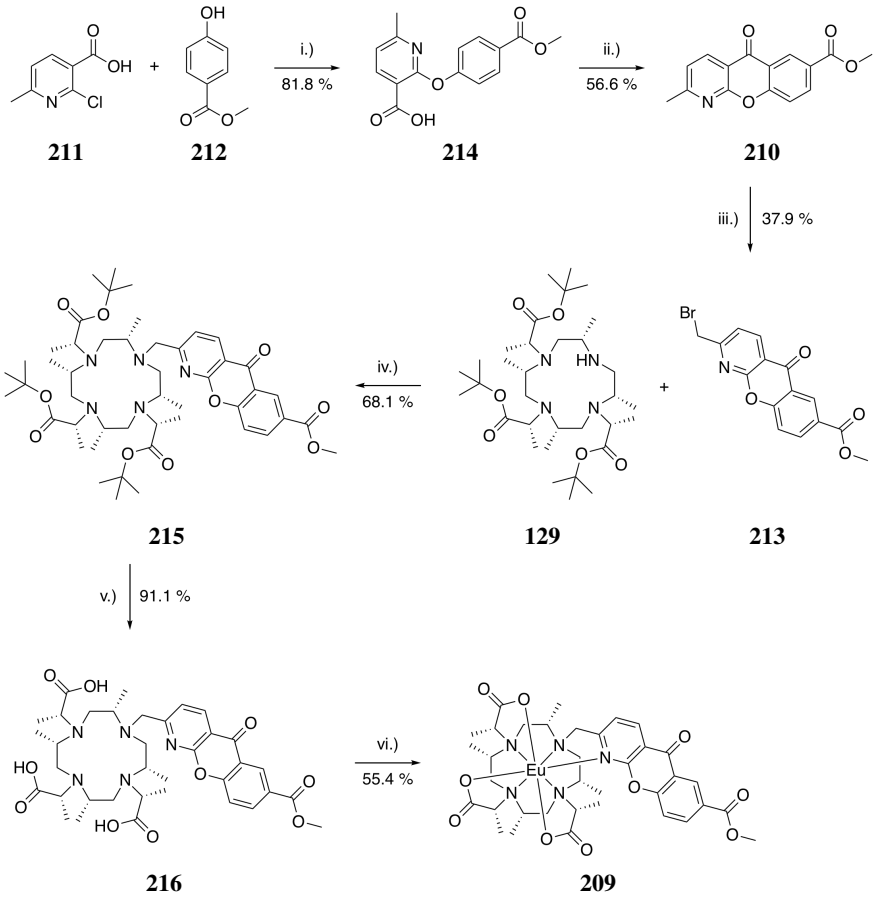

Scheme 51: Synthesis of compound **209**. Reaction Conditions: i.) NaOMe, neat, 125 °C, 24 h; ii.) polyphosphoric acid, 120 °C, 18 h; iii.) NBS, AIBN, CCl_4, reflux, 4 d; iv.) K_2CO_3, MeCN, 20-25 °C, 18 h; v.) TFA, 20-25 °C, 7 h; vi.) Eu^{3+}, aq. NH_4OAc 100 mM, 80 °C, 18 h

We measured UV/Vis absorption and emission spectra of Eu-Azaxanthon-M7-DOTA **209** (see Figure A.6) and we found that the complex absorbs in the UV range with maxima at 248 nm, 289 nm and 334 nm. Very typical for europium complex we found one very strong and narrow emission band at 614 nm corresponding to the $^5D_0 \rightarrow {}^7F_2$ transition. This preliminary results clearly indicate that M7-DOTA-based tags could potentially be used for FRET analysis if and only if they are conjugated to a UV harvesting antenna molecule.

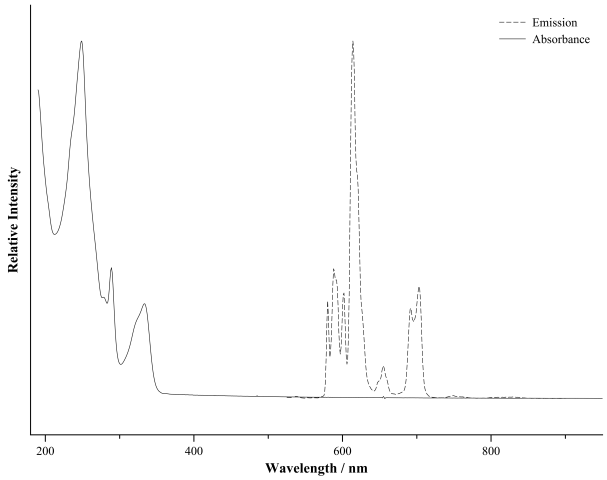

Figure 10.1: UV/Vis absorption and emission spectrum of Eu-Azaxanthon-M7-DOTA **209** measured in acetonitrile at 20-25 °C. λ_{ex}=250 nm.

10.2 CONJUGATION OF M8-DOTA TO SMALL MOLECULES

10.2.1 *Conjugation of M8-DOTA to polyproline*

This section describes a collaboration project with Dr. Marc-Olivier Ebert from the ETH Zurich. The Ebert group was interested in studies of a polyproline hexamer. Due to the relative small chemical shift range an assignment is difficult to obtain. We therefore envisioned that conjugation of a M8-DOTA paramagnetic tag to the *N*-terminus via an amide bond should greatly increase the observable chemical shift range. We received the Fmoc-protected polyproline **217** polymer bound. Starting from the Fmoc-protected polyproline polymer bound we first performed a deprotection step with piperidine in dimethylformamide following standard solid phase synthesis procedure (see Scheme 52). After deprotection we performed a HATU mediated peptide coupling with the free acid **218** of M8-DOTA. To our surprise we detected no conjugation to the polyproline. We found that during this reaction the free acid side-arm got cleaved off forming compound **129**. Further investigations showed that it was possible to conjugate Cbz-alanine **24** to polyproline and it was also possible to conjugate *tert*-butyl alanine **25** to the free acid **218** of M8-DOTA. Therefore, we conclude that only the combination of the anilin **219** and the free acid **218** of M8-DOTA was problematic. Future experiments should be conducted with a terminal alanine or glycine on the polyproline side.

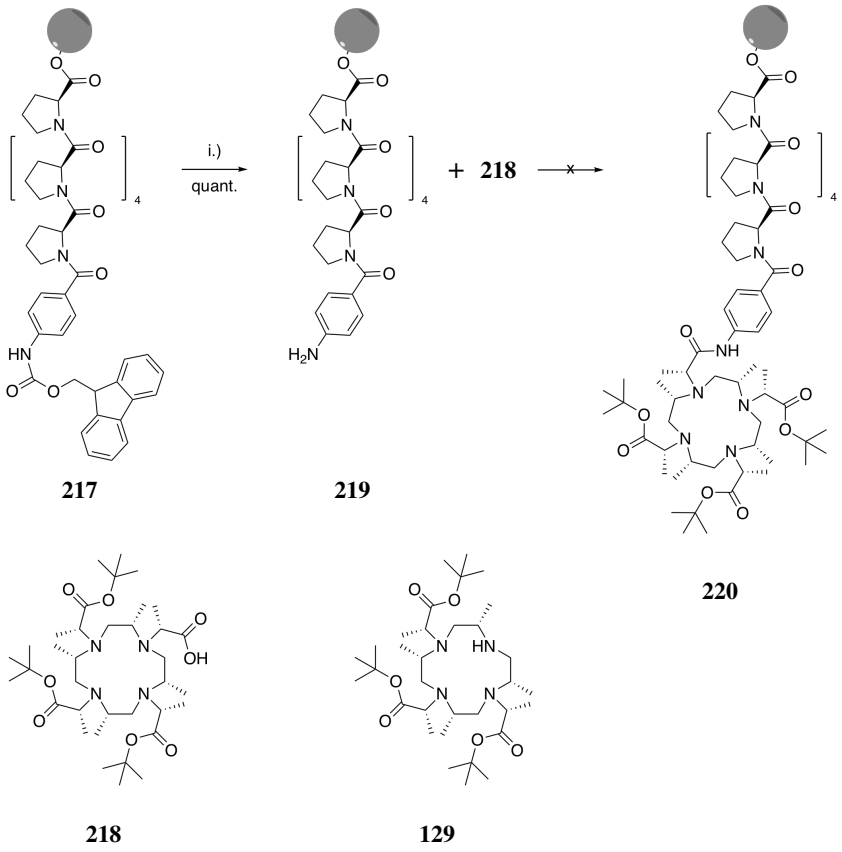

Scheme 52: Reaction Conditions: i.) Piperidine, DMF, 20-25 °C, 30 min.

10.2.2 *Conjugation of M8-DOTA to Pittsburgh compound B*

This section describes a collaboration project with Dr. Carlos Geraldes from the university of Coimbra. Their research focused on the Pittsburgh compound B (PiB) which has been used as amyloid affinity probe for the *in-vivo* positron emission tomography detection of amyloid beta deposits in the brain caused by Alzheimer's disease.[132,133] The key idea was to produce a M8-DOTA-PiB conjugate which efficiently binds to Gd^{3+} or Ga^{3+} and has a positive logP in order to be able to cross the blood-brain barrier. Our study focused on the conjugation of M8-DOTA to PiB and the formation of a Gd^{3+} complex. We received samples of the free amine with a C6 and C10 linker. We coupled the free amine **221** with the C6 linker to the free acid **218** of M8-DOTA and deprotected the *tert*-butyl groups with hydrogen bromide solution in acetic acid. The free ligand **222** was not soluble in water and the metallation was conducted in dimethylformamide (see Scheme 53). The final product was purified by preparative HPLC and sent back for further studies. We also tried the same procedure for the C10 analogue but all yields were significantly lower and the final metallation step failed.

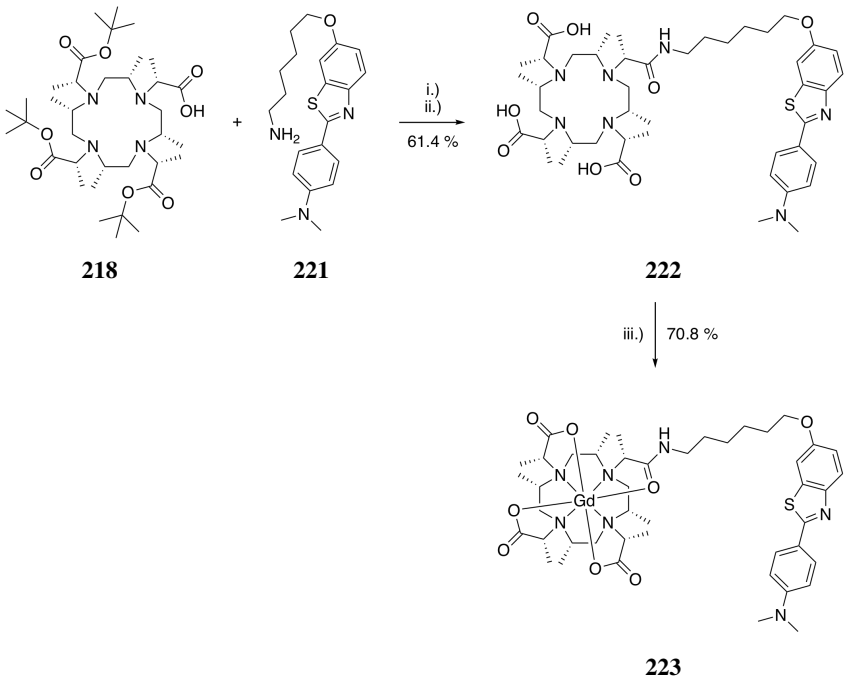

218 **221** **222** **223**

Scheme 53: Synthesis of compound **223**. Reaction Conditions: i.) HATU, DIPEA, MeCN, 20-25 °C, 1 h; ii.) HBr in AcOH, 40 °C, 20 min.

10.3 PROSPECTIVE INVESTIGATIONS FOR A DOTA-TYPE TAG SUITABLE FOR PCS NMR SPECTROSCOPY ON RNA

Generating pseudocontact shifts on a DNA or RNA most often requires conjugation of the tag to the backbone. Wu *et al.*[134] showed that DOTA-type tags can be conjugated to a phosphorothioate group. If this group resides in between the backbone two diastereomers are formed. Avoiding the formation of two diastereomers would only be possible upon conjugation of the tag to a terminal phosphorothioate group. However, attaching a tag at the end will most likely result in a very flexible and highly mobile tag which generates only little PCS.

10.3.1 *Design and Synthesis of a π-π stacking linker*

We envisioned that a biphenyl linker could provide additional non-covalent interactions to stabilize the tag in one specific location (see Figure 10.2). We proposed that such a tag could be easily synthesized by reaction of Ln-M7FPy-DOTA with an excess of 4,4′-Bis(mercaptomethyl)biphenyl followed by the activation with 2,2′-Dithiodipyridine.

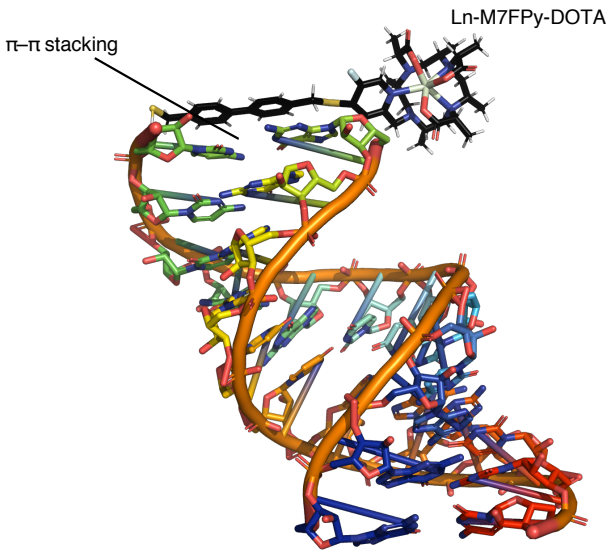

Figure 10.2: Representation of the envisioned interaction between the biphenyl linker and the last base pair.

We first synthesized the paramagnetic Tm-M7-FPy-S-Biphenyl-SSPy-DOTA **224** starting from Tm-M7FPy-DOTA **158**. The phenyl sulfone was substituted and the intermediate product was purified by preparative HPLC

and further activated with 2,2′-Dithiodipyridine in an overall yield of 24 % (see Scheme 54). The yields were low, especially for the nucleophilic aromatic substitution. Although we used a large excess of the thiol, the dimerized compound could still be detected. Nevertheless, the tag could be synthesized and the identity was confirmed by HR-ESI-MS. Further experiments should reveal its potential for PCS NMR spectroscopy of DNA and or RNA.

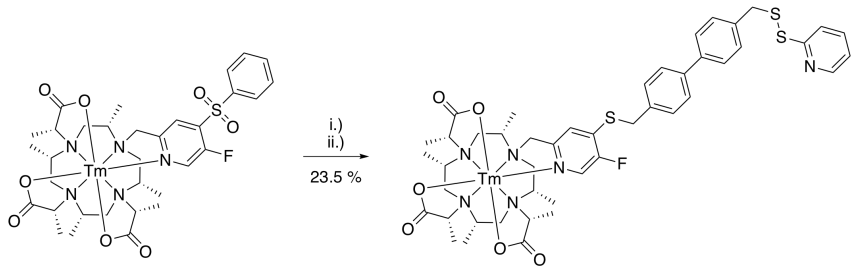

158 **224**

Scheme 54: Synthesis of compound **224**. Reaction Conditions: i.) 4,4′-Bis(mercaptomethyl)biphenyl, K_2CO_3, MeCN, 2 h, 20-25 °C; ii.) 2,2′-Dithiodipyridine, AcOH, MeOH, 2 h, 20-25 °C.

Part IV

EXPERIMENTAL PART

11

METHODS AND MATERIALS

REAGENTS

All chemicals were used as purchased without further purification if not stated otherwise.

NMR SPECTROSCOPY

All NMR experiments were performed at 298 K if not stated otherwise.

Small molecules

NMR 250 MHz, 400 MHz and 500 MHz experiments were performed on a Bruker Avance III NMR spectrometer equipped with a direct observe 5 mm BBFO smart probe. NMR 600 MHz experiments were either recorded on a Bruker Avance III NMR spectrometer equipped with a direct observe 5 mm BBFO smart probe or on a Bruker Avance III HD NMR spectromete equipped with a cryogenic 5 mm four-channel QCI probe (H/C/N/F). NMR samples were purified by preparative HPLC and stabilized with trifluoroacetic acid if needed.

Protein Samples

GB1 protein NMR samples were recorded in 20 mM phosphate buffer pH 7.00. All ubiquitin samples were recorded in 10 mM phosphate buffer pH 6.00. All spectra were either recorded on a Bruker Avance III NMR spectrometer equipped with a direct observe 5 mm BBFO smart probe or on a Bruker Avance III HD NMR spectrometer equipped with a cryogenic 5 mm four-channel QCI probe (H/C/N/F).

MS SPECTROSCOPY

Small organic molecules were measured on a Bruker Daltonics Esquire 3000 plus spectrometer using concentrations between 1-10 µg mL^{-1} in methanol or acetonitrile with 0.1 % trifluoroacetic acid or using the direct injection mode

of the analytic HPLC-ESI-MS.

HR-ESI-MS spectra were measured on a Bruker MaXis 4G HiRes ESI Mass Spectrometer using concentrations between 1-10 µg mL^{-1} in methanol or acetonitrile with 0.1 % trifluoroacetic acid.

HPLC-ESI-MS

A Shimadzu LC 20 System equipped with a Shimadzu Fraction Collector (FRC-10A) and a Shimadzu LSMS-2020 was used. Oven temperature was set to 40 °C.

Analytical method

- Column: ReprosilPur120 ODS-3 3 µm 150x3 mm
- Solvent A: Water + 0.1 % TFA
- Solvent B: 90 % Acetonitrile + 10 % water + 0.085 % TFA.
- Flow rate: 1.0 ml/min
- UV Detector: set to 254 and 280 nm
- Gradient: 2 minutes at 5 % B followed by a gradient over 4 min from 5 % B to 100 % B. These conditions were kept for 8 min followed by a gradient from 100 % B to 5 % B over 1 min. These conditions were kept constant for another 7 min.
- ESI-MS: positive mode 100-1500 m/z.

Preparative method

- Column: Reprosil-Pur 120 ODS-3 5 µm 30x20 mm
- Solvent A: Water + 0.1 % TFA
- Solvent B: 90 % Acetonitrile + 10 % water + 0.085 % TFA.
- Flow rate: 10.0 ml/min
- UV Detector: set to 254 and 280 nm
- Gradient: 2 minutes at 5 % B followed by a gradient over 7 min from 5 % B to 100 % B. These conditions were kept for 7 min followed by a gradient from 100 % B to 5 % B over 1 min. These conditions were kept constant for another 2 min.
- ESI-MS: positive mode 100-1500 m/z.
- Fraction Collector sample volume: 5-10 mL

HPLC

A Waters Prep LC 4000 System equipped with a Waters 2487 Dual Absorbance Detector and a Waters 740 Data Module was used.

Preparative method

- Column: Reprosil-Pur 120 ODS-3 5 µm 30x20 mm
- Solvent A: Water + 0.1 % TFA
- Solvent B: 90 % Acetonitrile + 10 % water + 0.085 % TFA.
- Flow rate: 10.0 ml/min
- UV Detector: set to 254 and 280 nm
- Gradient: 2 minutes at 10 % B followed by a gradient over 20 min from 10 % B to 50 % B. These conditions were kept for 3 min followed by a gradient from 50 % B to 100 % B over 10 min. These conditions were kept constant for another 10 min before the column was equilibrated to the starting conditions.
- Fraction Collector sample volume: 10-20 mL

UV-VIS SPECTROSCOPY

UV-VIS spectra were recorded on an Agilent Technologies UV-Visible 8453 spectrophotometer in HPLC-grade solvents.

PHOTOLUMINESCENCE

The photoluminescence measurements were performed on a Shimadzu RF-5301PC spectrofluorophotometer or on a Fluorolog Horiba Jobin Yvon spectrofluorophotometer.

PROTEIN TAGGING

All protein samples were incubated for 1-18 h in a 10 mM phosphate buffer pH 7.00 with 2 mM TCEP. The buffer was exchanged by means of serial ultrafiltration (3x) in 10 mM phosphate buffer, 0.45 mM TCEP at pH 7.0 (Amicon Ultra-4, MWCO 3 kDa, Millipore). Protein tagging reactions were carried out in 10 mM phosphate buffer pH 7.00 at 20-25 °C for 2-24 h. The protein concentration was adjusted to 100-150 µM and a 4-6 fold excess of tag was used. Protein samples were shaken in a Thermo-Shaker Grant-bio.

GB1 protein samples were tagged in 50 mM phosphate buffer pH 7.6, 0.5 mM TCEP at 40-45 °C and protein concentrations were adjusted to 300 µM.

DFT CALCULATIONS

DFT calculations were performed at sciCORE (http://scicore.unibas.ch/) scientific computing core facility at University of Basel. All lanthanide containing complexes were geometry optimized using ORCA[135,136] the SARC2[137] basis set, BP86 functional and the zeroth order regular approximation (ZORA).

CENTRIFUGATION

Centrifugation steps were carried out using a Hettich Universal 320 R centrifuge at 7380 rpm (6750 g).

12

EXPERIMENTAL PART

tert-BUTYL ((BENZYLOXY)CARBONYL)-*L*-ALANYL-*L*-ALANINATE (**26**).

N-Benzyloxycarbonyl-*L*-alanine (12.3 g, 55.1 mmol, 1.0 eq.) and HATU (23.0 g, 60.6 mmol, 1.1 eq.) were suspended in acetonitrile (100 mL). *N*-ethyl diisopropylamine (7.85 g, 60.6 mmol, 1.1 eq.) was added and the mixture turned to a yellow solution. A solution of *L*-alanine *tert*-butyl ester hydrochloride (10.0 g, 55.1 mmol, 1.0 eq.) and *N*-ethyl diisopropylamine (7.85 g, 60.6 mmol, 1.1 eq.) in acetonitrile (100 mL) was added while maintaining the temperature between 20-25 °C. The yellow solution was stirred for 3.5 h and then evaporated to dryness yielding a dark yellow oil. This oil was dissolved in ethyl acetate (200 mL) and extracted with aqueous citric acid (10 %, 4x 50 mL), aqueous saturated sodium hydrogen carbonate (2x 50 mL) and brine (50 mL). The organic layer was dried with sodium sulphate and evaporated to dryness yielding a yellow oil (33.5 g). The yellow oil was purified by flash column chromatography (SiO_2, ethyl acetate) yielding a yellowish oil. The oil was dried under high vacuum yielding a white foam (18.9 g, 54.0 mmol, 97.9 %).

HR-ESI-MS: calcd. for [**26**+Na]$^+$ $C_{18}H_{26}N_2NaO_5$ m/z= 373.1734, found m/z= 373.1733.

^{1}H-NMR (500.13 MHz, 298 K, DMSO−d_6): δ = 8.15 (d, $^3J_{HH}$ = 7.1 Hz, 1 H, H_5), 7.40 (d, $^3J_{HH}$ = 7.6 Hz, 1 H, H_1), 7.38-7.28 (m, 5 H, H_{14}, H_{15}, H_{16}), 5.02 (d, $^2J_{HH}$ = 12.9 Hz, 1 H, H_{12a}), 4.99 (d, $^2J_{HH}$ = 12.9 Hz, 1 H, H_{12b}), 4.11 (dq, $^3J_{HH}$ = 7.1 Hz, $^3J_{HH}$ = 7.3 Hz, 1 H, H_6), 4.08 (dq, $^3J_{HH}$ = 7.6 Hz, $^3J_{HH}$ = 7.3 Hz, 1 H, H_2), 1.38 (s, 9 H, H_{10}), 1.24 (d, $^3J_{HH}$ = 7.3 Hz, 3 H, H_8), 1.21 (d, $^3J_{HH}$ = 7.3 Hz, 3 H, H_4).

^{13}C{H}-NMR (125.77 MHz, 298 K, DMSO−d_6): δ = 172.32 (1 C, C_3), 171.68 (1 C, C_7), 155.60 (1 C, C_{11}), 137.06 (1 C, C_{13}), 128.32 (2 C, C_{15}), 127.75 (1 C, C_{16}), 127.69 (2 C, C_{14}), 80.26 (1 C, C_9), 65.27 (1 C, C_{12}), 49.58 (1 C, C_2), 48.25 (1 C, C_6), 27.57 (3 C, C_{10}), 18.21 (1 C, C_4), 16.89 (1 C, C_8).

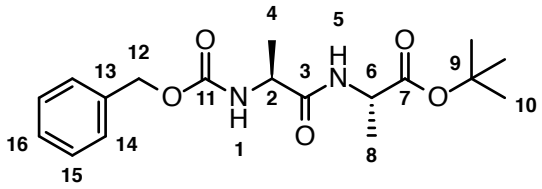

26

((BENZYLOXY)CARBONYL)-*L*-ALANYL-*L*-ALANINE (**27**).

tert-Butyl ((benzyloxy)carbonyl)-*L*-alanyl-*L*-alaninate (**26**) (19.3 g, 55.1 mmol, 1.0 eq.) was dissolved in dichloromethane (100 mL), trifluoroacetic acid (40 mL) and water (4 mL) at 0-5 °C. The reaction mixture was warmed up to 20-25 °C and stirred for 2 h before filtered through celite. The filtrate was evaporated to dryness yielding a yellowish oil. The oil was dissolved in ethyl acetate (100 mL) and extracted with aqueous saturated sodium hydrogen carbonate (1x 100 mL, 2x 50.0 mL). The combined aqueous layers were acidified with aqueous hydrochloric acid (37 %) and extracted with ethyl acetate (3x 80.0 mL). The combined organic layers were dried with sodium sulphate and evaporated to dryness yielding a yellowish oil. The oil was dried under high vacuum yielding an off-white solid (15.3 g, 52.0 mmol, 94.3 %).

HR-ESI-MS: calcd. for [**27**+Na]$^+$ $C_{14}H_{18}N_2NaO_5$ m/z= 317.1108, found m/z= 317.1107.

^{1}H-NMR (500.13 MHz, 298 K, DMSO−d_6): δ = 8.12 (d, $^3J_{HH}$ = 7.3 Hz, 1 H, H_5), 7.40 (d, $^3J_{HH}$ = 7.8 Hz, 1 H, H_1), 7.39-7.25 (m, 5 H, H_{12}, H_{13}, H_{14}), 5.03 (d, $^2J_{HH}$ = 12.5 Hz, 1 H, H_{10a}), 4.99 (d, $^2J_{HH}$ = 12.5 Hz, 1 H, H_{10b}), 4.19 (dq, $^3J_{HH}$ = 7.8 Hz, $^3J_{HH}$ = 7.4 Hz, 1 H, H_2), 4.07 (dq, $^3J_{HH}$ = 7.3 Hz, $^3J_{HH}$ = 7.2 Hz, 1 H, H_6), 1.27 (d, $^3J_{HH}$ = 7.4 Hz, 3 H, H_4), 1.20 (d, $^3J_{HH}$ = 7.2 Hz, 3 H, H_8).

^{13}C{H}-NMR (125.77 MHz, 298 K, DMSO−d_6): δ = 174.49 (1 C, C_7), 172.75 (1 C, C_3), 156.07 (1 C, C_9), 137.52 (1 C, C_{11}), 128.80 (2 C, C_{13}), 128.24 (1 C, C_{14}), 128.18 (2 C, C_{12}), 65.77 (2 C, C_{10}, C_6), 47.85 (1 C, C_2), 18.62 (1 C, C_8), 17.62 (1 C, C_4).

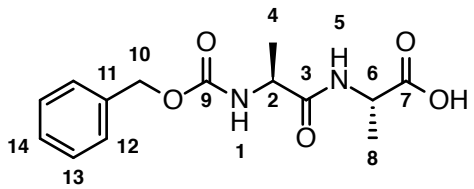

27

tert-BUTYL *L*-ALANYL*L*-ALANINATE (**28**).

tert-Butyl ((benzyloxy)carbonyl)-*L*-alanyl-*L*-alaninate (**26**) (51.3 g, 146 mmol, 1.0 eq.) was dissolved in methanol (300 mL). Palladium on activated charcoal (moistened with water, 10 % Pd basis, 15 g) was added and the mixture was stirred at 20-25 °C under 1.0 bar of hydrogen for 2 h. The suspension was filtered through celite, washed with methanol (50.0 mL) and evaporated to dryness yielding a yellowish oil (29.4 g, 136 mmol, 93.1 %).

HR-ESI-MS: calcd. for [**28**+H]$^+$ $C_{10}H_{21}N_2O_3$ m/z= 217.1547, found m/z= 217.1548.

^{1}H-NMR (500.13 MHz, 298 K, DMSO−d_6): δ = 8.05 (d, $^3J_{HH}$ = 7.1 Hz, 1 H, H_5), 4.12 (dq, $^3J_{HH}$ = 7.1 Hz, $^3J_{HH}$ = 7.3 Hz, 1 H, H_6), 3.26 (q, $^3J_{HH}$ = 6.8 Hz, 1 H, H_2), 1.98 (bs, 2 H, H_1), 1.39 (s, 9 H, H_{10}), 1.25 (d, $^3J_{HH}$ = 7.3 Hz, 3 H, H_8), 1.12 (d, $^3J_{HH}$ = 6.8 Hz, 3 H, H_4).

^{13}C{H}-NMR (125.77 MHz, 298 K, DMSO−d_6): δ = 175.49 (1 C, C_3), 171.82 (1 C, C_7), 80.39 (1 C, C_9), 49.85 (1 C, C_2), 47.95 (1 C, C_6), 27.89 (3 C, C_{10}), 21.57 (1 C, C_4), 17.31 (1 C, C_8).

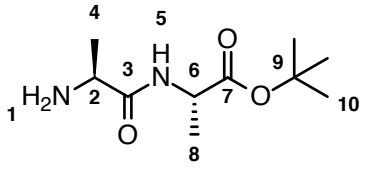

28

tert-BUTYL ((BENZYLOXY)CARBONYL)-*L*-ALANYL-*L*-ALANYL-*L*-ALANYL-*L*-ALANINATE (**29**).

((Benzyloxy)carbonyl)-*L*-alanyl-*L*-alanine (**27**) (40.0 g, 136 mmol, 1.0 eq.) was suspended in acetonitrile (450 mL) and *N*-ethyl diisopropylamine (27 mL). To this suspension dimethylformamide (18.0 g) was added forming a clear solution. To this solution HATU (51.7 g, 163 mmol, 1.2 eq.) was added. The solution turned yellow immediately and was further stirred for 5 min. A solution of *tert*-butyl *L*-alanyl*L*-alaninate (**28**) (29.4 g, 136 mmol, 1.0 eq.) in acetonitrile (100 mL) was added while maintaining the temperature between 20-25 °C. The resulting suspension was stirred for 2 h at 20-25 °C before the product was filtered off and washed with acetonitrile (100 mL) and diethyl ether (200 mL). The product was dried and recrystallized from acetonitrile yielding an off-white solid (31.0 g, 62.9 mmol, 46.3 %).

HR-ESI-MS: calcd. for [**29**+H]$^+$ $C_{24}H_{37}N_4O_7$ m/z= 493.2657, found m/z= 493.2656.

^{1}H-NMR (500.13 MHz, 298 K, DMSO−d_6): δ = 8.14 (d, $^{3}J_{HH}$ = 7.0 Hz, 1 H, H_{13}), 7.96 (d, $^{3}J_{HH}$ = 7.4 Hz, 1 H, H_5), 7.87 (d, $^{3}J_{HH}$ = 7.5 Hz, 1 H, H_9), 7.48 (d, $^{3}J_{HH}$ = 7.5 Hz, 1 H, H_1), 7.38-7.26 (m, 5 H, H_{20}, H_{21}, H_{22}), 5.03 (d, $^{2}J_{HH}$ = 12.9 Hz, 1 H, H_{18a}), 5.00 (d, $^{2}J_{HH}$ = 12.9 Hz, 1 H, H_{18b}), 4.28 (dq, $^{3}J_{HH}$ = 7.5 Hz, $^{3}J_{HH}$ = 7.4 Hz, 1 H, H_{10}), 4.26 (dq, $^{3}J_{HH}$ = 7.4 Hz, $^{3}J_{HH}$ = 7.5 Hz, 1 H, H_6), 4.09 (dq, $^{3}J_{HH}$ = 7.0 Hz, $^{3}J_{HH}$ = 7.4 Hz, 1 H, H_{14}), 4.04 (dq, $^{3}J_{HH}$ = 7.5 Hz, $^{3}J_{HH}$ = 7.3 Hz, 1 H, H_2), 1.38 (s, 9 H, H_{24}), 1.24 (d, $^{3}J_{HH}$ = 7.4 Hz, 3 H, H_{16}), 1.21 (d, $^{3}J_{HH}$ = 7.4 Hz, 3 H, H_{12}), 1.20 (d, $^{3}J_{HH}$ = 7.5 Hz, 3 H, H_8), 1.20 (d, $^{3}J_{HH}$ = 7.5 Hz, 3 H, H_4).

^{13}C{H}-NMR (125.77 MHz, 298 K, DMSO−d_6): δ = 171.06 (1 C, C_3), 170.69 (1 C, C_{11}), 170.48 (1 C, C_7), 170.46 (1 C, C_{15}), 154.65 (1 C, C_{17}), 135.88 (1 C, C_{19}), 127.20 (2 C, C_{21}), 126.62 (1 C, C_{22}), 126.54 (2 C, C_{20}), 79.16 (1 C, C_{23}), 64.2 (1 C, C_{18}), 48.84 (1 C, C_2), 47.12 (1 C, C_{14}), 46.84 (1 C, C_6), 46.42 (1 C, C_{10}), 26.43 (3 C, C_{24}), 17.22 (1 C, C_{12}), 16.98 (1 C, C_8), 16.91 (1 C, C_4), 15.71 (1 C, C_{16}).

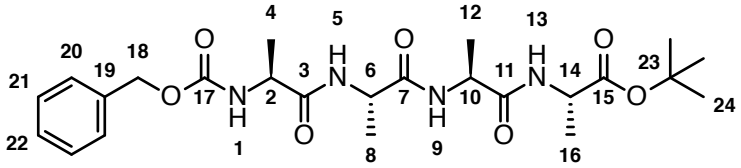

29

((BENZYLOXY)CARBONYL)-*L*-ALANYL-*L*-ALANYL-*L*-ALANYL-*L*-ALANINE (**30**).

tert-Butyl ((benzyloxy)carbonyl)-*L*-alanyl-*L*-alanyl-*L*-alanyl-*L*-alaninate (**29**) (3.00 g, 6.09 mmol, 1.0 eq.) was dissolved in trifluoroacetic acid (4.50 mL) and water (450 µL). The solution was stirred at 20-25 °C for 30 min. The reaction mixture was evaporated to dryness yielding a white waxy solid (2.65 g, 6.07 mmol, 99.7 %).

HR-ESI-MS: calcd. for [**30**+Na]$^{+}$ $C_{20}H_{28}N_4NaO_7$ m/z= 459.1850, found m/z= 459.1848.

^{1}H-NMR (600.13 MHz, 298 K, DMSO−d_6): δ = 8.09 (d, $^{3}J_{HH}$ = 7.1 Hz, 1 H, H_{13}), 7.97 (d, $^{3}J_{HH}$ = 7.5 Hz, 1 H, H_5), 7.87 (d, $^{3}J_{HH}$ = 7.5 Hz, 1 H, H_9), 7.46 (d, $^{3}J_{HH}$ = 7.5 Hz, 1 H, H_1), 7.40-7.27 (m, 5 H, H_{20}, H_{21}, H_{22}), 5.03 (d, $^{2}J_{HH}$ = 12.9 Hz, 1 H, H_{18a}), 5.00 (d, $^{2}J_{HH}$ = 12.9 Hz, 1 H, H_{18b}), 4.28 (dq, $^{3}J_{HH}$ = 7.5 Hz, $^{3}J_{HH}$ = 7.2 Hz, 1 H, H_{10}), 4.26 (dq, $^{3}J_{HH}$ = 7.5 Hz, $^{3}J_{HH}$ = 7.2 Hz, 1 H, H_6), 4.18 (dq, $^{3}J_{HH}$ = 7.1 Hz, $^{3}J_{HH}$ = 7.2 Hz, 1 H, H_{14}), 4.05 (dq, $^{3}J_{HH}$ = 7.5 Hz, $^{3}J_{HH}$ = 7.2 Hz, 1 H, H_2), 1.26 (d, $^{3}J_{HH}$ = 7.2 Hz, 3 H, H_{16}), 1.20 (d, $^{3}J_{HH}$ = 7.2 Hz, 3 H, H_{12}), 1.20 (d, $^{3}J_{HH}$ = 7.2 Hz, 3 H, H_8), 1.20 (d, $^{3}J_{HH}$ = 7.2 Hz, 3 H, H_4).

^{13}C{H}-NMR (150.95 MHz, 298 K, DMSO−d_6): δ = 173.83 (1 C, C_{15}), 172.14 (1 C, C_3), 171.67 (1 C, C_{11}), 171.53 (1 C, C_7), 155.58 (1 C, C_{17}), 136.90 (1 C, C_{19}), 128.21 (2 C, C_{21}), 127.67 (1 C, C_{22}), 127.57 (2 C, C_{20}), 65.24 (1 C, C_{18}), 49.87 (1 C, C_2), 47.87 (1 C, C_6), 47.58 (1 C, C_{10}), 47.29 (1 C, C_{14}), 18.12 (1 C, C_8), 18.00 (1 C, C_4), 17.96 (1 C, C_{12}), 17.02 (1 C, C_{16}).

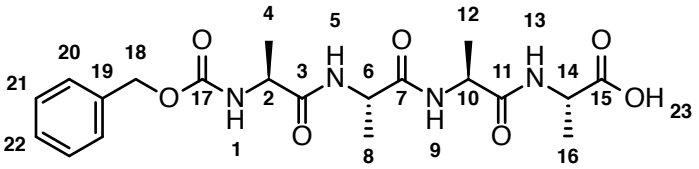

30

L-ALANYL-*L*-ALANYL-*L*-ALANYL-*L*-ALANINE (**35**).

((Benzyloxy)carbonyl)-*L*-alanyl-*L*-alanyl-*L*-alanyl-*L*-alanine (**30**) (1.50 g, 3.44 mmol, 1.0 eq.) was dissolved in methanol (15 mL). Palladium on activated charcoal (moistened with water, 10 % Pd basis, 150 mg) was added and the mixture was stirred at 20-25 °C under 1.0 bar of hydrogen for 2 h. The suspension was filtered through celite, washed with methanol (10 mL) and evaporated to dryness yielding a white solid (950 mg, 3.14 mmol, 91.3 %).

HR-ESI-MS: calcd. for [**35**+H]$^+$ $C_{12}H_{23}N_4O_5$ m/z= 303.1663, found m/z= 303.1664.

^{1}H-NMR (600.13 MHz, 298 K, D_2O): δ = 8.59 (d, $^3J_{HH}$ = 5.2 Hz, 1 H, H_5), 8.41 (d, $^3J_{HH}$ = 6.0 Hz, 1 H, H_9), 8.10 (d, $^3J_{HH}$ = 6.8 Hz, 1 H, H_{13}), 4.34 (dq, $^3J_{HH}$ = 5.2 Hz, $^3J_{HH}$ = 7.2 Hz, 1 H, H_6), 4.29 (dq, $^3J_{HH}$ = 6.0 Hz, $^3J_{HH}$ = 7.1 Hz, 1 H, H_{10}), 4.20 (dq, $^3J_{HH}$ = 6.8 Hz, $^3J_{HH}$ = 7.3 Hz, 1 H, H_{14}), 4.08 (q, $^3J_{HH}$ = 7.3 Hz, 1 H, H_2), 1.53 (d, $^3J_{HH}$ = 7.3 Hz, 3 H, H_4), 1.41 (d, $^3J_{HH}$ = 7.2 Hz, 3 H, H_8), 1.37 (d, $^3J_{HH}$ = 7.1 Hz, 3 H, H_{12}), 1.36 (d, $^3J_{HH}$ = 7.3 Hz, 3 H, H_{16}).

^{13}C{H}-NMR (from HMBC, 150.95 MHz, 298 K, D_2O): δ = 178.54 (1 C, C_{15}), 174.26 (1 C, C_7), 173.82 (1 C, C_{11}), 170.52 (1 C, C_3), 50.25 (1 C, C_{14}), 49.61 (2 C, C_6, C_{10}), 49.02 (1 C, C_2), 17.02 (1 C, C_{16}), 16.58 (1 C, C_4), 16.53 (2 C, C_8, C_{12}).

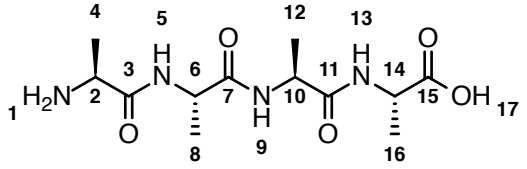

35

4-(HYDROXYMETHYL)-2-NITROPHENOL (**33**).

4-Hydroxy-3-nitro-benzoic acid (8.20 g, 43.9 mmol, 1.0 eq.) was dissolved in dry tetrahydrofuran (100 mL) at 20-25 °C under argon atmosphere. Boron trifluoride diethyl etherate (48 %, 13.0 g, 43.9 mmol, 1.0 eq.) was added followed by the addition of borane-tetrahydrofuran complex (1 M, 154 mL, 154 mmol, 3.5 eq.) over 15 min. The solution was stirred for 18 h and then carefully quenched with methanol (20.0 mL) and water (10.0 mL). The solution was evaporated to dryness under reduced pressure and the remaining crude oil was dissolved in water (350 mL) and ethyl acetate (150 mL). The layers were separated and the aqueous layer was extracted with ethyl acetate (3x 200 mL). The combined organic layers were extracted with brine (100 mL), dried over sodium sulphate and evaporated to dryness yielding a yellow crude product. This crude product was purified by flash column chromatography (SiO_2, hexane / ethyl acetate (1:1)) yielding a yellow crystalline solid (10.8 g, 63.8 mmol, 72.7 %).

HR-ESI-MS: calcd. for [**33**+Na]$^+$ $C_7H_7NNaO_4$ m/z= 192.0267, found m/z= 192.0266.

^{1}H-NMR (500.13 MHz, 298 K, $CDCl_3$): δ = 10.59 (s, 1 H, H_7), 8.12 (d, $^4J_{HH}$ = 2.1 Hz, 1 H, H_5), 7.61 (dd, $^3J_{HH}$ = 8.6 Hz, $^4J_{HH}$ = 2.1 Hz, 1 H, H_1), 7.17 (d, $^3J_{HH}$ = 8.6 Hz, 1 H, H_2), 4.70 (s, 2 H, H_8).

^{13}C{H}-NMR (125.77 MHz, 298 K, $CDCl_3$): δ = 154.65 (1 C, C_3), 136.37 (1 C, C_1), 133.34 (1 C, C_4), 133.24 (1 C, C_6), 123.16 (1 C, C_5), 120.26 (1 C, C_2), 63.73 (1 C, C_8).

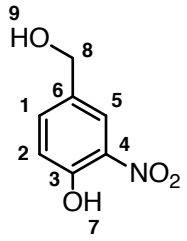

33

4-(CHLOROMETHYL)-2-NITROPHENOL (**31**).

4-(Hydroxymethyl)-2-nitrophenol (**33**) (4.30 g, 25.4 mmol, 1.0 eq.) was suspended chloroform (100 mL) wetted with aqueous hydrochloric acid (37 %, 1 mL). The suspension was saturated with hydrogen chloride gas. Sulphuric acid (98 %, cat.) was added and the reaction mixture was left stirring under an hydrogen chloride atmosphere for 18 h. The aqueous layer was separated and the organic layer was evaporated to dryness. The crude product was crystallized from methyl *tert*-butyl ether / hexane yielding a

yellow solid (2.09 g, 11.2 mmol, 43.9 %).

^{1}H-NMR (500.13 MHz, 298 K, $CDCl_3$): δ = 8.14 (d, $^{4}J_{HH}$ = 2.2 Hz, 1 H, H_5), 7.63 (dd, $^{3}J_{HH}$ = 8.7 Hz, $^{4}J_{HH}$ = 2.2 Hz, 1 H, H_1), 7.18 (d, $^{3}J_{HH}$ = 8.7 Hz, 1 H, H_2), 4.57 (s, 2 H, H_8).

^{13}C{H}-NMR (125.77 MHz, 298 K, $CDCl_3$): δ = 155.16 (1 C, C_3), 137.89 (1 C, C_1), 133.35 (1 C, C_4), 130.08 (1 C, C_6), 125.03 (1 C, C_5), 120.85 (1 C, C_2), 44.68 (1 C, C_8).

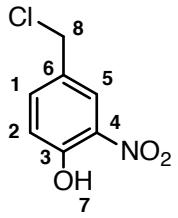

31

4-ACETOXY-3-NITROBENZOIC ACID (**34**).

4-Hydroxy-3-nitro-benzoic acid (15.0 g, 81.9 mmol, 1.0 eq.) and *N*-ethyl diisopropylamine (31.8 g, 246 mmol, 3.0 eq.) were suspended in tetrahydrofuran (150 mL). The suspension was cooled to 0-5 °C and a solution of acetyl chloride (9.64 g, 123 mmol, 1.5 eq.) in tetrahydrofuran (20.0 mL) was added dropwise. The reaction was allowed to warm up to 20-25 °C and was left stirring for 18 h. The reaction mixture was evaporated to dryness and the crude product was dissolved in ethyl acetate (100 mL) and water (100 mL). The layers were separated and the organic layer was extracted with aqueous saturated sodium hydrogen carbonate (2x 100 mL). The combined aqueous layers were acidified with hydrochloric acid (37 %) and extracted with ethyl acetate (2x 100 mL). The organic layers were dried with sodium sulphate and evaporated to dryness yielding a yellow solid (10.5 g, 46.6 mmol, 85.4 %).

HR-ESI-MS: calcd. for [**34**+Na]$^{+}$ $C_9H_7NNaO_6$ m/z= 248.0166, found m/z= 248.0169.

^{1}H-NMR (500.13 MHz, 298 K, $CDCl_3$): δ = 10.70 (bs, 1 H, H_8), 8.82 (d, $^{3}J_{HH}$ = 2.1 Hz, 1 H, H_5), 8.38 (dd, $^{3}J_{HH}$ = 8.5 Hz, $^{4}J_{HH}$ = 2.1 Hz, 1 H, H_1), 7.39 (d, $^{3}J_{HH}$ = 8.5 Hz, 1 H, H_2), 2.41 (s, 3 H, H_{10}).

^{13}C{H}-NMR (125.77 MHz, 298 K, $CDCl_3$): δ = 169.38 (1 C, C_7), 168.17 (1 C, C_9), 148.26 (1 C, C_3), 141.93 (1 C, C_4), 136.12 (1 C, C_1), 128.08 (1 C, C_6), 128.07 (1 C, C_5), 125.99 (1 C, C_2), 20.93 (1 C, C_{10}).

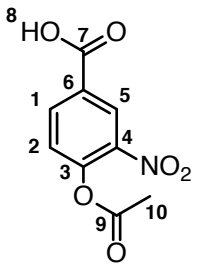

34

POLYMER FUNCTIONALIZATION

*Polymer A **225***

Poly(styrene-divinylbenzene) (2 % cross-linked, 200-400 mesh, 3.00 g) and 4-(chloromethyl)-2-nitrophenol (**31**) (1.80 g, 115 mmol, 1.0 eq.) were suspended in nitrobenzol (60 mL) and heated to 65 °C. A solution of aluminium trichloride (15.3 g, 115 mmol, 12 eq.) in nitrobenzol (60 mL) was added. The mixture was stirred for 48 h at 65 °C. The reaction mixture was filtered and the polymer was washed with chloroform (100 mL), water (100 mL), hydrochloric acid (1 M, 100 mL), 1,4-dioxane (100 mL) and methanol (100 mL). The solid was dried yielding a black powder (4.06 g, 2.08 mmol N/g).

EA: found C 79.38 %, H 6.35 %, N 2.88 %.

*Polymer B **226***

4-Acetoxy-3-nitrobenzoic acid (**34**) (5.70 g, 25.3 mmol, 1.0 eq.) was dissolved in nitrobenzol (150). Oxalylchloride (7.71 g, 60.7 mmol, 2.4 eq.) and dimethylformamide (cat.) was added. The reaction mixture was stirred at 20-25 °C for 45 min. Then aluminium trichloride (6.75 g, 50.6 mmol, 2.0 eq.) was added. After 10 min poly(styrene-divinylbenzene) (2 % cross-linked, 200-400 mesh, 15.0 g) was added and the reaction was heated to 40 °C for 18 h. The reaction mixture was filtered and the polymer was washed with acetone (100 mL), methanol (100 mL) and diethyl ether (100 mL). The yellow polymer was dried and suspended in methanol (40 mL) and aqueous sodium hydroxide (4 M, 40 mL). The suspension was stirred at 40 °C for 4 h. The polymer was filtered off and washed with methanol (100 mL). The solid was dried yielding an orange powder (18.8 g, 1.06 mmol N/g).

EA: found C 81.10 %, H 6.80 %, N 1.78 %.

*Polymer C **227***

Phenol, polymer-bound (1 % cross-linked, 100-200 mesh, extent of labeling: 0.5-1.5 mmol g^{-1}, 3.00 g) was suspended in nitric acid (68 %, 100 mL). The

suspension was stirred at 20-25 °C for 5 h. Then the polymer was filtered off and washed with water (50 mL), dimethylformamide (50 mL), ethanol (50 mL), acetone (50 mL), diethyl ether (50 mL). The solid was dried yielding an orange powder (3.14 g, 750 µmol N/g).

EA: found C 88.49 %, H 7.52 %, N 0.57 %.

POLYMER LOADING

Polymer **225** or **226** (1.00 g) was suspended in dimethylformamide (15.0 mL) and *N*-ethyl diisopropylamine (600 µL, 3.45 mmol, 3.0 eq.). To this suspension HATU (451 mg, 1.15 mmol, 1.0 eq.) and ((benzyloxy)carbonyl)--*L*-alanyl-*L*-alanyl-*L*-alanyl-*L*-alanine (**30**) (500 mg, 1.15 mmol, 1.0 eq.) was added. The suspension was stirred at 20-25 °C for 18 h. Then the polymer was filtered off and washed with dimethylformamide (50 mL), ethanol (50 mL), acetone (50 mL) and diethyl ether (50 mL). The polymer was dried under vacuum. Polymer loading: for Polymer A **225** (400 mg), Polymer B **226** (190 mg).

GENERAL PROCEDURE: POLYMER DEPROTECTION AND CYLIZATION

Loaded polymer (1-2 g) was suspended in hydrobromic acid solution (48 %, 5.00 mL) and stirred for 1 h at 20-25 °C. Then the polymer was washed with acetic acid (50 mL), dimethylformamide (50 mL), ethanol (50 mL) and diethyl ether (50 mL). The polymer was further suspended in dimethylformamide (10 mL) and *N*-ethyl diisopropylamine (5.0 mL) was added. After 18 h at 20-25 °C the polymer was filtered off and washed with dimethylformamide (5.0 mL). The filtrate was evaporated yielding the crude product from the cyclization.

(*S*)-2-(((*S*)-2-(((*S*)-2-(((*S*)-2-AMINOPROPYL)AMINO)PROPYL)AMINO)PROPYL)AMINO)PROPAN-1-OL (**36**).

L-Alanyl-*L*-alanyl-*L*-alanyl-*L*-alanine (**35**) (250 mg, 827 µmol, 1.0 eq.) was suspended in tetrahydrofuran (10 mL) and lithium aluminium hydride solution (2 M in tetrahydrofuran, 8.3 mL, 16.5 mmol, 20 eq.) was added and the suspension was refluxed for 8 h. The reaction mixture was cooled to 20-25 °C and stirred for 16 h. The reaction was quenched with aqueous potassium hydroxide (2 M, 2.0 mL) and ethyl acetate (10.0 mL). The suspension was diluted with tetrahydrofuran (10 mL) and ethyl acetate (10 mL). The suspension was dried with sodium sulphate. The suspension was filtered and washed with ethyl acetate (50 mL). The solvent was removed under reduced pressure yielding a colorless oil (140 mg, 568 µmol, 68.7 %). The product

was used without further purification.

HR-ESI-MS: calcd. for [**36**+H]$^+$ $C_{12}H_{31}N_4O$ m/z= 247.2492, found m/z= 247.2496.

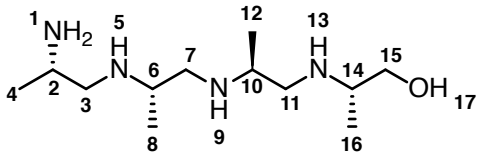

36

(*S*)-2-((*tert*-BUTOXYCARBONYL)AMINO)PROPYL 4-METHYLBENZENESULFONATE (**47**).

tert-Butyl (*S*)-(1-hydroxypropan-2-yl)carbamate (1.00 g, 5.71 mmol, 1.0 eq.) was dissolved in dichloromethane (20 mL) and cooled to 0-5 °C. 4-Methylbenzol-1-sulfonylchlorid (1.63 g, 8.57 mmol, 1.5 eq.) was added and the reaction was warmed up to 20-25 °C. The solution was stirred at 20-25 °C for 18 h. The solution was extracted with water (20 mL), aqueous saturated sodium hydrogen carbonate (20 mL) and water (20 mL). The organic layer was dried over sodium sulphate and evaporated to dryness. The crude oil was purified by (SiO_2, ethyl acetate / cyclohexane (3:7)) yielding a white solid (1.33 g, 4.04 mmol, 70.7 %).

^{1}H-NMR (600.13 MHz, 298 K, $CDCl_3$): δ = 7.72 (d, $^3J_{HH}$ = 8.3 Hz, 2 H, H_6), 7.40 (d, $^3J_{HH}$ = 8.3 Hz, 2 H, H_7), 4.57 (d, $^3J_{HH}$ = 8.8 Hz, 1 H, H_1), 4.05-4.00 (m, 1 H, H_{3a}), 3.93 (dd, $^2J_{HH}$ = 9.9 Hz, $^3J_{HH}$ = 4.2 Hz, 1 H, H_{3b}), 3.92-3.84 (m, 1 H, H_2), 2.45 (s, 3 H, H_9), 1.40 (s, 9 H, H_{12}), 1.35 (d, $^3J_{HH}$ = 7.2 Hz, 3 H, H_4).

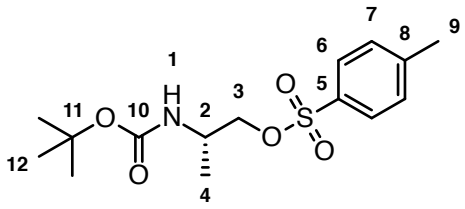

47

(*S*)-2-((*tert*-BUTOXYCARBONYL)AMINO)PROPYL METHANESULFONATE (**50**).

tert-Butyl (*S*)-(1-hydroxypropan-2-yl)carbamate (200 mg, 1.14 mmol, 1.0 eq.) was dissolved in dichloromethane (5.0 mL) and cooled to 0-5 °C. Methanesulfonyl chloride (157 mg, 1.37 mmol, 1.2 eq.) was added and the reaction was stirred at 0-5 °C for 3 h. The solution was extracted with

water (3x 5.0 mL). The organic layer was dried over sodium sulphate and evaporated to dryness yielding a white solid (280 mg, 1.11 mmol, 97.0 %).

^{1}H-NMR (600.13 MHz, 298 K, $CDCl_3$): δ = 4.57 (bs, 1 H, H_1), 4.26-4.20 (m, 1 H, H_{3a}), 4.14 (dd, $^2J_{HH}$ = 10.1 Hz, $^3J_{HH}$ = 4.3 Hz, 1 H, H_{3b}), 4.00-3.91 (m, 1 H, H_2), 3.03 (s, 3 H, H_5), 1.44 (s, 9 H, H_8), 1.23 (d, $^3J_{HH}$ = 6.9 Hz, 3 H, H_4).

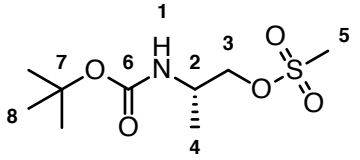

50

(*S*)-2-METHYL-1-((4-NITROPHENYL)SULFONYL)AZIRIDINE (**55**).

L-Alaninol (6.00 g, 79.9 mmol, 1.0 eq.) was dissolved in pyridine (25.3 g, 320 mmol, 4.0 eq.). This solution was added to a slurry of 4-nitrobenzene sulfonyl chloride (41.6 g, 188 mmol, 2.3 eq.) in acetonitrile (50 mL) at 0-5 °C. The reaction mixture was stirred at 0-5 °C for 2 h. Ethyl acetate (150 mL) and water (75 mL) were added and the mixture was stirred for another 10 min. The aqueous layer was removed and the organic layer was washed with aqueous citric acid (1 mM, 2x 50 mL) and water (40 mL). The organic solution was cooled to 10 °C and *N*-ethyl diisopropylamine (21.1 mL, 128 mmol, 1.6 eq.) was added. The reaction was stirred at 20-25 °C for 30 min. The lower layer was removed and the organic layer was extracted with aqueous citric acid (1 M, 2x 50 mL) and water (2x 40 mL). The organic layer was dried with sodium sulphate and concentrated under reduced pressure to approximately 50 mL. Isopropanol (50 mL) was added and more ethyl acetate was removed under reduced pressure. The resulting slurry was cooled to 0-5 °C. The suspension was filtered and the filter cake was washed with cold isopropanol (10 mL). The product was dried under vacuum at 20-25 °C yielding a yellow solid (12.1 g, 49.9 mmol, 62.5 %).

^{1}H-NMR (500.13 MHz, 298 K, $CDCl_3$): δ = 8.40-8.36 (m, 2 H, H_6), 8.17-8.12 (m, 2 H, H_5), 2.97 (ddd, $^3J_{HH}$ = 7.0 Hz, $^3J_{HH}$ = 5.6 Hz, $^3J_{HH}$ = 4.7 Hz, 1 H, H_2), 2.72 (d, $^3J_{HH}$ = 7.0 Hz, 1 H, H_{3a}), 2.12 (d, $^3J_{HH}$ = 4.7 Hz, 1 H, H_{3b}), 1.29 (d, $^3J_{HH}$ = 5.6 Hz, 3 H, H_1).

^{13}C{H}-NMR (125.77 MHz, 298 K, $CDCl_3$): δ = 150.72 (1 C, C_7), 144.43 (1 C, C_4), 129.21 (2 C, C_5), 124.41 (2 C, C_6), 36.95 (1 C, C_2), 35.61 (1 C, C_3), 16.88 (1 C, C_1).

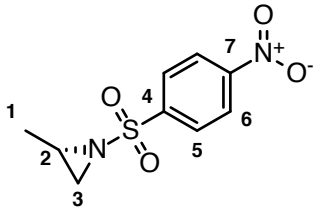

55

tert-BUTYL ((*S*)-2-((4-NITROPHENYL)SULFONAMIDO)PROPYL)-*L*-ALANINATE (**52**).

(*S*)-2-Methyl-1-((4-nitrophenyl)sulfonyl)aziridine (**55**) (6.20 g, 25.6 mmol, 1.0 eq.), tert-butyl *L*-alaninate (5.58 g, 38.4 mmol, 1.5 eq.) and *N*-ethyl diisopropylamine (6.35 mL, 38.4 mmol, 1.5 eq.) were dissolved in tetrahydrofuran (60 mL) and stirred at 60 °C for 18 h. The reaction mixture was evaporated to dryness and the crude product was purified by flash column chromatography (SiO_2, ethyl acetate / cyclohexane / triethylamine (50:50:1)) yielding a yellow solid (7.48 g, 19.3 mmol, 75.4 %).

HR-ESI-MS: calcd. for [**52**+H]$^+$ $C_{16}H_{26}N_3O_6S$ m/z= 388.1537, found m/z= 388.1542.

^{1}H-NMR (600.13 MHz, 298 K, $CDCl_3$): δ = 8.36-8.32 (m, 2 H, H_{11}), 8.10-8.06 (m, 2 H, H_{10}), 5.77 (bs, 1 H, H_1), 3.20 (ddq, $^3J_{HH}$ = 7.7 Hz, $^3J_{HH}$ = 4.2 Hz, $^3J_{HH}$ = Hz, 1 H, H_2), 3.08 (q, $^3J_{HH}$ = 7.0 Hz, 1 H, H_6), 2.64 (dd, $^2J_{HH}$ = 12.2 Hz, $^3J_{HH}$ = 4.2 Hz, 1 H, H_{3a}), 2.31 (dd, $^2J_{HH}$ = 12.2 Hz, $^3J_{HH}$ = 7.7 Hz, 1 H, H_{3b}), 1.44 (s, 9 H, H_{14}), 1.19 (d, $^3J_{HH}$ = 7.0 Hz, 3 H, H_8), 1.14 (d, $^3J_{HH}$ = 6.5 Hz, 3 H, H_4).

^{13}C{H}-NMR (150.95 MHz, 298 K, $CDCl_3$): δ = 174.75 (1 C, C_7), 150.06 (1 C, C_{12}), 146.72 (1 C, C_9), 128.58 (2 C, C_{11}), 124.37 (2 C, C_{10}), 81.59 (1 C, C_{13}), 57.27 (1 C, C_6), 52.36 (1 C, C_3), 50.10 (1 C, C_2), 28.17 (3 C, C_{14}), 19.57 (1 C, C_4), 19.22 (1 C, C_8).

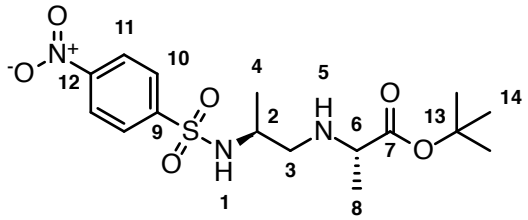

52

tert-BUTYL *N*-BENZYL-*N*-((*S*)-2-((4-NITROPHENYL)SULFONAMIDO)PROPYL)-*L*-ALANINATE (**53**).

tert-Butyl ((*S*)-2-((4-nitrophenyl)sulfonamido)propyl)-*L*-alaninate (**52**) (6.40 g, 16.5 mmol, 1.0 eq.) and potassium carbonate (4.56 g, 33.0 mmol, 2.0 eq.) were suspended in acetonitrile. To this suspension benzyl bromide (7.06 g, 41.3 mmol, 2.5 eq.) was added and the mixture was stirred at 50 °C for 18 h. Excess benzyl bromide was quenched with triethylamine (5.0 mL). The suspension was filtered and the filtrate was evaporated to dryness. The crude oil was purified by flash column chromatography (SiO_2, ethyl acetate / cyclohexane / triethylamine (30:70:1)) yielding a yellowish waxy solid (5.08 g, 10.6 mmol, 64.5 %).

HR-ESI-MS: calcd. for [**53**+H]$^+$ $C_{23}H_{32}N_3O_6S$ m/z= 478.2006, found m/z= 478.2009.

^{1}H-NMR (500.13 MHz, 298 K, $CDCl_3$): δ = 8.20-8.17 (m, 2 H, H_{11}), 8.02-7.98 (m, 2 H, H_{10}), 7.35-7.25 (m, 3 H, H_{18}, H_{19}), 7.13-7.06 (m, 2 H, H_{17}), 3.49 (d, $^2J_{HH}$ = 14.5 Hz, 1 H, H_{15a}), 3.45 (d, $^2J_{HH}$ = 14.5 Hz, 1 H, H_{15b}), 3.35-3.30 (m, 1 H, H_2), 3.34 (q, $^3J_{HH}$ = 7.0 Hz, 1 H, H_6), 2.51 (dd, $^2J_{HH}$ = 13.7 Hz, $^3J_{HH}$ = 4.2 Hz, 1 H, H_{3a}), 2.42 (dd, $^2J_{HH}$ = 13.7 Hz, $^3J_{HH}$ = 10.2 Hz, 1 H, H_{3b}), 1.51 (s, 9 H, H_{14}), 1.18 (d, $^3J_{HH}$ = 6.3 Hz, 3 H, H_4), 1.14 (d, $^3J_{HH}$ = 7.0 Hz, 3 H, H_8).

^{13}C{H}-NMR (125.77 MHz, 298 K, $CDCl_3$): δ = 173.37 (1 C, C_7), 149.75 (1 C, C_{12}), 146.71 (1 C, C_9), 138.07 (1 C, C_{16}), 128.68 (2 C, C_{18}), 128.22 (2 C, C_{11}), 128.00 (2 C, C_{17}), 127.50 (1 C, C_{19}), 124.11 (2 C, C_{10}), 81.93 (1 C, C_{13}), 57.65 (1 C, C_6), 55.61 (1 C, C_3), 54.93 (1 C, C_{15}), 47.77 (1 C, C_2), 28.16 (3 C, C_{14}), 19.80 (1 C, C_4), 10.29 (1 C, C_8).

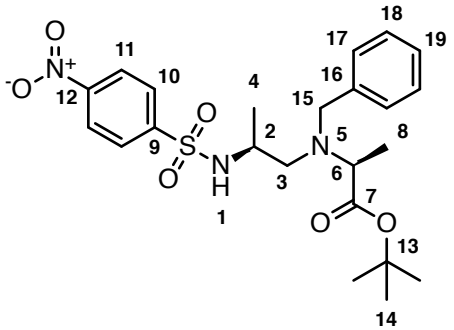

53

tert-BUTYL *N*-((*S*)-2-AMINOPROPYL)-*N*-BENZYL-*L*-ALANINATE (**56**).

Method A

tert-Butyl *N*-benzyl-*N*-((*S*)-2-((4-nitrophenyl)sulfonamido)propyl)-*L*-alaninate (**53**) (2.50 g, 5.23 mmol, 1.0 eq.), dodecanthiol (2.5 mL, 10.5 mmol, 2.0 eq.) and potassium carbonate were suspended in acetonitrile (20 mL). The suspension was heated to 50 °C for 18 h. The mixture was cooled to 20-25 °C filtered and evaporated to dryness. The crude product was dissolved in ethyl acetate. The organic solution was extracted with hydrochloric acid (1 M, 3x 20 mL). The combined aqueous layers were extracted with ethyl acetate (3x 20 mL). The pH of the aqueous layer was adjusted to 14 with aqueous sodium hydroxide (40 %). The product was extracted with ethyl acetate (3x 20 mL). The combined organic layers were dried with sodium sulphate and evaporated to dryness yielding a yellowish oil (1.14 g, 3.89 mmol, 74.5 %).

Method B

tert-Butyl *N*-benzyl-*N*-((S)-2 (((benzyloxy)carbonyl)amino)propyl)-*L*-alaninate (**63**) (751 mg, 1.76 mmol, 1.0 eq.) was dissolved in methanol (5.0 mL). Palladium on barium sulphate (60.0 mg, 5 % Pd/$BaSO_4$) was added and the reaction flask was flushed with nitrogen. Then hydrogen was bubbled through the solution for 5 min and the reaction mixture was left stirring under 1 bar hydrogen at 20-25 °C for 2 h. The suspension was filtered through celite and washed with methanol (3 x 5.0 mL). The filtrate was evaporated to dryness yielding a yellowish oil (480 mg, 1.64 mmol, 93.3 %).

HR-ESI-MS: calcd. for [**56**+H]$^+$ $C_{17}H_{29}N_2O_2$ m/z= 293.2224, found m/z= 293.2228.

^{1}H-NMR (600.13 MHz, 298 K, $CDCl_3$): δ = 7.36-7.33 (m, 2 H, H_{13}), 7.32-7.28 (m, 2 H, H_{14}), 7.25-7.21 (m, 1 H, H_{15}), 3.76 (d, $^2J_{HH}$ = 14.8 Hz, 1 H, H_{11a}), 3.73 (d, $^2J_{HH}$ = 14.8 Hz, 1 H, H_{11b}), 3.40 (q, $^3J_{HH}$ = 7.1 Hz, 1 H, H_6), 2.84 (ddq, $^3J_{HH}$ = 8.5 Hz, $^3J_{HH}$ = 5.1 Hz, $^3J_{HH}$ = 6.3 Hz, 1 H, H_2), 2.57 (dd, $^2J_{HH}$ = 13.2 Hz, $^3J_{HH}$ = 5.1 Hz, 1 H, H_{3a}), 2.33 (dd, $^2J_{HH}$ = 13.2 Hz, $^3J_{HH}$ = 8.5 Hz, 1 H, H_{3b}), 1.48 (s, 9 H, H_{10}), 1.23 (d, $^3J_{HH}$ = 7.1 Hz, 3 H, H_8), 0.98 (d, $^3J_{HH}$ = 6.3 Hz, 3 H, H_4).

^{13}C{H}-NMR (150.95 MHz, 298 K, $CDCl_3$): δ = 173.18 (1 C, C_7), 140.41 (1 C, C_{12}), 128.46 (2 C, C_{13}), 128.27 (2 C, C_{14}), 126.91 (1 C, C_{15}), 80.71 (1 C, C_9), 60.89 (1 C, C_{11}), 59.71 (1 C, C_6), 56.11 (1 C, C_3), 45.26 (1 C, C_2), 28.28 (3 C, C_{10}), 21.16 (1 C, C_4), 13.75 (1 C, C_8).

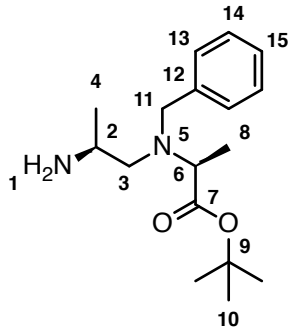

56

N-BENZYL-*N*-((*S*)-2-((4-NITROPHENYL)SULFONAMIDO)PROPYL)-*L*-ALANINE (**57**).

tert-Butyl *N*-benzyl-*N*-((*S*)-2-((4-nitrophenyl)sulfonamido)propyl)-*L*-alaninate (**53**) (2.50 g, 5.23 mmol, 1.0 eq.) was dissolved in acetonitrile (40 mL) and hydrochloric acid (4 M, 40 mL). The solution was stirred at 50 °C and stirred for 6 h. The reaction mixture was evaporated to dryness yielding the title compound as hydrochloride salt (2.31 g, 5.04 mmol, 96.5 %).

HR-ESI-MS: calcd. for [**57**+H]$^+$ $C_{19}H_{24}N_3O_6S$ m/z= 422.1380, found m/z= 422.1386.

^{1}H-NMR (500.13 MHz, 298 K, $CDCl_3$): δ = 8.38-8.33 (m, 2 H, H_{11}), 8.22-8.18 (m, 2 H, H_{10}), 7.36-7.26 (m, 5 H, H_{15}, H_{16}, H_{17}), 4.42 (ddq, $^3J_{HH}$ = 3.2 Hz, $^3J_{HH}$ = 2.4 Hz, $^3J_{HH}$ = 6.2 Hz, 1 H, H_2), 4.04 (d, $^2J_{HH}$ = 13.5 Hz, 1 H, H_{13a}), 3.15 (d, $^2J_{HH}$ = 13.5 Hz, 1 H, H_{13b}), 3.04 (q, $^3J_{HH}$ = 6.8 Hz, 1 H, H_6), 2.81 (dd, $^2J_{HH}$ = 12.4 Hz, $^3J_{HH}$ = 2.4 Hz, 1 H, H_{3a}), 2.50 (dd, $^2J_{HH}$ = 12.4 Hz, $^3J_{HH}$ = 3.2 Hz, 1 H, H_{3b}), 1.52 (d, $^3J_{HH}$ = 6.2 Hz, 3 H, H_4), 1.47 (d, $^3J_{HH}$ = 6.8 Hz, 3 H, H_8).

^{13}C{H}-NMR (125.77 MHz, 298 K, $CDCl_3$): δ = 170.89 (1 C, C_7), 150.69 (1 C, C_{12}), 144.92 (1 C, C_9), 137.28 (1 C, C_{14}), 130.34 (2 C, C_{10}), 128.86 (2 C, C_{16}), 128.67 (2 C, C_{15}), 127.75 (1 C, C_{17}), 124.02 (2 C, C_{11}), 62.89 (1 C, C_6), 58.35 (1 C, C_{13}), 54.35 (1 C, C_3), 53.06 (1 C, C_2), 21.32 (1 C, C_4), 17.18 (1 C, C_8).

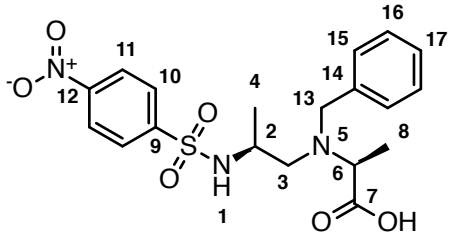

57

tert-BUTYL ((*S*)-2-AMINOPROPYL)-*L*-ALANINATE (**228**).

Method A

tert-Butyl ((*S*)-2-((4-nitrophenyl)sulfonamido)propyl)-*L*-alaninate (**52**) (2.00 g, 5.16 mmol, 1.0 eq.) was dissolved in acetonitrile (20 mL). Then potassium carbonate (1.07 g, 7.74 mmol, 1.5 eq.) and dodecanthiol (2.5 mL, 10.3 mmol, 2.0 eq.) were added and the reaction mixture was stirred at 60 °C for 18 h. The mixture was filtered and evaporated to dryness. The residue was taken up in ethyl acetate (30 mL) and extracted with aqueous formic acid (1 M, 3x 30 mL). The combined aqueous layers were extracted with ethyl acetate (20 mL). The pH of the aqueous layer was adjusted to 14 with aqueous sodium hydroxide (4 M). The product was extracted with ethyl acetate (3x 20 mL). The combined organic layers were dried with sodium sulphate and evaporated to dryness yielding a yellowish oil (540 mg, 2.67 mmol, 51.7 %).

Method B

tert-Butyl ((*S*)-2-(((benzyloxy)carbonyl)amino)propyl)-*L*-alaninate (**62**) (600 mg, 1.78 mmol, 1.0 eq.) was dissolved in methanol (10 mL) and palladium on activated charcoal (moistened with water, 10 % Pd basis, 60.0 mg) was added. The suspension was hydrogenated at 1.0 bar hydrogen for 4 h. The reaction mixture was filtered over celite and the solvent was removed under reduced pressure yielding a yellowish oil (355 mg, 1.76 mmol, 98.6 %).

HR-ESI-MS: calcd. for [**228**+H]$^+$ $C_{10}H_{23}N_2O_2$ m/z= 203.1754, found m/z= 203.1753.

^{1}H-NMR (500.13 MHz, 298 K, $CDCl_3$): δ = 3.16 (q, $^3J_{HH}$ = 7.0 Hz, 1 H, H_6), 2.91 (ddq, $^3J_{HH}$ = 8.4 Hz, $^3J_{HH}$ = 4.3 Hz, $^3J_{HH}$ = 6.4 Hz, 1 H, H_2), 2.63 (dd, $^2J_{HH}$ = 11.3 Hz, $^3J_{HH}$ = 4.3 Hz, 1 H, H_{3a}), 2.19 (dd, $^2J_{HH}$ = 11.3 Hz, $^3J_{HH}$ = 8.4 Hz, 1 H, H_{3b}), 1.46 (s, 9 H, H_{10}), 1.24 (d, $^3J_{HH}$ = 7.0 Hz, 3 H, H_8), 1.04 (d, $^3J_{HH}$ = 6.4 Hz, 3 H, H_4).

^{13}C{H}-NMR (125.77 MHz, 298 K, $CDCl_3$): δ = 175.58 (1 C, C_7), 80.96 (1 C, C_9), 57.91 (1 C, C_6), 56.76 (1 C, C_3), 47.23 (1 C, C_2), 28.23 (3 C, C_{10}), 21.67 (1 C, C_4), 19.42 (1 C, C_8).

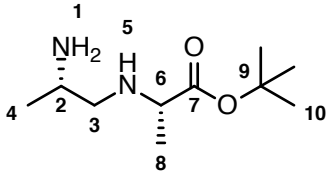

228

((*S*)-2-AMINOPROPYL)-*L*-ALANINE (**229**).

tert-Butyl ((*S*)-2-aminopropyl)-*L*-alaninate (**228**) (50.0 mg, 258 µmol, 1.0 eq.) was dissolved in hydrochloric acid (1 M, 10.0 mL) and stirred at 45 °C for 30 min. The solvent was evaporated yielding the title compound as hydrochloride salt (55.3 mg, 252 µmol, 97.8 %).

HR-ESI-MS: calcd. for [**229**+H]$^+$ $C_6H_{15}N_2O_2$ m/z= 147.1128, found m/z= 147.1127.

^{1}H-NMR (600.13 MHz, 298 K, D_2O): δ = 4.11 (q, $^3J_{HH}$ = 7.2 Hz, 1 H, H_6), 3.81 (ddq, $^3J_{HH}$ = 6.4 Hz, $^3J_{HH}$ = 6.2 Hz, $^3J_{HH}$ = 6.8 Hz, 1 H, H_2), 3.44 (dd, $^2J_{HH}$ = 13.4 Hz, $^3J_{HH}$ = 6.2 Hz, 1 H, H_{3a}), 3.36 (dd, $^2J_{HH}$ = 13.4 Hz, $^3J_{HH}$ = 6.4 Hz, 1 H, H_{3b}), 1.60 (d, $^3J_{HH}$ = 7.2 Hz, 3 H, H_8), 1.45 (d, $^3J_{HH}$ = 6.8 Hz, 3 H, H_4).

^{13}C{H}-NMR (150.95 MHz, 298 K, D_2O): δ = 172.03 (1 C, C_7), 56.92 (1 C, C_6), 48.31 (1 C, C_3), 44.58 (1 C, C_2), 16.06 (1 C, C_4), 14.25 (1 C, C_8).

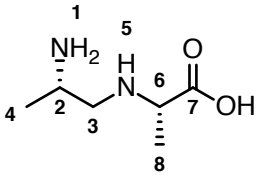

229

((*S*)-2-((4-NITROPHENYL)SULFONAMIDO)PROPYL)-*L*-ALANINE (**230**).

tert-Butyl ((*S*)-2-((4-nitrophenyl)sulfonamido)propyl)-*L*-alaninate (**52**) (1.00 g, 2.58 mmol, 1.0 eq.) was dissolved in hydrogen chloride solution (conc. in 1,4-dioxane, 10 mL) and stirred at 45 °C for 1 h. The solvent was evaporated yielding the title compound as hydrochloride salt (930 mg, 2.53 mmol, 98.0 %).

HR-ESI-MS: calcd. for [**230**+H]$^+$ $C_{12}H_{18}N_3O_6S$ m/z= 332.0911, found m/z= 332.0913.

^{1}H-NMR (500.13 MHz, 298 K, DMSO−d_6): δ = 8.46-8.41 (m, 2 H, H_{11}), 8.16-8.11 (m, 2 H, H_{10}), 8.52 (d, $^3J_{HH}$ = 8.0 Hz, 1 H, H_1), 3.99 (q, $^3J_{HH}$ = 7.2 Hz, 1 H, H_6), 3.77-3.67 (m, 1 H, H_2), 3.01-2.88 (m, 2 H, H_3), 1.45 (d, $^3J_{HH}$ = 7.2 Hz, 3 H, H_8), 0.96 (d, $^3J_{HH}$ = 6.7 Hz, 3 H, H_4).

^{13}C{H}-NMR (125.77 MHz, 298 K, DMSO−d_6): δ = 170.62 (1 C, C_7), 149.66 (1 C, C_{12}), 146.83 (1 C, C_9), 128.16 (2 C, C_{11}), 124.72 (2 C, C_{10}), 54.72 (1 C, C_6), 49.65 (1 C, C_3), 46.60 (1 C, C_2), 18.53 (1 C, C_4), 13.82 (1 C,

C_8).

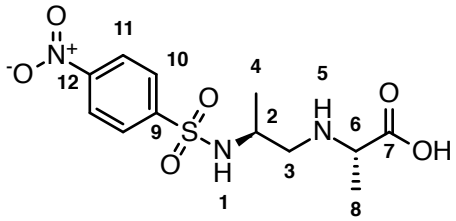

230

BENZYL (*S*)-(1-HYDROXYPROPAN-2-YL)CARBAMATE (**61**).

Sodium carbonate (245 g, 2.32 mol, 3.1 eq.) was dissolved in water (500 mL). A solution of (*S*)-alaninol (57.0 g, 759 mmol, 1.0 eq.) in ethyl acetate (180 mL) was added at 20-25 °C. The biphasic mixture was stirred vigorously and benzyl chloroformate (133 g, 782 mmol, 1.03 eq.) was added at 20-25 °C. After addition the biphasic mixture was further stirred for 1 h before diluted with water (500 mL) and ethyl acetate (600 mL). The clear layers were separated and the aqueous layer was extracted with ethyl acetate (250 mL). The combined organic layers were extracted with water (250 mL), dried over sodium sulphate and evaporated to dryness. The crude product was recrystallized from ethyl acetate / cyclohexane yielding a white solid (149 g, 711 mmol, 93.8 %).

HR-ESI-MS: calcd. for [**61**+Na]$^+$ $C_{11}H_{15}NNaO_3$ m/z= 232.0944, found m/z= 232.0944.

^{1}H-NMR (600.13 MHz, 298 K, $CDCl_3$): δ = 7.41-7.28 (m, 5 H, H_9,H_{10},H_{11}), 5.10 (d, $^2J_{HH}$ = 12.1 Hz, 1 H, H_{7a}), 5.07 (d, $^2J_{HH}$ = 12.1 Hz, 1 H, H_{7b}), 5.06 (bs, 1 H, H_5), 3.82 (ddd, $^3J_{HH}$ = 6.8 Hz, $^3J_{HH}$ = 5.6 Hz, $^3J_{HH}$ = 2.4 Hz, 1 H, H_3), 3.63 (dd, $^2J_{HH}$ = 10.2 Hz, $^3J_{HH}$ = 2.4 Hz, 1 H, H_{2a}), 3.50 (dd, $^2J_{HH}$ = 10.2 Hz, $^3J_{HH}$ = 5.6 Hz, 1 H, H_{2b}), 2.73 (bs, 1 H, H_1), 1.15 (d, $^3J_{HH}$ = 6.8 Hz, 3 H, H_4).

^{13}C{H}-NMR (150.9 MHz, 298 K, $CDCl_3$): δ = 156.70 (1 C, C_6), 136.46 (1 C, C_8), 128.64 (2 C, C_{10}), 128.27 (1 C, C_{11}), 128.23 (2 C, C_9), 66.93 (1 C, C_7), 66.83 (1 C, C_2), 49.05 (1 C, C_3), 17.32 (1 C, C_4).

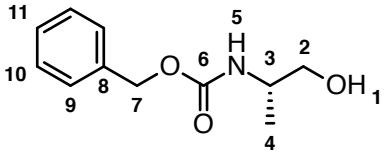

61

BENZYL (*S*)-(1-OXOPROPAN-2-YL)CARBAMATE (**60**).

(*S*)-(1-Hydroxypropan-2-yl)carbamate (**61**) (45.0 g, 215 mmol, 1.0 eq.), 2-iodoxybenzoic acid (IBX) (90.3 g, 322 mmol, 1.5 eq.) were suspended in ethyl acetate (450 mL). The suspension was heated to reflux. At reflux dimethyl sulfoxide (46 mL, 645 mmol, 3.0 eq.) was added. The suspension was further refluxed for 3.5 h before cooled down to 0-5 °C. The suspension was filtered and washed with ethyl acetate (150 mL). The filtrate was extracted with aqueous saturated sodium hydrogen carbonate (450 mL), water (450 mL) and brine (300 mL). The organic layer was dried with sodium sulphate and evaporated to dryness yielding a colourless oil (41.5 g, 200 mmol, 93.1 %).

HR-ESI-MS: calcd. for [**60**+H]$^+$ $C_{11}H_{14}NO_3$ m/z= 208.0968, found m/z= 208.0967.

^{1}H-NMR (250.13 MHz, 298 K, CD_3CN): δ = 9.51 (d, $^3J_{HH}$ = 0.5 Hz, 1 H, H_1), 7.54-7.11 (m, 5 H, H_8,H_9,H_{10}), 5.10 (s, 2 H, H_6), 4.08 (qdd, $^3J_{HH}$ = 7.4 Hz, $^3J_{HH}$ = 7.0 Hz, $^3J_{HH}$ = 0.5 Hz, 1 H, H_2), 1.27 (d, $^3J_{HH}$ = 7.4 Hz, 3 H, H_3).

^{13}C{H}-NMR (125.8 MHz, 298 K, $CDCl_3$): δ = 198.97 (1 C, C_1), 155.82 (1 C, C_5), 136.15 (1 C, C_7), 128.59 (2 C, C_9), 128.29 (1 C, C_{10}), 128.17 (2 C, C_8), 67.09 (1 C, C_6), 55.93 (1 C, C_2), 14.86 (1 C, C_3).

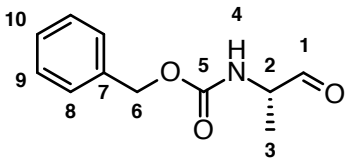

60

BENZYL (*R*)-(1-OXOPROPAN-2-YL)CARBAMATE (**122**).

(*R*)-(1-Hydroxypropan-2-yl)carbamate (1.06 g, 5.07 mmol, 1.0 eq.), 2-iodoxybenzoic acid (IBX) (3.27 g, 11.7 mmol, 2.3 eq.) were suspended in ethyl acetate (20 mL). The suspension was heated to reflux. At reflux dimethyl sulfoxide (1.7 mL, 23.3 mmol, 4.6 eq.) was added. The suspension was further refluxed for 3.5 h before cooled down to 0-5 °C. The suspension was filtered and washed with ethyl acetate (10 mL). The filtrate was extracted with aqueous saturated sodium hydrogen carbonate (20 mL), water (20 mL) and brine (20 mL). The organic layer was dried with sodium sulphate and evaporated to dryness yielding a colourless oil (1.04 g, 5.07 mol, 99.0 %).

^{1}H-NMR (250.13 MHz, 298 K, CD_3CN): δ = 9.51 (d, $^3J_{HH}$ = 0.5 Hz, 1 H, H_1), 7.54-7.11 (m, 5 H, H_8,H_9,H_{10}), 5.10 (s, 2 H, H_6), 4.08 (qdd, $^3J_{HH}$ = 7.4 Hz, $^3J_{HH}$ = 7.0 Hz, $^3J_{HH}$ = 0.5 Hz, 1 H, H_2), 1.27 (d, $^3J_{HH}$ = 7.4 Hz, 3 H, H_3).

$^{13}C\{H\}$-NMR (125.8 MHz, 298 K, $CDCl_3$): δ = 198.97 (1 C, C_1), 155.82 (1 C, C_5), 136.15 (1 C, C_7), 128.59 (2 C, C_9), 128.29 (1 C, C_{10}), 128.17 (2 C, C_8), 67.09 (1 C, C_6), 55.93 (1 C, C_2), 14.86 (1 C, C_3).

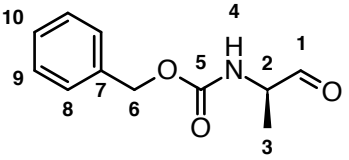

122

tert-BUTYL ((*S*)-2-(((BENZYLOXY)CARBONYL)AMINO)PROPYL)-*L*-ALANINATE (**62**).

Benzyl (*S*)-(1-oxopropan-2-yl)carbamate (**60**) (41.4 g, 200 mmol, 1.0 eq.) was dissolved in dichloromethane (600 mL). To this solution *L*-alanine *tert*-butyl ester (30.6 g, 200 mmol, 1.0 eq.) was added. The solution was stirred at 20-25 °C for 5 min followed by the addition of sodium triacetoxyborohydride (141 g, 600 mmol, 3.0 eq.). The reaction mixture was stirred at 20-25 °C for 16 h. The excess of sodium triacetoxyborohydride was quenched with aqueous saturated sodium hydrogen carbonate (450 mL) and the pH adjusted to >9 by addition of triethylamine (100 mL). The two layers were separated and the organic layer was washed with water (250 mL) and dried with sodium sulphate. The organic layer was evaporated to dryness yielding a colourless oil that slowly crystallised forming a white solid (66.0 g, 196 mmol, 98.1 %).

HR-ESI-MS: calcd. for [**62**+H]$^+$ $C_{18}H_{29}N_2O_4$ m/z= 337.2122, found m/z= 337.2121.

^{1}H-NMR (600.13 MHz, 298 K, DMSO−d_6): δ = 7.38-7.33 (m, 3 H, H_{15},H_{16}), 7.32-7.28 (m, 2 H, H_{14}), 7.09 (d, $^3J_{HH}$ = 8.1 Hz, 1 H, H_1), 5.01 (d, $^2J_{HH}$ = 12.8 Hz, 1 H, H_{12a}), 4.98 (d, $^2J_{HH}$ = 12.8 Hz, 1 H, H_{12b}), 3.54 (dddq, $^3J_{HH}$ = 8.1 Hz, $^3J_{HH}$ = 6.3 Hz, $^3J_{HH}$ = 6.2 Hz, $^3J_{HH}$ = 6.6 Hz, 1 H, H_2), 3.09 (q, $^3J_{HH}$ = 6.9 Hz, 1 H, H_6), 2.47 (dd, $^2J_{HH}$ = 11.5 Hz, $^3J_{HH}$ = 6.2 Hz, 1 H, H_{3a}), 2.40 (dd, $^2J_{HH}$ = 11.5 Hz, $^3J_{HH}$ = 6.3 Hz, 1 H, H_{3b}), 1.86 (bs, 1 H, H_5), 1.40 (s, 9 H, H_{10}), 1.11 (d, $^3J_{HH}$ = 6.9 Hz, 3 H, H_8), 1.03 (d, $^3J_{HH}$ = 6.6 Hz, 3 H, H_4).

$^{13}C\{H\}$-NMR (150.9 MHz, 298 K, DMSO−d_6): δ = 174.46 (1 C, C_7), 155.53 (1 C, C_{11}), 137.25 (1 C, C_{13}), 128.31 (2 C, C_{15}), 127.72 (3 C, C_{14}, C_{16}), 79.91 (1 C, C_9), 65.03 (1 C, C_{12}), 56.67 (1 C, C_6), 52.18 (1 C, C_3), 46.61 (1 C, C_2), 27.69 (3 C, C_{10}), 18.66 (1 C, C_8), 18.58 (1 C, C_4).

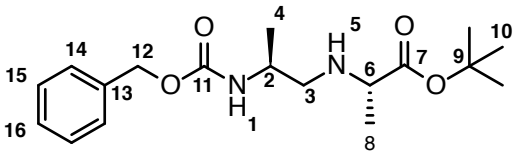

62

((*S*)-2-(((BENZYLOXY)CARBONYL)AMINO)PROPYL)-*L*-ALANINE (**231**).

tert-Butyl ((*S*)-2-(((benzyloxy)carbonyl)amino)propyl)-*L*-alaninate (**62**) (600 mg, 1.78 mmol, 1.0 eq.) was dissolved in methanol (10 mL) and hydrochloric acid (1 M, 10 mL). The solution was stirred at 40 °C before it was evaporated to dryness yielding a off-white solid (550 mg, 1.74 mmol, 97.5 %).

HR-ESI-MS: calcd. for [**231**+H]$^+$ $C_{14}H_{21}N_2O_4$ m/z= 281.1496, found m/z= 281.1499.

^{1}H-NMR (500.13 MHz, 298 K, DMSO−d_6): δ = 7.45-7.28 (m, 5 H, H_{12},H_{13}, H_{14}), 5.07 (d, $^2J_{HH}$ = 12.3 Hz, 1 H, H_{10a}), 5.02 (d, $^2J_{HH}$ = 12.3 Hz, 1 H, H_{10b}), 4.01 (q, $^3J_{HH}$ = 7.2 Hz, 1 H, H_2), 3.93 (ddq, $^3J_{HH}$ = 8.7 Hz, $^3J_{HH}$ = 5.1 Hz, $^3J_{HH}$ = 6.2 Hz, 1 H, H_6), 3.02 (dd, $^2J_{HH}$ = 12.8 Hz, $^3J_{HH}$ = 8.7 Hz, 1 H, H_{7a}), 2.96 (dd, $^2J_{HH}$ = 12.8 Hz, $^3J_{HH}$ = 5.1 Hz, 1 H, H_{7b}), 1.46 (d, $^3J_{HH}$ = 7.2 Hz, 3 H, H_4), 1.14 (d, $^3J_{HH}$ = 6.2 Hz, 3 H, H_8).

^{13}C{H}-NMR (125.77 MHz, 298 K, DMSO−d_6): δ = 170.79 (1 C, C_3), 155.65 (1 C, C_9), 136.85 (1 C, C_{11}), 128.39 (2 C, C_{13}), 127.89 (2 C, C_{12}), 127.85 (1 C, C_{14}), 65.55 (1 C, C_{10}), 54.80 (1 C, C_2), 49.44 (1 C, C_7), 44.05 (1 C, C_6), 18.64 (1 C, C_8), 13.99 (1 C, C_4).

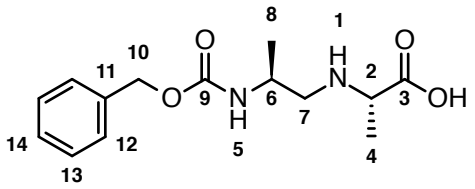

231

TERT-BUTYL *N*-BENZYL-*N*-((S)-2 (((BENZYLOXY)CARBONYL)-AMINO)PROPYL)-*L*-ALANINATE (**63**).

tert-Butyl ((*S*)-2-(((benzyloxy)carbonyl)amino)propyl)-*L*-alaninate (**62**) (23.7 g, 70.4 mmol, 1.0 eq.) was dissolved in acetonitrile (200 mL) and potassium carbonate (10.7 g, 77.4 mmol, 1.1 eq.) was added. To this suspension benzyl bromide (12.6 g, 73.9 mmol, 1.05 eq.) was added and the reaction mixture was stirred at 50 °C for 16 h. Excess of benzyl bromide was quenched with triethylamine (15 mL). The reaction mixture was then

cooled to 20-25 °C filtered and evaporated to dryness yielding a crude yellow oil. The crude product was purified by flash column chromatography (SiO_2, ethyl acetate / cyclohexane (7:3)) yielding a yellowish oil (25.3 g, 59.3 mmol, 84.2 %).

HR-ESI-MS: calcd. for [**63**+H]$^+$ $C_{25}H_{35}N_2O_4$ m/z= 427.2591, found m/z= 427.2596.

^{1}H-NMR (600.13 MHz, 298 K, CD_3CN): δ = 7.41-7.17 (m, 10 H, H_{14}, H_{15}, H_{16}, H_{19}, H_{20}, H_{21}), 5.81 (bs, 1 H, H_1), 5.06 (d, $^2J_{HH}$ = 12.6 Hz, 1 H, H_{12a}), 5.01 (d, $^2J_{HH}$ = 12.6 Hz, 1 H, H_{12b}), 3.76 (d, $^2J_{HH}$ = 14.2 Hz, 1 H, H_{17a}), 3.71 (d, $^2J_{HH}$ = 14.2 Hz, 1 H, H_{17b}), 3.59 (m, 1 H, H_2), 3.28 (q, $^3J_{HH}$ = 7.1 Hz, 1 H, H_6), 2.58 (dd, $^2J_{HH}$ = 13.4 Hz, $^3J_{HH}$ = 8.1 Hz, 1 H, H_{3a}), 2.52 (dd, $^2J_{HH}$ = 13.4 Hz, $^3J_{HH}$ = 6.3 Hz, 1 H, H_{3b}), 1.44 (s, 9 H, H_{10}), 1.17 (d, $^3J_{HH}$ = 7.1 Hz, 3 H, H_8), 1.09 (d, $^3J_{HH}$ = 6.3 Hz, 3 H, H_4).

^{13}C{H}-NMR (100.61 MHz, 298 K, CD_3CN): δ = 174.05 (1 C, C_7), 156.97 (1 C, C_{11}), 141.08 (1 C, C_{18}), 138.59 (1 C, C_{13}), 129.50 ($C_{arom.}$), 129.40 ($C_{arom.}$), 129.19 ($C_{arom.}$), 128.76 (2 C, C_{19}), 128.66 (2 C, C_{14}), 127.87 ($C_{arom.}$), 81.57 (1 C, C_9), 66.52 (1 C, C_{12}), 59.00 (1 C, C_6), 56.55 (1 C, C_3), 56.55 (1 C, C_{17}), 46.64 (1 C, C_2), 28.37 (3 C, C_{10}), 19.25 (1 C, C_4), 13.88 (1 C, C_8).

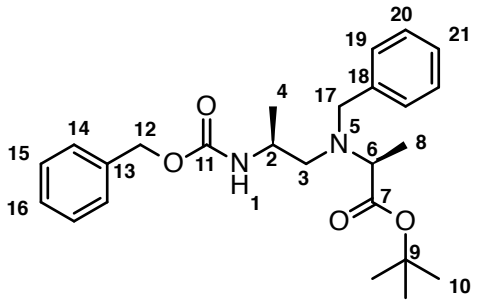

63

N-BENZYL-*N*-((*S*)-2-(((BENZYLOXY)CARBONYL)AMINO)-PROPYL)-*L*-ALANINE (**64**).

tert-Butyl *N*-benzyl-*N*-((*S*)-2-(((benzyloxy) carbonyl)amino)propyl)-*L*-alaninate (**63**) (4.01 g, 9.40 mmol, 1.0 eq.) was dissolved in hydrogen chloride solution (conc. in 1,4-dioxane, 30.0 mL). The reaction mixture was heated to 40 °C and stirred for 18 h. The solution was evaporated to dryness yielding the title compound as a hydrochloride salt (3.81 g, 9.36 mmol, quant.). The product was used in the next step without additional purification.

HR-ESI-MS: calcd. for [**64**+H]$^+$ $C_{21}H_{27}N_2O_4$ m/z= 371.1965, found m/z= 371.1970.

^{1}H-NMR (500.13 MHz, 298 K, CD_3CN): δ = 7.58-7.31 (m, 10 H, H_{13}, H_{14}, H_{15}, H_{18}, H_{19}, H_{20}), 5.08 (d, $^{2}J_{HH}$ = 12.2 Hz, 1 H, H_{11a}), 5.05 (d, $^{2}J_{HH}$ = 12.2 Hz, 1 H, H_{11b}), 4.66 (d, $^{2}J_{HH}$ = 12.9 Hz, 1 H, H_{16a}), 4.17-4.06 (m, 1 H, H_2), 4.07 (q, $^{3}J_{HH}$ = 7.2 Hz, 1 H, H_6), 3.96 (d, $^{2}J_{HH}$ = 12.9 Hz, 1 H, H_{16b}), 3.22 (dd, $^{2}J_{HH}$ = 13.6 Hz, $^{3}J_{HH}$ = 1.8 Hz, 1 H, H_{3a}), 3.10 (dd, $^{2}J_{HH}$ = 13.6 Hz, $^{3}J_{HH}$ = 10.4 Hz, 1 H, H_{3b}), 1.55 (d, $^{3}J_{HH}$ = 7.2 Hz, 3 H, H_8), 1.16 (d, $^{3}J_{HH}$ = 6.9 Hz, 3 H, H_4).

^{13}C{H}-NMR (125.75 MHz, 298 K, CD_3CN): δ = 171.12 (1 C, C_7), 159.86 (1 C, C_{10}), 137.40 (1 C, C_{12}), 131.47 (1 C, C_{17}), 131.07 (2 C, C_{18}), 131.03 ($C_{arom.}$), 130.42 ($C_{arom.}$), 129.54 ($C_{arom.}$), 129.17 ($C_{arom.}$), 128.97 (2 C, C_{13}), 68.13 (1 C, C_{11}), 61.08 (1 C, C_6), 59.53 (1 C, C_3), 56.69 (1 C, C_{16}), 44.69 (1 C, C_2), 18.05 (1 C, C_4), 9.64 (1 C, C_8).

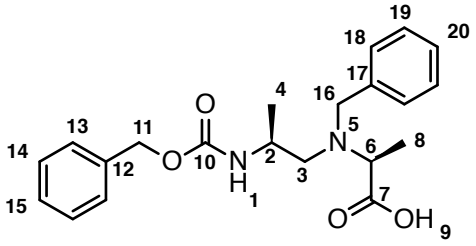

64

tert-BUTYL (5*S*,8*S*,11*S*,14*S*)-7,13-DIBENZYL-5,8,11,14-TETRAMETHYL-3,9-DIOXO-1-PHENYL-2-OXA-4,7,10,13-TETRAAZAPENTADECAN-15-OATE (**65**).

Method A

tert-Butyl ((*S*)-2-((*S*)-2-(((*S*)-2-(((benzyloxy)carbonyl)amino)propyl)amino)propanamido)propyl)-*L*-alaninate (**75**) (410 mg, 882 µmol, 1.0 eq.) was dissolved in acetonitrile (20 mL). Benzyl bromide (462 mg, 2.65 mmol, 3.0 eq.) and potassium carbonate (366 mg, 2.65 mmol, 3.0 eq.) were added and the suspension was stirred at 40 °C for 18 h. The suspension was filtered and evaporated to dryness. The crude oil was purified by flash column chromatography (SiO_2, ethyl acetate) yielding a yellowish oil (511 mg, 792 µmol, 89.8 %).

Method B

tert-butyl *N*-((*S*)-2-aminopropyl)-*N*-benzyl-*L*-alaninate (**56**) (380 mg, 1.30 mmol, 1.0 eq.), *N*-benzyl-*N*-((*S*)-2-(((benzyloxy)carbonyl)amino)propyl)-*L*-alanine (**64**) trifluoroacetate salt (630 mg, 1.30 mmol, 1.0 eq.) and *N*-ethyl diisopropylamine (430 µL, 2.60 mmol, 2.0 eq.) were dissolved in acetonitrile (10 mL). HATU (519 mg, 1.37 mmol, 1.1 eq.) was added. The

reaction mixture was stirred at 20-25 °C for 16 h. The solvent was removed under vacuum and the crude oil was dissolved in ethyl acetate (10 mL) and extracted with water (2x 5.0 mL) and brine (2.0 mL). The organic layer was dried with sodium sulphate and evaporated to dryness. The resulting oil was purified by flash column chromatography (SiO_2, ethyl acetate / cyclohexane (5:5)) yielding a white solid (580 g, 899 µmol, 69.2 %).

HR-ESI-MS: calcd. for [**65**+H]$^+$ $C_{38}H_{53}N_4O_5$ m/z= 645.4010, found m/z= 645.4009.

^{1}H-NMR (500.13 MHz, 298 K, $CDCl_3$): δ = 7.40-7.14 (m, 15 H, H_{19}, H_{20}, H_{21}, H_{24}, H_{25}, H_{26}, H_{32}, H_{33}, H_{34}), 5.12 (d, $^2J_{HH}$ = 12.2 Hz, 1 H, H_{30a}), 4.94 (d, $^2J_{HH}$ = 12.2 Hz, 1 H, H_{30b}), 4.70 (d, $^3J_{HH}$ = 7.8 Hz, 1 H, H_1), 3.99 (ddq, $^3J_{HH}$ = 7.8 Hz, $^3J_{HH}$ = 6.1 Hz, $^3J_{HH}$ = 6.5 Hz, 1 H, H_{10}), 3.87-3.80 (m, 1 H, H_2), 3.85 (d, $^2J_{HH}$ = 14.1 Hz, 1 H, H_{22a}), 3.72 (d, $^2J_{HH}$ = 14.1 Hz, 1 H, H_{22b}), 3.72 (d, $^2J_{HH}$ = 13.4 Hz, 1 H, H_{17a}), 3.38 (d, $^2J_{HH}$ = 13.4 Hz, 1 H, H_{17b}), 3.36 (q, $^3J_{HH}$ = 6.9 Hz, 1 H, H_6), 3.28 (q, $^3J_{HH}$ = 6.9 Hz, 1 H, H_{14}), 2.67 (dd, $^2J_{HH}$ = 13.5 Hz, $^3J_{HH}$ = 6.1 Hz, 1 H, H_{11a}), 2.59 (dd, $^2J_{HH}$ = 13.5 Hz, $^3J_{HH}$ = 7.8 Hz, 1 H, H_{11b}), 2.48 (dd, $^2J_{HH}$ = 13.3 Hz, $^3J_{HH}$ = 3.6 Hz, 1 H, H_{3a}), 2.28 (dd, $^2J_{HH}$ = 13.3 Hz, $^3J_{HH}$ = 9.3 Hz, 1 H, H_{3b}), 1.44 (s, 9 H, H_{28}), 1.19 (d, $^3J_{HH}$ = 6.9 Hz, 3 H, H_8), 1.17 (d, $^3J_{HH}$ = 6.5 Hz, 3 H, H_{12}), 1.16 (d, $^3J_{HH}$ = 7.0 Hz, 3 H, H_{16}), 1.05 (d, $^3J_{HH}$ = 6.6 Hz, 3 H, H_4).

^{13}C{H}-NMR (125.77 MHz, 298 K, $CDCl_3$): δ = 173.41 (1 C, C_{15}), 172.98 (1 C, C_7), 156.45 (1 C, C_{29}), 140.06 (1 C, C_{23}), 139.23 (1 C, C_{18}), 136.71 (1 C, C_{31}), 129.09 (2 C, C_{19}), 128.63 ($C_{arom.}$), 128.59 (2 C, C_{24}), 128.44 ($C_{arom.}$), 128.28 ($C_{arom.}$), 128.24 (2 C, C_{32}), 128.13 ($C_{arom.}$), 127.28 ($C_{arom.}$), 126.92 ($C_{arom.}$), 80.89 (1 C, C_{27}), 66.63 (1 C, C_{30}), 58.47 (1 C, C_6), 57.77 (1 C, C_{14}), 56.48 (1 C, C_3), 56.36 (1 C, C_{22}), 55.70 (1 C, C_{11}), 54.88 (1 C, C_{17}), 45.19 (1 C, C_2), 44.30 (1 C, C_{10}), 28.28 (3 C, C_{28}), 19.50 (1 C, C_4), 19.17 (1 C, C_{12}), 15.29 (1 C, C_{16}), 8.31 (1 C, C_8).

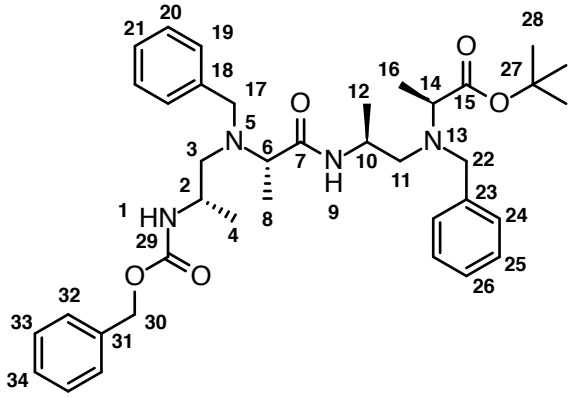

65

N-((*S*)-2-((*S*)-2-(((*S*)-2-AMINOPROPYL)(BENZYL)AMINO)PROPANAMIDO)PROPYL)-*N*-BENZYL-*L*-ALANINE (**66**).

tert-Butyl (5*S*,8*S*,11*S*,14*S*)-7,13-dibenzyl-5,8,11,14-tetramethyl-3,9-dioxo-1-phenyl-2-oxa-4,7,10,13-tetraazapentadecan-15-oate (**65**) (1.73 g, 2.68 mmol, 1.0 eq.) was dissolved in hydrobromic acid solution (16 % wt. in acetic acid, 15.0 mL) and stirred at 40 °C for 30 min. The solvent was removed under reduced pressure yielding a brownish oil. This oil was further suspended in acetonitrile (15 mL) and hydrochloric acid (37 %, 5.0 mL). This mixture was again evaporated to dryness. The procedure was repeated three times to remove residual acetic acid from the product. Finally, the product was dissolved in methanol (15.0 mL) and evaporated to dryness, yielding a light brown foam. This foam was extensively dried under high vacuum at 40 °C for 2 d. The product (1.89 g) is obtained as a mixture of HCl and HBr salt with minimal acetate content and was further used without additional purification.

HR-ESI-MS: calcd. for [**66**+H]$^+$ $C_{26}H_{39}N_4O_3$ m/z= 455.3017, found m/z= 455.3022.

^{1}H-NMR (500.13 MHz, 298 K, DMSO−d_6): δ = 9.96 (bs, 1 H, H_{27}), 8.64 (bs, 2 H, H_1), 7.51-7.40 (m, 2 H, $H_{arom.}$), 7.35-7.22 (m, 5 H, $H_{arom.}$), 7.21-7.11 (m, 3 H, $H_{arom.}$), 3.67 (d, $^2J_{HH}$ = 14.5 Hz, 1 H, H_{22a}), 3.62 (d, $^2J_{HH}$ = 14.5 Hz, 1 H, H_{22b}), 3.61 (m, 1 H, H_{10}), 3.44 (q, $^3J_{HH}$ = 6.9 Hz, 1 H, H_6), 3.47 (d, $^2J_{HH}$ = 14.1 Hz, 1 H, H_{17a}), 3.42 (d, $^2J_{HH}$ = 14.2 Hz, 1 H, H_{17b}), 3.32-3.24 (m, 1 H, H_2), 2.99 (q, $^3J_{HH}$ = 7.3 Hz, 1 H, H_{14}), 2.77 (dd, $^2J_{HH}$ = 13.8 Hz, $^3J_{HH}$ = 11.5 Hz, 1 H, H_{11a}), 2.54 (dd, $^2J_{HH}$ = 13.6 Hz, $^3J_{HH}$ = 8.6 Hz, 1 H, H_{3a}), 2.39-2.31 (m, 2 H, H_{11b}, H_{3b}), 1.10 (d, $^3J_{HH}$ = 6.9 Hz, 3 H, H_8), 1.08 (d, $^3J_{HH}$ = 7.0 Hz, 3 H, H_{16}), 1.00 (d, $^3J_{HH}$ = 6.5 Hz, 3 H, H_4), 0.98 (d, $^3J_{HH}$ = 6.2 Hz, 3 H, H_{12}).

^{13}C{H}-NMR (125.77 MHz, 298 K, DMSO−d_6): δ = 177.43 (1 C, C_{15}), 171.50 (1 C, C_7), 140.74 (1 C, C_{23}), 138.50 (1 C, C_{18}), 129.01 ($C_{arom.}$), 128.15 ($C_{arom.}$), 128.11 ($C_{arom.}$), 127.95 ($C_{arom.}$), 126.87 ($C_{arom.}$), 126.42 ($C_{arom.}$), 59.12 (1 C, C_{14}), 57.44 (1 C, C_6), 55.87 (1 C, C_{22}), 55.03 (1 C, C_{11}), 53.63 (1 C, C_{17}), 53.46 (1 C, C_3), 44.61 (1 C, C_{10}), 43.31 (1 C, C_2), 18.29 (1 C, C_{12}), 17.37 (1 C, C_4), 10.8 (1 C, C_8), 10.19 (1 C, C_{16}).

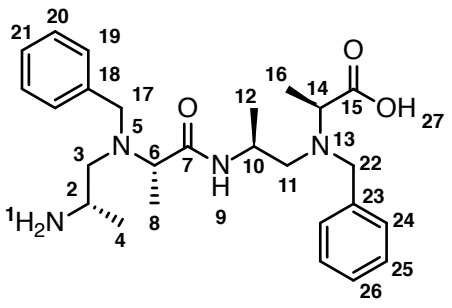

66

(3*S*,6*S*,9*S*,12*S*)-4,10-DIBENZYL-3,6,9,12-TETRA-METHYL-1,4,7,10-TETRAAZACYCLODODECANE-2,8-DIONE (**67**).

Method A

(3*S*,6*S*,9*S*,12*S*)-3,6,9,12-tetramethyl-1,4,7,10-tetraazacyclododecane-2,8-dione (**69**) (660 mg, 2.57 mmol, 1.0 eq.) was dissolved in acetonitrile (5.0 mL) and potassium carbonate (1.42 g, 10.3 mmol, 4.0 eq.) was added. To this suspension benzyl bromide (987 mg, 5.65 mmol, 2.2 eq.) was added and the reaction mixture was heated to 55 °C for 16 h. Excess benzyl bromide was quenched with triethylamine (2.0 mL). The reaction mixture was then cooled to 20-25 °C, filtered and evaporated to dryness yielding a crude yellow oil. The crude product was purified by flash column chromatography (SiO_2, ethyl acetate / triethylamine (100:1)) yielding a white solid (890 mg, 2.04 mmol, 79.3 %).

Method B

N-((*S*)-2-((*S*)-2-(((*S*)-2-aminopropyl)(benzyl)amino)propanamido)propyl)-*N*-benzyl-*L*-alanine (**66**) (1.89 g, 2.68 mmol, 1.0 eq.) and *N*-ethyl diisopropylamine (2.2 m L, 13.4 mmol, 5.0 eq.) were dissolved in acetonitrile (1.8 L). HATU (1.26 g, 3.22 mmol, 1.2 eq.) was added and the solution was stirred at 20-25 °C for 20 min. The solvent was removed under vacuum. The crude product was combined and purified by flash column chromatography (SiO_2, ethyl acetate / cyclohexane (7:3)) yielding a white solid (950 mg, 2.18 mmol, 81.2 % yield calculated over 2 steps starting from **65**).

HR-ESI-MS: calcd. for [**67**+H]$^+$ $C_{26}H_{37}N_4O_2$ m/z= 437.2911, found m/z= 437.2917.

^{1}H-NMR (600.13 MHz, 298 K, DMSO−d_6): δ = 7.73 (d, $^3J_{HH}$ = 4.8 Hz, 2 H, H_5), 7.45-7.42 (m, 4 H, H_{11}), 7.33-7.25 (m, 6 H, H_{12},H_{13}), 3.90 (d, $^2J_{HH}$ = 13.3 Hz, 2 H, H_{9a}), 3.57 (d, $^2J_{HH}$ = 13.3 Hz, 2 H, H_{9b}), 3.34 (dddq, $^3J_{HH}$ = 10.8 Hz, $^3J_{HH}$ = 4.8 Hz, $^3J_{HH}$ = 2.8 Hz, $^3J_{HH}$ = 6.6 Hz, 2 H, H_6), 3.20 (q, $^3J_{HH}$ = 7.0 Hz, 2 H, H_2), 2.77 (dd, $^2J_{HH}$ = 13.4 Hz, $^3J_{HH}$ = 10.8 Hz, 2 H, H_{7a}), 2.29 (dd, $^2J_{HH}$ = 13.4 Hz, $^3J_{HH}$ = 2.8 Hz, 2 H, H_{7b}), 1.15 (d, $^3J_{HH}$ = 6.6 Hz, 6 H, H_8), 1.05 (d, $^3J_{HH}$ = 7.0 Hz, 6 H, H_4).

^{13}C{H}-NMR (150.95 MHz, 298 K, DMSO−d_6): δ = 172.14 (2 C, C_3), 139.20 (2 C, C_{10}), 129.05 (4 C, C_{11}), 128.18 (4 C, C_{12}), 127.11 (2 C, C_{13}), 59.65 (2 C, C_2), 56.87 (2 C, C_9), 55.14 (2 C, C_7), 44.08 (2 C, C_6), 17.71 (2 C, C_8), 8.54 (2 C, C_4).

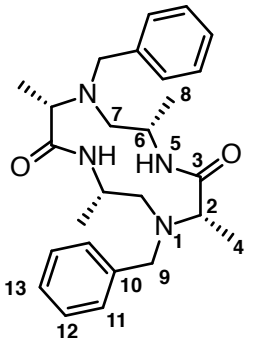

67

(2*S*,5*S*,8*S*,11*S*)-1,7-DIBENZYL-2,5,8,11-TETRA-METHYL-1,4,7,10-TETRAAZACYCLODODECANE (**68**).

(3*S*,6*S*,9*S*,12*S*)-4,10-dibenzyl-3,6,9,12-tetramethyl-1,4,7,10-tetraazacyclododecane-2,8-dione (**67**) (1.90 g, 4.35 mmol, 1.0 eq.) was dissolved in dichloromethane (50 mL) and cooled to 0-5 °C. Trimethylsilyl chloride (2.60 g, 23.9 mmol, 5.5 eq.) was slowly added. After completion, the reaction mixture was stirred at 0-5 °C for 30 min followed by the addition of lithium aluminium hydride (6.1 mL, 2 M in tetrahydrofuran, 12.2 mmol, 2.8 eq.). The reaction mixture was allowed to warm to 20-25 °C and was further stirred for 3 h. The reaction mixture was cooled to 0-5 °C and saturated aqueous sodium hydrogen carbonate (5.0 mL) was slowly added. To the resulting suspension sodium sulphate (5.00 g) was added. The suspension was filtered and evaporated to dryness yielding a white solid (1.65 g, 4.04 mmol, 92.8 %).

HR-ESI-MS: calcd. for [**68**+H]$^+$ $C_{26}H_{41}N_4$ m/z= 409.3326, found m/z= 409.3330.

^{1}H-NMR (600.13 MHz, 298 K, $CDCl_3$): δ = 7.40-7.34 (m, 8 H, H_{11},H_{12}), 7.29-7.26 (m, 2 H, H_{13}), 3.81 (d, $^2J_{HH}$ = 12.8 Hz, 2 H, H_{9a}), 3.13-3.02 (bs, 2 H, H_6), 2.98 (d, $^2J_{HH}$ = 12.8 Hz, 2 H, H_{9b}), 2.94 (bs, 2 H, H_5), 2.88-2.76 (m, 4 H, H_2,H_{7a}), 2.45 (d, $^2J_{HH}$ = 11.8 Hz, 2 H, H_{3a}), 2.40 (dd, $^2J_{HH}$ = 13.4 Hz, $^3J_{HH}$ = 13.1 Hz, 2 H, H_{7b}), 2.25 (dd, $^2J_{HH}$ = 11.8 Hz, $^3J_{HH}$ = 11.8 Hz, 2 H, H_{3b}), 0.91 (d, $^3J_{HH}$ = 6.5 Hz, 6 H, H_8), 0.87 (d, $^3J_{HH}$ = 5.5 Hz, 6 H, H_4).

^{13}C{H}-NMR (150.95 MHz, 298 K, $CDCl_3$): δ = 139.97 (2 C, C_{10}), 129.41 (4 C, C_{12}), 128.50 (4 C, C_{11}), 127.30 (2 C, C_{13}), 56.62 (2 C, C_3), 51.72 (2 C, C_9), 50.04 (2 C, C_6), 47.83 (2 C, C_7), 46.47 (2 C, C_2), 18.71 (2 C, C_4), 10.20 (2 C, C_8).

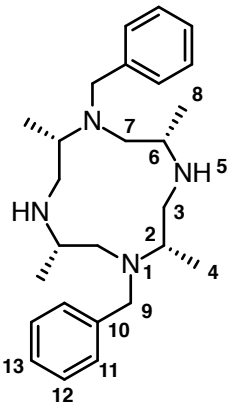

68

(2*S*,5*S*,8*S*,11*S*)-2,5,8,11-TETRAMETHYL-1,4,7,10-TETRAAZACYCLODODECANE (**22**).

Method A

(2*S*,5*S*,8*S*,11*S*)-1,7-dibenzyl-2,5,8,11-tetramethyl-1,4,7,10-tetraazacyclododecane (**68**) (1.50 g, 3.67 mmol, 1.0 eq.), palladium hydroxide on carbon (20 wt % loading, 750 mg) and ammonium formate (5.00 g, 79.3 mmol, 10 eq.) were suspended in ethanol (50 mL) and heated to reflux. The suspension was refluxed for 16 h, cooled to 20-25 °C, filtered over celite and evaporated to dryness. The crude product was washed with cold acetone (1.0 mL). The title compound was obtained as a white solid (650 mg, 2.85 mmol 77.6 %).

Method B

(3*S*,6*S*,9*S*,12*S*)-3,6,9,12-tetramethyl-1,4,7,10-tetraazacyclododecane-2,8-dione **69** (430 mg, 1.68 mmol, 1.0 eq.) was dissolved in dichloromethane (10 mL) and cooled to 0-5 °C. Trimethylsilyl chloride (1.10 g, 10.1 mmol, 6.0 eq.) was slowly added. After completion, the reaction mixture was stirred at 0-5 °C for 30 min followed by the addition of lithium aluminium hydride (2 M in tetrahydrofuran, 8.4 mL, 16.8 mmol, 10 eq.). The reaction mixture was allowed to warm to 20-25 °C and was further stirred for 3 h. The reaction mixture was cooled to 0-5 °C and saturated aqueous sodium hydrogen carbonate (5.0 mL) was slowly added. To the resulting suspension sodium sulphate (5.00 g) was added. The suspension was filtered and the filter cake was washed with dichloromethane (5x 50 mL). The filtrate was evaporated to dryness yielding a white solid (350 mg, 1.53 mmol, 91.2 %).

ESI-MS: calcd. for [**22**+H]$^+$ $C_{12}H_{29}N_4$ m/z= 229.23, found m/z= 229.15.

^{1}H-NMR (500.13 MHz, 298 K, $CDCl_3$): δ = 2.70-2.60 (m, 8 H, H_2, H_{3eq}), 2.38 (dd, $^2J_{HH}$ = 13.4 Hz, $^3J_{HH}$ = 10.6 Hz, 4 H, H_{3ax}), 2.01 (bs, 4 H, H_1), 0.95

(d, $^{3}J_{HH}$ = 6.1 Hz, 12 H, H_4).

^{13}C{H}-NMR (125.77 MHz, 298 K, $CDCl_3$): δ = 52.32 (4 C, C_2), 47.67 (4 C, C_3), 18.42 (4 C, C_4).

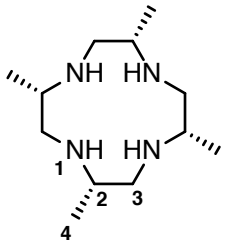

22

BENZYL (*S*)-(1,1-DIMETHOXYPROPAN-2-YL)CARBAMATE (**77**).

Benzyl (*S*)-(1-oxopropan-2-yl)carbamate (**60**) (2.00 g, 9.65 mmol, 1.0 eq.) and trimethyl orthoformate (1.54 g, 14.5 mmol, 1.5 eq.) were dissolved in methanol (10 mL) and stirred at 20-25 °C for 18 h. The solution was evaporated to dryness yielding a yellowish solid (2.38 g, 9.40 mmol, 97.4 %).

HR-ESI-MS: calcd. for [**77**+Na]$^{+}$ $C_{13}H_{19}NNaO_4$ m/z= 276.1206, found m/z= 276.1211.

^{1}H-NMR (600.13 MHz, 298 K, CD_3CN): δ = 7.39-7.30 (m, 5 H, H_{10}, H_{11}, H_{12}), 5.51 (bs, 1 H, H_6), 5.05 (s, 2 H, H_8), 4.16 (d, $^{3}J_{HH}$ = 4.6 Hz, 1 H, H_3), 3.76 (qd, $^{3}J_{HH}$ = 6.8 Hz, $^{3}J_{HH}$ = 4.6 Hz, 1 H, H_4), 3.35 (s, 3 H, $H_{2/1}$), 3.34 (s, 3 H, $H_{1/2}$), 1.05 (d, $^{3}J_{HH}$ = 6.8 Hz, 3 H, H_5).

^{13}C{H}-NMR (150.95 MHz, 298 K, CD_3CN): δ = 156.77 (1 C, C_7), 138.43 (1 C, C_9), 129.38 (2 C, C_{11}), 128.77 (1 C, C_{12}), 128.59 (2 C, C_{10}), 107.21 (1 C, C_3), 66.68 (1 C, C_8), 56.08 (1 C, $C_{2/1}$), 55.50 (1 C, $C_{1/2}$), 49.35 (1 C, C_4), 15.65 (1 C, C_5).

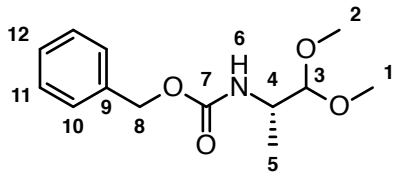

77

(*S*)-1,1-DIMETHOXYPROPAN-2-AMINE (**74**).

Benzyl (*S*)-(1,1-dimethoxypropan-2-yl)carbamate (**77**) (2.38 g, 9.40 mmol, 1.0 eq.) was dissolved in methanol (100 mL). Palladium on activated charcoal (moistened with water, 10 % Pd basis, 200 mg) was added and the mixture was stirred at 20-25 °C under 1.0 bar of hydrogen for 6 h. The suspension was filtered through celite and evaporated to dryness yielding a yellowish liquid (790 mg, 6.63 mmol, 70.5 %).

^{1}H-NMR (600.13 MHz, 298 K, CD_3CN): δ = 3.92 (d, $^3J_{HH}$ = 6.1 Hz, 1 H, H_3), 2.86 (qd, $^3J_{HH}$ = 6.6 Hz, $^3J_{HH}$ = 6.1 Hz, 1 H, H_4), 3.35 (s, 3 H, $H_{2/1}$), 3.33 (s, 3 H, $H_{1/2}$), 1.05 (d, $^3J_{HH}$ = 6.8 Hz, 3 H, H_5).

^{13}C{H}-NMR (150.95 MHz, 298 K, CD_3CN): δ = 110.20 (1 C, C_3), 55.12 (1 C, $C_{2/1}$), 55.10 (1 C, $C_{1/2}$), 49.17 (1 C, C_4), 18.13 (1 C, C_5).

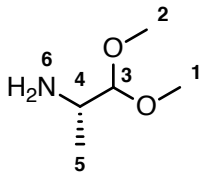

74

BENZYL ((*S*)-1-(((*S*)-1,1-DIMETHOXYPROPAN-2-YL)AMINO)-1-OXOPROPAN-2-YL)CARBAMATE (**78**).

N-Carbobenzyloxy-*L*-alanine (656 mg, 2.94 mmol, 1.0 eq.) and (*S*)-1,1-dimethoxypropan-2-amine (350 mg, 2.94 mmol, 1.0 eq.) was dissolved in ethyl acetate (10 mL). Propylphosphonic anhydride solution (50 wt. % in ethyl acetate, 2.6 mL, 4.41 mmol, 1.5 eq.) and *N*,*N*-diisopropylethylamine (1.0 mL, 5.88 mmol, 2.0 eq.) were added and the solution was stirred at 20-25 °C for 18 h. The solution was extracted with hydrochloric acid (1 M, 20.0 mL), aqueous saturated sodium hydrogen carbonate (20.0 mL) and brine (20.0 mL). The organic layer was evaporated to dryness yielding a white solid (810 mg, 2.50 mmol, 84.9 %).

HR-ESI-MS: calcd. for [**78**+Na]$^+$ $C_{16}H_{24}N_2NaO_5$ m/z= 347.1577, found m/z= 347.1584.

^{1}H-NMR (600.13 MHz, 298 K, $CDCl_3$): δ = 7.39-7.30 (m, 5 H, H_{14}, H_{15}, H_{16}), 6.00 (d, $^3J_{HH}$ = 6.4 Hz, 1 H, H_5), 5.31 (d, $^3J_{HH}$ = 5.1 Hz, 1 H, H_1), 5.12 (d, $^2J_{HH}$ = 12.9 Hz, 1 H, H_{12a}), 5.09 (d, $^2J_{HH}$ = 12.9 Hz, 1 H, H_{12b}), 4.25-4.10 (m, 3 H, H_2, H_6, H_7), 3.42 (s, 3 H, $H_{9/10}$), 3.40 (s, 3 H, $H_{10/9}$), 1.38 (d, $^3J_{HH}$ = 7.10 Hz, 3 H, H_3), 1.11 (d, $^3J_{HH}$ = 6.4 Hz, 3 H, H_8).

$^{13}C\{H\}$-NMR (150.95 MHz, 298 K, $CDCl_3$): δ = 171.79 (1 C, C_4), 155.97 (1 C, C_{11}), 136.37 (1 C, C_{13}), 128.71 (2 C, C_{15}), 128.37 (1 C, C_{16}), 128.23 (2 C, C_{14}), 106.10 (1 C, C_7), 67.12 (1 C, C_{12}), 56.17 (1 C, $C_{10/9}$), 55.91 (1 C, $C_{9/10}$), 50.82 (1 C, C_2), 46.67 (1 C, C_6), 19.02 (1 C, C_3), 14.87 (1 C, C_8).

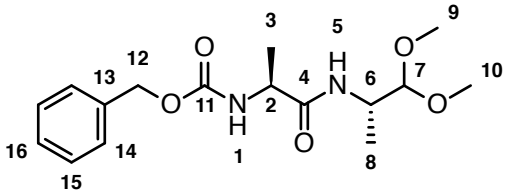

78

METHYL ((BENZYLOXY)CARBONYL)-*L*-ALANYL-*L*-ALANINATE (**80**).

N-Carbobenzyloxy-*L*-alanine (68.3 g, 306 mmol, 1.0 eq.), *L*-alanine methyl ester hydrochloride (42.7 g, 306 mmol, 1.0 eq.) and *N*,*N*-diisopropylethylamine (177 mL, 1.07 mol, 3.5 eq.) were suspended in ethyl acetate (500 mL). Propylphosphonic anhydride solution (50 wt. % in ethyl acetate, 214 g, 337 mmol, 1.1 eq.) was added and the mixture was stirred at 20-25 °C for 18 h. The mixture was diluted with hydrochloric acid (2 M, 500 mL) and the layers were separated. The aqueous layer was extracted with ethyl acetate (200 mL). The combined organic layers were extracted with aqueous saturated sodium hydrogen carbonate (500 mL) and brine (300 mL). The organic layer was dried with sodium sulphate and evaporated to dryness yielding a white solid (79.5 g, 258 mmol, 84.3 %).

HR-ESI-MS: calcd. for [**80**+Na]$^+$ $C_{15}H_{20}N_2NaO_5$ m/z= 331.1264, found m/z= 331.1265.

^1H-NMR (600.13 MHz, 298 K, $CDCl_3$): δ = 7.37-7.28 (m, 5 H, H_{13}, H_{14}, H_{15}), 6.65 (d, $^3J_{HH}$ = 4.3 Hz, 1 H, H_5), 5.43 (d, $^3J_{HH}$ = 6.2 Hz, 1 H, H_1), 5.10 (s, 2 H, H_{11}), 4.54 (qd, $^3J_{HH}$ = 7.2 Hz, $^3J_{HH}$ = 4.3 Hz, 1 H, H_6), 4.25 (qd, $^3J_{HH}$ = 7.2 Hz, $^3J_{HH}$ = 6.2 Hz, 1 H, H_2), 3.73 (s, 3 H, H_9), 1.380 (d, $^3J_{HH}$ = 7.2 Hz, 3 H, H_8), 1.379 (s, $^3J_{HH}$ = 7.2 Hz, 3 H, H_4).

$^{13}C\{H\}$-NMR (150.95 MHz, 298 K, $CDCl_3$): δ = 173.32 (1 C, C_7), 171.96 (1 C, C_3), 155.94 (1 C, C_{10}), 136.31 (1 C, C_{12}), 128.67 (2 C, C_{14}), 128.32 (1 C, C_{15}), 128.19 (2 C, C_{13}), 67.13 (1 C, C_{11}), 52.63 (1 C, C_9), 50.51 (1 C, C_2), 48.18 (1 C, C_6), 18.78 (1 C, C_4), 18.37 (1 C, C_8).

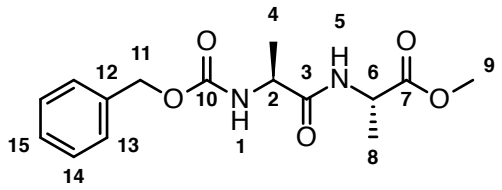

80

BENZYL ((*S*)-1-(((*S*)-1-HYDROXYPROPAN-2-YL)AMINO)-1-OXOPROPAN-2-YL)CARBAMATE (**73**).

Methyl ((benzyloxy)carbonyl)-*L*-alanyl-*L*-alaninate (**80**) (20.0 g, 64.9 mmol, 1.0 eq.) was dissolved in tetrahydrofuran (60 mL) and methanol (60 mL) and cooled to 0-5 °C. A solution of sodium borohydride (15.3 g, 389 mmol, 6.0 eq.) in methanol / water 8:2 (225 mL) was added dropwise and the mixture was allowed to warm up to 20-25 °C and was left stirring for 18 h. The pH was adjusted to 7 with hydrochloric acid (4 M). Volatile organic solvents were removed on the rotary evaporator. The white suspension was diluted with ethyl acetate (200 mL). The two layers were separated and the aqueous layer was extracted with ethyl acetate (100 mL). The combined organic layers were extracted with aqueous saturated sodium hydrogen carbonate (200 mL) and water (100 mL). The organic layer was dried with sodium sulphate and evaporated to dryness yielding a white solid (15.3 g, 54.6 mmol, 84.1 %).

HR-ESI-MS: calcd. for [**73**+Na]$^+$ $C_{14}H_{20}N_2NaO_4$ m/z= 303.1315, found m/z= 303.1317.

^{1}H-NMR (600.13 MHz, 298 K, $CDCl_3$): δ = 7.39-7.30 (m, 5 H, H_{13}, H_{14}, H_{15}), 6.17 (bs, 1 H, H_1), 5.25 (bs, 1 H, H_6), 5.11 (s, 2 H, H_{11}), 4.18 (qd, $^3J_{HH}$ = 6.8 Hz, $^3J_{HH}$ = 6.2 Hz, 1 H, H_7), 4.07-3.98 (m, 1 H, H_2), 3.73 (bs, 1 H, H_{3a}), 3.53-3.45 (m, 1 H, H_{3b}), 1.38 (d, $^3J_{HH}$ = 6.8 Hz, 3 H, H_9), 1.14 (d, $^3J_{HH}$ = 6.9 Hz, 3 H, H_4).

^{13}C{H}-NMR (150.95 MHz, 298 K, $CDCl_3$): δ = 172.71 (1 C, C_8), 156.16 (1 C, C_{10}), 136.19 (1 C, C_{12}), 128.74 (2 C, C_{14}), 128.44 (1 C, C_{15}), 128.32 (2 C, C_{13}), 67.35 (1 C, C_{11}), 66.82 (1 C, C_3), 50.98 (1 C, C_7), 47.94 (1 C, C_2), 18.54 (1 C, C_9), 16.97 (1 C, C_4).

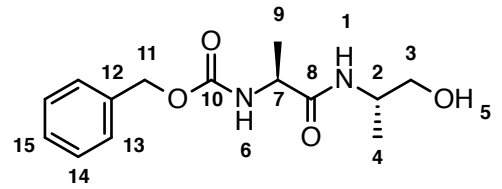

73

BENZYL ((*S*)-1-OXO-1-(((*S*)-1-OXOPROPAN-2-YL)AMINO)PROPAN-2-YL)CARBAMATE (**71**).

Benzyl ((*S*)-1-(((*S*)-1-hydroxypropan-2-yl)amino)-1-oxopropan-2-yl)carbamate (**73** (12.2 g, 43.5 mmol, 1.0 eq.) was dissolved in acetonitrile (200 mL). 2-Iodoxybenzoic acid (30.5 g, 109 mmol, 2.5 eq.) was added and the suspension was stirred at 80 °C for 2 h. The reaction mixture was cooled to 20-25 °C and diluted with ethyl acetate (600 mL). The suspension was filtered and the filtrate was evaporated to dryness. The residue was redissolved in ethtyl acetate (100 mL) and extracted with aqueous saturated sodium hydrogen carbonate (100 mL) and water (100 mL). The organic layer was dried with sodium sulphate and evaporated to dryness yielding a yellowish oil that slowly crystallized yielding a yellowish solid (11.2 g, 40.2 mmol, 92.5 %).

HR-ESI-MS: calcd. for [**71**+H]$^+$ $C_{14}H_{19}N_2O_4$ m/z= 279.1339, found m/z= 279.1334.

^{1}H-NMR (600.13 MHz, 298 K, $CDCl_3$): δ = 9.53 (s, 1 H, H_3), 7.39-7.30 (m, 5 H, H_{12}, H_{13}, H_{14}), 6.57 (bs, 1 H, H_1), 5.24 (bs, 1 H, H_5), 5.12 (s, 2 H, H_{10}), 4.47 (dq, $^3J_{HH}$ = 7.0 Hz, $^3J_{HH}$ = 6.6 Hz, 1 H, H_2), 4.32-4.23 (m, 1 H, H_6), 1.41 (d, $^3J_{HH}$ = 7.0 Hz, 3 H, H_8), 1.35 (d, $^3J_{HH}$ = 6.6 Hz, 3 H, H_4).

^{13}C{H}-NMR (150.95 MHz, 298 K, $CDCl_3$): δ = 198.69 (1 C, C_3), 172.29 (1 C, C_7), 155.94 (1 C, C_9), 136.21 (1 C, C_{11}), 128.73 (2 C, C_{13}), 128.46 (1 C, C_{14}), 128.30 (2 C, C_{12}), 67.33 (1 C, C_{10}), 54.71 (1 C, C_2), 50.61 (1 C, C_7), 18.60 (1 C, C_8), 14.60 (1 C, C_4).

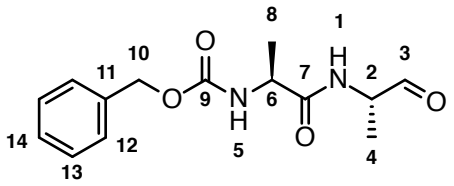

71

tert-BUTYL ((*S*)-2-((*S*)-2-(((BENZYLOXY)CARBONYL)AMINO)-PROPANAMIDO)PROPYL)-*L*-ALANINATE (**81**).

Benzyl ((*S*)-1-oxo-1-(((*S*)-1-oxopropan-2-yl)amino)propan-2-yl)carbamate (**71**) (11.2 g, 40.2 mmol, 1.0 eq.) was dissolved in dichloromethane (200 mL) and *tert*-butyl *L*-alaninate (5.84 g, 40.2 mmol) was added. The solution was stirred at 20-25 °C for 5 min followed by the addition of sodium triacetoxyborohydride (21.3 g, 101 mmol, 2.5 eq.). The suspension was stirred at 20-25 °C for 4 h. The reaction mixture was extracted with aqueous saturated sodium hydrogen carbonate (100 mL) and water (100 mL). The organic layer was dried with sodium sulphate and evaporated to dryness yielding a

yellowish oil. The oil was purified by flash column chromatography (SiO_2, ethyl acetate) yielding a colorless oil (14.2 g, 34.8 mmol, 86.7 %).

HR-ESI-MS: calcd. for [**81**+H]$^+$ $C_{21}H_{34}N_3O_5$ m/z= 408.2493, found m/z= 408.2500.

^{1}H-NMR (600.13 MHz, 298 K, $CDCl_3$): δ = 7.38-7.28 (m, 5 H, H_{18}, H_{19}, H_{20}), 6.43 (bs, 1 H, H_5), 5.44 (bs, 1 H, H_9), 5.09 (s, 2 H, H_{16}), 4.25-4.16 (m, 1 H, H_{10}), 3.95-3.86 (m, 1 H, H_6), 3.20 (q, $^3J_{HH}$ = 6.9 Hz, 1 H, H_2), 2.63 (dd, $^2J_{HH}$ = 10.9 Hz, $^3J_{HH}$ = 3.3 Hz, 1 H, H_{7a}), 2.53 (dd, $^2J_{HH}$ = 10.9 Hz, $^3J_{HH}$ = 4.3 Hz, 1 H, H_{7b}), 1.45 (s, 9 H, H_{14}), 1.38 (d, $^3J_{HH}$ = 7.0 Hz, 3 H, H_{12}), 1.23 (d, $^3J_{HH}$ = 7.2 Hz, 3 H, H_4), 1.14 (d, $^3J_{HH}$ = 6.9 Hz, 3 H, H_8).

^{13}C{H}-NMR (150.95 MHz, 298 K, $CDCl_3$): δ = 175.09 (1 C, C_3), 171.81 (1 C, C_{11}), 155.95 (1 C, C_{15}), 136.48 (1 C, C_{17}), 128.67 (2 C, C_{19}), 128.30 (1 C, C_{20}), 128.20 (2 C, C_{18}), 81.23 (1 C, C_{13}), 67.02 (1 C, C_{16}), 57.38 (1 C, C_2), 50.77 (1 C, C_{10}), 52.00 (1 C, C_7), 45.75 (1 C, C_6), 28.22 (3 C, C_{14}), 19.26 (1 C, C_{12}), 18.56 (1 C, C_8), 13.09 (1 C, C_4).

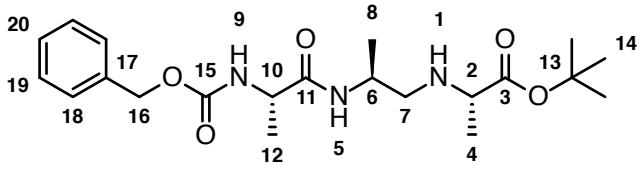

81

tert-BUTYL ((*S*)-2-((*S*)-2-AMINOPROPANAMIDO)PROPYL)-*L*-ALANINATE (**76**).

tert-Butyl ((*S*)-2-((*S*)-2-(((benzyloxy)carbonyl)amino)propanamido)propyl)-*L*-alaninate (**81**) (9.54 g, 23.4 mmol, 1.0 eq.) was dissolved in methanol (250 mL). Palladium on activated charcoal (moistened with water, 10 % Pd basis, 500 mg) was added and the mixture was stirred at 20-25 °C under 1.0 bar of hydrogen for 6 h. The suspension was filtered through celite and evaporated to dryness yielding a yellowish oil (6.28 g, 23.0 mmol, 98.2 %).

HR-ESI-MS: calcd. for [**76**+H]$^+$ $C_{13}H_{28}N_3O_3$ m/z= 274.2125, found m/z= 274.2130.

^{1}H-NMR (600.13 MHz, 298 K, $CDCl_3$): δ = 7.2 (bs, 1 H, H_5), 4.00-3.90 (m, 1 H, H_6), 3.47 (q, $^3J_{HH}$ = 7.0 Hz, 1 H, H_{10}), 3.20 (q, $^3J_{HH}$ = 6.9 Hz, 1 H, H_2), 2.64 (dd, $^2J_{HH}$ = 11.90 Hz, $^3J_{HH}$ = 5.5 Hz, 1 H, H_{7a}), 2.54 (dd, $^2J_{HH}$ = 11.90 Hz, $^3J_{HH}$ = 3.3 Hz, 1 H, H_{7b}), 1.45 (s, 9 H, H_{14}), 1.31 (d, $^3J_{HH}$ = 6.9 Hz, 3 H, H_{12}), 1.24 (d, $^3J_{HH}$ = 7.0 Hz, 3 H, H_4), 1.16 (3J=6., ($^3J_{HH}$ = 6.7 Hz, 3 H, H_8).

$^{13}C\{H\}$-NMR (150.95 MHz, 298 K, $CDCl_3$): δ = 175.35 (1 C, C_{11}), 175.02 (1 C, C_3), 80.96 (1 C, C_{13}), 57.31 (1 C, C_2), 52.43 (1 C, C_7), 50.89 (1 C, C_{10}), 44.89 (1 C, C_6), 28.09 (3 C, C_{14}), 21.78 (1 C, C_{12}), 18.93 (1 C, C_4), 18.68 (1 C, C_8).

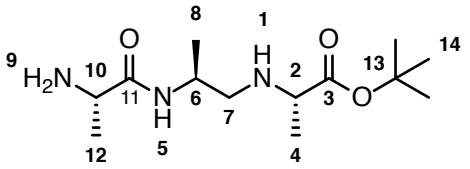

76

TERT-BUTYL ((*S*)-2-((*S*)-2-(((*S*)-2-(((BENZYLOXY)CARBONYL)AMINO)PROPYL)AMINO)PROPANAMIDO)PROPYL)-*L*-ALANINATE (**75**).

tert-Butyl ((*S*)-2-((*S*)-2-aminopropanamido)propyl)-*L*-alaninate (**76**) (331 mg, 1.21 mmol, 1.0 eq.) and benzyl (*S*)-(1-oxopropan-2-yl)carbamate (**60**) (251 mg, 1.21 mmol, 1.0 eq.) were dissolved in dichloromethane (20 mL). The solution was stirred at 20-25 °C for 5 min followed by the addition of sodium triacetoxyborohydride (769 mg, 3.63 mmol, 3.0 eq.). The reaction mixture was stirred at 20-25 °C for 16 h. The excess of sodium triacetoxyborohydride was quenched with aqueous saturated sodium hydrogencarbonate (20.0 mL) and the pH adjusted to >9 by addition of triethylamine (2.0 mL). The two layers were separated and the organic layer was washed with water (20 mL) and dried with sodium sulphate. The organic layer was evaporated to dryness yielding a colourless oil (410 mg, 882 µmol, 72.9 %).

HR-ESI-MS: calcd. for [**75**+H]$^+$ $C_{24}H_{41}N_4O_5$ m/z= 465.3071, found m/z= 465.3076.

^1H-NMR (600.13 MHz, 298 K, $CDCl_3$): δ = 7.38-7.26 (m, 5 H, H_{20}, H_{21}, H_{22}), 5.47 (d, $^3J_{HH}$ = 6.7 Hz, 1 H, H_{13}), 5.08 (s, 2 H, H_{18}), 4.00-3.92 (m, 1 H, H_6), 3.76-3.73 (m, 1 H, H_{14}), 3.15 (q, $^3J_{HH}$ = 7.0 Hz, 1 H, H_2), 3.07 (q, $^3J_{HH}$ = 6.9 Hz, 1 H, H_{10}), 2.77 (dd, $^2J_{HH}$ = 12.9 Hz, $^3J_{HH}$ = 7.1 Hz, 1 H, H_{15a}), 2.67 (dd, $^2J_{HH}$ = 11.7 Hz, $^3J_{HH}$ = 4.7 Hz, 1 H, H_{7a}), 2.59 (dd, $^2J_{HH}$ = 12.9 Hz, $^3J_{HH}$ = 5.0 Hz, 1 H, H_{15b}), 2.45 (dd, $^2J_{HH}$ = 11.7 Hz, $^3J_{HH}$ = 5.1 Hz, 1 H, H_{7b}), 1.43 (s, 9 H, H_{24}), 1.26 (d, $^3J_{HH}$ = 7.0 Hz, 3 H, H_{12}), 1.19 (d, $^3J_{HH}$ = 7.0 Hz, 3 H, H_{16}), 1.19 (d, $^3J_{HH}$ = 7.0 Hz, 3 H, H_4), 1.11 (d, $^3J_{HH}$ = 6.7 Hz, 3 H, H_8).

$^{13}C\{H\}$-NMR (150.95 MHz, 298 K, $CDCl_3$): δ = 174.90 (1 C, C_3), 174.65 (1 C, C_{11}), 156.00 (1 C, C_{17}), 136.61 (1 C, C_{19}), 128.53 (2 C, C_{21}), 128.19 (1 C, C_{22}), 128.12 (2 C, C_{20}), 81.00 (1 C, C_{23}), 66.57 (1 C, C_{18}), 59.12 (1 C, C_{10}), 57.14 (1 C, C_2), 53.92 (1 C, C_{15}), 52.36 (1 C, C_7), 47.23 (1 C, C_{14}), 44.75 (1 C, C_6), 28.08 (3 C, C_{24}), 20.10 (1 C, C_{12}), 18.85 (1 C, C_{16}), 18.85 (1 C, C_4),

18.84 (1 C, C_8).

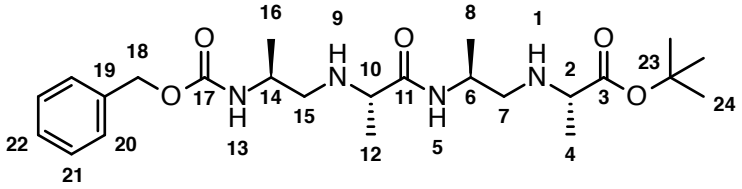

75

tert-BUTYL *N*-((*S*)-2-(((BENZYLOXY)CARBONYL)AMINO)-PROPYL)-*N*-(4-FLUOROBENZYL)-*L*-ALANINATE (**85**)

tert-Butyl ((*S*)-2-(((benzyloxy)carbonyl)amino)propyl)-*L*-alaninate (**62**) (65.0 g, 189 mmol, 1.0 eq.) was dissolved in acetonitrile (200 mL) and potassium carbonate (53.3 g, 386 mmol, 2.0 eq.) was added. To this suspension 1-(bromomethyl)-4-fluorobenzene (43.8 g, 232 mmol, 1.2 eq.) was added and the reaction mixture was stirred at 45 °C for 16 h. Excess of 1-(bromomethyl)--4-fluorobenzene was quenched with triethylamine (50.0 mL). The reaction mixture was cooled to 20-25 °C filtered and evaporated to dryness yielding a crude oil. The crude product was purified by flash column chromatography (SiO_2, ethyl acetate / cyclohexane (7:3)) yielding a yellowish oil (78.3 g, 176 mmol, 91.3 %).

HR-ESI-MS: calcd. for [**85**+H]$^+$ $C_{25}H_{34}FN_2O_4$ m/z= 445.2497, found m/z= 445.2498.

^{1}H-NMR (600.13 MHz, 298 K, DMSO−d_6): δ = 7.37-7.28 (m, 7 H, H_{14}, H_{15}, H_{16}, H_{19}), 7.11 (dd, $^3J_{HH}$ = 8.8 Hz, $^3J_{HH}$ = 8.8 Hz, 2 H, H_{20}), 7.05 (d, $^3J_{HH}$ = 8.0 Hz, 1 H, H_1), 5.02 (d, $^2J_{HH}$ = 12.6 Hz, 1 H, H_{12a}), 4.97 (d, $^2J_{HH}$ = 12.6 Hz, 1 H, H_{12b}), 3.80 (d, $^2J_{HH}$ = 14.3 Hz, 1 H, H_{17a}), 3.64 (d, $^2J_{HH}$ = 14.3 Hz, 1 H, H_{17b}), 3.54 (dddq, $^3J_{HH}$ = 8.7 Hz, $^3J_{HH}$ = 8.0 Hz, $^3J_{HH}$ = 5.8 Hz, $^3J_{HH}$ = 6.7 Hz, 1 H, H_2), 3.20 (q, $^3J_{HH}$ = 7.1 Hz, 1 H, H_6), 2.52 (dd, $^2J_{HH}$ = 13.1 Hz, $^3J_{HH}$ = 5.8 Hz, 1 H, H_{3a}), 2.48 (dd, $^2J_{HH}$ = 13.1 Hz, $^3J_{HH}$ = 8.7 Hz, 1 H, H_{3b}), 1.42 (s, 9 H, H_{10}), 1.10 (d, $^3J_{HH}$ = 7.1 Hz, 3 H, H_8), 1.02 (d, $^3J_{HH}$ = 6.7 Hz, 3 H, H_4).

^{13}C{H}-NMR (150.9 MHz, 298 K, DMSO−d_6): δ = 172.13 (1 C, C_7), 161.18 (d, $^1J_{CF}$ = 242.1 Hz, 1 C, C_{21}), 155.48 (1 C, C_{11}), 137.29 (1 C, C_{13}), 135.89 (d, $^4J_{CF}$ = 2.9 Hz, 1 C, C_{18}), 130.05 (d, $^3J_{CF}$ = 8.0 Hz, 2 C, C_{19}), 128.30 (2 C, C_{15}), 127.72 (1 C, C_{16}), 127.68 (2 C, C_{14}), 114.86 (d, $^2J_{CF}$ = 21.1 Hz, 2 C, C_{20}), 80.25 (1 C, C_9), 65.02 (1 C, C_{12}), 57.28 (1 C, C_6), 55.58 (1 C, C_3), 55.05 (1 C, C_{17}), 45.47 (1 C, C_2), 27.89 (3 C, C_{10}), 18.58 (1 C, C_4), 15.58 (1 C, C_8).

^{19}F{H}-NMR (564.6 MHz, 298 K, DMSO−d_6): δ = −114.86 (1 F, F_{21}).

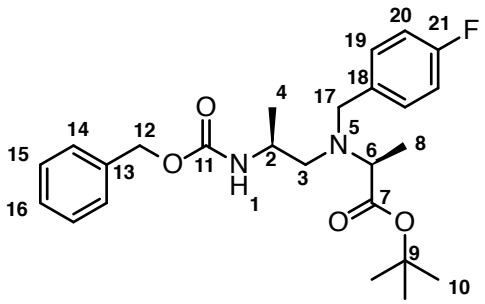

85

tert-BUTYL *N*-((*S*)-2-AMINOPROPYL)-*N*-(4-FLUOROBENZYL)-*L*-ALANINATE (**88**).

Ammonium formate (8.50 g, 135 mmol, 8.0 eq.) was dissolved in ethanol (485 mL) and palladium on activated charcoal (moistened with water, 10 % Pd basis, 750 mg) was added. The reaction mixture was then heated to 50 °C for 15 min (H_2 evolution!) followed by the addition of *tert*-butyl *N*-((*S*)-2--(((benzyloxy)carbonyl)amino)propyl)-*N*-(4-fluorobenzyl)-*L*-alaninate (**85**) (7.50 g, 16.9 mmol, 1.0 eq.) dissolved in ethanol (15.0 mL). The reaction progress was carefully monitored by LC/MS. The reaction was stopped once the starting material was consumed completely (approximately after 1 h). The hot suspension was then immediately filtered through celite and triethylamine (20.0 mL) was added. The solution was evaporated to dryness yielding a yellowish oil (4.80 g, 15.4 mmol, 91.5 %) that was used without further purification.

HR-ESI-MS: calcd. for [**88**+H]$^+$ $C_{17}H_{28}FN_2O_2$ m/z= 311.2129, found m/z= 311.2128.

^{1}H-NMR (600.13 MHz, 298 K, DMSO−d_6): δ = 7.37-7.32 (m, 2 H, H_{13}), 7.16-7.11 (m, 2 H, H_{14}), 3.70 (d, $^2J_{HH}$ = 14.3 Hz, 1 H, H_{11a}), 3.62 (d, $^2J_{HH}$ = 14.3 Hz, 1 H, H_{11b}), 3.25 (q, $^3J_{HH}$ = 7.0 Hz, 1 H, H_6), 2.75 (ddq, $^3J_{HH}$ = 7.0 Hz, $^3J_{HH}$ = 6.5 Hz, $^3J_{HH}$ = Hz, 1 H, H_2), 2.36 (dd, $^2J_{HH}$ = 12.8 Hz, $^3J_{HH}$ = 7.0 Hz, 1 H, H_{3a}), 2.26 (dd, $^2J_{HH}$ = 12.8 Hz, $^3J_{HH}$ = 6.5 Hz, 1 H, H_{3b}), 1.44 (s, 9 H, H_{10}), 1.11 (d, $^3J_{HH}$ = 7.0 Hz, 3 H, H_8), 0.87 (d, $^3J_{HH}$ = 6.3 Hz, 3 H, H_4).

^{13}C{H}-NMR (150.95 MHz, 298 K, DMSO−d_6): δ = 172.21 (1 C, C_7), 161.14 (d, $^1J_{CF}$ = 242.0 Hz, 1 C, C_{15}), 136.35 (d, $^4J_{CF}$ = 2.9 Hz, 1 C, C_{12}), 130.02 (d, $^3J_{CF}$ = 8.0 Hz, 2 C, C_{13}), 114.86 (d, $^2J_{CF}$ = 21.1 Hz, 2 C, C_{14}), 80.05 (1 C, C_9), 59.72 (1 C, C_3), 57.96 (1 C, C_6), 54.77 (1 C, C_{11}), 44.70 (1 C, C_2), 27.88 (3 C, C_{10}), 21.48 (1 C, C_4), 14.08 (1 C, C_8).

^{19}F{H}-NMR (564.6 MHz, 298 K, DMSO−d_6): δ = −116.31 (1 F, F_{15}).

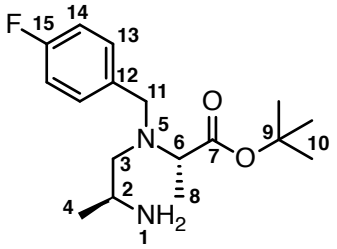

88

N-((*S*)-2-(((BENZYLOXY)CARBONYL)AMINO)PROPYL)-*N*-(4-FLUOROBENZYL)-*L*-ALANINE (**87**).

tert-Butyl *N*-((*S*)-2-(((benzyloxy)carbonyl)amino)propyl)-*N*-(4-fluorobenzyl)-*L*-alaninate (**85**) (33.0 g, 74.2 mmol, 1.0 eq.) was dissolved in hydrogen chloride solution (4 M in 1,4-dioxane) and stirred at 20-25 °C. The reaction progress was monitored by LC/MS and once the starting material was consumed (approximately 12 h) the solution was evaporated to dryness. The crude oil was then dissolved in dichloromethane (100 mL) and triethylamine (30 mL) was added. The organic layer was extracted with water (2x 100 mL), dried with sodium sulphate and evaporated to dryness yielding the title compound as a triethylammonium salt (35.4 g. 72.3 mmol, 97.4 %). The off-white foam was used in the next step without further purification.

HR-ESI-MS: calcd. for [**87**+H]$^+$ $C_{21}H_{26}FN_2O_4$ m/z= 389.1871, found m/z= 389.1866.

^{1}H-NMR (600.13 MHz, 298 K, DMSO−d_6): δ = 12.35 (bs, 1 H, H_9), 7.38-7.26 (m, 7 H, H_{13},H_{14},H_{15},H_{18}), 7.09 (d, $^3J_{HH}$ = 8.0 Hz, 1 H, H_1), 7.11-7.03 (m, 2 H, H_{19}), 5.01 (d, $^2J_{HH}$ = 12.5 Hz, 1 H, H_{11a}), 4.98 (d, $^2J_{HH}$ = 12.5 Hz, 1 H, H_{11b}), 3.76 (d, $^2J_{HH}$ = 14.4 Hz, 1 H, H_{16a}), 3.66 (d, $^2J_{HH}$ = 14.4 Hz, 1 H, H_{16b}), 3.52 (dddq, $^3J_{HH}$ = 8.0 Hz, $^3J_{HH}$ = 8.0 Hz, $^3J_{HH}$ = 6.1 Hz, $^3J_{HH}$ = 6.6 Hz, 1 H, H_2), 3.29 (q, $^3J_{HH}$ = 7.1 Hz, 1 H, H_6), 2.56 (dd, $^2J_{HH}$ = 13.2 Hz, $^3J_{HH}$ = 6.1 Hz, 1 H, H_{3a}), 2.47 (dd, $^2J_{HH}$ = 13.2 Hz, 1 H, H_{3b}), 1.16 (d, $^3J_{HH}$ = 7.1 Hz, 3 H, H_8), 1.01 (d, $^3J_{HH}$ = 6.6 Hz, 3 H, H_4).

^{13}C{H}-NMR (150.95 MHz, 298 K, DMSO−d_6): δ = 174.64 (1 C, C_7), 161.16 (d, $^1J_{CF}$ = 242.1 Hz, 1 C, C_{20}), 155.61 (1 C, C_{10}), 137.27 (1 C, C_{12}), 136.09 (1 C, C_{17}), 130.02 (d, $^3J_{CF}$ = 8.0 Hz, 2 C, C_{18}), 128.33 (2 C, C_{14}), 127.73 (3 C, C_{13},C_{15}), 114.83 (d, $^2J_{CF}$ = 21.1 Hz, 2 C, C_{19}), 65.07 (1 C, C_{11}), 56.96 (1 C, C_6), 55.93 (1 C, C_3), 55.00 (1 C, C_{16}), 45.57 (1 C, C_2), 18.59 (1 C, C_4), 15.25 (1 C, C_8).

^{19}F{H}-NMR (564.6 MHz, 298 K, DMSO−d_6): δ = −116.26 (1 F, F_{20}).

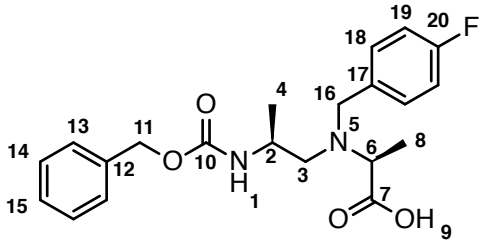

87

tert-BUTYL (5*S*,8*S*,11*S*,14*S*)-7,13-BIS(4-FLUOROBENZYL)-5,8,11,14-TETRAMETHYL-3,9-DIOXO-1-PHENYL-2-OXA-4,7,10,13-TETRAAZAPENTADECAN-15-OATE (**86**).

tert-Butyl *N*-(((*S*))-2-aminopropyl)-*N*-(4-fluorobenzyl)-*L*-alaninate (**88**) (18.0 g, 58.0 mmol, 1.0 eq.), N-((*S*)-2-(((benzyloxy)carbonyl)amino)propyl)-*N*-(4-fluorobenzyl)-*L*-alanine (**87**) triethylammonium salt (28.4 g, 58.0 mmol, 1.0 eq.) and *N*-ethyl diisopropylamine (19.2 mL, 116 mmol, 2.0 eq.) were dissolved in acetonitrile (300 mL) and HATU (22.1 g, 58.0 mmol, 1.0 eq.) was added. The reaction mixture was stirred at 20-25 °C for 16 h. The solvent was removed under vacuum and the crude oil was dissolved in ethyl acetate (300 mL) and extracted with water (2x 100 mL) and brine (50.0 mL). The organic layer was dried with sodium sulphate and evaporated to dryness. The crude oil was first plugged through a short silica gel column (100 g SiO_2). The fractions containing the product were combined and evaporated to dryness. The resulting oil was further purified by flash column chromatography (SiO_2, ethyl acetate / cyclohexane (3:7)) yielding a white foam (21.9 g, 32.1 mmol, 55.4 %).

HR-ESI-MS: calcd. for [**86**+H]$^+$ $C_{38}H_{51}F_2N_4O_5$ m/z= 681.3822, found m/z= 681.3826.

^{1}H-NMR (600.13 MHz, 298 K, DMSO−d_6): δ = 7.58 (d, $^3J_{HH}$ = 8.2 Hz, 1 H, H_9), 7.40-7.25 (m, 9 H, H_{34},H_{33},H_{32},H_{24},H_{19}), 7.12-7.06 (m, 2 H, H_{25}), 7.04-6.97 (m, 2 H, H_{20}), 5.05 (d, $^2J_{HH}$ = 12.5 Hz, 1 H, H_{30a}), 4.98 (d, $^2J_{HH}$ = 12.5 Hz, 1 H, H_{30b}), 3.86-3.77 (m, 1 H, H_{10}), 3.81 (d, $^2J_{HH}$ = 14.3 Hz, 1 H, H_{22a}), 3.64 (m, 1 H, H_2), 3.62 (d, $^2J_{HH}$ = 14.3 Hz, 1 H, H_{22b}), 3.50 (d, $^2J_{HH}$ = 14.4 Hz, 1 H, H_{17a}), 3.45 (d, $^2J_{HH}$ = 14.4 Hz, 1 H, H_{17b}), 3.29 (q, $^3J_{HH}$ = 6.9 Hz, 1 H, H_6), 3.21 (q, $^3J_{HH}$ = 6.6 Hz, 1 H, H_{14}), 2.57-2.51 (m, 2 H, H_{11}), 2.46 (dd, $^2J_{HH}$ = 13.3 Hz, $^3J_{HH}$ = 4.8 Hz, 1 H, H_{3a}), 2.28 (dd, $^2J_{HH}$ = 13.3 Hz, $^3J_{HH}$ = 8.2 Hz, 1 H, H_{3b}), 1.41 (s, 9 H, H_{28}), 1.10 (d, $^3J_{HH}$ = 7.2 Hz, 3 H, H_{16}), 1.08 (d, $^3J_{HH}$ = 6.9 Hz, 3 H, H_8), 1.04 (d, $^3J_{HH}$ = 6.6 Hz, 3 H, H_{12}), 0.96 (d, $^3J_{HH}$ = 6.7 Hz, 3 H, H_4).

^{13}C{H}-NMR (150.95 MHz, 298 K, DMSO−d_6): δ = 172.14 (1 C, C_{15}), 171.86 (1 C, C_7), 161.15 (d, $^1J_{CF}$ = 242.1 Hz, 1 C, C_{26}), 161.13 (d, $^1J_{CF}$ = 242.1 Hz, 1 C, C_{21}), 156.06 (1 C, C_{29}), 137.10 (1 C, C_{31}), 135.97

(d, $^4J_{CF}$ = Hz, 1 C, C_{23}), 135.88 (d, $^4J_{CF}$ = 2.3 Hz, 1 C, C_{18}), 130.17 (d, $^3J_{CF}$ = Hz, 2 C, C_{19}), 129.97 (d, $^3J_{CF}$ = Hz, 2 C, C_{24}), 128.34 (2 C, C_{33}), 127.84 (1 C, C_{34}), 127.80 (2 C, C_{32}), 114.84 (d, $^2J_{CF}$ = 21.1 Hz, 2 C, C_{25}), 114.69 (d, $^2J_{CF}$ = Hz, 2 C, C_{20}), 80.23 (1 C, C_{27}), 65.15 (1 C, C_{30}), 57.57 (1 C, C_6), 57.34 (1 C, C_{14}), 56.54 (1 C, C_3), 55.51 (1 C, C_{11}), 55.00 (1 C, C_{22}), 53.78 (1 C, C_{17}), 44.98 (1 C, C_2), 43.32 (1 C, C_{10}), 27.88 (3 C, C_{28}), 18.68 (2 C, C_{12},C_4), 15.86 (1 C, C_{16}), 10.63 (1 C, C_8).

^{19}F{H}-NMR (564.6 MHz, 298 K, DMSO−d_6): δ = −116.20 (1 F, F_{26}), −116.37 (1 F, F_{21}).

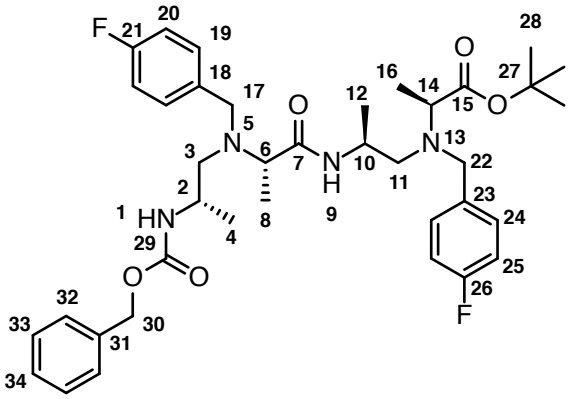

86

N-((*S*)-2-((*S*)-2-(((*S*)-2-AMINOPROPYL)(4-FLUOROBENZYL)AMINO)PROPANAMIDO)PROPYL)-*N*-(4-FLUOROBENZYL)-*L*-ALANINE (**90**).

tert-Butyl (5*S*,8*S*,11*S*,14*S*)-7,13-bis(4-fluorobenzyl)-5,8,11,14-tetramethyl-3,9-dioxo-1-phenyl-2-oxa-4,7,10,13-tetraazapentadecan-15-oate (**86**) (21.0 g, 30.8 mmol, 1.0 eq.) was dissolved in hydrogen bromide solution (16 % wt. in acetic acid, 100 mL) and stirred at 40 °C for 30 min. The solvent was removed under reduced pressure yielding a brownish oil. This oil was further suspended in acetonitrile (100 mL) and aqueous hydrochloric acid (37 %, 5.0 mL). This mixture was again evaporated to dryness. This procedure was repeated three times to remove residual acetic acid from the product. Finally, the product was dissolved in methanol (100 mL) and evaporated to dryness, yielding a brownish foam. This foam was extensively dried under high vacuum at 40 °C for 5 d. The product (21.3 g) is obtained as a mixture of HCl and HBr salt with minimal acetate content and was further used without additional purification.

HR-ESI-MS: calcd. for [**90**+H]$^+$ $C_{26}H_{36}F_2N_4O_3$ m/z= 491.2828, found m/z= 491.2831.

^{1}H-NMR (600.13 MHz, 298 K, DMSO−d_6): δ = 10.13 (s, 1 H, H_{27}), 8.60 (bs, 3 H, H_1), 7.53-7.48 (m, 2 H, H_{19}), 7.32-7.24 (m, 2 H, H_{24}), 7.10-7.05 (m, 2 H, H_{20}), 7.01-6.94 (m, 2 H, H_{25}), 3.61 (d, $^{2}J_{HH}$ = 14.9 Hz, 1 H, H_{22a}), 3.59 (d, $^{2}J_{HH}$ = 14.9 Hz, 1 H, H_{22b}), 3.53 (m, 1 H, H_{10}), 3.47 (q, $^{3}J_{HH}$ = 6.8 Hz, 1 H, H_6), 3.40 (s, 2 H, H_{17}), 3.30 (m, 1 H, H_2), 2.94 (q, $^{3}J_{HH}$ = 7.0 Hz, 1 H, H_{14}), 2.73 (dd, $^{2}J_{HH}$ = 13.3 Hz, $^{3}J_{HH}$ = 11.7 Hz, 1 H, H_{11a}), 2.46 (dd, $^{2}J_{HH}$ = 13.6 Hz, $^{3}J_{HH}$ = 9.0 Hz, 1 H, H_{3a}), 2.39-2.32 (m, 2 H, H_{3b},H_{11b}), 1.09 (d, $^{3}J_{HH}$ = 6.8 Hz, 3 H, H_8), 1.06 (d, $^{3}J_{HH}$ = 7.1 Hz, 3 H, H_{16}), 1.00 (d, $^{3}J_{HH}$ = 6.6 Hz, 3 H, H_4), 0.95 (d, $^{3}J_{HH}$ = 6.2 Hz, 3 H, H_{12}).

^{13}C{H}-NMR (150.95 MHz, 298 K, DMSO−d_6): δ = 177.48 (1 C, C_{15}), 171.50 (1 C, C_7), 161.29 (d, $^{1}J_{CF}$ = 242.1 Hz, 1 C, C_{21}), 160.92 (d, $^{1}J_{CF}$ = 242.1 Hz, 1 C, C_{26}), 136.99 (d, $^{4}J_{CF}$ = 2.8 Hz, 1 C, C_{23}), 134.79 (1 C, C_{18}), 130.82 (d, $^{3}J_{CF}$ = 7.6 Hz, 2 C, C_{19}), 129.73 (d, $^{3}J_{CF}$ = 7.9 Hz, 2 C, C_{24}), 114.81 (d, $^{2}J_{CF}$ = 20.9 Hz, 2 C, C_{20}), 114.59 ($^{(2}J_{CF}$ = 30.0 Hz, 2 C, C_{25}), 59.42 (1 C, C_{14}), 57.39 (1 C, C_6), 55.03 (1 C, C_{22}), 54.87 (1 C, C_{11}), 53.49 (1 C, C_3), 52.78 (1 C, C_{17}), 44.67 (1 C, C_{10}), 43.16 (1 C, C_2), 18.27 (1 C, C_{12}), 17.39 (1 C, C_4), 10.04 (1 C, C_{16}), 9.63 (1 C, C_8).

^{19}F{H}-NMR (564.6 MHz, 298 K, DMSO−d_6): δ = −116.21 (1 F, F_{21}), −116.76 (1 F, F_{26}).

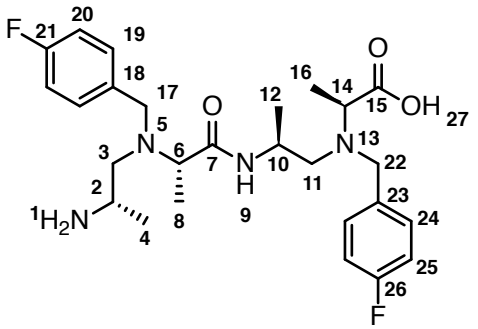

90

(3*S*,6*S*,9*S*,12*S*)-4,10-BIS(4-FLUOROBENZYL)-3,6,9,12-TETRAMETHYL-1,4,7,10-TETRAAZA-CYCLODODECANE-2,8-DIONE (**92**).

A total of 21.3 g of N-((*S*)-2-((*S*)-2-(((*S*)-2-aminopropyl)(4-fluoro benzyl)-amino)propanamido)propyl)-*N*-(4-fluorobenzyl)-*L*-alanine (**90**) salt was cyclized in several portions of max. 2.00 g. N-((*S*)-2-((*S*)-2-(((*S*)-2-amino-propyl)(4-fluorobenzyl) amino) propanamido) propyl)-*N*-(4-fluorobenzyl)-*L*-alanine (**90**) salt (2.00 g, 4.08 mmol, 1.0 eq.) and *N*-ethyl diisopropylamine (3.4 mL, 20.4 mmol, 5 eq.) were dissolved in acetonitrile (2.0 L). HATU (1.55 g, 4.08 mmol, 1.0 eq.) was added and the solution was stirred at 20-25 °C for 20 min. The solvent was removed under vacuum. The crude product from all batches was combined and purified by flash column chromatography

(SiO_2, ethyl acetate / cyclohexane (7:3)) yielding a white solid (10.4 g, 22.0 mmol, 68.5 % yield calculated over 2 steps starting from **86**).

HR-ESI-MS: calcd. for [**92**+H]$^+$ $C_{26}H_{35}F_2N_4O_2$ m/z= 473.2723, found m/z= 473.2720.

^{1}H-NMR (600.13 MHz, 298 K, DMSO−d_6): δ = 7.71 (d, $^3J_{HH}$ = 4.9 Hz, 2 H, H_5), 7.44 (dd, $^3J_{HH}$ = 8.4 Hz, $^4J_{HF}$ = 6.0 Hz, 4 H, H_{11}), 7.09 (dd, $^3J_{HH}$ = 8.4 Hz, $^3J_{HF}$ = 8.8 Hz, 4 H, H_{12}), 3.86 (d, $^2J_{HH}$ = 13.4 Hz, 2 H, H_{9a}), 3.57 (d, $^2J_{HH}$ = 13.4 Hz, 2 H, H_{9b}), 3.35 (dddq, $^3J_{HH}$ = 10.8 Hz, $^3J_{HH}$ = 4.9 Hz, $^3J_{HH}$ = 2.8 Hz, 2 H, H_6), 3.20 (q, 2 H, H_2), 2.75 (dd, $^2J_{HH}$ = 13.4 Hz, $^3J_{HH}$ = 10.8 Hz, 2 H, H_{7a}), 2.29 (dd, $^2J_{HH}$ = 13.4 Hz, $^3J_{HH}$ = 2.8 Hz, 2 H, H_{7b}), 1.14 (d, $^3J_{HH}$ = 6.5 Hz, 6 H, H_8), 1.04 (d, $^3J_{HH}$ = 7.0 Hz, 6 H, H_4).

^{13}C{H}-NMR (150.95 MHz, 298 K, DMSO−d_6): δ = 172.12 (2 C, C_3), 161.33 (d, $^1J_{CF}$ = 242.7 Hz, 2 C, C_{13}), 135.34 (2 C, C_{10}), 130.97 (d, $^3J_{CF}$ = 7.8 Hz, 4 C, C_{11}), 114.81 (d, $^2J_{CF}$ = 21.0 Hz, 4 C, C_{12}), 59.66 (2 C, C_2), 55.92 (2 C, C_9), 54.94 (2 C, C_7), 43.96 (2 C, C_6), 17.69 (2 C, C_8), 8.73 (2 C, C_4).

^{19}F{H}-NMR (564.6 MHz, 298 K, DMSO−d_6): δ = −115.65 (1 F, F_{13}).

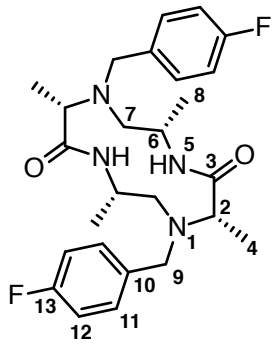

92

(2*S*,5*S*,8*S*,11*S*)-1,7-BIS(4-FLUOROBENZYL)-2,5,8,11-TETRAMETHYL-1,4,7,10-TETRAAZACYCLODODECANE (**91**).

(3*S*,6*S*,9*S*,12*S*)-4,10-Bis(4-fluorobenzyl)-3,6,9,12-tetramethyl-1,4,7,10-tetraaza-cyclododecane-2,8-dione (**92**) (120 mg, 254 µmol, 1.0 eq.) was dissolved in dichloromethane (5.0 mL) and cooled to 0-5 °C. Trimethylsilyl chloride (152 mg, 1.40 mmol, 5.5 eq.) was slowly added. After completion, the reaction mixture was stirred at 0-5 °C for 30 min followed by the addition of a lithium aluminium hydride solution (2.5 mL, 2 M in tetrahydrofuran, 5.08 mmol, 20.0 eq.). The reaction mixture was allowed to warm to 20-25 °C and was further stirred for 3 h. The reaction mixture was cooled to 0-5 °C and saturated aqueous sodium hydrogen carbonate (2.0 mL) was slowly

added. To the resulting suspension sodium sulphate (4.00 g) was added. The suspension was filtered and evaporated to dryness yielding a white solid (103 mg, 232 µmol, 91.2 %).

HR-ESI-MS: calcd. for [**91**+H]$^+$ $C_{26}H_{39}F_2N_4$ m/z= 445.3137, found m/z= 445.3146.

^{1}H-NMR (500.13 MHz, 298 K, $CDCl_3$): δ = 7.31-7.28 (m, 4 H, H_{11}), 7.06-7.00 (m, 4 H, H_{12}), 3.75 (d, $^2J_{HH}$ = 13.0 Hz, 2 H, H_{9a}), 3.11-3.00 (m, 2 H, H_2), 2.97 (bs, 2 H, H_{9b}), 2.90-2.74 (m, 4 H, H_{3a}, H_6), 2.49-2.34 (m, 4 H, H_{3b}, H_{7a}), 2.27-2.11 (m, 2 H, H_{7b}), 0.91 (d, $^3J_{HH}$ = 6.4 Hz, 6 H, H_8), 0.89 (d, $^3J_{HH}$ = 6.0 Hz, 6 H, H_4).

^{13}C{H}-NMR (125.77 MHz, 298 K, $CDCl_3$): δ = 162.19 (d, $^1J_{CF}$ = 245.6 Hz, 2 C, C_{13}), 135.58 (d, $^4J_{CF}$ = 1.5 Hz, 2 C, C_{10}), 130.68 (d, $^3J_{CF}$ = 7.9 Hz, 4 C, C_{11}), 115.39 (d, $^2J_{CF}$ = 21.5 Hz, 4 C, C_{12}), 56.59 (2 C, C_7), 51.01 (2 C, C_9), 50.17 (2 C, C_2), 47.91 (2 C, C_3), 46.58 (2 C, C_6), 18.78 (2 C, C_4), 10.24 (2 C, C_8).

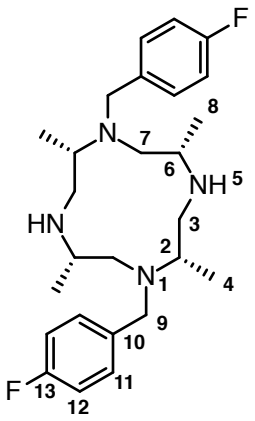

91

(3*S*,6*S*,9*S*,12*S*)-3,6,9,12-TETRAMETHYL-1,4,7,10-TETRAAZACYCLODODECANE-2,8-DIONE (**69**).

Method A

(3*S*,6*S*,9*S*,12*S*)-4,10-Bis(4-fluorobenzyl)-3,6,9,12-tetramethyl-1,4,7,10-tetraazacyclododecane-2,8-dione (**92**) (2.50 g, 5.29 mmol, 1.0 eq.) was dissolved in acetic acid (40 mL) and trifluoroacetic acid (2.0 mL). Palladium on charcoal (moistened with water, 10 % Pd basis, 200 mg) was added and the suspension was hydrogenated at 45 bar for 16 h. The suspension was filtered through celite and the solvent was removed under reduced pressure. The residue was dissolved in dichloromethane (5.0 mL) and aqueous sodium hydroxide (2 M, 5.0 mL). The layers were separated and the organic layer

was washed with aqueous sodium hydroxide (2 M, 5.0 mL). The organic layer was dried with sodium sulphate and evaporated to dryness yielding the title compound as a white solid (1.14 g, 4.45 mmol, 84.1 %).

Method B

(3*S*,6*S*,9*S*,12*S*)-4-Benzyl-10-(4-fluorobenzyl)-3,6,9,12-tetramethyl-1,4,7,10-tetraazacyclododecane-2,8-dione (**94**) (3.69 g, 8.12 mmol, 1.0 eq.) was dissolved in acetic acid (50.0 mL) and trifluoroacetic acid (2.0 mL). Palladium on charcoal (moistened with water, 10 % Pd basis, 350 mg) was added and the suspension was hydrogenated at 45 bar for 16 h. The suspension was filtered through celite and the solvent was removed under reduced pressure. The residue was dissolved in dichloromethane (10.0 mL) and aqueous sodium hydroxide (2 M, 10.0 mL). The layers were separated and the organic layer was washed with aqueous sodium hydroxide (2 M, 10.0 mL). The organic layer was dried with sodium sulphate and evaporated to dryness yielding the title compound as a white solid (1.85 g, 7.22 mmol, 88.9 %).

Method C

(3*S*,6*S*,9*S*,12*S*)-4,10-Dibenzyl-3,6,9,12-tetra-methyl-1,4,7,10-tetraazacyclododecane-2,8-dione (**67**) (50.0 mg, 115 µmol, 1.0 eq.) was dissolved in methanol (5.00 mL). Palladium on charcoal (moistened with water, 10 % Pd basis, 50.0 mg) was added and the suspension was hydrogenated at 1 bar for 16 h. The suspension was filtered through celite and the solvent was removed under reduced pressure yielding the title compound as a white solid (25.0 mg, 97.5 µmol, 84.8 %).

HR-ESI-MS: calcd. for [**69**+H]$^+$ $C_{12}H_{25}N_4O_2$ m/z= 257.1972, found m/z= 257.1975.

^{1}H-NMR (600.13 MHz, 298 K, DMSO−d_6): δ = 7.78 (d, $^3J_{HH}$ = 9.1 Hz, 2 H, H_5), 3.79 (dddq, $^3J_{HH}$ = 9.1 Hz, $^3J_{HH}$ = 3.4 Hz, $^3J_{HH}$ = 3.0 Hz, $^3J_{HH}$ = 6.9 Hz, 2 H, H_6), 2.88 (q, $^3J_{HH}$ = 6.9 Hz, 2 H, H_2), 2.79 (ddd, $^2J_{HH}$ = 12.5 Hz, $^3J_{HH}$ = 6.1 Hz, $^3J_{HH}$ = 3.0 Hz, 2 H, H_{7a}), 2.40 (dd, $^3J_{HH}$ = 10.3 Hz, $^3J_{HH}$ = 6.1 Hz, 2 H, H_1), 2.05 (ddd, $^2J_{HH}$ = 12.5 Hz, $^3J_{HH}$ = 10.3 Hz, $^3J_{HH}$ = 3.4 Hz, 2 H, H_{7b}), 1.17 (d, $^3J_{HH}$ = 6.9 Hz, 6 H, H_4), 1.02 (d, $^3J_{HH}$ = 6.9 Hz, 6 H, H_8).

^{13}C{H}-NMR (150.95 MHz, 298 K, DMSO−d_6): δ = 173.76 (2 C, C_3), 59.41 (2 C, C_2), 52.62 (2 C, C_7), 42.64 (2 C, C_6), 19.21 (2 C, C_4), 17.74 (2 C, C_8).

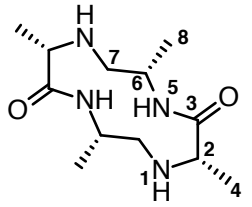

69

tert-BUTYL (5*S*,8*S*,11*S*,14*S*)-7-BENZYL-13-(4-FLUOROBENZYL)-5,8,11,14-TETRAMETHYL-3,9-DIOXO-1-PHENYL-2-OXA-4,7,10,13-TETRAAZAPENTADECAN-15-OATE (**93**).

tert-Butyl *N*-(((*S*))-2-aminopropyl)-*N*-(4-fluorobenzyl)-*L*-alaninate (**88**) (7.36 g, 23.7 mmol, 1.0 eq.), *N*-benzyl-*N*-((*S*)-2-(((benzyloxy)carbonyl)-amino)propyl)-*L*-alanine (**64**) triethylammonium salt (10.3 g, 21.9 mmol, 0.9 eq.) and *N*-ethyl diisopropylamine (7.8 mL, 47.4 mmol, 2.0 eq.) were dissolved in acetonitrile (100 mL). HATU (9.01 g, 23.7 mmol, 1.0 eq.) was added. The reaction mixture was stirred at 20-25 °C for 16 h. The solvent was removed under vacuum and the crude oil was dissolved in ethyl acetate (100 mL) and extracted with water (2x 50 mL) and brine (20.0 mL). The organic layer was dried with sodium sulphate and evaporated to dryness. The crude oil was first plugged through a short silica gel column (150 g SiO_2). The fractions containing the product were combined and evaporated to dryness. The resulting oil was further purified by flash column chromatography (SiO_2, ethyl acetate / cyclohexane (3:7)) yielding a white solid (7.66 g, 11.6 mmol, 48.8 %).

HR-ESI-MS: calcd. for [**93**+H]$^+$ $C_{38}H_{52}FN_4O_5$ m/z= 663.3916, found m/z= 663.3905.

^{1}H-NMR (500.13 MHz, 298 K, $CDCl_3$): δ = 7.38-7.19 (m, 12 H, H_{19}, H_{20}, H_{21}, H_{24}, H_{32}, H_{33}, H_{34}), 6.94-6.89 (m, 2 H, H_{25}), 5.14 (d, $^2J_{HH}$ = 12.3 Hz, 1 H, H_{30a}), 4.99 (d, $^2J_{HH}$ = 12.3 Hz, 1 H, H_{30b}), 4.61 (d, $^3J_{HH}$ = 8.0 Hz, 1 H, H_1), 3.98 (ddq, $^3J_{HH}$ = 8.0 Hz, $^3J_{HH}$ = 6.1 Hz, $^3J_{HH}$ = 7.0 Hz, 1 H, H_{10}), 3.90-3.83 (m, 1 H, H_2), 3.82 (d, $^2J_{HH}$ = 14.3 Hz, 1 H, H_{22a}), 3.71 (d, $^2J_{HH}$ = 13.4 Hz, 1 H, H_{17a}), 3.68 (d, $^2J_{HH}$ = 14.3 Hz, 1 H, H_{22b}), 3.38 (q, $^3J_{HH}$ = 6.9 Hz, 1 H, H_6), 3.37 (d, $^2J_{HH}$ = 13.4 Hz, 1 H, H_{17b}), 3.25 (q, $^3J_{HH}$ = 7.2 Hz, 1 H, H_{14}), 2.66 (dd, $^2J_{HH}$ = 13.7 Hz, $^3J_{HH}$ = 6.1 Hz, 1 H, H_{11a}), 2.59 (dd, $^2J_{HH}$ = 13.7 Hz, $^3J_{HH}$ = 6.1 Hz, 1 H, H_{11b}), 2.49 (dd, $^2J_{HH}$ = 13.5 Hz, $^3J_{HH}$ = 3.3 Hz, 1 H, H_{3a}), 2.26 (dd, $^2J_{HH}$ = 13.5 Hz, $^3J_{HH}$ = 10.6 Hz, 1 H, H_{3b}), 1.45 (s, 9 H, H_{28}), 1.21 (d, $^3J_{HH}$ = 6.9 Hz, 3 H, H_8), 1.17 (d, $^3J_{HH}$ = 7.0 Hz, 3 H, H_{12}), 1.16 (d, $^3J_{HH}$ = 7.2 Hz, 3 H, H_{16}), 1.05 (d, $^3J_{HH}$ = 6.8 Hz, 3 H, H_4).

^{13}C{H}-NMR (125.77 MHz, 298 K, $CDCl_3$): δ = 173.27 (1 C, C_{15}), 172.95 (1 C, C_7), 161.95 (1 C, C_{26}), 156.47 (1 C, C_{29}), 139.24 (1 C, C_{18}), 136.63 (1 C, C_{31}), 135.74 (1 C, C_{23}), 130.07 (2 C, C_{24}), 129.10 (2 C, C_{19}), 128.64 (2

C, C_{33}), 128.46 (2 C, C_{20}), 128.24 (1 C, C_{34}), 128.21 (2 C, C_{32}), 127.31 (1 C, C_{21}), 115.06 (2 C, C_{25}), 80.97 (1 C, C_{27}), 66.65 (1 C, C_{30}), 58.45 (1 C, C_6), 57.72 (1 C, C_{14}), 56.61 (1 C, C_3), 55.78 (1 C, C_{11}), 55.68 (1 C, C_{22}), 54.81 (1 C, C_{17}), 45.20 (1 C, C_2), 44.33 (1 C, C_{10}), 28.42 (3 C, C_{28}), 19.51 (1 C, C_4), 19.17 (1 C, C_{12}), 15.5 (1 C, C_{16}), 8.12 (1 C, C_8).

^{19}F{H}-NMR (564.76 MHz, 298 K, $CDCl_3$): $\delta = -116.22$ (1 F, F_{26}).

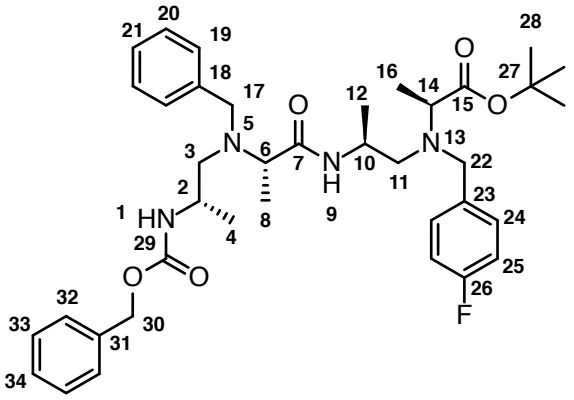

93

N-((*S*)-2-((*S*)-2-(((*S*)-2-AMINOPROPYL)(BENZYL)AMINO)-PROPANAMIDO)PROPYL)-*N*-(4-FLUOROBENZYL)-*L*-ALANINE (**95**).

tert-Butyl (5*S*,8*S*,11*S*,14*S*)-7-benzyl-13-(4-fluorobenzyl)-5,8,11,14-tetramethyl-3,9-dioxo-1-phenyl-2-oxa-4,7,10,13-tetraazapentadecan-15-oate (**93**) (7.66 g, 11.6 mmol, 1.0 eq.) was dissolved in hydrogen bromide solution (16 % wt. in acetic acid, 40 mL) and stirred at 40 °C for 30 min. The solvent was removed under reduced pressure yielding a brownish oil. This oil was further suspended in acetonitrile (50 mL) and aqueous hydrochloric acid (37 %, 2.0 mL). This mixture was again evaporated to dryness. This procedure was repeated three times to remove residual acetic acid from the product. Finally, the product was dissolved in methanol (30.0 mL) and evaporated to dryness, yielding a yellowish foam. This foam was extensively dried under high vacuum at 40 °C for 5 d. The product (7.91 g) is obtained as a mixture of HCl and HBr salt with minimal acetate content and was used without further purification.

HR-ESI-MS: calcd. for [**95**+H]$^+$ $C_{26}H_{38}FN_4O_3$ m/z= 473.2922, found m/z= 473.2930.

^{1}H-NMR (500.13 MHz, 298 K, DMSO−d_6): δ = 7.46-7.40 (m, 2 H, H_{25}), 7.20-7.14 (m, 2 H, H_{24}), 7.36-7.23 (m, 5 H, H_{19}, H_{20}, H_{21}), 4.06-3.88 (m, 3 H, H_{22}, H_{10}), 3.65-3.58 (m, 1 H, H_6), 3.65 (bs, 2 H, H_{17}), 3.30 (q, $^3J_{HH} = 6.8$ Hz, 1 H, H_{14}), 3.23-3.13 (m, 1 H, H_2), 2.77 (bs, 2 H, H_{11}), 2.64 (d, $^3J_{HH} = 6.9$ Hz,

2 H, H_3), 1.30 (d, $^3J_{HH}$ = 6.9 Hz, 3 H, H_8), 1.12 (d, $^3J_{HH}$ = 6.8 Hz, 3 H, H_{16}), 1.11 (d, $^3J_{HH}$ = 6.8 Hz, 3 H, H_4), 1.06 (d, $^3J_{HH}$ = 6.7 Hz, 3 H, H_{12}).

^{13}C{H}-NMR (125.77 MHz, 298 K, DMSO−d_6): δ = 173.64 (1 C, C_{15}), 173.05 (1 C, C_7), 161.77 (1 C, C_{26}), 138.78 (1 C, C_{18}), 131.18 (1 C, C_{23}), 128.58 (2 C, C_{20}), 128.32 (2 C, C_{19}), 127.16 (1 C, C_{21}), 117.42 (2 C, C_{24}), 115.27 (2 C, C_{25}), 57.70 (1 C, C_6), 57.56 (1 C, C_{14}), 56.44 (1 C, C_{11}), 55.60 (1 C, C_{17}), 54.74 (1 C, C_{22}), 53.85 (1 C, C_3), 45.16 (1 C, C_2), 43.10 (1 C, C_{10}), 18.27 (1 C, C_{12}), 16.44 (1 C, C_4), 13.26 (1 C, C_8), 12.52 (1 C, C_{16}).

^{19}F{H}-NMR (564.76 MHz, 298 K, DMSO−d_6): δ = −114.44 (1 F, F_{26}).

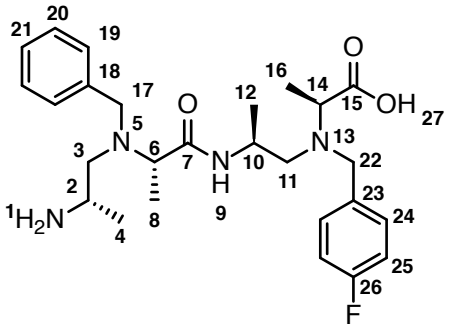

95

(3*S*,6*S*,9*S*,12*S*)-4-BENZYL-10-(4-FLUOROBENZYL)-3,6,9,12-TETRAMETHYL-1,4,7,10-TETRAAZACYCLODODECANE-2,8-DIONE (**94**).

A total of 7.91 g of *N*-((*S*)-2-((*S*)-2-(((*S*)-2-aminopropyl)(benzyl)amino)propanamido)propyl)-*N*-(4-fluorobenzyl)-*L*-alanine (**95**) salt was cyclized in several portions of max. 2.00 g. *N*-((*S*)-2-((*S*)-2-(((*S*)-2-Aminopropyl)(benzyl)amino)propanamido)propyl)-*N*-(4-fluorobenzyl)-*L*-alanine (**95**) salt (2.00 g, 4.24 mmol, 1.0 eq.) and *N*-ethyl diisopropylamine (2.74 mL, 21.2 mmol, 5.0 eq.) were dissolved in acetonitrile (2.0 L). HATU (1.61 g, 4.24 mmol, 1.0 eq.) was added and the solution was stirred at 20-25 °C for 20 min. The solvent was removed under vacuum. The crude product from all batches was combined and purified by flash column chromatography (SiO_2, ethyl acetate / cyclohexane (7:3)) yielding a white solid (3.69 g, 8.12 mmol, 70.0 % yield calculated over 2 steps starting from **93**).

HR-ESI-MS: calcd. for [**94**+H]$^+$ $C_{26}H_{36}FN_4O_2$ m/z= 455.2817, found m/z= 455.2826.

^{1}H-NMR (500.13 MHz, 298 K, DMSO−d_6): δ = 7.72 (d, $^3J_{HH}$ = 4.7 Hz, 1 H, H_{13}), 7.70 (d, $^3J_{HH}$ = 4.6 Hz, 1 H, H_5), 7.47-7.43 (m, 2 H, H_{19}), 7.43-7.40 (m, 2 H, H_{25}), 7.32-7.27 (m, 3 H, H_{26}, H_{24}), 7.11-7.06 (m, 2 H, H_{20}), 3.89 (d, $^2J_{HH}$ = 13.2 Hz, 1 H, H_{22a}), 3.85 (d, $^2J_{HH}$ = 13.3 Hz, 1 H, H_{17a}), 3.57 (d,

$^{2}J_{HH}$ = 13.3 Hz, 1 H, H_{17b}), 3.56 (d, $^{2}J_{HH}$ = 13.3 Hz, 1 H, H_{22b}), 3.40-3.32 (m, 1 H, H_6), 3.36-3.28 (m, 1 H, H_{14}), 3.21 (q, $^{3}J_{HH}$ = 7.0 Hz, 1 H, H_2), 3.20 (q, $^{3}J_{HH}$ = 7.0 Hz, 1 H, H_{10}), 2.81-2.71 (m, 2 H, H_{7a}, H_{15a}), 2.32-2.26 (m, 2 H, H_{7b}, H_{15b}), 1.15 (d, $^{3}J_{HH}$ = 6.7 Hz, 3 H, H_8), 1.14 (d, $^{3}J_{HH}$ = 6.6 Hz, 3 H, H_{16}), 1.05 (d, $^{3}J_{HH}$ = 7.0 Hz, 3 H, H_4), 1.04 (d, $^{3}J_{HH}$ = 7.0 Hz, 3 H, H_{12}).

$^{13}C\{H\}$-NMR (125.77 MHz, 298 K, DMSO−d_6): δ = 172.18 (1 C, C_3), 172.06 (1 C, C_{11}), 161.32 (1 C, C_{21}), 139.15 (1 C, C_{23}), 135.37 (1 C, C_{18}), 130.93 (2 C, C_{19}), 129.06 (2 C, C_{25}), 128.14 (2 C, C_{24}), 127.12 (1 C, C_{26}), 114.78 (2 C, C_{20}), 59.69 (1 C, C_2), 59.60 (1 C, C_{10}), 56.75 (1 C, C_{22}), 56.04 (1 C, C_{17}), 55.05 (1 C, C_{15}), 55.04 (1 C, C_7), 44.10 (1 C, C_6), 43.96 (1 C, C_{14}), 17.69 (1 C, C_{16}), 17.66 (1 C, C_8), 8.65 (1 C, C_4), 8.55 (1 C, C_{12}).

$^{19}F\{H\}$-NMR (564.76 MHz, 298 K, $CDCl_3$): δ = −115.64 (1 F, F_{21}).

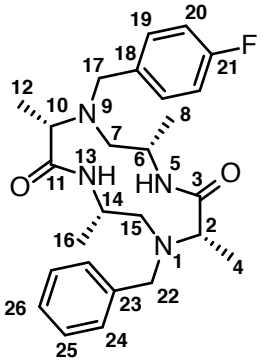

94

tert-BUTYL ((*S*)-2-(((BENZYLOXY)CARBONYL)AMINO)PROPYL)-*L*-VALINATE (**103**).

Benzyl (*S*)-(1-oxopropan-2-yl)carbamate (**60**) (12.6 g, 60.8 mmol, 1.0 eq.) was dissolved in dichloromethane (120 mL). To this solution *L*-valine *tert*-butyl ester (10.7 g, 62.0 mmol, 1.0 eq.) was added. The solution was stirred at 20-25 °C for 5 min followed by the addition of sodium triacetoxyborohydride (52.3 g, 246 mmol, 4.1 eq.). The reaction mixture was stirred at 20-25 °C for 16 h. The excess of sodium triacetoxyborohydride was quenched with aqueous saturated sodium hydrogen carbonate (150 mL) and the pH adjusted to >9 by addition of triethylamine (20.0 mL). The two layers were separated and the organic layer was washed with aqueous saturated sodium hydrogen carbonate (2x 100 mL), water (50.0 mL) and dried with sodium sulphate. The organic layer was evaporated to dryness and the crude oil was purified by flash column chromatography (SiO_2, cyclohexane / ethyl acetate / triethylamine (70:30:1)) yielding a yellowish oil (19.4 g, 53.2 mmol, 87.5 %).

HR-ESI-MS: calcd. for [**103**+H]$^+$ $C_{20}H_{33}N_2O_4$ m/z= 365.2435, found m/z= 365.2439.

^{1}H-NMR (400.13 MHz, 298 K, CD_3CN): δ = 7.41-7.25 (m, 5 H, H_{14},H_{15},H_{16}), 5.56 (bs, 1 H, H_1), 5.06 (d, $^2J_{HH}$ = 13.4 Hz, 1 H, H_{12a}), 5.02 (d, $^2J_{HH}$ = 13.4 Hz, 1 H, H_{12b}), 3.61 (qdd, $^3J_{HH}$ = 6.6 Hz, $^3J_{HH}$ = 6.4 Hz, $^3J_{HH}$ = 5.8 Hz, 1 H, H_2), 2.76 (d, $^3J_{HH}$ = 6.3 Hz, 1 H, H_6), 2.62 (dd, $^2J_{HH}$ = 11.9 Hz, $^3J_{HH}$ = 5.8 Hz, 1 H, H_{3a}), 2.37 (dd, $^2J_{HH}$ = 11.9 Hz, 1 H, H_{3b}), 1.81 (dqq, $^3J_{HH}$ = 6.3 Hz, $^3J_{HH}$ = 6.8 Hz, $^3J_{HH}$ = 6.8 Hz, 1 H, H_8), 1.44 (s, 9 H, H_{18}), 1.17 (d, $^3J_{HH}$ = 6.6 Hz, 3 H, H_4), 0.91 (d, $^3J_{HH}$ = 6.8 Hz, 3 H, $H_{9/10}$), 0.90 (d, $^3J_{HH}$ = 6.8 Hz, 3 H, $H_{9/10)}$).

^{13}C{H}-NMR (100.61 MHz, 298 K, CD_3CN): δ = 171.15 (1 C, C_7), 156.88 (1 C, C_{11}), 138.54 (1 C, C_{13}), 129.41 (2 C, C_{15}), 128.77 (1 C, C_{16}), 128.66 (2 C, C_{14}), 81.36 (1 C, C_{17}), 69.20 (1 C, C_6), 66.59 (1 C, C_{12}), 54.20 (1 C, C_3), 48.32 (1 C, C_2), 32.42 (1 C, C_8), 28.35 (3 C, C_{18}), 19.66 (1 C, $C_{9/10}$), 19.02 (1 C, C_4), 18.94 (1 C, $C_{9/10}$).

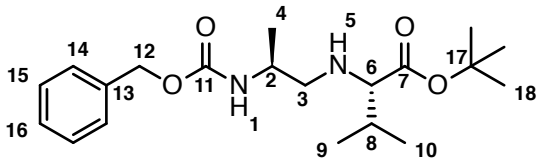

103

tert-BUTYL ((*R*)-2-(((BENZYLOXY)CARBONYL)AMINO)PROPYL)-*L*-VALINATE (**123**).

Benzyl (*R*)-(1-oxopropan-2-yl)carbamate (**122**) (1.05 g, 5.07 mmol, 1.0 eq.) was dissolved in dichloromethane (20 mL). To this solution *L*-valine *tert*-butyl ester (878 mg, 5.07 mmol, 1.0 eq.) was added. The solution was stirred at 20-25 °C for 5 min followed by the addition of sodium triacetoxyborohydride (4.30 g, 20.3 mmol, 4.1 eq.). The reaction mixture was stirred at 20-25 °C for 16 h. The excess of sodium triacetoxyborohydride was quenched with aqueous saturated sodium hydrogen carbonate (20 mL) and the pH adjusted to >9 by the addition of triethylamine (3.0 mL). The two layers were separated and the organic layer was washed with aqueous saturated sodium hydrogen carbonate (2x 20 mL), water (20 mL) and dried with sodium sulphate. The organic layer was evaporated to dryness yielding a colorless oil (1.79 g, 4.91 mmol, 96.9 %).

^{1}H-NMR (400.13 MHz, 298 K, $CDCl_3$): δ = 7.40-7.26 (m, 5 H, H_{14},H_{15},H_{16}), 5.24 (bs, 1 H, H_1), 5.10 (s, 2 H, H_{12}), 3.78 (qdd, $^3J_{HH}$ = 6.5 Hz, $^3J_{HH}$ = 6.0 Hz, $^3J_{HH}$ = 4.4 Hz, 1 H, H_2), 2.77 (d, $^3J_{HH}$ = 6.1 Hz, 1 H, H_6), 2.65 (dd, $^2J_{HH}$ = 12.4 Hz, $^3J_{HH}$ = 6.0 Hz, 1 H, H_{3a}), 2.44 (dd, $^2J_{HH}$ = 12.4 Hz, $^3J_{HH}$ = 4.4 Hz, 1 H, H_{3b}), 1.85 (dqq, $^3J_{HH}$ = 6.1 Hz, $^3J_{HH}$ = 6.7 Hz,

$^3J_{HH}$ = 6.7 Hz, 1 H, H_8), 1.46 (s, 9 H, H_{18}), 1.15 (d, $^3J_{HH}$ = 6.5 Hz, 3 H, H_4), 0.92 (d, $^3J_{HH}$ = 6.7 Hz, 3 H, $H_{9/10}$), 0.90 (d, $^3J_{HH}$ = 6.7 Hz, 3 H, $H_{9/10}$).

$^{13}C\{H\}$-NMR (100.61 MHz, 298 K, $CDCl_3$): δ = 174.51 (1 C, C_7), 156.14 (1 C, C_{11}), 136.89 (1 C, C_{13}), 128.59 (2 C, C_{15}), 128.15 (1 C, C_{16}), 128.11 (2 C, C_{14}), 81.15 (1 C, C_{17}), 67.91 (1 C, C_6), 66.53 (1 C, C_{12}), 53.16 (1 C, C_3), 46.60 (1 C, C_2), 31.84 (1 C, C_8), 28.29 (3 C, C_{18}), 19.49 (1 C, $C_{9/10}$), 19.04 (1 C, C_4), 18.61 (1 C, $C_{9/10}$).

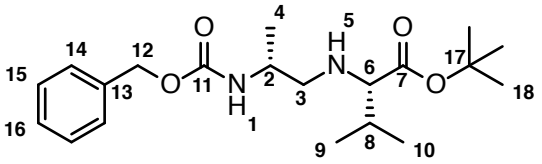

123

tert-BUTYL *N*-BENZYL-*N*-((*S*)-2-(((BENZYLOXY)CARBONYL) AMINO)PROPYL)-*L*-VALINATE (**100**).

tert-Butyl ((*S*)-2-(((benzyloxy)carbonyl)amino)propyl)-*L*-valinate (**103**) (19.4 g, 53.2 mmol, 1.0 eq.) was dissolved in acetonitrile (200 mL) and potassium carbonate (8.09 g, 58.5 mmol, 1.1 eq.) was added. To this suspension benzyl bromide (9.50 mL, 79.8 mmol, 1.5 eq.) was added over a period of 5 min. The reaction mixture was heated to 65 °C and stirred for 2 d under an argon atmosphere. Excess of benzyl bromide was quenched with triethylamine (30.0 mL). The suspension was stirred at 50 °C for 30 min and an additional 30 min at 20-25 °C. The reaction mixture was filtered, washed with acetonitrile (50.0 mL) and evaporated to dryness. The crude oil was purified by flash column chromatography (SiO_2, cyclohexane / ethyl acetate / triethylamine (80:20:1)) yielding a colorless oil (21.0 g, 46.2 mmol, 86.9 %).

HR-ESI-MS: calcd. for [**100**+H]$^+$ $C_{27}H_{39}N_2O_4$ m/z= 455.2904, found m/z= 455.2908.

^{1}H-NMR (400.13 MHz, 298 K, CD_3CN): δ = 7.36-7.15 (m, 10 H, H_{19}, H_{20}, H_{21}, H_{14}, H_{15}, H_{16}), 5.47 (bs, 1 H, H_1), 5.02 (d, $^2J_{HH}$ = 12.5 Hz, 1 H, H_{12a}), 4.96 (d, $^2J_{HH}$ = 12.5 Hz, 1 H, H_{12b}), 3.96 (d, $^2J_{HH}$ = 14.0 Hz, 1 H, H_{17a}), 3.72 (ddq, $^3J_{HH}$ = 8.8 Hz, $^3J_{HH}$ = 5.5 Hz, $^3J_{HH}$ = 6.2 Hz, 1 H,H_2), 3.41 (d, $^2J_{HH}$ = 14.0 Hz, 1 H, H_{17b}), 2.63 (d, $^3J_{HH}$ = 10.8 Hz, 1 H, H_6), 2.57 (dd, $^2J_{HH}$ = 13.0 Hz, $^3J_{HH}$ = 8.8 Hz, 1 H, H_{3a}), 2.49 (dd, $^2J_{HH}$ = 13.0 Hz, $^3J_{HH}$ = 5.5 Hz, 1 H, H_{3b}), 1.97 (ddq, $^3J_{HH}$ = 10.8 Hz, $^3J_{HH}$ = 6.5 Hz, $^3J_{HH}$ = 6.5 Hz, 1 H, H_8), 1.47 (s, 9 H, H_{23}), 1.08 (d, $^3J_{HH}$ = 6.6 Hz, 3 H, H_4), 0.95 (d, $^3J_{HH}$ = 6.5 Hz, 3 H, $H_{9/10}$), 0.81 (d, $^3J_{HH}$ = 6.5 Hz, 3 H, $H_{9/10}$).

$^{13}C\{H\}$-NMR (100.61 MHz, 298 K, CD_3CN): δ = 172.07 (1 C, C_7), 156.65 (1 C, C_{11}), 140.84 (1 C, C_{18}), 138.47 (1 C, C_{13}), 129.92 (2 C, C_{20}), 129.36 (1

C, C_{21}), 129.05 (2 C, C_{19}), 128.74 (2 C, C_{15}), 128.64 (1 C, C_{16}), 127.82 (2 C, C_{14}), 81.68 (1 C, C_{22}), 71.04 (1 C, C_6), 66.56 (1 C, C_{12}), 56.96 (1 C, C_3), 56.71 (1 C, C_{17}), 46.77 (1 C, C_2), 28.55 (3 C, C_{23}), 28.27 (1 C, C_8), 20.11 (1 C, $C_{9/10}$), 20.10 (1 C, $C_{9/10}$), 19.41 (1 C, C_4).

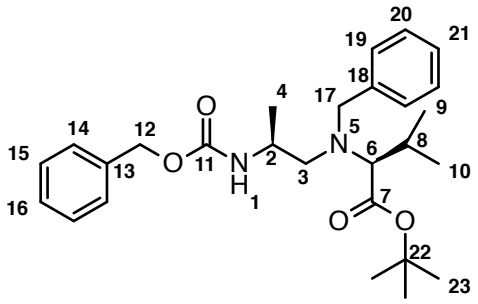

100

tert-BUTYL *N*-BENZYL-*N*-((*R*)-2-(((BENZYLOXY)CARBONYL) AMINO)PROPYL)-*L*-VALINATE (**120**).

tert-Butyl ((*R*)-2-(((benzyloxy)carbonyl)amino)propyl)-*L*-valinate (**123**) (1.20 g, 3.29 mmol, 1.0 eq.) was dissolved in acetonitrile (20 mL) and potassium carbonate (1.36 g, 9.87 mmol, 3.0 eq.) was added. To this suspension benzyl bromide (1.4 mL, 8.23 mmol, 2.5 eq.) was added over a period of 1 min. The reaction mixture was heated to 65 °C and stirred for 18 h under an argon atmosphere. Excess of benzyl bromide was quenched with triethylamine (1.0 mL). The suspension was stirred at 50 °C for 30 min and an additional 30 min at 20-25 °C. The reaction mixture was filtered, washed with acetonitrile (10 mL) and evaporated to dryness yielding a white solid. The solid was recrystallized from ethyl acetate / cyclohexane yielding a white solid (960 mg, 2.11 mmol, 64.2 %).

^{1}H-NMR (600.13 MHz, 298 K, $CDCl_3$): δ = 7.38-7.18 (m, 10 H, H_{19}, H_{20}, H_{21}, H_{14}, H_{15}, H_{16}), 6.95 (d, $^3J_{HH}$ = 8.9 Hz, 1 H, H_1), 5.09 (d, $^2J_{HH}$ = 12.6 Hz, 1 H, H_{12a}), 4.96 (d, $^2J_{HH}$ = 12.6 Hz, 1 H, H_{12b}), 3.95 (d, $^2J_{HH}$ = 13.6 Hz, 1 H, H_{17a}), 3.82 (ddq, $^3J_{HH}$ = 10.1 Hz, $^3J_{HH}$ = 3.9 Hz, $^3J_{HH}$ = 6.8 Hz, 1 H, H_2), 3.32 (d, $^2J_{HH}$ = 13.6 Hz, 1 H, H_{17b}), 2.74 (dd, $^2J_{HH}$ = 13.6 Hz, $^3J_{HH}$ = 10.1 Hz, 1 H, H_{3a}), 2.52 (d, $^3J_{HH}$ = 10.8 Hz, 1 H, H_6), 2.19 (dd, $^2J_{HH}$ = 13.6 Hz, $^3J_{HH}$ = 3.9 Hz, 1 H, H_{3b}), 1.88 (ddq, $^3J_{HH}$ = 10.8 Hz, $^3J_{HH}$ = 6.4 Hz, $^3J_{HH}$ = 6.4 Hz, 1 H, H_8), 1.45 (s, 9 H, H_{23}), 1.02 (d, $^3J_{HH}$ = 6.8 Hz, 3 H, H_4), 0.73 (d, $^3J_{HH}$ = 6.4 Hz, 3 H, $H_{9/10}$), 0.67 (d, $^3J_{HH}$ = 6.4 Hz, 3 H, $H_{9/10}$).

^{13}C{H}-NMR (150.92 MHz, 298 K, $CDCl_3$): δ = 170.45 (1 C, C_7), 155.62 (1 C, C_{11}), 139.17 (1 C, C_{18}), 137.42 (1 C, C_{13}), 128.91 (2 C, C_{20}), 128.24 (1 C, C_{21}), 127.87 (2 C, C_{19}), 127.63 (2 C, C_{15}), 127.62 (1 C, C_{16}), 126.27 (2 C, C_{14}), 80.17 (1 C, C_{22}), 68.42 (1 C, C_6), 64.93 (1 C, C_{12}), 56.41 (1 C, C_3), 55.47 (1 C, C_{17}), 44.38 (1 C, C_2), 28.02 (3 C, C_{23}), 26.53 (1 C, C_8), 19.52 (1

C, $C_{9/10}$), 19.30 (1 C, $C_{9/10}$), 19.12 (1 C, C_4).

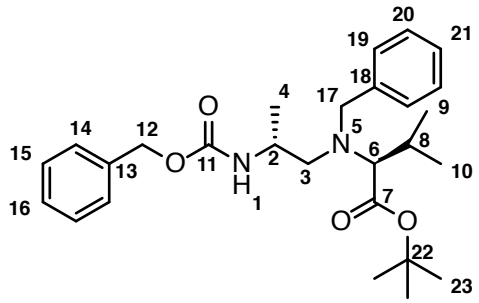

120

tert-BUTYL *N*-((*S*)-2-AMINOPROPYL)-*N*-BENZYL-*L*-VALINATE (**101**).

tert-Butyl *N*-benzyl-*N*-((*S*)-2-(((benzyloxy) carbonyl) amino) propyl)-*L*-valinate (**100**) (10.7 g, 23.5 mmol, 1.0 eq.) was dissolved in methlanol (100 mL). Palladium on barium sulphate (1.80 g, 5 % Pd/$BaSO_4$) was added and the reaction flask was flushed with nitrogen. Then hydrogen was bubbled through the solution for 5 min and the reaction mixture was left stirring under 1 bar hydrogen at 20-25 °C for 3 h. The suspension was filtered through celite and washed with methanol (3 x 50 mL). The filtrate was evaporated to dryness yielding a yellowish oil (6.82 g, 21.3 mmol, 90.6 %).

HR-ESI-MS: calcd. for [**101**+H]$^+$ $C_{19}H_{33}N_2O_2$ m/z= 321.2537, found m/z= 321.2539.

^{1}H-NMR (400.13 MHz, 298 K, DMSO−d_6): δ = 7.40-7.16 (m, 5 H, H_{13}, H_{14}, H_{15}), 3.93 (d, $^2J_{HH}$ = 14.1 Hz, 1 H, H_{11a}), 3.35 (d, $^2J_{HH}$ = 14.1 Hz, 1 H, H_{11b}), 3.27 (bs, 2 H, H_1), 2.96 (m, 1 H, H_2), 2.60 (d, $^3J_{HH}$ = 10.8 Hz, 1 H, H_6), 2.42 (dd, $^2J_{HH}$ = 13.1 Hz, $^3J_{HH}$ = 8.9 Hz, 1 H, H_{3a}), 2.35 (dd, $^2J_{HH}$ = 13.1 Hz, 1 H, H_{3b}), 1.93 (dqq, $^3J_{HH}$ = 10.8 Hz, $^3J_{HH}$ = 6.6 Hz, $^3J_{HH}$ = 6.5 Hz, 1 H, H_8), 1.47 (s, 9 H, H_{17}), 0.97 (d, $^3J_{HH}$ = 6.3 Hz, 3 H, H_4), 0.90 (d, $^3J_{HH}$ = 6.6 Hz, 3 H, $H_{9/10}$), 0.76 (d, $^3J_{HH}$ = 6.6 Hz, 3 H, $H_{9/10}$).

^{13}C{H}-NMR (100.61 MHz, 298 K, DMSO−d_6): δ = 170.32 (1 C, C_7), 139.56 (1 C, C_{12}), 128.64 (2 C, C_{14}), 128.12 (2 C, C_{13}), 126.87 (1 C, C_{15}), 80.33 (1 C, C_{16}), 69.76 (1 C, C_6), 58.57 (1 C, C_3), 55.44 (1 C, C_{11}), 44.80 (1 C, C_2), 28.01 (3 C, C_{17}), 26.81 (1 C, C_8), 20.87 (1 C, C_4), 19.58 (1 C, $C_{9/10}$), 19.42 (1 C, $C_{9/10}$).

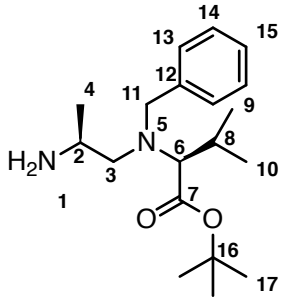

101

N-BENZYL-*N*-((S)-2-(((BENZYLOXY)CARBONYL)AMINO)PROPYL)-*L*-VALINE (**102**).

tert-Butyl *N*-benzyl-*N*-((*S*)-2-(((benzyloxy) carbonyl)amino)propyl)-*L*-valinate (**100**) (5.77 g, 12.7 mmol, 1.0 eq.) was dissolved in hydrogen chloride solution (conc. in 1,4-dioxane, 50 mL) and heated to 40 °C for 16 h. The reaction mixture was evaporated to dryness yielding the title compound as a hydrochloride salt (5.41 g, 12.4 mmol, 98.0 %). The product was used in the next step without further purification.

HR-ESI-MS: calcd. for [**102**+H]$^+$ $C_{23}H_{31}N_2O_4$ m/z= 399.2278, found m/z= 399.2283.

^{1}H-NMR (400.13 MHz, 298 K, CD_3CN): δ = 7.46-6.90 (m, 10 H, H_{14}, H_{15}, H_{16}, H_{18}, H_{19}, H_{20}), 5.57 (d, $^3J_{HH}$ = 8.1 Hz, 1 H, H_1), 5.05 (d, $^2J_{HH}$ = 12.6 Hz, 1 H, H_{12a}), 4.92 (d, $^2J_{HH}$ = 12.6 Hz, 1 H, H_{12b}), 4.08 (d, $^2J_{HH}$ = 14.6 Hz, 1 H, H_{17a}), 3.91 (m, 1 H, H_2), 3.21 (d, ($^2J_{HH}$ = 14.6 Hz, 1 H, H_{17b}), 2.79 (d, $^3J_{HH}$ = 10.6 Hz, 1 H, H_6), 2.64 (dd, $^2J_{HH}$ = 12.1 Hz, $^3J_{HH}$ = 3.6 Hz, 1 H, H_{3a}), 2.12-1.97 (m, 2 H, H_{3b}, H_8), 1.03 (d, $^3J_{HH}$ = 6.5 Hz, 3 H, H_4), 0.96 (d, $^3J_{HH}$ = 6.6 Hz, 3 H, $H_{9/10}$), 0.90 (d, $^3J_{HH}$ = 6.4 Hz, 3 H, $H_{9/10}$).

^{13}C{H}-NMR (100.61 MHz, 298 K, CD_3CN): δ = 177.55 (1 C, C_7), 156.37 (1 C, C_{11}), 141.25 (1 C, C_{18}), 136.52 (1 C, C_{13}), 128.43 (1 C, $C_{arom.}$), 128.10 (1 C, $C_{arom.}$), 127.61 (3 C, $C_{arom.}$), 125.98 (1 C, $C_{arom.}$), 71.86 (1 C, C_6), 65.94 (1 C, C_{12}), 55.99 (1 C, C_3), 53.55 (1 C, C_{17}), 44.19 (1 C, C_2), 26.83 (1 C, C_8), 19.81 (1 C, $C_{9/10}$), 18.93 (1 C, $C_{9/10}$), 16.88 (1 C, C_4).

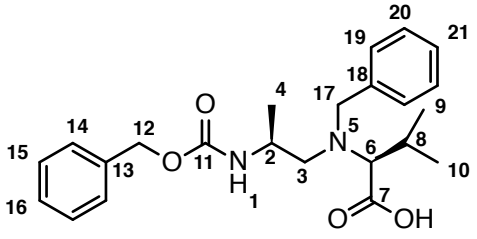

102

tert-BUTYL (5*S*,8*S*,11*S*,14*S*)-7,13-DIBENZYL-8,14-DIISOPROPYL-5,11-DIMETHYL-3,9-DIOXO-1-PHENYL-2-OXA-4,7,10,13-TETRAAZAPENTADECAN-15-OATE (**104**).

N-benzyl-*N*-((*S*)-2-(((benzyloxy)carbonyl)amino)propyl)-*L*-valine hydrochloride (**102**) (5.00 g, 11.5 mmol, 1.0 eq.), *tert*-butyl *N*-((*S*)-2-aminopropyl)-*N*-benzyl-*L*-valinate (**101**) (3.64 g, 11.4 mmol, 1.01 eq.) and *N*-ethyl diisopropylamine (6.0 mL, 36.3 mmol, 3.2 eq.) were dissolved in acetonitrile (70 mL). To this solution HATU (4.93 g, 13.0 mmol, 1.1 eq.) was added. After 40 min, additional HATU (1.06 g, 2.79 mmol, 0.2 eq.) was added and the solution was stirred for another 2 h. The solvent was removed under reduced pressure and the crude oil was purified by flash column chromatography (SiO_2, pentane / methyl *tert*-butyl ether / triethylamine (70:30:1)) yielding a colorless oil (6.05 g, 8.63 mmol, 75.7 %).

HR-ESI-MS: calcd. for [**104**+H]$^+$ $C_{42}H_{61}N_4O_5$ m/z= 701.4636, found m/z= 701.4640.

^{1}H-NMR (600.13 MHz, 298 K, DMSO−d_6): δ = 7.44-7.21 (m, 15 H, H_{25}, H_{26}, H_{27}, H_{31}, H_{32}, H_{33}, H_{36}, H_{37}, H_{38}), 5.00 (d, $^2J_{HH}$ = 12.9 Hz, 1 H, H_{29a}), 4.98 (d, $^2J_{HH}$ = 12.9 Hz, 1 H, H_{29b}), 4.09 (m, 1 H, H_{12}), 4.02 (d, $^2J_{HH}$ = 14.0 Hz, 1 H, H_{23a}), 4.00 (d, $^2J_{HH}$ = 13.7 Hz, 1 H, H_{34a}), 3.60 (bs, 1 H, H_2), 3.48 (bs, 1 H, H_{34b}), 3.41 (d, $^2J_{HH}$ = 14.0 Hz, 1 H, H_{23b}), 2.79 (bs, 1 H, H_6), 2.72 (d, $^3J_{HH}$ = 10.4 Hz, 1 H, H_{16}), 2.65-2.59 (m, 1 H, H_{3a}), 2.57-2.51 (m, 1 H, H_{3b}), 2.54-2.48 (m, 2 H, H_{13}), 2.06 (m, 1 H, H_8), 1.97 (dqq, $^3J_{HH}$ = 10.4 Hz, $^3J_{HH}$ = 6.5 Hz, $^3J_{HH}$ = 6.5 Hz, 1 H, H_{18}), 1.46 (s, 9 H, H_{22}), 1.08 (d, $^3J_{HH}$ = 6.7 Hz, 3 H, H_{14}), 0.99 (d, $^3J_{HH}$ = 6.7 Hz, 3 H, $H_{10/9}$), 0.96 (d, $^3J_{HH}$ = 6.7 Hz, 3 H, H_4), 0.94 (d, $^3J_{HH}$ = 6.5 Hz, 3 H, $H_{19/20}$), 0.82 (d, $^3J_{HH}$ = 6.5 Hz, 3 H, $H_{9/10}$), 0.815 (d, $^3J_{HH}$ = 6.5 Hz, 3 H, $H_{20/19}$).

^{13}C{H}-NMR (from HMBC/HMQC, 600.13 MHz, 298 K, DMSO−d_6): δ = 169.45 (1 C, C_{17}), 155.00 (1 C, C_{28}), 138.59 (1 C, C_{24}), 136.37 (1 C, C_{30}), 127.48 (2 C, C_{25}), 126.8 (2 C, C_{31}), 79.86 (1 C, C_{21}), 69.82 (1 C, C_6), 69.05 (1 C, C_{16}), 64.7 (1 C, C_{29}), 56.18 (1 C, C_3), 55.43 (1 C, C_{13}), 55.02 (1 C, C_{34}), 54.65 (1 C, C_{23}), 44.83 (1 C, C_2), 42.40 (1 C, C_{12}), 27.49 (3 C, C_{22}), 26.22 (1 C, C_{18}), 26.08 (1 C, C_8), 19.26 (1 C, $C_{9/10}$), 18.92 (1 C, $C_{19/20}$), 18.89 (1 C, $C_{9/10}$), 18.86 (1 C, $C_{19/20}$), 18.42 (1 C, C_{14}), 17.97 (1 C, C_4).

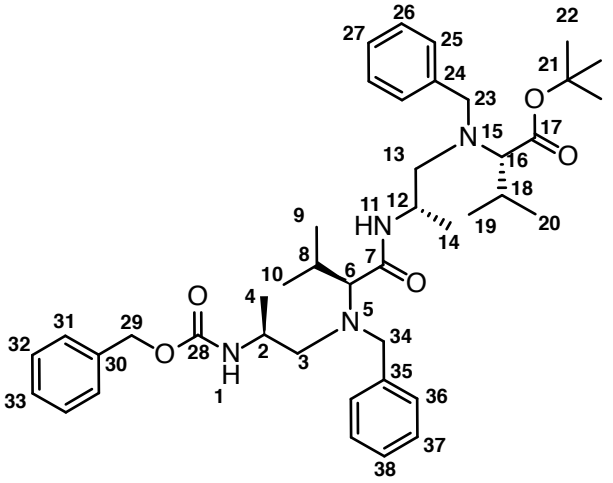

104

N-((*S*)-2-((*S*)-2-(((*S*)-2-AMINOPROPYL)(BENZYL)AMINO)-3-METHYLBUTANAMIDO)PROPYL)-*N*-BENZYL-*L*-VALINE (**98**).

tert-Butyl (5*S*,8*S*,11*S*,14*S*)-7,13-dibenzyl-8,14-diisopropyl-5,11-dimethyl-3,9-dioxo-1-phenyl-2-oxa-4,7,10,13-tetraazapenta-decan-15-oate (**104**) (8.55 g, 12.2 mmol, 1.0 eq.) was dissolved in acetic acid (60 mL) and hydrogen bromide solution (33 wt.% in acetic acid, 60 mL) was added. The solution was stirred at 40 °C for 30 min and evaporated to dryness. This oil was further suspended in acetonitrile (20 mL) and hydrochloric acid (37 %, 1.0 mL). This mixture was again evaporated to dryness. This procedure was repeated three times to remove residual acetic acid from the product. Finally, methanol (20 mL) was added and the solvent was removed under reduced pressure yielding a yellowish foam. This foam was extensively dried under high vacuum at 40 °C for 2 d. The product (9.04 g) is obtained as a mixture of HCl and HBr salt with minimal acetate content and was used without further purification.

HR-ESI-MS: calcd. for [**98**+H]$^+$ $C_{30}H_{47}N_4O_3$ m/z= 511.3643, found m/z= 511.3650.

^{1}H-NMR (500.13 MHz, 298 K, DMSO−d_6): δ = 7.81-7.71 (m, 3 H, H_{11}, H_1), 7.39 (7.2, 10 H, H_{24}, H_{25}, H_{26}, H_{29}, H_{30}, H_{31}), 4.10-4.03 (m, 1 H, H_{12}), 3.98 (d, $^2J_{HH}$ = 14.0 Hz, 1 H, H_{22a}), 3.91 (d, $^2J_{HH}$ = 14.6 Hz, 1 H, H_{27a}), 3.40 (d, $^2J_{HH}$ = 14.6 Hz, 1 H, H_{27b}), 3.35 (d, $^2J_{HH}$ = 14.0 Hz, 1 H, H_{22b}), 3.28-3.17 (m, 1 H, H_2), 2.70 (d, $^3J_{HH}$ = 10.8 Hz, 1 H, H_{16}), 2.67-2.57 (m, 2 H, H_3), 2.59 (d, $^3J_{HH}$ = 10.8 Hz, 1 H, H_6), 2.49-2.39 (m, 2 H, H_{13}), 2.02-1.96 (m, 2 H, H_{18}, H_8), 1.11 (d, $^3J_{HH}$ = 6.6 Hz, 3 H, H_{14}), 1.06 (d, $^3J_{HH}$ = 6.5 Hz, 3 H, H_4), 0.97 (d, $^3J_{HH}$ = 6.5 Hz, 3 H, $H_{9/10}$), 0.95 (d, $^3J_{HH}$ = 6.5 Hz, 3 H, $H_{19/20}$), 0.82 (d, $^3J_{HH}$ = 6.5 Hz, 3 H, $H_{19/20}$), 0.78 (d, $^3J_{HH}$ = 6.5 Hz, 3 H, $H_{9/10}$).

$^{13}C\{H\}$-NMR (125.75 MHz, 298 K, DMSO−d_6): δ = 172.19 (1 C, C_{17}), 169.39 (1 C, C_7), 139.86 (1 C, C_{28}, C_{23}), 128.78 (2 C, C_{24}), 128.39 (2 C, C_{29}), 128.26 (2 C, C_{25}), 128.17 (2 C, C_{30}), 126.94 (1 C, C_{31}), 126.88 (1 C, C_{26}), 69.82 (1 C, C_6), 68.74 (1 C, C_{16}), 55.58 (1 C, C_{27}), 55.47 (1 C, C_{13}), 55.06 (1 C, C_{22}), 53.68 (1 C, C_3), 44.92 (1 C, C_2), 42.66 (1 C, C_{12}), 26.70 (1 C, C_8), 26.62 (1 C, C_{18}), 19.83 (2 C, $C_{19/20}$, $C_{9/10}$), 19.75 (1 C, $C_{9/10}$), 19.55 (1 C, $C_{19/20}$), 19.21 (1 C, C_{14}), 16.66 (1 C, C_4).

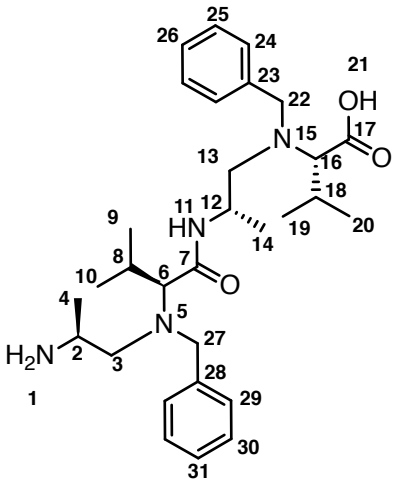

98

(3*S*,6*S*,9*S*,12*S*)-4,10-DIBENZYL-3,9-DIISOPROPYL-6,12-DIMETHYL-1,4,7,10-TETRAAZACYCLODODECANE-2,8-DIONE (**97**).

A total of 9.03 g of N-((*S*)-2-((*S*)-2-(((*S*)-2-aminopropyl)(benzyl)amino)--3-methylbutanamido)propyl)-*N*-benzyl-*L*-valine (**98**) salt was cyclized in several portions of max. 2.0 g. N-((*S*)-2-((*S*)-2-(((*S*)-2-aminopropyl)(benzyl)amino)-3-methylbutanamido)propyl)-*N*-benzyl-*L*-valine (**98**) salt (2.00 g, 4.08 mmol, 1.0 eq.) and *N*-ethyl diisopropylamine (3.4 mL, 20.4 mmol, 5 eq.) were dissolved in acetonitrile (2.0 L). HATU (1.55 g, 4.08 mmol, 1.0 eq.) was added and the solution was stirred at 20-25 °C for 20 min. The solvent was removed under vacuum. The crude products from all batches were combined and purified by flash column chromatography (SiO_2, ethyl acetate / cyclohexane / triethylamine (90:10:1)) yielding a yellowish solid (3.54 g, 7.18 mmol, 58.9 % yield calculated over 2 steps starting from **104**).

HR-ESI-MS: calcd. for [**97**+H]$^+$ $C_{30}H_{45}N_4O_2$ m/z= 493.3537, found m/z= 493.3539.

^{1}H-NMR (600.13 MHz, 298 K, $CDCl_3$): δ = 7.37-7.23 (m, 10 H, H_{14}, H_{15}, H_{16}), 3.98 (d, $^2J_{HH}$ = 14.2 Hz, 2 H, H_{12a}), 3.90 (d, $^2J_{HH}$ = 14.2 Hz, 2 H, H_{12b}), 3.74-3.64 (m, 2 H, H_8), 3.20 (dd, $^2J_{HH}$ = 13.7 Hz, $^3J_{HH}$ = 11.3 Hz, 2 H, H_{10a}), 2.96 (d, $^3J_{HH}$ = 8.1 Hz, 2 H, H_2), 2.72 (dd, $^2J_{HH}$ = 13.7 Hz, $^3J_{HH}$ = 3.1 Hz, 2

H, H_{10b}), 2.16 (dqq, $^3J_{HH}$ = 8.1 Hz, $^3J_{HH}$ = 6.7 Hz, $^3J_{HH}$ = 6.7 Hz, 2 H, H_4), 1.19 (d, $^3J_{HH}$ = 6.6 Hz, 6 H, H_9), 1.02 (d, $^3J_{HH}$ = 6.7 Hz, 6 H, $H_{5/6}$), 0.90 (d, $^3J_{HH}$ = 6.7 Hz, 6 H, $H_{5/6}$).

$^{13}C\{H\}$-NMR (150.9 MHz, 298 K, $CDCl_3$): δ = 173.85 (2 C, C_3), 139.25 (2 C, C_{13}), 129.18 (4 C, C_{15}), 128.69 (4 C, C_{14}), 127.53 (2 C, C_{16}), 71.77 (2 C, C_2), 58.46 (2 C, C_{12}), 54.08 (2 C, C_{10}), 45.04 (2 C, C_8), 28.06 (2 C, C_4), 22.20 (2 C, $C_{5/6}$), 20.06 (2 C, $C_{5/6}$), 18.44 (2 C, C_9).

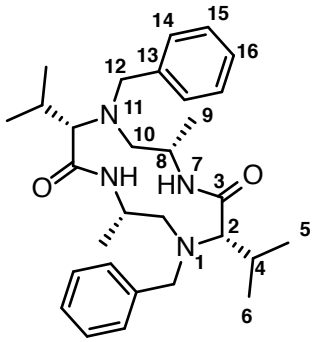

97

(2*S*,5*S*,8*S*,11*S*)-1,7-DIBENZYL-2,8-DIISOPROPYL-5,11-DIMETHYL-1,4,7,10-TETRAAZACYCLODODECANE (**107**).

(3*S*,6*S*,9*S*,12*S*)-4,10-Dibenzyl-3,9-diisopropyl-6,12-dimethyl-1,4,7,10-tetraazacyclododecane-2,8-dione (**97**) (1.49 g, 3.02 mmol, 1.0 eq.) was dissolved in dichloromethane (50 mL) and was cooled to 0-5 °C. Trimethylchlorosilane (2.2 mL, 17.5 mmol, 5.8 eq.) was added and the solution was stirred for 1 h at 0-5 °C. A suspension of lithium aluminium hydride (490 mg, 12.9 mmol, 4.3 eq.) in tetrahydrofuran (10 mL) was prepared under inert conditions and added dropwise to the reaction mixture at 0-5 °C. After 3 h the excess of lithium aluminium hydride was quenched with aqueous potassium hydroxide (1 M, 2.0 mL). The suspension was dried over sodium sulphate, filtered and the filter cake was washed with dichloromethane (5 x 20 mL). The filtrate was evaporated to dryness and was purified by flash column chromatography (SiO_2, ethyl acetate / triethylamine (100:1)) yielding a white solid (1.29 g, 2.77 mmol, 91.9 %).

HR-ESI-MS: calcd. for [**107**+H]$^+$ $C_{30}H_{49}N_4$ m/z= 465.3952, found m/z= 465.3958.

^1H-NMR (500.13 MHz, 298 K, $CDCl_3$): δ = 7.5-7.1 (m, 10 H, H_{14}, H_{15}, H_{16}), 4.03 (d, $^2J_{HH}$ = 11.5 Hz, 2 H, H_{12a}), 3.16 (d, $^2J_{HH}$ = 11.5 Hz, 2 H, H_{12b}), 2.86-2.74 (m, 4 H, H_{3a}, H_8), 2.65-2.59 (m, 4 H, H_{10a}, H_2), 2.53 (bs, 2 H, H_{3b}), 2.34-2.25 (m, 2 H, H_{10b}), 2.20-2.03 (m, 2 H, H_4), 1.00 (d, $^3J_{HH}$ = 6.6 Hz, 6 H,

$H_{5/6}$), 0.92 (d, $^3J_{HH}$ = 6.7 Hz, 6 H, $H_{5/6}$), 0.87 (bs, 6 H, H_9).

$^{13}C\{H\}$-NMR (125.75 MHz, 298 K, $CDCl_3$): δ = 140.30 (2 C, C_{13}), 129.24 (2 C, C_{15}), 128.49 (2 C, C_{14}), 127.30 (2 C, C_{16}), 59.22 (2 C, C_2), 56.62 (2 C, C_{10}), 53.15 (2 C, C_{12}), 45.74 (2 C, C_8), 41.46 (2 C, C_3), 24.43 (2 C, C_4), 24.18 (2 C, $C_{5/6}$), 19.34 (2 C, $C_{5/6}$), 18.82 (2 C, C_9).

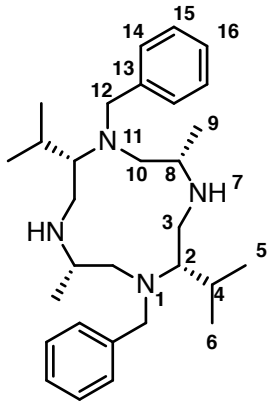

107

(2*S*,5*S*,8*S*,11*S*)-2,8-DIISOPROPYL-5,11-DIMETHYL-1,4,7,10-TETRAAZACYCLODODECANE (**96**).

(2*S*,5*S*,8*S*,11*S*)-1,7-Dibenzyl-2,8-diisopropyl-5,11-dimethyl-1,4,7,10-tetraazacyclododecane (**107**) (197 mg, 423 µmol, 1.0 eq.) was dissolved in ethanol (30 mL) and ethyl acetate (3.0 mL). Palladium on activated charcoal (101 mg, 10 % Pd) and ammonium formate (612 mg, 9.71 mmol, 23.0 eq.) were added and the resulting suspension was refluxed for 16 h. The suspension was cooled to 20-25 °C, filtered through celite and washed with methanol (3 x 20 mL). The solvent was removed under reduced pressure yielding a white solid (118 mg, 415 µmol, 98.2 %).

HR-ESI-MS: calcd. for [**96**+H]$^+$ $C_{16}H_{37}N_4$ *m*/*z*= 285.3013, found *m*/*z*= 285.3013.

^1H-NMR (500.13 MHz, 298 K, $CDCl_3$): δ = 2.70 (dd, $^2J_{HH}$ = 13.1 Hz, $^3J_{HH}$ = 2.8 Hz, 2 H, H_{10a}), 2.64 (dd, $^2J_{HH}$ = 13.0 Hz, $^3J_{HH}$ = 1.9 Hz, 2 H, H_{3a}), 2.64-2.59 (m, 2 H, H_8), 2.46-2.35 (m, 6 H, H_{3b}, H_{10b}, H_2), 1.94-1.86 (m, 2 H, H_4), 0.94 (d, $^3J_{HH}$ = 7.0 Hz, 6 H, $H_{5/6}$), 0.91 (d, $^3J_{HH}$ = 6.3 Hz, 6 H, H_9), 0.85 (d, $^3J_{HH}$ = 7.0 Hz, 6 H, $H_{5/6}$).

$^{13}C\{H\}$-NMR (125.75 MHz, 298 K, $CDCl_3$): δ = 57.13 (2 C, C_2), 52.60 (2 C, C_{10}), 47.64 (2 C, C_8), 44.98 (2 C, C_3), 28.13 (2 C, C_4), 20.29 (2 C, $C_{5/6}$), 18.16 (2 C, C_9), 16.62 (2 C, $C_{5/6}$).

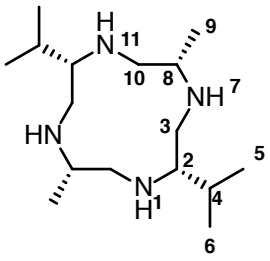

96

tert-BUTYL *N*-((*S*)-2-(((BENZYLOXY)CARBONYL)AMINO)-PROPYL)-*O*-(*tert*-BUTYL)-*L*-SERINATE (**114**).

Benzyl (*S*)-(1-oxopropan-2-yl)carbamate (**60**) (2.60 g, 12.5 mmol, 1.1 eq.) was dissolved in dichloromethane (20 mL). To this solution *tert*-butyl *O*-(*tert*-butyl)-*L*-serinate (2.52 g, 12.5 mmol, 1.0 eq.) was added. The solution was stirred at 20-25 °C for 5 min followed by the addition of sodium triacetoxyborohydride (10.9 g, 51.4 mmol, 4.4 eq.). The reaction mixture was stirred at 20-25 °C for 16 h. The excess of sodium triacetoxyborohydride was quenched with aqueous saturated sodium hydrogen carbonate (50.0 mL) and the pH adjusted to >9 by the addition of triethylamine (5.0 mL). The two layers were separated and the organic layer was washed with water (30 mL) and dried with sodium sulphate. The organic layer was evaporated to dryness yielding a yellowish oil (4.61 g, 11.3 mmol, 97.3 %).

HR-ESI-MS: calcd. for [**114**+H]$^+$ $C_{22}H_{37}N_2O_5$ m/z= 409.2697, found m/z= 409.2700.

^{1}H-NMR (500.13 MHz, 298 K, $CDCl_3$): δ = 7.40-7.27 (m, 5 H, H_{14}, H_{15}, H_{16}), 5.23 (bs, 1 H, H_1), 5.08 (s, 2 H, H_{12}), 3.73 (qdd, $^3J_{HH}$ = 6.7 Hz, $^3J_{HH}$ = 5.7 Hz, $^3J_{HH}$ = 5.2 Hz, 1 H, H_2), 3.52 (dd, $^2J_{HH}$ = 8.3 Hz, $^3J_{HH}$ = 5.4 Hz, 1 H, H_{8a}), 3.49 (dd, $^2J_{HH}$ = 8.3 Hz, $^3J_{HH}$ = 4.7 Hz, 1 H, H_{8b}), 3.24 (dd, $^3J_{HH}$ = 5.4 Hz, $^3J_{HH}$ = 4.7 Hz, 1 H, H_6), 2.75 (dd, $^2J_{HH}$ = 12.6 Hz, $^3J_{HH}$ = 5.2 Hz, 1 H, H_{3a}), 2.53 (dd, $^2J_{HH}$ = 12.6 Hz, $^3J_{HH}$ = 5.7 Hz, 1 H, H_{3b}), 1.45 (s, 9 H, H_{10}), 1.17 (d, $^3J_{HH}$ = 6.7 Hz, 3 H, H_4), 1.15 (s, 9 H, H_{18}).

^{13}C{H}-NMR (100.61 MHz, 298 K, $CDCl_3$): δ = 172.52 (1 C, C_7), 156.46 (1 C, C_{11}), 136.88 (1 C, C_{13}), 128.57 (2 C, C_{15}), 128.17 (2 C, C_{14}), 128.08 (1 C, C_{16}), 81.19 (1 C, C_9), 73.13 (1 C, C_{17}), 66.53 (1 C, C_{12}), 62.99 (1 C, C_8), 62.70 (1 C, C_6), 52.73 (1 C, C_3), 47.33 (1 C, C_2), 28.25 (3 C, C_{10}), 27.51 (3 C, C_{18}), 18.99 (1 C, C_4).

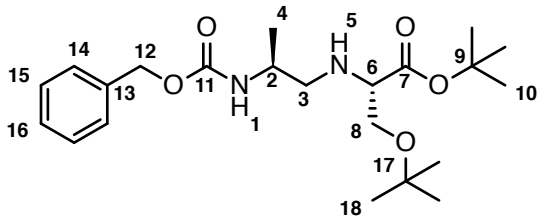

114

tert-BUTYL *N*-BENZYL-*N*-((*S*)-2-(((BENZYLOXY)CARBONYL) AMINO)PROPYL)-*O*-(*tert*-BUTYL)-*L*-SERINATE (**118**).

tert-Butyl *N*-((*S*)-2-(((benzyloxy)carbonyl)amino)propyl)-*O*-(*tert*-butyl)-*L*-serinate (**114**) (3.58 g, 8.76 mmol, 1.0 eq.) and potassium carbonate (1.37 g, 9.91 mmol, 1.1 eq.) were suspended in acetonitrile (35 mL). Over a period of 2 min benzyl bromide (1.3 mL, 10.9 mmol, 1.2 eq.) was added. The reaction mixture was heated to 40 °C and stirred for 18 h under an argon atmosphere. The excess of benzyl bromide was quenched with triethylamine (10 mL). The suspension was heated to 50 °C and stirred for 40 min followed by cooling to 20-25 °C. The reaction mixture was filtered and the filter cake was washed with acetonitrile (20 mL). The filtrate was evaporated to dryness and the crude oil was purified by flash column chromatography (SiO_2, cyclohexane / ethyl acetate / triethylamine (80:20:1)) yielding a colorless oil (2.99 g, 5.99 mmol, 68.4 %).

HR-ESI-MS: calcd. for [**118**+H]$^+$ $C_{29}H_{43}N_2O_5$ m/z= 499.3166, found m/z= 499.3173.

^{1}H-NMR (500.13 MHz, 298 K, $CDCl_3$): δ = 7.41-7.17 (m, 10 H, H_{14}, H_{15}, H_{16}, H_{19}, H_{20}, H_{21}), 5.79 (bs, 1 H, H_1), 5.11 (d, $^2J_{HH}$ = 12.3 Hz, 1 H, H_{12a}), 5.06 (d, $^2J_{HH}$ = 12.3 Hz, 1 H, H_{12b}), 3.89 (d, $^2J_{HH}$ = 14.4 Hz, 1 H, H_{17a}), 3.83 (d, $^2J_{HH}$ = 14.4 Hz, 1 H, H_{17b}), 3.73-3.64 (m, 1 H, H_2), 3.64 (dd, $^2J_{HH}$ = 9.4 Hz, $^3J_{HH}$ = 5.6 Hz, 1 H, H_{8a}), 3.57 (dd, $^2J_{HH}$ = 9.4 Hz, $^3J_{HH}$ = 7.1 Hz, 1 H, H_{8b}), 3.39 (dd, $^3J_{HH}$ = 7.1 Hz, $^3J_{HH}$ = 5.6 Hz, 1 H, H_6), 2.82 (dd, $^2J_{HH}$ = 13.3 Hz, $^3J_{HH}$ = 4.9 Hz, 1 H, H_{3a}), 2.73 (dd, $^2J_{HH}$ = 13.3 Hz, $^3J_{HH}$ = 7.1 Hz, 1 H, H_{3b}), 1.46 (s, 9 H, H_{24}), 1.16 (d, $^3J_{HH}$ = 7.6 Hz, 3 H, H_4), 1.15 (s, 9 H, H_{10}).

^{13}C{H}-NMR (125.76 MHz, 298 K, $CDCl_3$): δ = 171.22 (1 C, C_7), 156.34 (1 C, C_{11}), 139.69 (1 C, C_{18}), 137.04 (1 C, C_{13}), 128.59 (2 C, C_{19}), 128.38 (2 C, C_{20}), 128.22 (2 C, C_{15}), 128.01 (2 C, C_{14}), 127.82 (1 C, C_{21}), 126.92 (1 C, C_{16}), 81.18 (1 C, C_{23}), 73.24 (1 C, C_9), 66.18 (1 C, C_{12}), 63.59 (1 C, C_6), 60.32 (1 C, C_8), 57.03 (1 C, C_{17}), 56.49 (1 C, C_3), 46.11 (1 C, C_2), 28.22 (3 C, C_{24}), 27.34 (3 C, C_{10}), 19.28 (1 C, C_4).

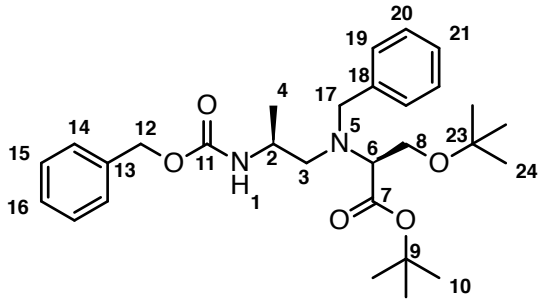

118

tert-BUTYL *N*-((*S*)-2-AMINOPROPYL)-*N*-BENZYL-*O*-(*tert*-BUTYL)-*L*-SERINATE (**110**).

tert-Butyl *N*-benzyl -*N*-((*S*)-2-(((benzyloxy)carbonyl)amino)propyl)-*O*--(*tert*-butyl)-*L*-serinate (**118**) (2.99 g, 6.00 mmol, 1.0 eq.), was dissolved in methanol (30 mL). Palladium (50 mg, 5 % Pd / $BaSO_4$) was added and the reaction flask was flushed with nitrogen. Then hydrogen was bubbled through the solution for 5 min and the reaction mixture was left stirring under 1 bar hydrogen at 20-25 °C for 24 h. The suspension was filtered through celite and washed with methanol (3x 50 mL). The filtrate was evaporated to dryness yielding a yellowish oil (2.02 g, 5.53 mmol, 92.4 %).

HR-ESI-MS: calcd. for [**110**+H]$^+$ $C_{17}H_{37}N_2O_3$ m/z= 365.2799, found m/z= 365.2803.

^{1}H-NMR (500.13 MHz, 298 K, CD_3CN): δ = 7.38-7.25 (m, 5 H, H_{15}, H_{16}, H_{17}), 3.90 (d, $^2J_{HH}$ = 13.8 Hz, 1 H, H_{13a}), 3.76 (d, $^2J_{HH}$ = 13.8 Hz, 1 H, H_{13b}), 3.63 (dd, $^2J_{HH}$ = 10.5 Hz, $^3J_{HH}$ = 5.1 Hz, 1 H, H_{8a}), 3.55 (dd, $^2J_{HH}$ = 10.5 Hz, $^3J_{HH}$ = 9.4 Hz, 1 H, H_{8b}), 3.42-3.34 (m, 1 H, H_2), 3.37 (dd, $^3J_{HH}$ = 5.1 Hz, $^3J_{HH}$ = 4.2 Hz, 1 H, H_6), 2.95 (dd, $^2J_{HH}$ = 14.3 Hz, $^3J_{HH}$ = 3.4 Hz, 1 H, H_{3a}), 2.73 (dd, $^2J_{HH}$ = 14.3 Hz, $^3J_{HH}$ = 11.7 Hz, 1 H, H_{3b}), 1.48 (s, 9 H, H_{10}), 1.21 (d, $^3J_{HH}$ = 6.6 Hz, 3 H, H_4), 1.15 (s, 9 H, H_{12}).

^{13}C{H}-NMR (125.76 MHz, 298 K, CD_3CN): δ = 171.17 (1 C, C_7), 139.83 (1 C, C_{14}), 130.03 (2 C, C_{16}), 129.45 (2 C, C_{15}), 128.33 (1 C, C_{17}), 82.63 (1 C, C_9), 75.25 (1 C, C_{11}), 63.36 (1 C, C_6), 60.02 (1 C, C_8), 57.32 (1 C, C_{13}), 54.53 (1 C, C_3), 47.57 (1 C, C_2), 28.43 (3 C, C_{10}), 27.57 (3 C, C_{12}), 15.77 (1 C, C_4).

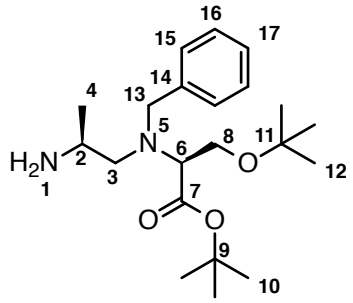

110

tert-BUTYL (5*S*,8*S*,11*S*,14*S*)-7,13-DIBENZYL-14-(*tert*-BUTOXYMETHYL)-5,8,11-TRIMETHYL-3,9-DIOXO-1-PHENYL-2-OXA-4,7,10,13-TETRAAZAPENTADECAN-15-OATE (**116**).

N-benzyl-*N*-((*S*)-2-(((benzyloxy) carbonyl)amino)propyl)-*L*-alanine hydrochloride (2.16 g, 5.32 mmol, 1.0 eq.), *tert*-butyl *N*-((*S*)-2-aminopropyl)-*N*-benzyl-*O*-(*tert*-butyl)-*L*-serinate (1.94 g, 5.32 mmol, 1.0 eq.) and *N*-ethyl diisopropylamine (2.7 mL, 16.4 mmol, 3.1 eq.) were dissolved in acetonitrile (30 mL). To this solution HATU (2.45 g, 6.44 mmol, 1.2 eq.) was added. The reaction mixture was stirred for 2 h. The solvent was removed under reduced pressure and the crude oil was purified by flash column chromatography (SiO_2, ethyl acetate / cyclohexane / triethylamine (70:30:1)) yielding a yellowish oil (3.35 g, 4.67 mmol, 87.8 %).

HR-ESI-MS: calcd. for [**116**+H]$^+$ $C_{42}H_{61}N_4O_6$ m/z= 717.4586, found m/z= 717.4588.

^{1}H-NMR (500.13 MHz, 298 K, $CDCl_3$): δ = 7.40-7.12 (m, 15 H, H_{19}, H_{20}, H_{21}, H_{24}, H_{25}, H_{26}, H_{32}, H_{33}, H_{34}), 5.10 (d, $^2J_{HH}$ = 12.6 Hz, 1 H, H_{30a}), 4.92 (d, $^2J_{HH}$ = 12.6 Hz, 1 H, H_{30b}), 4.75 (d, $^3J_{HH}$ = 6.8 Hz, 1 H, H_1), 4.02 (ddq, $^3J_{HH}$ = 7.2 Hz, $^3J_{HH}$ = 6.9 Hz, $^3J_{HH}$ = 6.5 Hz, 1 H, H_{10}), 3.92 (d, $^2J_{HH}$ = 14.7 Hz, 1 H, H_{22a}), 3.83-3.78 (m, 1 H, H_2), 3.76 (d, $^2J_{HH}$ = 14.7 Hz, 1 H, H_{22b}), 3.71 (d, $^2J_{HH}$ = 13.7 Hz, 1 H, H_{17a}), 3.64 (dd, $^2J_{HH}$ = 8.6 Hz, $^3J_{HH}$ = 5.4 Hz, 1 H, H_{16a}), 3.51 (dd, $^2J_{HH}$ = 8.6 Hz, $^3J_{HH}$ = 5.7 Hz, 1 H, H_{16b}), 3.40 (d, $^2J_{HH}$ = 13.7 Hz, 1 H, H_{17b}), 3.35 (dd, $^3J_{HH}$ = 5.7 Hz, $^3J_{HH}$ = 5.4 Hz, 1 H, H_{14}), 2.79 (dd, $^2J_{HH}$ = 13.3 Hz, $^3J_{HH}$ = 6.9 Hz, 1 H, H_{11a}), 2.75 (dd, $^2J_{HH}$ = 13.3 Hz, $^3J_{HH}$ = 7.2 Hz, 1 H, H_{11b}), 2.50 (dd, $^2J_{HH}$ = 13.5 Hz, $^3J_{HH}$ = 3.7 Hz, 1 H, H_{3a}), 2.32 (dd, $^2J_{HH}$ = 13.5 Hz, $^3J_{HH}$ = 10.5 Hz, 1 H, H_{3b}), 1.44 (s, 9 H, H_{28}), 1.21 (d, $^3J_{HH}$ = 6.9 Hz, 3 H, H_8), 1.17 (d, $^3J_{HH}$ = 6.5 Hz, 3 H, H_{12}), 1.13 (s, 9 H, H_{36}), 1.05 (d, $^3J_{HH}$ = 7.3 Hz, 3 H, H_4).

^{13}C{H}-NMR (125.77 MHz, 298 K, $CDCl_3$): δ = 173.03 (1 C, C_7), 171.42 (1 C, C_{15}), 156.45 (1 C, C_{29}), 140.20 (1 C, C_{23}), 139.37 (1 C, C_{18}), 136.84 (1 C, C_{31}), 129.05 (2 C, C_{19}), 128.68 (2 C, C_{24}), 128.58 ($C_{arom.}$), 128.43 ($C_{arom.}$), 128.28 ($C_{arom.}$), 128.23 (2 C, C_{32}), 128.14 ($C_{arom.}$), 127.22 ($C_{arom.}$), 126.85 ($C_{arom.}$), 80.95 (1 C, C_{27}), 72.99 (1 C, C_{35}), 66.62 (1 C, C_{30}), 63.13 (1 C, C_{14}),

58.54 (1 C, C_6), 57.24 (1 C, C_{22}), 57.08 (1 C, C_{11}), 56.42 (1 C, C_3), 54.99 (2 C, C_{16}, C_{17}), 45.25 (1 C, C_2), 44.68 (1 C, C_{10}), 28.41 (3 C, C_{28}), 27.51 (3 C, C_{36}), 19.50 (1 C, C_4), 19.18 (1 C, C_{12}), 8.63 (1 C, C_8).

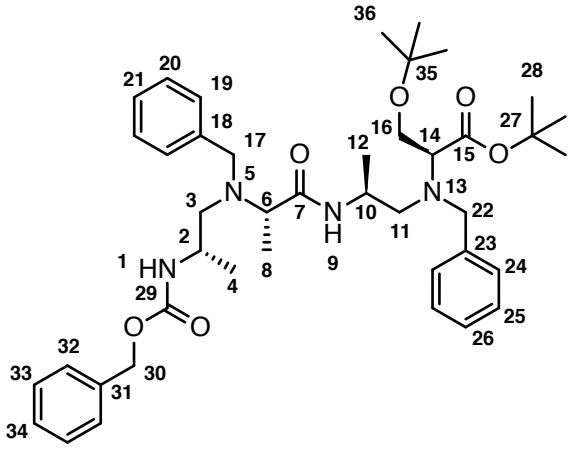

116

O-ACETYL-*N*-((*S*)-2-((*S*)-2-(((*S*)-2-AMINOPROPYL)(BENZYL) AMINO)PROPANAMIDO)PROPYL)-*N*-BENZYL-*L*-SERINE (**112**).

tert-Butyl (5*S*,8*S*,11*S*,14*S*)-7,13-dibenzyl-14-(*tert*-butoxymethyl)-5,8,11-trimethyl-3,9-dioxo-1-phenyl-2-oxa-4,7,10,13-tetra-azapentadecan-15-oate (**116**) (1.04 g, 1.45 mmol, 1.0 eq.) was dissolved in acetic acid (10.0 mL) and hydrogen bromide solution (33 wt.% in acetic acid, 10 mL). The solution was stirred at 40 °C for 30 min and evaporated to dryness. This oil was further suspended in acetonitrile (10 mL) and hydrochloric acid (37 %, 500 µL). This mixture was again evaporated to dryness. This procedure was repeated three times to remove residual acetic acid from the product. Finally, methanol (10 mL) was added and the solvent was removed under reduced pressure yielding a brown foam. The foam was extensively dried under high vacuum at 40 °C for 2 d. The product (1.12 g) is obtained as a mixture of HCl and HBr salt with minimal acetate content and was used without further purification.

HR-ESI-MS: calcd. for [**112**+H]$^+$ $C_{28}H_{41}N_4O_5$ m/z= 513.3071, found m/z= 513.3071.

^{1}H-NMR (500.13 MHz, 298 K, DMSO−d_6): δ = 7.40-7.21 (m, 10 H, H_{19}, H_{20}, H_{21}, H_{24}, H_{25}, H_{26}), 4.23 (dd, $^2J_{HH}$ = 11.5 Hz, $^3J_{HH}$ = 5.7 Hz, 1 H, H_{16a}), 4.11 (dd, $^2J_{HH}$ = 11.5 Hz, $^3J_{HH}$ = 7.8 Hz, 1 H, H_{16b}), 3.92-3.82 (m, 1 H, H_{10}), 3.87 (d, $^2J_{HH}$ = 14.1 Hz, 1 H, H_{22a}), 3.72 (d, $^2J_{HH}$ = 14.1 Hz, 1 H, H_{22b}), 3.68-3.63 (m, 2 H, H_{17}), 3.50 (dd, $^3J_{HH}$ = 7.8 Hz, $^3J_{HH}$ = 5.7 Hz, 1 H, H_{14}), 3.28 (q, $^3J_{HH}$ = 7.0 Hz, 1 H, H_6), 3.22-3.13 (m, 1 H, H_2), 2.69-2.59 (m, 2 H, H_3), 2.63 (dd, $^2J_{HH}$ = 12.5 Hz, $^3J_{HH}$ = 4.9 Hz, 1 H, H_{11a}), 2.46 (dd, $^2J_{HH}$ = 12.5 Hz, $^3J_{HH}$ = 9.2 Hz, 1 H, H_{11b}), 1.97 (s, 3 H, H_{28}), 1.13 (d, $^3J_{HH}$ = 7.0 Hz, 3 H, H_8),

1.10 (d, $^3J_{HH}$ = 6.5 Hz, 3 H, H_4), 1.02 (d, $^3J_{HH}$ = 6.6 Hz, 3 H, H_{12}).

$^{13}C\{H\}$-NMR (125.77 MHz, 298 K, DMSO−d_6): δ = 172.49 (1 C, C_7), 171.55 (1 C, C_{15}), 170.02 (1 C, C_{27}), 139.29 (1 C, C_{23}), 138.85 (1 C, C_{18}), 128.35 ($C_{arom.}$), 128.47 ($C_{arom.}$), 128.31 ($C_{arom.}$), 128.15 ($C_{arom.}$), 127.15 ($C_{arom.}$), 127.00 ($C_{arom.}$), 62.09 (1 C, C_{16}), 60.41 (1 C, C_{14}), 57.57 (1 C, C_6), 56.03 (1 C, C_{11}), 55.87 (1 C, C_{22}), 55.70 (1 C, C_{17}), 53.82 (1 C, C_3), 45.26 (1 C, C_2), 43.27 (1 C, C_{10}), 20.01 (1 C, C_{28}), 18.28 (1 C, C_{12}), 16.45 (1 C, C_4), 12.76 (1 C, C_8).

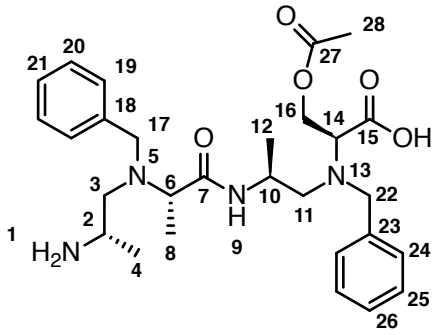

112

2-((2*S*,5*S*,8*S*,11*S*)-1,7-DIBENZYL-5,8,11-TRIMETHYL-3,9-DIOXO-1,4,7,10-TETRAAZACYCLODODECAN-2-YL)ETHYL ACETATE (**111**).

O-Acetyl-*N*-((*S*)-2-((*S*)-2-(((*S*)-2-aminopropyl)(benzyl)amino)propanamido)propyl)-*N*-benzyl-*L*-serine (**112**) salt (1.07 g, 1.40 mmol, 1.0 eq.) and *N*-ethyl diisopropylamine (1.4 mL, 8.60 mmol, 6.1 eq.) were dissolved in acetonitrile (1.0 L). Then HATU (900 mg, 2.37 mmol, 1.7 eq.) was added to the solution. After 1 h the solvent was removed under reduced pressure and the crude oil was purified by flash column chromatography (SiO_2, ethyl acetate / triethylamine (100:1)) yielding a yellowish solid (318 mg, 643 µmol, 44.8 % yield calculated over 2 steps starting from **116**).

HR-ESI-MS: calcd. for [**111**+H]$^+$ $C_{28}H_{39}N_4O_4$ m/z= 495.2966, found m/z= 495.2971.

^{1}H-NMR (400.13 MHz, 298 K, DMSO−d_6): δ = 7.90 (d, $^3J_{HH}$ = 5.3 Hz, 1 H, H_{13}), 7.68 (d, $^3J_{HH}$ = 4.1 Hz, 1 H, H_5), 7.47-7.43 (m, 2 H, H_{25}), 7.43-7.38 (m, 2 H, H_{19}), 7.37-7.24 (m, 6 H, H_{24}, H_{26}, H_{20}, H_{21}), 4.38 (dd, $^2J_{HH}$ = 11.7 Hz, $^3J_{HH}$ = 5.9 Hz, 1 H, H_{12a}), 4.32 (dd, $^2J_{HH}$ = 11.7 Hz, $^3J_{HH}$ = 7.5 Hz, 1 H, H_{12b}), 4.00 (d, $^2J_{HH}$ = 13.4 Hz, 1 H, H_{17a}), 3.93 (d, $^2J_{HH}$ = 13.4 Hz, 1 H, H_{22a}), 3.80 (d, $^2J_{HH}$ = 13.4 Hz, 1 H, H_{17b}), 3.53 (d, $^2J_{HH}$ = 13.4 Hz, 1 H, H_{22b}), 3.53-3.45 (m, 1 H, H_{14}), 3.51 (dd, $^3J_{HH}$ = 7.1 Hz, $^3J_{HH}$ = 5.9 Hz, 1 H, H_{10}), 3.24-3.15 (m, 1 H, H_6), 3.16 (q, $^3J_{HH}$ = 7.1 Hz, 1 H, H_2), 2.94

(dd, $^{2}J_{HH}$ = 13.3 Hz, $^{3}J_{HH}$ = 11.3 Hz, 1 H, H_{7a}), 2.78 (dd, $^{2}J_{HH}$ = 13.1 Hz, $^{3}J_{HH}$ = 11.3 Hz, 1 H, H_{15a}), 2.48 (dd, $^{2}J_{HH}$ = 13.3 Hz, $^{3}J_{HH}$ = 2.9 Hz, 1 H, H_{7b}), 2.29 (dd, $^{2}J_{HH}$ = 13.1 Hz, $^{3}J_{HH}$ = 2.5 Hz, 1 H, H_{15b}), 2.04 (s, 3 H, H_{28}), 1.18 (d, $^{3}J_{HH}$ = 6.5 Hz, 3 H, H_{16}), 1.11 (d, $^{3}J_{HH}$ = 6.4 Hz, 3 H, H_{8}), 1.04 (d, $^{3}J_{HH}$ = 7.1 Hz, 3 H, H_{4}).

^{13}C{H}-NMR (100.61 MHz, 298 K, DMSO−d_6): δ = 172.17 (1 C, C_3), 170.21 (1 C, C_{27}), 169.31 (1 C, C_{11}), 139.04 (1 C, C_{23}), 138.99 (1 C, C_{18}), 129.21 (2 C, C_{24}), 129.14 (2 C, C_{19}), 128.23 (2 C, C_{25}), 128.18 (2 C, C_{20}), 127.24 (1 C, C_{26}), 127.17 (1 C, C_{21}), 63.22 (1 C, C_{10}), 60.38 (1 C, C_{12}), 59.18 (1 C, C_2), 58.32 (1 C, C_{17}), 56.45 (1 C, C_{22}), 55.14 (1 C, C_7), 54.80 (1 C, C_{15}), 44.13 (1 C, C_{14}), 43.99 (1 C, C_6), 20.79 (1 C, C_{28}), 17.65 (1 C, C_{16}), 17.59 (1 C, C_8), 8.44 (1 C, C_4).

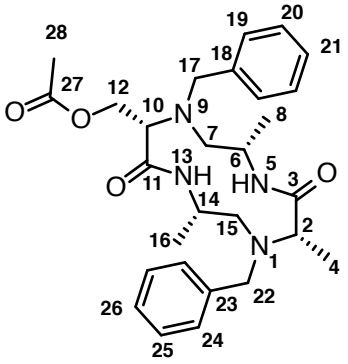

111

((2*R*,5*S*,8*S*,11*S*)-1,7-DIBENZYL-5,8,11-TRIMETHYL-1,4,7,10-TETRAAZACYCLODODECAN-2-YL)METHANOL (**119**).

((2*S*,5*S*,8*S*,11*S*)-1,7-dibenzyl-5,8,11-trimethyl-3,9-dioxo-1,4,7,10-tetraazacyclododecan-2-yl)methyl acetate (**111**) (152 mg, 307 µmol, 1.0 eq.) was dissolved in dichloromethane (15 mL) and cooled to 0-5 °C. To this solution trimethylchlorosilane (250 µL, 1.98 mmol, 6.5 eq.) was added and stirred for 30 min under an argon atmosphere. To the reaction mixture lithium aluminium hydride (2 M in tetrahydrofuran, 1.0 mL, 2.01 mmol, 6.5 eq.) was added drop wise. After 3 h additional lithium aluminium hydride (2 M in tetrahydrofuran, 1.0 mL, 2.01 mmol, 6.5 eq.) was added dropwise and the reaction mixture was stirred at 20-25 °C for 24 h. The excess of lithium aluminium hydride was quenched with aqueous potassium hydroxide (1 M, 1.0 mL). The suspension was dried with sodium sulphate, filtered and the filter cake was washed with dichloromethane (3 x 20 mL). The filtrate was evaporated to dryness yielding a yellowish solid (123 mg, 289 µmol, 94.1 %).

HR-ESI-MS: calcd. for [**119**+H]$^{+}$ $C_{26}H_{41}N_4O$ m/z= 425.3275, found m/z= 425.3279.

Proton NMR showed very broad lines at 298K. Few HMBC correlations could be obtained. Full assignment was not possible.

^{1}H-NMR (600.13 MHz, 298 K, DMSO−d_6): δ = 3.95 (d, $^{2}J_{HH}$ = 12.4 Hz, 1 H), 3.82-3.73 (m, 1 H), 3.43 (dd, $^{2}J_{HH}$ = 12.2 Hz, $^{3}J_{HH}$ = 6.7 Hz, 1 H), 3.25 (d, $^{2}J_{HH}$ = 11.1 Hz, 1 H), 3.06 (bs, 1 H), 3.01 (d, $^{2}J_{HH}$ = 11.2 Hz, 1 H), 2.93 (bs, 1 H), 2.89-2.59 (m, 1 H), 2.47 (bs, 1 H), 2.41 (bs, 1 H), 2.26 (bs, 1 H), 2.13 (bs, 1 H), 0.90 (d, $^{3}J_{HH}$ = 6.6 Hz, 1 H), 0.82 (bs, 1 H).

^{13}C{H}-NMR (150.9 MHz, 298 K, DMSO−d_6): δ = 141.03 (1 C, $C_{arom.}$), 140.90 (1 C, $C_{arom.}$), 129.75 ($C_{arom.}$), 129.49 ($C_{arom.}$), 128.59 ($C_{arom.}$), 128.58 ($C_{arom.}$), 127.25 ($C_{arom.}$), 60.06 (1 C, C_{CH}), 58.00 (1 C, C_{CH2}), 57.21 (1 C, C_{CH}), 56.56 (1 C, C_{CH2}), 53.10 (1 C, C_{CH2}), 51.42 (1 C, C_{CH2}), 49.50 (1 C, C_{CH}), 47.47 (1 C, C_{CH2}), 46.48 (1 C, C_{CH}), 46.36 (1 C, C_{CH}), 44.49 (1 C, C_{CH2}), 18.09 (1 C, C_{CH3}), 17.98 (1 C, C_{CH3}), 9.91 (1 C, C_{CH3}).

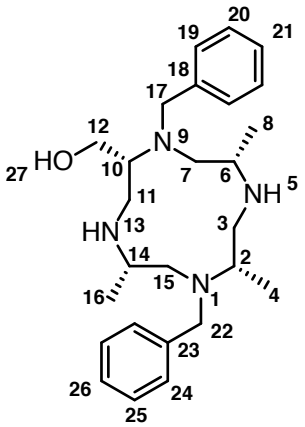

119

((2*R*,5*S*,8*S*,11*S*)-5,8,11-TRIMETHYL-1,4,7,10-TETRA-AZACYCLODODECAN-2-YL)METHANOL (**108**).

((2*R*,5*S*,8*S*,11*S*)-1,7-dibenzyl-5,8,11-trimethyl-1,4,7,10-tetraazacyclododecan-2-yl)methanol (**119**) (65.0 mg, 153 µmol, 1.0 eq.) was dissolved in methanol (2.0 mL) and trifluoroacetic acid (100 µL). Palladium on activated charcoal (moistened with water, 10 % Pd, 100 mg) was added and the suspension was hydrogenated at room temperature and 90 bar hydrogen pressure for 17 h. The suspension was filtered. The filtrate was evaporated to dryness yielding an off-white solid (32.0 mg, 131 µmol, 85.6 %).

HR-ESI-MS: calcd. for [**108**+H]$^{+}$ $C_{12}H_{29}N_4O$ m/z= 245.2336, found m/z= 245.2335.

The proton NMR spectrum is very crowded and shows the presence of multiple species. Possibly conformations, different protonation states and

remaining diastereoisomers.

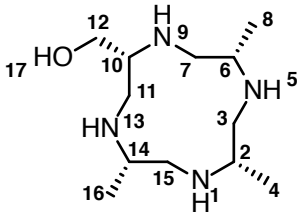

108

TRI-*tert*-BUTYL 2,2′,2′′-((2*S*,5*S*,8*S*,11*S*)-2,5,8,11-TETRAMETHYL-1,4,7,10-TETRAAZACYCLODODECANE-1,4,7-TRIYL)(2*R*,2′*R*,2′′*R*)-TRIPROPIONATE (**129**).

(2*S*,5*S*,8*S*,11*S*)-2,5,8,11-Tetramethyl-1,4,7,10-tetraazacyclododecane (**22**) (137 mg, 600 µmol, 1.0 eq.) and potassium carbonate (250 mg, 1.80 mmol, 3.0 eq.) were suspended in dichloromethane (20 mL). *tert*-Butyl (*S*)-2-((-(trifluoromethyl)sulfonyl)oxy)propanoate (500 mg, 1.80 mmol, 3.0 eq.) was dissolved in dichloromethane (6.0 mL) and was added to the reaction. The mixture was stirred for 3 h. Acetonitrile (20 mL) was added and the reaction was left stirring at 20-25 °C for 18 h. Excess tert-butyl (S)-2-(((trifluoromethyl)sulfonyl)oxy) was quenched with triethylamine (30.0 µL) and the suspension was filtered and evaporated to dryness. The crude product was purified by preparative HPLC (water / acetonitrile) yielding a white solid (330 mg, 538 µmol, 89.7 %).

ESI-MS: calcd. for [**129**+H]$^+$ $C_{33}H_{65}N_4O_6$ m/z= 613.48, found m/z= 613.70.

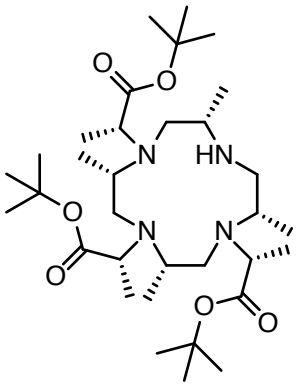

129

2-METHYL-4-(PHENYLSULFONYL)PYRIDINE (**127**).

4-Bromo-2-methylpyridine (8.60 g, 50.3 mmol, 1.0 eq.) was dissolved in dimethylformamide (30 mL). Potassium carbonate (8.42 g, 61.0 mmol,

1.2 eq.) and thiophenol (5.84 g, 53.1 mmol, 1.1 eq.) were added. The mixture was stirred at 90 °C for 22 h. The Suspension was filtered trough celite. The filtrate was split in half and one half was acidified with acetic acid (5.0 mL). Aqueous bleach (14 % Cl_2 basis, 90.0 mL) was added and the mixture was stirred at 20-25 °C until full conversion. The pH of the mixture was adjusted to 9 with aqueous sodium hydroxide and the product was extracted with dichloromethane (2x 50 mL). The combined organic layers were evaporated to dryness yielding a white solid (4.50 g, 19.3 mmol, 76.7 %).

^{1}H-NMR (500.13 MHz, 298 K, K): δ = 7.98-7.93 (m, 2 H, H_8), 7.66-7.62 (m, 2 H, H_1, H_{10}), 7.58-7.53 (m, (3 H, H_9, H_4), 2.63 (s, 3 H, H_6).

^{13}C{H}-NMR (125.77 MHz, 298 K, $CDCl_3$): δ = 160.71 (1 C, C_2), 150.56 (1 C, C_3), 149.99 (1 C, C_5), 139.92 (1 C, C_7), 134.05 (1 C, C_{10}), 129.59 (2 C, C_9), 128.10 (2 C, C_8), 120.04 (1 C, C_1), 117.71 (1 C, C_4), 24.68 (1 C, C_6).

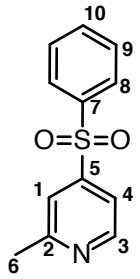

127

2-(BROMOMETHYL)-4-(PHENYLSULFONYL)PYRIDINE (**128**).

2-Methyl-4-(phenylsulfonyl) pyridine (**127**) (1.04 g, 4.46 mmol, 1.0 eq.) was dissolved in tetrachloromethane (20 mL) under an atmosphere of argon and the solution was heated to reflux. *N*-bromosuccinimide (730 mg, 4.01 mmol, 0.9 eq.) and AIBN (cat. 20.0 mg) were added in several portions over 10 h. After 10 h the reaction mixture was filtered and evaporated to dryness. The crude was purified by flash column chromatography (SiO_2, ethyl acetate / cyclohexane (1:9)) yielding a off-white solid (530 mg, 1.70 mmol, 38.0 %).

^{1}H-NMR (600.13 MHz, 298 K, $CDCl_3$): δ = 8.76 (d, $^3J_{HH}$ = 5.1 Hz, 1 H, H_3), 7.98 (m, 2 H, H_8), 7.90 (s, 1 H, H_1), 7.66 (m, 2 H, H_4, H_{10}), 7.58 (m, 2 H, H_9), 4.58 (s, 2 H, H_6).

^{13}C{H}-NMR (from HMQC, 150.95 MHz, 298 K, $CDCl_3$): δ = 151.16 (1 C, C_3), 134.34 (1 C, C_{10}), 129.91 (2 C, C_9), 128.36 (2 C, $C_{8)}$), 120.49 (1 C, C_1), 120.06 (1 C, C_4), 32.48 (1 C, C_6).

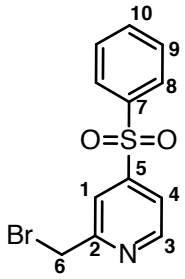

128

TRI-*tert*-BUTYL 2,2′,2′′-((2*S*,5*S*,8*S*,11*S*)-2,5,8,11-TETRAMETHYL-10-((4-(PHENYLSULFONYL)PYRIDIN-2-YL)METHYL)--1,4,7,10-TETRAAZACYCLODODECANE-1,4,7-TRIYL)(2*R*,2′*R*,2′′*R*)-TRIPROPIONATE (**131**).

Tri-*tert*-butyl 2,2',2′′-((2*S*,5*S*,8*S*,11*S*)-2,5,8,11-tetramethyl-1,4,7,10-tetraazacyclododecane-1,4,7-triyl)(2*R*,2′*R*,2′′*R*)-tripropionate (**129**) (224 mg, 365 µmol, 1.0 eq.) and potassium carbonate (100 mg, 723 µmol, 2.0 eq.) were suspended in acetonitrile (5.0 mL). To this suspension 2-(Bromomethyl)-4-(phenylsulfonyl)pyridine (**128**) (340 mg, 1.09 mmol, 2.9 eq.) was added and the mixture was stirred for 18 h at 20-25 °C. The mixture was filtered and evaporated to dryness. The residue was purified by preparative HPLC (water, acetonitrile) yielding a white solid (256 mg, 303 µmol, 82.9 %).

HR-ESI-MS: calcd. for [**131**+H]$^+$ $C_{45}H_{74}N_5O_8S$ m/z= 844.5264, found m/z= 844.5253.

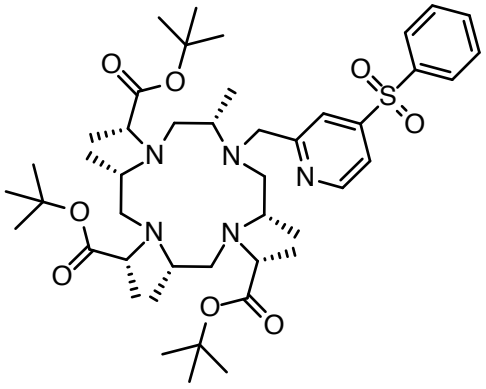

131

(2*R*,2′*R*,2″*R*)-2,2′,2″-((2*S*,5*S*,8*S*,11*S*)-2,5,8,11-TETRAMETHYL-10-((4-(PHENYLSULFONYL)PYRIDIN-2-YL)METHYL)--1,4,7,10-TETRAAZACYCLODODECANE-1,4,7-TRIYL)TRIPROPIONIC ACID (**21**).

Tri-*tert*-butyl 2,2′,2″-((2*S*,5*S*,8*S*,11*S*)-2,5,8,11-tetramethyl-10-((4-(phenylsulfonyl)pyridin-2-yl)methyl)-1,4,7,10-tetraazacyclododecane-1,4,7-triyl)-(2*R*,2′*R*,2″*R*)-tripropionate (**131**) (256 mg, 303 µmol, 1.0 eq.) was dissolved in acetonitrile (5.0 mL) and hydrochloric acid (1 M, 10.0 mL) was added. The solution was stirred at 80 °C for 4 h. The reaction mixture was concentrated and purified by preparative HPLC (water , acetonitrile) yielding a white solid (160 mg, 237 µmol, 78.2 %).

HR-ESI-MS: calcd. for [**21**+H]$^+$ $C_{33}H_{50}N_5O_8S$ m/z= 676.3375, found m/z= 676.3375.

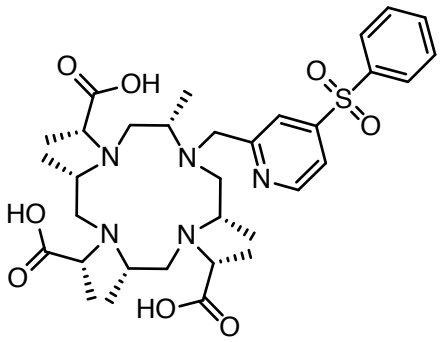

21

LU-M7-PY-SO_2-PHE-DOTA **132**.

(2*R*,2′*R*,2″*R*)-2,2′,2″-((2*S*,5*S*,8*S*,11*S*)-2,5,8,11-tetramethyl-10-((4-(phenylsulfonyl)pyridin-2-yl)methyl)-1,4,7,10-tetraazacyclododecane-1,4,7-triyl)tripropionic acid (**21**) (40.0 mg, 59.2 µmol, 1.0 eq.) was dissolved in aqueous ammonium acetate (100 mM, 5.0 mL) and $LuCl_3 \cdot 6\,H_2O$ (92.2 mg, 237 µmol, 4.0 eq.) was added. The reaction was heated to 80 °C and stirred for 18 h before purified by preparative HPLC (water, acetonitrile) yielding a white solid (38.8 mg, 45.7 µmol, 77.3 %).

HR-ESI-MS: calcd. for [**132**+H]$^+$ $C_{33}H_{47}LuN_5O_8S$ m/z= 848.2555, found m/z= 848.2548.

^{1}H-NMR (600.13 MHz, 298 K, $CDCl_3$): δ = 8.65 (d, $^3J_{HH}$ = 5.8 Hz, 1 H, H_{27}), 8.03 (m, 2 H, H_{29}), 8.02 (d, $^4J_{HH}$ = 1.5 Hz, 1 H, H_{24}), 7.99 (dd, $^3J_{HH}$ = 5.8 Hz, $^4J_{HH}$ = 1.5 Hz, 1 H, H_{26}), 7.80 (m, 1 H, H_{31}), 7.68 (m, 2 H, H_{30}), 4.57 (d, $^2J_{HH}$ = 17.9 Hz, 1 H, H_{22a}), 4.44 (d, $^2J_{HH}$ = 17.9 Hz, 1 H, H_{22b}), 3.82 (q, $^3J_{HH}$ = 7.4 Hz, 1 H, H_{17}), 3.79 (q, $^3J_{HH}$ = 7.4 Hz, 1 H, H_{20}), 3.43

(dd, $^2J_{HH}$ = 13.4 Hz, $^3J_{HH}$ = 13.4 Hz, 1 H, H_{1ax}), 3.14 (dq, $^3J_{HH}$ = 11.7 Hz, $^3J_{HH}$ = 6.6 Hz, 1 H, H_{11}), 3.08 (dq, $^3J_{HH}$ = 12.1 Hz, $^3J_{HH}$ = 6.5 Hz, 1 H, H_8), 3.06 (dd, $^2J_{HH}$ = 15.0 Hz, $^3J_{HH}$ = 11.7 Hz, 1 H, H_{10ax}), 3.02 (dd, $^2J_{HH}$ = 14.6 Hz, $^3J_{HH}$ = 13.4 Hz, 1 H, H_{7ax}), 3.00 (dd, $^2J_{HH}$ = 13.4 Hz, $^3J_{HH}$ = 13.4 Hz, 1 H, H_{4ax}), 3.00 (dq, $^3J_{HH}$ = 13.4 Hz, $^3J_{HH}$ = 6.1 Hz, 1 H, H_5), 2.84 (q, $^3J_{HH}$ = 7.4 Hz, 1 H, H_{14}), 2.81 (d, $^2J_{HH}$ = 15.0 Hz, 1 H, H_{10eq}), 2.71 (d, $^2J_{HH}$ = 14.6 Hz, 1 H, H_{7eq}), 2.62 (dq, $^3J_{HH}$ = 13.4 Hz, $^3J_{HH}$ = 6.4 Hz, 1 H, H_2), 2.61 (d, $^2J_{HH}$ = 13.4 Hz, 1 H, H_{4eq}), 2.59 (d, $^2J_{HH}$ = 13.4 Hz, 1 H, H_{1eq}), 1.46 (d, $^3J_{HH}$ = 7.5 Hz, 3 H, H_{16}), 1.44 (d, $^3J_{HH}$ = 7.5 Hz, 3 H, H_{19}), 1.25 (d, $^3J_{HH}$ = 7.1 Hz, 3 H, H_{13}), 1.19 (d, $^3J_{HH}$ = 6.6 Hz, 3 H, H_{12}), 1.17 (d, $^3J_{HH}$ = 6.5 Hz, 3 H, H_9), 1.16 (d, $^3J_{HH}$ = 6.1 Hz, 3 H, H_6), 0.97 (d, $^3J_{HH}$ = 6.4 Hz, 3 H, H_3).

$^{13}C\{H\}$-NMR (150.92 MHz, 298 K, $CDCl_3$): δ = 183.31 (1 C, C_{21}), 183.16 (1 C, C_{15}), 183.10 (1 C, C_{18}), 161.87 (1 C, C_{23}), 151.73 (1 C, C_{25}), 149.93 (1 C, C_{27}), 136.84 (1 C, C_{28}), 135.58 (1 C, C_{31}), 130.13 (2 C, C_{30}), 128.30 (2 C, C_{29}), 121.29 (1 C, C_{26}), 119.07 (1 C, C_{24}), 67.33 (1 C, C_{17}), 67.23 (1 C, C_{20}), 66.96 (1 C, C_{14}), 65.24 (1 C, C_{22}), 61.46 (1 C, C_{11}), 60.78 (1 C, C_2), 60.75 (1 C, C_8), 60.65 (1 C, C_5), 55.30 (1 C, C_1), 46.20 (1 C, C_7), 45.87 (1 C, C_4), 45.27 (1 C, C_{10}), 13.41 (1 C, C_{19}), 13.24 (2 C, C_{13}, C_{16}), 13.03 (1 C, C_6), 12.76 (1 C, C_9), 12.56 (1 C, C_3), 10.16 (1 C, C_{12}).

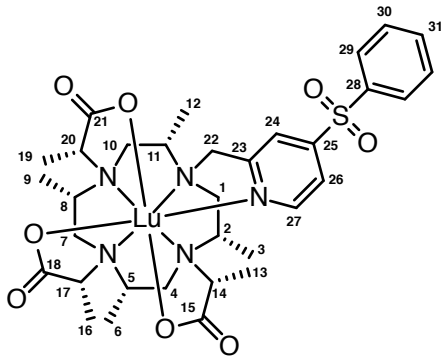

132

TM-M7-PY-SO_2-PHE-DOTA **133**.

(2*R*,2′*R*,2″*R*)-2,2′,2″-((2*S*,5*S*,8*S*,11*S*)-2,5,8,11-tetramethyl-10-((4-(phenylsulfonyl)pyridin-2-yl)methyl)-1,4,7,10-tetraazacyclododecane-1,4,7-triyl)tripropionic acid (**21**) (60.0 mg, 88.8 µmol, 1.0 eq.) was dissolved in aqueous ammonium acetate (100 mM, 5.0 mL) and $Tm(OTf)_3$ (219 mg, 355 µmol, 4.0 eq.) was added. The reaction was heated to 80 °C and stirred for 18 h before purified by preparative HPLC (water, acetonitrile) yielding a white solid (55.3 mg, 65.7 µmol, 74.0 %).

HR-ESI-MS: calcd. for [**133**+H]$^+$ $C_{33}H_{47}N_5O_8STm$ m/z= 842.2491, found m/z= 842.2482.

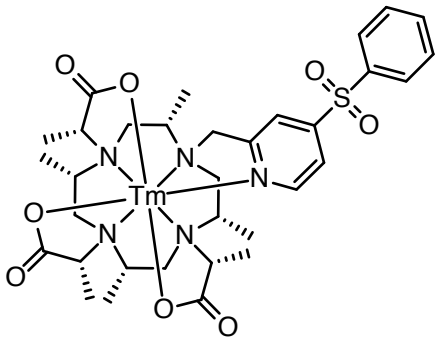

133

TB-M7-PY-SO_2-PHE-DOTA **134**.

(2*R*,2′*R*,2″*R*)-2,2′,2″-((2*S*,5*S*,8*S*,11*S*)-2,5,8,11-tetramethyl-10-((4-(phenylsulfonyl)pyridin-2-yl)methyl)-1,4,7,10-tetraazacyclododecane-1,4,7-triyl)tripropionic acid (**21**) (30.0 mg, 44.4 µmol, 1.0 eq.) was dissolved in aqueous ammonium acetate (100 mM, 5.0 mL) and $TbCl_3 \cdot 6\,H_2O$ (66.3 mg, 178 µmol, 4.0 eq.) was added. The reaction was heated to 80 °C and stirred for 18 h before purified by preparative HPLC (water, acetonitrile) yielding a white solid (31.3 mg, 37.7 µmol, 84.8 %).

HR-ESI-MS: calcd. for [**134**+H]$^+$ $C_{33}H_{47}N_5O_8STb$ m/z= 832.2395, found m/z= 832.2393.

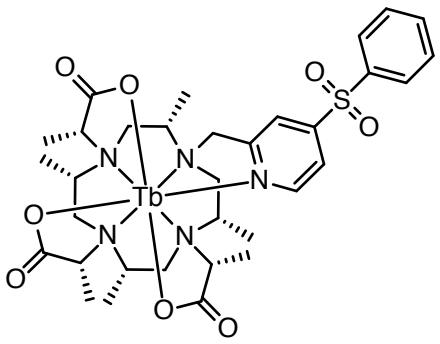

134

SM-M7-PY-SO_2-PHE-DOTA **135**.

(2*R*,2′*R*,2″*R*)-2,2′,2″-((2*S*,5*S*,8*S*,11*S*)-2,5,8,11-tetramethyl-10-((4-(phenylsulfonyl)pyridin-2-yl)methyl)-1,4,7,10-tetraazacyclododecane-1,4,7-triyl)tripropionic acid (**21**) (20.0 mg, 29.6 µmol, 1.0 eq.) was dissolved in aqueous ammonium acetate (100 mM, 5.0 mL) and $SmCl_3 \cdot 6\,H_2O$ (66.3 mg, 178 µmol,

4.0 eq.) was added. The reaction was heated to 80 °C and stirred for 18 h before purified by preparative HPLC (water, acetonitrile) yielding a white solid (24.0 mg, 29.2 µmol, 98.5 %).

HR-ESI-MS: calcd. for [**135**+H]$^+$ $C_{33}H_{47}N_5O_8SSm$ m/z= 825.2337, found m/z= 825.2332.

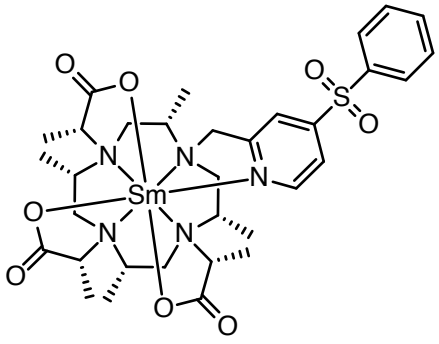

135

4-((3,5-BIS(TRIFLUOROMETHYL)PHENYL)SULFONYL)-2-METHYLPYRIDINE (**143**).

4-bromo-2-methylpyridine (710 mg, 4.13 mmol, 1.0 eq.), 3,5-Bis(trifluoromethyl) thiophenol (1.04 g, 4.13 mmol, 1.0 eq.) and potassium carbonate (680 mg, 4.96 mmol, 1.2 eq.) were suspended in dimethylformamide (10 mL). The mixture was stirred for 18 h at 80 °C. The mixture was cooled to 40 °C and acidified with acetic acid (10.0 mL). Bleach (10-15 % chlorine basis, 10 mL) was added and the mixture was stirred for 6 h. The pH was adjusted to > 10 with aqueous sodium hydroxide (4 M) and the mixture was extracted with dichloromethane (2x 15 mL). The organic layer was dried with sodium sulphate and evaporated to dryness yielding a brown oil. This brown oil was redissolved in methanol (10 mL), sodium tungstate dihydrate (608 mg, 2.07 mol, 0.5 eq.) and hydrogen peroxide (30 wt%, 2.0 mL, 5.0 eq.) was added. The mixture was stirred for 18 h at 20-25 °C. The reaction mixture was diluted with water (20 mL) and methanol was removed under reduced pressure. The product was extracted with dichloromethane (2x 20 mL). The organic layer was dried with sodium sulphate and evaporated to dryness. The crude product was purified by flash column chromatography (ethyl acetate / cyclohexane) yielding a yellowish solid (513 mg, 1.39 mmol, 33.6 %).

HR-ESI-MS: calcd. for [**143**+H]$^+$ $C_{14}H_{10}F_6NO_2S$ m/z= 370.0331, found m/z= 370.0337.

^{1}H-NMR (400.13 MHz, 298 K, $CDCl_3$): δ = 8.77 (d, $^3J_{HH}$ = 5.3 Hz, 1 H, H_3), 8.38 (bs, 2 H, H_8), 8.11 (bs, 1 H, H_{11}), 7.65 (d, $^4J_{HH}$ = 1.0 Hz, 1 H, H_1), 7.59

(dd, $^{3}J_{HH} = 5.3\,Hz$, $^{4}J_{HH} = 1.0\,Hz$, 1 H, H_4), 2.67 (s, 3 H, H_6).

$^{13}C\{H\}$-NMR (100.6 MHz, 298 K, $CDCl_3$): δ = 161.52 (1 C, C_2), 151.27 (1 C, C_3), 148.12 (1 C, C_5), 143.15 (1 C, C_7), 133.45 (q, $^{2}J_{CF} = 34.4\,Hz$, 2 C, C_9), 128.48 (2 C, C_8), 127.89 (1 C, C_{11}), 122.39 (q, $^{1}J_{CF} = 273.5\,Hz$, 2 C, C_{10}), 120.29 (1 C, C_1), 117.95 (1 C, C_4), 24.7 (1 C, C_6).

$^{19}F\{H\}$-NMR (376.5 MHz, 298 K, $CDCl_3$): δ = –62.92 (6 F, F_{10}).

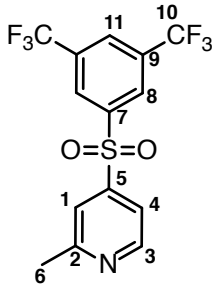

143

4-((3,5-BIS(TRIFLUOROMETHYL)PHENYL)SULFONYL)-2--(BROMOMETHYL) PYRIDINE (**140**).

4-((3,5-bis(trifluoromethyl)phenyl)sulfonyl)-2-methylpyridine (200 mg, 542 µmol, 1.0 eq.) was dissolved in carbon tetrachloride (20.0 mL) and heated to reflux. During 2.5 h *N*-bromosuccinimide (289 mg, 1.63 mmol, 3.0 eq.) and AIBN (cat. 5.0 mg) were added in small portions. The reaction was refluxed for 18 h, filtered and evaporated to dryness under vacuum at 40 °C. The crude reaction mixture was purified by flash column chromatography (pentane / methyl *tert*-butyl ether 7/3) yielding a slightly yellowish solid (64.4 mg, 117 µmol, 26.5 %).

^{1}H-NMR (600.13 MHz, 298 K, $CDCl_3$): δ = 8.85 (d, $^{3}J_{HH} = 5.0\,Hz$, 1 H, H_3), 8.41 (bs, 2 H, H_8), 8.15 (bs, 1 H, H_{11}), 7.97 (d, $^{4}J_{HH} = 1.7\,Hz$, 1 H, H_1), 7.71 (dd, $^{3}J_{HH} = 5.0\,Hz$, $^{4}J_{HH} = 1.7\,Hz$, 1 H, H_4), 4.61 (s, 2 H, H_6).

$^{13}C\{H\}$-NMR (150.9 MHz, 298 K, $CDCl_3$): δ = 159.89 (1 C, C_2), 151.68 (1 C, C_3), 149.24 (1 C, C_5), 142.80 (1 C, C_7), 133.93 (q, $^{2}J_{CF} = 35.6\,Hz$, 2 C, C_9), 128.55 (q, $^{3}J_{CF} = 3.6\,Hz$, 2 C, C_8), 128.12 (q, $^{3}J_{CF} = 3.6\,Hz$, 1 C, C_{11}), 122.19 (q, $^{1}J_{CF} = 269.9\,Hz$, 2 C, C_{10}), 120.68 (1 C, C_1), 120.18 (1 C, C_4), 32.24 (1 C, C_6).

$^{19}F\{H\}$-NMR (564.6 MHz, 298 K, $CDCl_3$): δ = –62.91 (6 F, F_{10}).

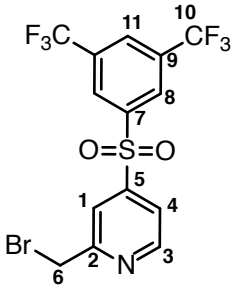

140

TRI-*tert*-BUTYL 2,2',2''-((2*S*,5*S*,8*S*,11*S*)-10-((4-((3,5-BIS-(TRIFLUOROMETHYL) PHENYL)SULFONYL)PYRIDIN-2-YL)-METHYL)-2,5,8,11-TETRAMETHYL-1,4,7,10-TETRAAZACY-CLODODECANE-1,4,7-TRIYL)(2*R*,2'*R*,2''*R*)-TRIPROPIONATE (**151**).

Tri-*tert*-butyl 2,2',2''-((2*S*,5*S*,8*S*,11*S*)-2,5,8,11-tetramethyl-1,4,7,10-tetraazacyclododecane-1,4,7-triyl)(2*R*,2'*R*,2''*R*)-tripropionate (**129**) (50.0 mg, 81.5 µmol, 1.0 eq.) and potassium carbonate (45.1 mg, 326 µmol, 4.0 eq.) were suspended in acetonitrile (6.0 mL). To this suspension 4-((3,5-bis(trifluoromethyl)phenyl)sulfonyl)-2-(bromomethyl)pyridine (**140**) (52.2 mg, 116 µmol, 1.4 eq.) was added and the mixture was stirred for 18 h at 20-25 °C. The mixture was filtered and evaporated to dryness. The residue was purified by preparative HPLC (water, acetonitrile) yielding a white solid (63.0 mg, 64.3 µmol, 78.8 %).

HR-ESI-MS: calcd. for [**151**+H]$^+$ $C_{47}H_{72}F_6N_5O_8S$ m/z= 980.5000, found m/z= 980.4989.

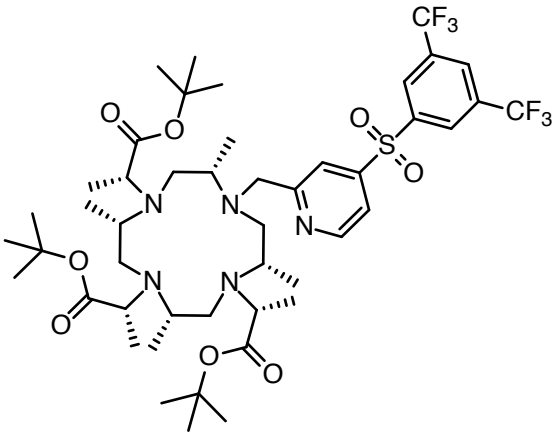

151

(2*R*,2'*R*,2''*R*)-2,2',2''-((2S,5S,8S,11S)-10-((4-((3,5-BIS (TRIFLUOROMETHYL) PHENYL)SULFONYL)PYRIDIN-2-YL) METHYL)-2,5,8,11-TETRAMETHYL-1,4,7,10-TETRAAZACYCLODODECANE-1,4,7-TRIYL) TRIPROPIONIC ACID (**152**).

Tri-*tert*-butyl 2,2',2''-((2*S*,5*S*,8*S*,11*S*)-10-((4-((3,5-bis (trifluoromethyl)-phenyl)sulfonyl)pyridin-2-yl)methyl)-2,5,8,11-tetramethyl-1,4,7,10-tetra-azacyclododecane-1,4,7-triyl)(2*R*,2'*R*,2''*R*)-tripropionate (**151**) (63.0 mg, 64.3 µmol, 1.0 eq.) was dissolved in acetonitrile (2.0 mL) and aqueous hydrochloric acid (1 M, 5.0 mL). The solution was stirred at 80 °C for 4 h. The solution was concentrated under reduced pressure at 50 °C and the residue was purified by preparative HPLC (water, acetonitrile) yielding a white solid (42.0 mg, 51.7 µmol 80.5 %).

HR-ESI-MS: calcd. for [**152**+H]$^+$ $C_{35}H_{48}F_6N_5O_8S$ m/z= 812.3122, found m/z= 812.3112.

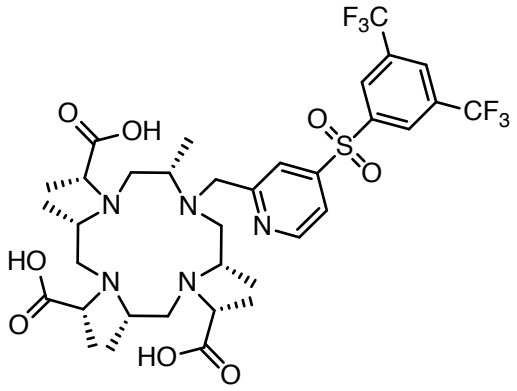

152

LU-DOTA-M7-PY-SO_2-BIS-CF_3-PHE **150**.

To a solution of (2*R*,2'*R*,2''*R*)-2,2',2''-((2S,5S,8S,11S)-10-((4-((3,5-bis(trifluoromethyl)phenyl)sulfonyl)pyridin-2-yl)methyl)-2,5,8,11-tetramethyl-1,4,7,10-tetraazacyclododecane-1,4,7-triyl) tripropionic acid (**152**) (20.0 mg, 24.6 µmol, 1.0 eq.) in aqueous ammonium acetate (100 mM, 10 mL) was added $Lu(OTf)_3$ (61.2 mg, 98.5 µmol, 4.0 eq.). The mixture was stirred at 80 °C for 18 h before purified by preparative HPLC (water, acetonitrile) yielding a white solid (17.2 mg, 17.5 µmol, 71.1 %).

HR-ESI-MS: calcd. for [**150**+H]$^+$ $C_{35}H_{45}F_6LuN_5O_8S$ m/z= 984.2295, found m/z= 984.2294.

^{1}H-NMR (600.13 MHz, 298 K, CD_3CN): δ = 8.98 (bs, 1 H, H_{26}), 8.56 (bs, 2 H, H_{29}), 8.37 (bs, 1 H, H_{31}), 8.20 (bs, 1 H, H_{27}), 7.76 (bs, 1 H, H_{24}), 4.56 (d, $^2J_{HH}$ = 17.5 Hz, 1 H, H_{22a}), 4.36 (d, $^2J_{HH}$ = 17.5 Hz, 1 H, H_{22b}), 3.90

(q, $^3J_{HH}$ = 7.2 Hz, 1 H, H_{17}), 3.73 (q, $^3J_{HH}$ = 7.0 Hz, 1 H, H_{20}), 3.32 (dd, $^2J_{HH}$ = 16.2 Hz, $^3J_{HH}$ = 12.3 Hz, 1 H, H_{1ax}), 3.28-3.16 (m, 2 H, H_{11}, H_8), 3.11-2.90 (m, 5 H, H_{14}, H_5, H_{7ax}, H_{4ax}, H_{10ax}), 2.83 (d, $^2J_{HH}$ = 14.8 Hz, 1 H, H_{10eq}), 2.75-2.50 (m, 4 H, H_2, H_{1eq}, H_{4eq}, H_{7eq}), 1.54 (d, $^3J_{HH}$ = 7.2 Hz, 3 H, H_{16}), 1.49 (d, $^3J_{HH}$ = 7.0 Hz, 3 H, H_{19}), 1.26 (d, $^3J_{HH}$ = 6.8 Hz, 3 H, H_{12}), 1.25 (d, $^3J_{HH}$ = 7.2 Hz, 3 H, H_{13}), 1.18 (d, $^3J_{HH}$ = 6.3 Hz, 3 H, H_9), 1.15 (d, $^3J_{HH}$ = 5.3 Hz, 3 H, H_6), 0.98 (d, $^3J_{HH}$ = 6.3 Hz, 3 H, H_3).

^{13}C{H}-NMR (150.92 MHz, 298 K, CD_3CN): δ = 187.35 (1 C, C_{18}), 185.42 (1 C, C_{15}), 179.53 (1 C, C_{21}), 162.10 (1 C, C_{23}), 151.91 (1 C, C_{25}), 150.04 (1 C, C_{27}), 142.34 (1 C, C_{28}), 133.65 (q, $^2J_{CF}$ = 34.3 Hz, 2 C, C_{30}), 130.53 (2 C, C_{29}), 129.88 (1 C, C_{31}), 125.41 (1 C, C_{26}), 123.66 (q, $^1J_{CF}$ = 274.0 Hz, 2 C, C_{32}), 120.41 (1 C, C_{24}), 68.93 (1 C, C_{20}), 67.57 (1 C, C_{17}), 66.73 (1 C, C_{14}), 66.52 (1 C, C_{22}), 63.00 (1 C, C_{11}), 62.47 (1 C, C_5), 61.52 (1 C, C_8), 61.47 (1 C, C_2), 56.28 (1 C, C_1), 47.60 (1 C, C_7), 46.70 (1 C, C_4), 46.32 (1 C, C_{10}), 14.69 (1 C, C_{16}), 14.43 (1 C, C_6), 14.14 (1 C, C_{19}), 13.83 (1 C, C_9), 13.72 (1 C, C_3), 13.66 (1 C, C_{13}), 11.60 (1 C, C_{12}).

^{19}F{H}-NMR (564.6 MHz, 298 K, CD_3CN): δ = −63.07 (6 F, F_{32}).

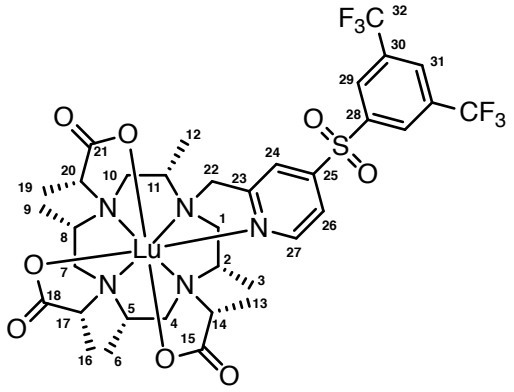

150

TM-DOTA-M7-PY-SO_2-BIS-CF_3-PHE **149**.

To a solution of (2*R*,2'*R*,2''*R*)-2,2',2''-((2S,5S,8S,11S)-10-((4-((3,5-bis(trifluoromethyl)phenyl)sulfonyl)pyridin-2-yl)methyl)-2,5,8,11-tetramethyl-1,4,7,10-tetraazacyclododecane-1,4,7-triyl) tripropionic acid (**152**) (20.0 mg, 24.6 µmol, 1.0 eq.) in aqueous ammonium acetate (100 mM, 10 mL) was added $Tm(OTf)_3$ (60.6 mg, 98.5 µmol, 4.0 eq.). The mixture was stirred at 80 °C for 18 h before purified by preparative HPLC (water, acetonitrile) yielding a white solid (13.4 mg, 13.7 µmol, 52.3 %).

HR-ESI-MS: calcd. for [**149**+H]$^+$ $C_{35}H_{45}F_6N_5O_8STm$ m/z= 978.2230, found m/z= 978.2225.

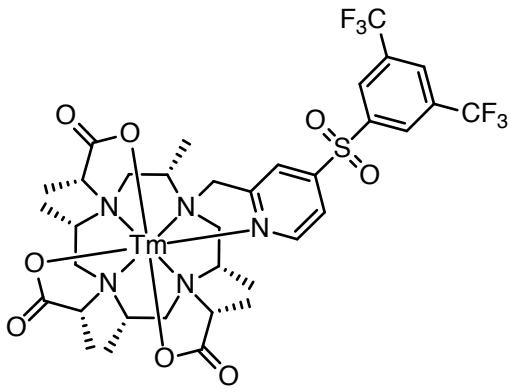

149

2-METHYL-4-((4-(TRIFLUOROMETHYL)PHENYL)SULFONYL) PYRIDINE (**142**).

4-bromo-2-methylpyridine (980 mg, 5.67 mmol, 1.0 eq.), 4-(trifluoromethyl)-benzenethiol (1.00 g, 5.61 mmol, 1.0 eq.) and potassium carbonate (930 mg, 6.73 mmol, 1.2 eq.) were suspended in acetonitrile (50 mL) and stirred at 65 °C for 18 h. The reaction mixture was filtered over celite and evaporated to dryness. The residue was dissolved in methanol (40.0 mL) and water (5.0 mL). Sodium tungstate dihydrate (930 g, 2.81 mmol, 0.5 eq.) and aqueous hydrogen peroxide (30 wt%, 1.3 mL, 11.2 mmol, 2.0 eq.) were added. The mixture was stirred at 20-25 °C for 18 h. Water (50.0 mL) was added and methanol was removed under reduced pressure. The product was extracted with dichloromethane (2x 50.0 mL). The organic layers were combined, dried with sodium sulphate and evaporated to dryness. The crude product was purified by flash column chromatography (pentane / methyl *tert*-butyl ether 5/5) yielding a yellowish solid (640 mg, 2.15 mmol, 37.9 %).

HR-ESI-MS: calcd. for [**142**+H]$^+$ $C_{13}H_{11}F_3NO_2S$ m/z= 302.0457, found m/z= 302.0453.

^{1}H-NMR (600.13 MHz, 298 K, $CDCl_3$): δ = 8.73 (d, $^3J_{HH}$ = 5.1 Hz, 1 H, H_3), 8.09 (d, $^3J_{HH}$ = 8.2 Hz, 2 H, H_8), 7.82 (d, $^3J_{HH}$ = 8.2 Hz, 2 H, H_9), 7.63 (d, $^4J_{HH}$ = 1.4 Hz, 1 H, H_1), 7.57 (dd, $^3J_{HH}$ = 5.1 Hz, $^4J_{HH}$ = 1.4 Hz, 1 H, H_4), 2.66 (s, 3 H, H_6).

^{13}C{H}-NMR (150.9 MHz, 298 K, $CDCl_3$): δ = 161.22 (1 C, C_2), 151.07 (1 C, C_3), 149.11 (1 C, C_5), 143.70 (1 C, C_7), 135.84 (q, $^2J_{CF}$ = 33.3 Hz, 1 C, C_{11}), 128.82 (2 C, C_8), 126.89 (q, $^3J_{CF}$ = 3.7 Hz, 2 C, C_9), 123.08 (q, $^1J_{CF}$ = 273.6 Hz, 1 C, C_{10}), 120.29 (1 C, C_1), 117.92 (1 C, C_4), 24.86 (1 C, C_6).

^{19}F{H}-NMR (564.6 MHz, 298 K, $CDCl_3$): δ = –63.29 (3 F, F_{10}).

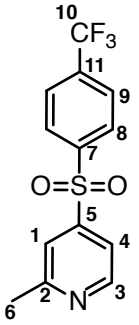

142

2-(BROMOMETHYL)-4-((4-(TRIFLUOROMETHYL)PHENYL)-SULFONYL)PYRIDINE (**139**).

2-methyl-4-((4-(trifluoromethyl)phenyl)sulfonyl)pyridine (**142**) (200 mg, 664 µmol, 1.0 eq.) was dissolved in carbon tetrachloride (20 mL) and heated to reflux. During 5 h *N*-bromosuccinimide (380 mg, 2.14 mmol, 3.2 eq.) and AIBN (cat. 5.0 mg) were added in small portions. The reaction was refluxed for 18 h, filtered and evaporated to dryness under vacuum at 40 °C. The crude reaction mixture was purified by flash chromatography (pentane / methyl tert-butyl ether 7/3) yielding a yellowish wax (58.1 mg, 153 µmol, 23.2 %).

^{1}H-NMR (600.13 MHz, 298 K, $CDCl_3$): δ = 8.80 (dd, $^{3}J_{HH}$ = 5.1 Hz, $^{5}J_{HH}$ = 0.7 Hz, 1 H, H_3), 8.10 (d, $^{3}J_{HH}$ = 8.4 Hz, 2 H, H_8), 7.94 (dd, $^{4}J_{HH}$ = 1.7 Hz, $^{5}J_{HH}$ = 0.7 Hz, 1 H, H_1), 7.84 (d, $^{3}J_{HH}$ = 8.4 Hz, 2 H, H_9), 7.68 (dd, $^{3}J_{HH}$ = 5.1 Hz, $^{4}J_{HH}$ = 1.7 Hz, 1 H, H_4), 4.59 (s, 2 H, H_6).

^{13}C{H}-NMR (150.9 MHz, 298 K, $CDCl_3$): δ = 159.47 (1 C, C_2), 151.38 (1 C, C_3), 150.14 (1 C, C_5), 143.34 (1 C, C_7), 136.11 (q, $^{2}J_{CF}$ = 33.1 Hz, 1 C, C_{11}), 128.93 (2 C, C_8), 127.05 (q, $^{3}J_{CF}$ = 3.7 Hz, 2 C, C_9), 123.07 (q, $^{1}J_{CF}$ = 274.4 Hz, 1 C, C_{10}), 120.61 (1 C, C_1), 120.15 (1 C, C_4), 32.45 (1 C, C_6).

^{19}F{H}-NMR (564.6 MHz, 298 K, $CDCl_3$): δ = −63.31 (3 F, F_{10}).

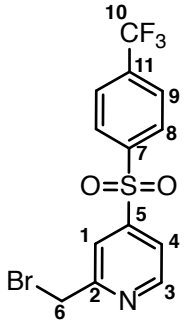

139

TRI-*tert*-BUTYL 2,2′,2″-((2*S*,5*S*,8*S*,11*S*)-2,5,8,11-TETRAMETHYL-10-((4-((4-(TRIFLUOROMETHYL)PHENYL)SULFONYL)PYRIDIN-2-YL)METHYL)-1,4,7,10-TETRAAZACYCLODODECANE-1,4,7-TRIYL)(2*R*,2′*R*,2″*R*)-TRIPROPIONATE (**147**).

Tri-*tert*-butyl 2,2',2″-((2*S*,5*S*,8*S*,11*S*)-2,5,8,11-tetramethyl-1,4,7,10-tetraazacyclododecane-1,4,7-triyl)(2*R*,2′*R*,2″*R*)-tripropionate (**129**) (100 mg, 163 µmol, 1.0 eq.) and potassium carbonate (90.1 mg, 651 µmol, 4.0 eq.) were suspended in acetonitrile (5.0 mL). To this suspension 2-(bromomethyl)--4-((4-(trifluoromethyl)phenyl)sulfonyl)pyridine (**139**) (74.4 mg, 196 µmol, 1.2 eq.) was added and the mixture was stirred for 18 h at 20-25 °C. The mixture was filtered and evaporated to dryness. The residue was purified by preparative HPLC (water, acetonitrile) yielding a white solid (70.0 mg, 76.7 µmol, 47.1 %).

HR-ESI-MS: calcd. for [**147**+H]$^+$ $C_{46}H_{73}F_3N_5O_8S$ m/z= 912.5126, found m/z= 912.5116.

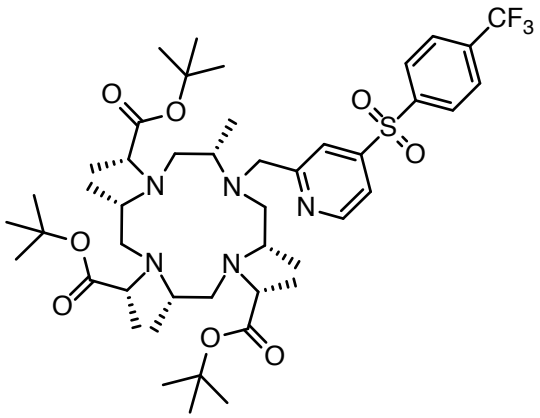

147

(2*R*,2′*R*,2″*R*)-2,2′,2″-((2*S*,5*S*,8*S*,11*S*)-2,5,8,11-TETRAMETHYL-10-((4-((4-(TRIFLUOROMETHYL)PHENYL)SULFONYL)PYRIDIN-2-YL)METHYL)-1,4,7,10-TETRAAZACYCLODODECANE-1,4,7-TRIYL)TRIPROPIONIC ACID (**148**).

Tri-*tert*-butyl 2,2′,2″-((2*S*,5*S*,8*S*,11*S*)-2,5,8,11-tetramethyl-10-((4-((4-(trifluoromethyl)phenyl)sulfonyl)pyridin-2-yl)methyl)-1,4,7,10-tetraazacyclododecane-1,4,7-triyl)(2*R*,2′*R*,2″*R*)-tripropionate (70.0 mg, 76.7 µmol, 1.0 eq.) was dissolved in acetontirile (2.0 mL) and hydrochloric acid (1 M, 5.0 mL). The solution was stirred at 80 °C for 4 h. The solution was concentrated under reduced pressure at 50 °C and the residue was purified by preparative HPLC (water, acetonitrile) yielding a white solid (40.0 mg, 53.7 µmol 70.1 %).

HR-ESI-MS: calcd. for [**148**+H]$^+$ $C_{34}H_{49}F_3N_5O_8S$ m/z= 744.3248, found m/z= 744.3243.

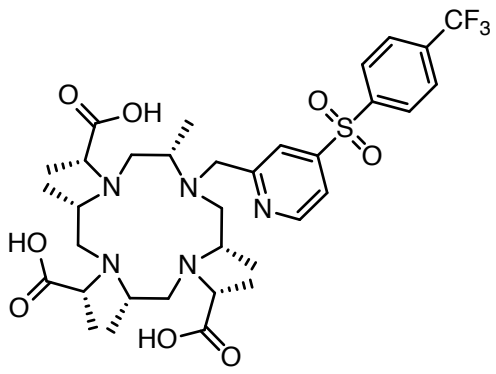

148

LU-DOTA-M7-PY-SO_2-MONO-CF_3-PHE **146**.

To a solution of (2*R*,2′*R*,2″*R*)-2,2′,2″-((2*S*,5*S*,8*S*,11*S*)-2,5,8,11-tetramethyl-10-((4-((4-(trifluoromethyl)phenyl)sulfonyl)pyridin-2-yl)methyl)-1,4,7,10-tetraazacyclododecane-1,4,7-triyl)tripropionic acid (**148**) (20.0 mg, 26.9 µmol, 1.0 eq.) in aqueous ammonium acetate (100 mM, 10 mL) was added $Lu(OTf)_3$ (66.9 mg, 108 µmol, 4.0 eq.). The mixture was stirred at 80 °C for 18 h before purified by preparative HPLC (water, acetonitrile) yielding a white solid (17.2 mg, 18.8 µmol, 71.1 %).

HR-ESI-MS: calcd. for [**146**+H]$^+$ $C_{34}H_{46}F_3LuN_5O_8S$ m/z= 916.2421, found m/z= 916.2417.

^{1}H-NMR (600.13 MHz, 298 K, CD_3CN): δ = 8.90 (bs, 1 H, H_{26}), 8.20 (d, $^3J_{HH}$ = 8.3 Hz, 2 H, H_{29}), 8.17 (bs, 1 H, H_{27}), 7.53 (bs, 1 H, H_{24}), 7.96 (d, $^3J_{HH}$ = 8.3 Hz, 2 H, H_{30}), 4.52 (d, $^2J_{HH}$ = 17.5 Hz, 1 H, H_{22a}), 4.15 (d, $^2J_{HH}$ = 17.5 Hz, 1 H, H_{22b}), 3.87 (q, $^3J_{HH}$ = 6.2 Hz, 1 H, H_{17}), 3.76 (q, $^3J_{HH}$ = 7.0 Hz, 1 H, H_{20}), 3.36 (dd, $^2J_{HH}$ = 15.8 Hz, $^3J_{HH}$ = 12.3 Hz, 1 H, H_{1ax}), 3.28-3.16 (m, 2 H, H_{11}, H_8), 3.12-2.88 (m, 5 H, H_{14}, H_5, H_{7ax}, H_{4ax}, H_{10ax}), 2.83 (d, $^2J_{HH}$ = 14.5 Hz, 1 H, H_{10eq}), 2.69-2.49 (m, 4 H, H_2, H_{1eq}, H_{4eq}, H_{7eq}), 1.54 (d, $^3J_{HH}$ = 6.2 Hz, 6 H, H_{19}, H_{16}), 1.25 (d, $^3J_{HH}$ = 6.1 Hz, 3 H, H_{12}), 1.24 (d, $^3J_{HH}$ = 6.1 Hz, 3 H, H_{13}), 1.19 (d, $^3J_{HH}$ = 6.0 Hz, 3 H, H_9), 1.15 (d, $^3J_{HH}$ = 6.3 Hz, 3 H, H_6), 0.96 (d, $^3J_{HH}$ = 6.2 Hz, 3 H, H_3).

^{13}C{H}-NMR (150.92 MHz, 298 K, CD_3CN): δ = 187.36 (1 C, C_{18}), 185.48 (1 C, C_{15}), 179.71 (1 C, C_{21}), 161.60 (1 C, C_{23}), 152.61 (1 C, C_{25}), 150.10 (1 C, C_{27}), 143.25 (1 C, C_{28}), 136.12 (q, $^2J_{CF}$ = 33.3 Hz, 1 C, C_{31}), 130.96 (2 C, C_{29}), 127.87 (q, $^3J_{CF}$ = 3.2 Hz, 2 C, C_{30}), 125.37 (1 C, C_{26}), 124.49 (q, $^1J_{CF}$ = 273.0 Hz, 1 C, C_{32}), 119.43 (1 C, C_{24}), 68.87 (1 C, C_{20}), 67.61 (1 C, C_{17}), 66.49 (1 C, C_{14}), 66.43 (1 C, C_{22}), 63.20 (1 C, C_{11}), 62.45 (1 C, C_5), 61.58 (1 C, C_8), 61.21 (1 C, C_2), 56.23 (1 C, C_1), 47.64 (1 C, C_7), 46.79 (1

C, C_4), 46.44 (1 C, C_{10}), 14.65 (1 C, C_{16}), 14.49 (1 C, C_6), 14.31 (1 C, C_{19}), 13.86 (1 C, C_9), 13.72 (1 C, C_3), 13.60 (1 C, C_{13}), 11.68 (1 C, C_{12}).

^{19}F{H}-NMR (564.6 MHz, 298 K, CD_3CN): $\delta = -63.40$ (3 F, F_{32}).

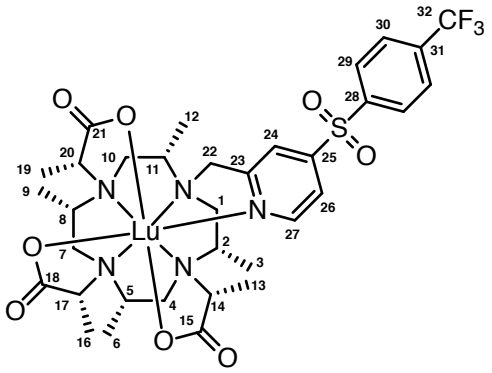

146

TM-DOTA-M7-PY-SO_2-MONO-CF_3-PHE **145**.

To a solution of (2*R*,2′*R*,2″*R*)-2,2′,2″-((2*S*,5*S*,8*S*,11*S*)-2,5,8,11-tetramethyl-10-((4-((4-(trifluoromethyl)phenyl)sulfonyl)pyridin-2-yl)methyl)-1,4,7,10-tetraazacyclododecane-1,4,7-triyl)tripropionic acid (**148**) (20.0 mg, 26.9 µmol, 1.0 eq.) in aqueous ammonium acetate (100 mM, 10 mL) was added $Tm(OTf)_3$ (66.3 mg, 108 µmol, 4.0 eq.). The mixture was stirred at 80 °C for 18 h before purified by preparative HPLC (water, acetonitrile) yielding a white solid (14.9 mg, 16.4 µmol, 60.9 %).

HR-ESI-MS: calcd. for [**145**+H]$^+$ $C_{34}H_{46}F_3N_5O_8STm$ m/z= 910.2356, found m/z= 910.2363.

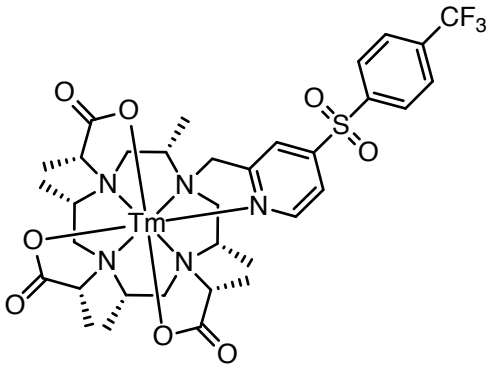

145

5-FLUORO-2-METHYL-4-(PHENYLSULFONYL)PYRIDINE (**156**).

Potassium carbonate (180 mg, 1.33 mmol, 1.2 eq.) was suspended in dimethylformamide (3.0 mL) and 4-bromo-5-fluoro-2-methyl pyridine (211 mg, 1.11 mmol, 1.0 eq.) was added followed by thiophenol (103 µL, 1.00 mmol, 0.9 eq.). The resulting white suspension was stirred at 70 °C for 1 h. The reaction mixture was concentrated under reduced pressure at 50 °C to give a white solid, which was dissolved in dichloromethane (10 mL) and washed with water (5.00 mL). The organic layer was dried over sodium sulphate, filtered and evaporated to dryness yielding a yellow oil (220 mg, 93.0 % crude yield). The crude product was dissolved in methanol (5.0 mL), sodium tungstate dihydrate (82.5 mg, 250 µmol, 0.3 eq.) and aqueous hydrogen peroxide (300 µL, 30 %, 10.6 mmol, 11 eq.) were added. The reaction mixture was stirred at 20-25 °C for 16 h. LC-MS showed incomplete conversion therefore, additional sodium tungstate dihydrate (58.0 mg, 175 µmol, 0.2 eq.) and aqueous hydrogen peroxide (900 µL, 30 %, 31.8 mmol, 30 eq.) were added. The mixture was left stirring at 20-25 °C for another 24 h. After completion, the reaction was diluted with water (5.0 mL) and methanol was removed under reduced pressure at 40 °C. The aqueous heterogeneous mixture was extracted with ethyl acetate (2x 15 mL). The combined organic layers were washed with water (10 mL), brine (10 mL), dried over sodium sulphate, filtered and evaporated to dryness yielding a white solid (248 mg, 998 µmol, 90.7 %).

HR-ESI-MS: calcd. for [**156**+H]$^+$ $C_{12}H_{10}FNO_2S$ m/z= 252.0489, found m/z= 252.0492.

^{1}H-NMR (600.13 MHz, 298 K, $CDCl_3$): δ = 8.42 (d, $^3J_{HF}$ = 1.0 Hz, 1 H, H_3), 8.03 (d, $^3J_{HH}$ = 8.5 Hz, 2 H, H_8), 7.78 (d, $^4J_{HF}$ = 5.4 Hz, 1 H, H_1), 7.68 (ddd, $^3J_{HH}$ = 8.5 Hz, $^3J_{HH}$ = 7.4 Hz, $^4J_{HH}$ = 1.7 Hz, 2 H, H_9), 7.58 (ddd, $^3J_{HH}$ = 7.5 Hz, $^3J_{HH}$ = 7.4 Hz, $^4J_{HH}$ = 1.2 Hz, 2 H, H_{10}), 2.64 (d, $^4J_{HH}$ = 1.0 Hz, 3 H, H_6).

^{13}C{H}-NMR (150.92 MHz, 298 K, $CDCl_3$): δ = 156.17 (1 C, C_1), 152.83 (1 C, C_4), 139.51 (1 C, C_7), 139.34 (1 C, C_5), 136.62 (1 C, C_3), 134.50 (1 C, C_{10}), 129.44 (2 C, C_9), 128.56 (2 C, C_8), 121.16 (1 C, C_2), 23.91 (1 C, C_6).

^{19}F{H}-NMR (564.6 MHz, 298 K, $CDCl_3$): δ = −129.49 (1 F, F_4).

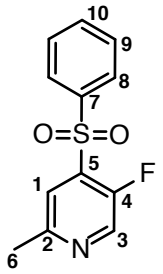

156

2-(BROMOMETHYL)-5-FLUORO-4-(PHENYLSULFONYL)PYRIDINE (**154**).

5-Fluoro-2-methyl-4-(phenylsulfonyl) pyridine (**156**) (230 mg, 91.7 µmol, 1.0 eq.) was dissolved in tetrachloromethane (20.0 mL) under an atmosphere of argon and the solution was refluxed. *N*-bromosuccinimide (330 mg, 1.83 mmol, 2.0 eq.) and AIBN (cat. 2.0 mg) were added in five portions over 4 h. After 6 h the reaction mixture was filtered and evaporated to dryness. The crude was immediately purified by flash column chromatography (SiO_2, ethyl acetate / cyclohexane (1:9)) yielding a colourless oil (82.5 mg, 248 µmol, 27.0 %).

HR-ESI-MS: calcd. for [**154**+H]$^+$ $C_{12}H_9BrFNO_2S$ m/z= 329.9594, found m/z= 329.9596.

^{1}H-NMR (600.13 MHz, 298 K, $CDCl_3$): δ = 8.49 (d, $^3J_{HF}$ = 1.2 Hz, 1 H, H_3), 8.07 (d, $^4J_{HF}$ = Hz, 2 H, H_1), 8.04 (d, $^3J_{HH}$ = 8.7 Hz, $^4J_{HH}$ = 1.3 Hz, 1 H, H_8), 7.70 (dddd, $^3J_{HH}$ = Hz, $^3J_{HH}$ = 7.1 Hz, $^4J_{HH}$ = 2.2 Hz, $^4J_{HH}$ = 1.0 Hz, 1 H, H_{10}), 7.60 (m, 2 H, H_9), 4.59 (s, 2 H, H_6).

^{13}C{H}-NMR (150.92 MHz, 298 K, $CDCl_3$): δ = 154.74 (1 C, C_1), 153.93 (1 C, C_4), 140.30 (1 C, C_7), 139.28 (1 C, C_5), 137.76 (1 C, C_3), 134.96 (1 C, C_{10}), 129.77 (2 C, C_9), 128.89 (2 C, C_8), 122.15 (1 C, C_2), 31.93 (1 C, C_6).

^{19}F{H}-NMR (564.6 MHz, 298 K, $CDCl_3$): δ = −124.34 (1 F, F_4).

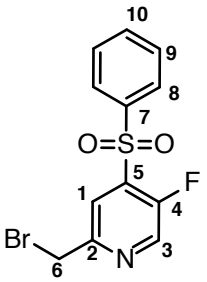

154

TRI-*tert*-BUTYL 2,2′,2″-((2*S*,5*S*,8*S*,11*S*)-10-((5-FLUORO-4--(PHENYLSULFONYL)PYRIDIN-2-YL)METHYL)-2,5,8,11-TETRAMETHYL-1,4,7,10-TETRAAZACYCLODODECANE-1,4,7-TRIYL) (2*R*,2′*R*,2″*R*)-TRIPROPIONATE (**160**).

Tri-*tert*-butyl 2,2',2″-((2*S*,5*S*,8*S*,11*S*)-2,5,8,11-tetramethyl-1,4,7,10-tetraazacyclododecane-1,4,7-triyl)(2*R*,2′*R*,2″*R*)-tripropionate (**129**) (100 mg, 163 µmol, 1.0 eq.) and potassium carbonate (45.1 mg, 326 µmol, 2.0 eq.) were suspended in acetonitrile (3.0 mL). To this suspension 2-(bromomethyl)-5-fluoro-4-(phenylsulfonyl)pyridine (**154**) (56.5 mg, 171 µmol, 1.1 eq.) was added and the mixture was stirred at 20-25 °C for 18 h. The mixture was filtered, washed with acetonitrile (2.0 mL) and evaporated to dryness. The residue was purified by preparative HPLC (water, acetonitrile) yielding a white solid (85.0 mg, 98.5 µmol, 60.5 %).

HR-ESI-MS: calcd. for [**160**+H]$^+$ $C_{45}H_{73}FN_5O_8S$ m/z= 862.5158, found m/z= 862.5161.

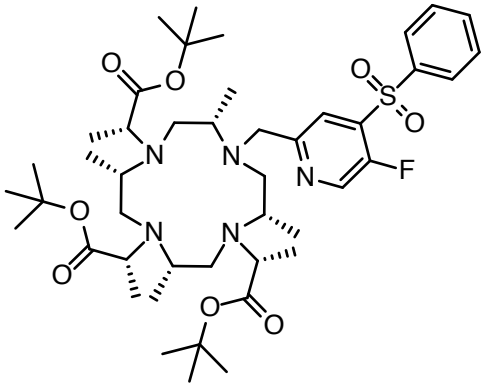

160

(2*R*,2′*R*,2″*R*)-2,2′,2″-((2*S*,5*S*,8*S*,11*S*)-10-((5-FLUORO-4--(PHENYLSULFONYL)PYRIDIN-2-YL)METHYL)-2,5,8,11-TETRAMETHYL-1,4,7,10-TETRAAZACYCLODODECANE-1,4,7-TRIYL)TRIPROPIONIC ACID (**161**).

Tri-*tert*-butyl 2,2′,2″-((2*S*,5*S*,8*S*,11*S*)-10-((5-fluoro-4-(phenylsulfonyl)pyridin-2-yl)methyl)-2,5,8,11-tetramethyl-1,4,7,10-tetraazacyclododecane-1,4,7-triyl) (2*R*,2′*R*,2″*R*)-tripropionate (**160**) (85.0 mg, 98.5 µmol, 1.0 h) was dissolved in acetonitrile (5.0 mL) and hydrochloric acid (1 M, 10.0 mL) was added. The yellow solution was stirred at 65 °C for 2 h. The reaction mixture was concentrated and purified by preparative HPLC (water, acetonitrile) yielding a white solid (51.0 mg, 73.5 µmol, 74.6 %).

HR-ESI-MS: calcd. for [**161**+H]$^+$ $C_{33}H_{49}FN_5O_8S$ m/z= 694.3280, found m/z= 694.3287.

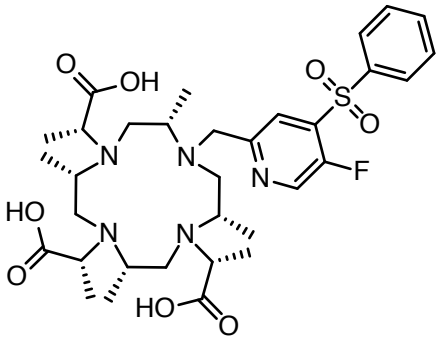

161

LU-M7-FPY-SO_2-PHE-DOTA **159**.

(2*R*,2′*R*,2″*R*)-2,2′,2″-((2*S*,5*S*,8*S*,11*S*)-10-((5-fluoro-4-(phenylsulfonyl)pyridin-2-yl)methyl)-2,5,8,11-tetramethyl-1,4,7,10-tetraazacyclododecane-1,4,7-triyl)tripropionic acid (**161**) (9.8 mg, 14.1 µmol, 1.0 eq.) was dissolved in aqueous ammonium acetate (100 mM, 5.0 mL) and Lu(OTf_3) (17.9 mg, 28.2 µmol, 2.0 eq.) was added. The reaction was heated to 80 °C and stirred for 18 h before purified by preparative HPLC (water, acetonitrile) yielding a white solid (7.9 mg, 9.12 µmol, 64.7 %).

HR-ESI-MS: calcd. for [**159**+H]$^+$ $C_{33}H_{45}FLuN_5O_8S$ m/z= 866.2453, found m/z= 866.2444.

^{1}H-NMR (600.13 MHz, 298 K, D_2O): δ = 8.46 (d, $^3J_{HF}$ = 2.6 Hz, 1 H, H_{27}), 8.15 (d, $^4J_{HF}$ = 5.5 Hz, 1 H, H_{24}), 8.07 (d, $^3J_{HH}$ = 7.9 Hz, 2 H, H_{29}), 7.85-7.81 (m, 1 H, H_{31}), 7.72-7.67 (m, 2 H, H_{30}), 4.65 (d, $^2J_{HH}$ = 17.9 Hz, 1 H, H_{22a}), 4.45 (d, $^2J_{HH}$ = 17.9 Hz, 1 H, H_{22b}), 3.81 (q, $^3J_{HH}$ = 7.2 Hz, 1 H, H_{17}), 3.80 (q, $^3J_{HH}$ = 7.2 Hz, 1 H, H_{20}), 3.45 (dd, $^2J_{HH}$ = 15.0 Hz, $^3J_{HH}$ = 12.3 Hz, 1 H, H_{1ax}), 3.20-3.12 (m, 1 H, H_{11}), 3.12-2.99 (m, 5 H, H_5, H_8, H_{4ax}, H_{7ax}, H_{10ax}), 2.97 (q, $^3J_{HH}$ = 7.2 Hz, 1 H, H_{14}), 2.84 (d, $^2J_{HH}$ = 14.8 Hz, 1 H, H_{10eq}), 2.73-2.68 (m, 1 H, H_2), 2.72 (d, $^2J_{HH}$ = 14.5 Hz, 1 H, H_{7eq}), 2.66-2.60 (m, 2 H, H_{4eq}, H_{1eq}), 1.46 (d, $^3J_{HH}$ = 7.2 Hz, 3 H, H_{16}), 1.45 (d, $^3J_{HH}$ = 7.2 Hz, 3 H, H_{19}), 1.29 (d, $^3J_{HH}$ = 7.0 Hz, 3 H, H_{13}), 1.22 (d, $^3J_{HH}$ = 6.6 Hz, 3 H, H_{12}), 1.19 (d, $^3J_{HH}$ = 6.6 Hz, 3 H, H_9), 1.18 (d, $^3J_{HH}$ = 6.3 Hz, 3 H, H_6), 1.02 (d, $^3J_{HH}$ = 6.4 Hz, 3 H, H_3).

^{13}C{H,F}-NMR (150.92 MHz, 298 K, D_2O): δ = 183.22 (1 C, C_{21}), 183.08 (1 C, C_{15}), 182.95 (1 C, C_{18}), 157.57 (1 C, C_{23}), 154.42 (1 C, C_{26}), 138.94 (1 C, C_{27}), 138.88 (1 C, C_{25}), 136.64 (1 C, C_{28}), 135.94 (1 C, C_{31}), 129.96 (2 C, C_{30}), 128.56 (2 C, C_{29}), 121.95 (1 C, C_{24}), 67.37 (1 C, C_{20}), 67.27 (1 C, C_{17}), 66.89 (1 C, C_{14}), 64.80 (1 C, C_{22}), 61.47 (1 C, C_{11}), 60.78 (1 C, C_2), 60.70

(1 C, C_8), 60.64 (1 C, C_5), 55.29 (1 C, C_1), 46.18 (1 C, C_7), 45.84 (1 C, C_4), 45.22 (1 C, C_{10}), 13.39 (1 C, C_{19}), 13.26 (1 C, C_{13}), 13.22 (1 C, C_{16}), 13.01 (1 C, C_6), 12.74 (1 C, C_9), 12.54 (1 C, C_3), 10.18 (1 C, C_{12}).

^{19}F{H}-NMR (564.76 MHz, 298 K, D_2O): δ = −122.72 (1 F, F_{26}).

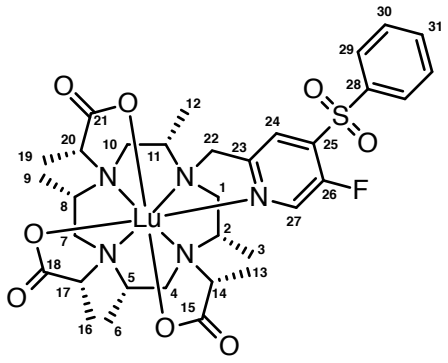

159

TM-M7-FPY-SO_2-PHE-DOTA **158**.

(2*R*,2′*R*,2″*R*)-2,2′,2″-((2*S*,5*S*,8*S*,11*S*)-10-((5-fluoro-4-(phenylsulfonyl)pyridin-2-yl)methyl)-2,5,8,11-tetramethyl-1,4,7,10-tetraazacyclododecane-1,4,7-triyl)tripropionic acid (**161**) (50.0 mg, 72.0 µmol, 1.0 eq.) was dissolved in aqueous ammonium acetate (100 mM, 8.0 mL) and Tm(OTf_3) (153.3 mg, 86.4 µmol, 1.2 eq.) was added. The reaction was heated to 80 °C and stirred for 18 h before purified by preparative HPLC (water, acetonitrile) yielding a white solid (51.0 mg, 59.3 µmol, 82.3 %).

HR-ESI-MS: calcd. for [**158**+H]$^+$ $C_{33}H_{45}FN_5O_8STm$ m/z= 860.2388, found m/z= 860.2391.

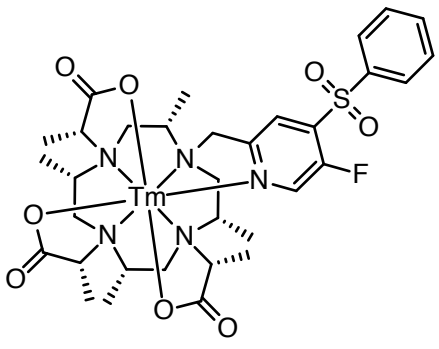

158

TM-M7-FPY-S-C_2H_4-TMS-DOTA **168**.

Tm-M7-FPy-SO_2-Phe-DOTA **158** (50.0 mg, 58.2 µmol, 1.0 eq.) was dissolved in acetonitrile (5.0 mL), 2-(tri|meth|ylsilyl)ethanethiol (18.4 µL, 116 µmol, 2.0 eq.) and potassium carbonate (32.2 mg, 233 µmol, 4.0 eq.) were added. The suspension was stirred at 20-25 °C for 2 h. The mixture was filtered and evaporated to dryness. The crude product was purified by preparative HPLC (water, acetonitrile) yielding a white solid (43.2 mg, 50.7 µmol, 87.1 %).

HR-ESI-MS: calcd. for [**168**+H]$^+$ $C_{32}H_{54}FN_5O_6SSiTm$ m/z= 852.2885, found m/z= 852.2882.

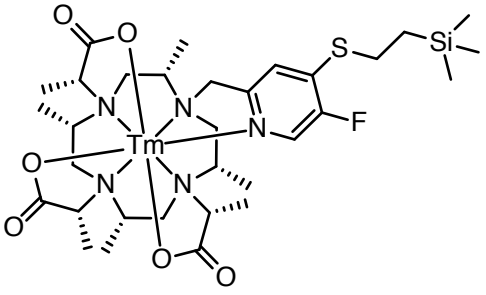

168

TM-M7-FPY-SO_2-C_2H_4-TMS-DOTA **169**.

Tm-M7-FPy-S-C_2H_4-TMS-DOTA **168** (43.2 mg, 50.7 µmol, 1.0 eq.) was dissolved in methanol (10 mL). Sodium tungstate dihydrate (5.0 mg, 15.1 µmol, 0.3 eq.) and aqueous hydrogen peroxide (300 µL, 30 %, 2.94 mmol, 60.0 eq.) was added. The reaction mixture was stirred at 20-25 °C for 18 h. After completion the reaction mixture was concentrated to a final volume of 2-4 mL. The remaining suspension was filtered and the filtrate was purified by preparative HPLC (water, acetonitrile) yielding a white solid (32.3 mg, 36.6 µmol, 71.7 %).

HR-ESI-MS: calcd. for [**169**+H]$^+$ $C_{32}H_{54}FN_5O_8SSiTm$ m/z= 884.2783, found m/z= 884.2781.

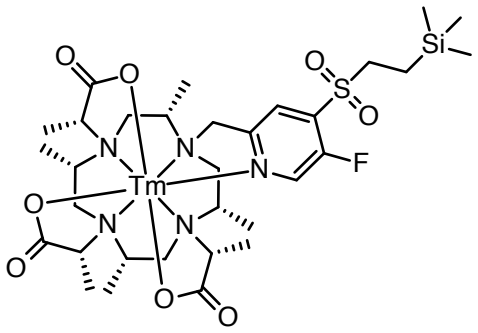

169

TM-M7-FPY-SO_2NH_2-DOTA **170**.

Tm-M7-FPy-SO_2-C_2H_4-TMS-DOTA (**169**) (15.0 mg, 17.0 µmol, 1.0 eq.) was dissolved in tetrahydrofuran (2.0 mL) and acetonitirle (2.00 mL). Tetrabutylammonium fluoride (1 M in tetrahydrofuran, 34.0 µL, 34.0 µmol, 2.0 eq.) was added and the solution was stirred at 20-25 °C for 30 min. The reaction mixture was evaporated to dryness and redissolved in water (5.0 mL). Sodium acetate (13.9 mg, 170 µmol, 10.0 eq.) and hydroxylamine-o-sulfonic acid (9.6 mg, 85.0 µmol, 5.0 eq.) were added. The reaction was stirred at 20-25 °C for 6 h before the solution was directly subjected to preparative HPLC (water, acetonitrile) yielding a white solid (7.1 mg, 8.89 µmol, 52.3 %).

HR-ESI-MS: calcd. for [**170**+H]$^+$ $C_{27}H_{43}FN_6O_8STm$ m/z= 799.2184, found m/z= 799.2187.

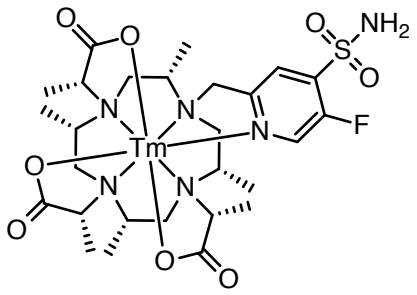

170

TM-M7-FPY-SH-DOTA **171**.

Tm-M7-FPy-SO_2-C_2H_4-TMS-DOTA (**169**) (50.0 mg, 58.7 µmol, 1.0 eq.) was dissolved in tetrahydrofuran (5.00 mL) and acetonitirle (5.00 mL). tetrabutylammonium fluoride (1 M in tetrahydrofuran, 120 µL, 120 µmol, 2.0 eq.) was added and the solution was stirred at 20-25 °C for 30 min. The reaction mixture was evaporated to dryness and the residue was purified by preparative HPLC (water, acetonitrile) yielding a white solid (32.2 mg,

42.8 µmol, 73.0 %).

HR-ESI-MS: calcd. for [**171**+H]$^+$ $C_{27}H_{42}FN_5O_6STm$ m/z= 752.2176, found m/z= 752.2166.

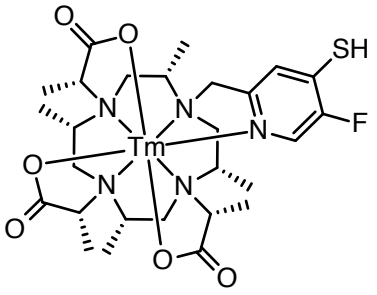

171

TM-M7-FPY-SME-DOTA **172**.

Tm-M7-FPy-SH-DOTA **171** (32.2 mg, 42.8 µmol, 1.0 eq.) and potassium carbonate (11.0 mg, 80.3 mmol, 1.9 eq.) were suspended in acetonitrile (5.0 mL). Iodomethane (4.0 µL, 64.3 µmol, 1.5 eq.) was added and the mixture was stirred at 20-25 °C for 2 h. The mixture was filtered and evaporated to dryness yielding a off-white solid (33.0 mg, 43.4 µmol, quant.).

HR-ESI-MS: calcd. for [**172**+H]$^+$ $C_{28}H_{44}FN_5O_6STm$ m/z= 766.2333, found m/z= 766.2337.

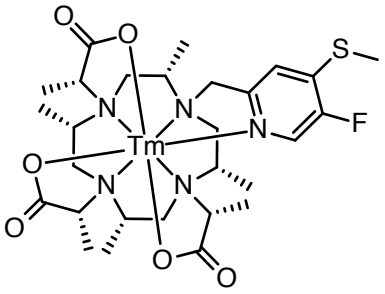

172

TM-M7-FPY-SO$_2$ME-DOTA **173**.

Tm-M7-FPy-SMe-DOTA **172** (33.0 mg, 43.4 µmol, 1.0 eq.) was dissolved in methanol (5.0 mL). Sodium tungstate dihydrate (6.6 mg, 20.0 µmol, 0.5 eq.) and aqueous hydrogen peroxide (30 wt%, 100 µL, 1.06 mmol, 26.0 eq.) were added. The reaction mixture was stirred at 20-25 °C fro 18 h before concentrated to a final volume of 2-4 mL. The resulting suspension was filtered and the filtrate was purified by preperative HPLC (water, acetonitrile)

yielding a white solid (22.1 mg, 27.7 µmol, 64.4 %).

HR-ESI-MS: calcd. for [**173**+H]$^+$ $C_{28}H_{44}FN_5O_8STm$ m/z= 798.2231, found m/z= 798.2236.

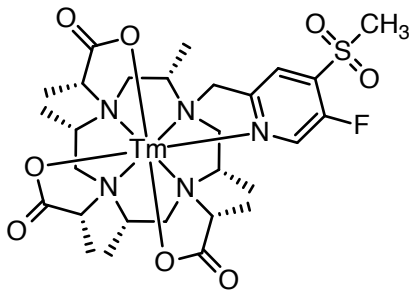

173

4-BROMO-2-(BROMOMETHYL)-5-FLUOROPYRIDINE (**232**).

4-bromo-5-fluoro-2-methylpyridine (75.1 mg, 395 µmol, 1.0 eq.) was dissolved in tetrachloromethane (8.0 mL) under an atmosphere of argon and the solution was heated to 60 °C. *N*-bromosuccinimide (211 mg, 1.19 mmol, 3.0 eq.) and AIBN (cat. 5.0 mg) were added in five portions over 5 h. After 6 h the reaction mixture was filtered and evaporated to dryness. The crude was immediately purified by flash column chromatography (SiO_2, ethyl acetate / cyclohexane (1:9)) yielding a white solid (55.8 mg, 207 µmol, 52.5 %).

^{1}H-NMR (400.13 MHz, 298 K, $CDCl_3$): δ = 8.39 (s, 1 H, H_3), 7.69 (d, $^4J_{HF}$ = 5.3 Hz, 1 H, H_1), 4.49 (s, 2 H, H_6).

^{13}C{H}-NMR (100.62 MHz, 298 K, $CDCl_3$): δ = 156.12 (d, $^1J_{CF}$ = 258.6 Hz, 1 C, C_4), 153.75 (d, $^4J_{CF}$ = 5.4 Hz, 1 C, C_2), 138.09 (d, $^2J_{CF}$ = 25.1 Hz, 1 C, C_3), 128.28 (1 C, C_1), 119.88 ($^{(2}J_{CF}$ = 18.9 Hz, 1 C, C_5), 31.82 (1 C, C_6).

^{19}F{H}-NMR (376.46 MHz, 298 K, $CDCl_3$): δ = −122.97 (1 F, F_4).

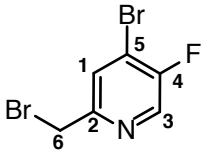

232

TRI-*tert*-BUTYL 2,2′,2″-((2*S*,5*S*,8*S*,11*S*)-10-((4-BROMO-5-FLUOROPYRIDIN-2-YL)METHYL)-2,5,8,11-TETRAMETHYL-1,4,7,10-TETRAAZACYCLODODECANE-1,4,7-TRIYL)(2*R*,2′*R*,2″*R*)-TRIPROPIONATE (**233**).

Tri-*tert*-butyl 2,2',2″-((2*S*,5*S*,8*S*,11*S*)-2,5,8,11-tetramethyl-1,4,7,10-tetraazacyclododecane-1,4,7-triyl)(2*R*,2′*R*,2″*R*)-tripropionate (**129**) (91.9 mg, 150 µmol, 1.0 eq.) and potassium carbonate (82.9 mg, 600 µmol, 4.0 eq.) were suspended in acetonitrile (10 mL). To this suspension 4-bromo-2--(bromomethyl)-5-fluoropyridine (**232**) (40.3 mg, 150 µmol, 1.0 eq.) was added and the mixture was stirred for 18 h at 20-25 °C. The mixture was filtered and evaporated to dryness. The residue was purified by preparative HPLC (water, acetonitrile) yielding a white solid (107 mg, 134 µmol, 89.1 %).

HR-ESI-MS: calcd. for [**233**+H]$^+$ $C_{39}H_{68}BrFN_5O_6$ m/z= 800.4332, found m/z= 800.4330.

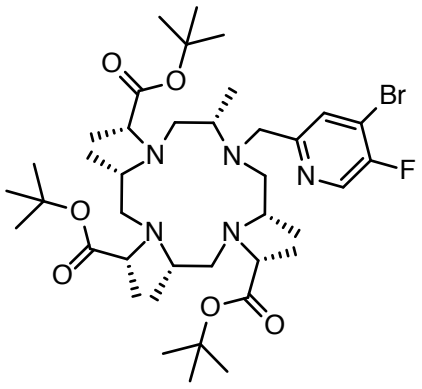

233

(2*R*,2'*R*,2''*R*)-2,2′,2″-((2*S*,5*S*,8*S*,11*S*)-10-((4-((3,5-BIS(TRIFLUOROMETHYL) PHENYL)SULFONYL)PYRIDIN-2-YL)-METHYL)-2,5,8,11-TETRAMETHYL-1,4,7,10-TETRAAZACYCLODODECANE-1,4,7-TRIYL) TRIPROPIONIC ACID (**234**).

Tri-*tert*-butyl 2,2′,2″-((2*S*,5*S*,8*S*,11*S*)-10-((4-bromo-5-fluoropyridin-2-yl)-methyl)-2,5,8,11-tetramethyl-1,4,7,10-tetraazacyclododecane-1,4,7-triyl) (2*R*,2′*R*,2″*R*)-tripropionate (**233**) (107 mg, 134 µmol, 1.0 eq.) was dissolved in acetontirile (5.0 mL) and hydrochloric acid (1 M, 10 mL). The solution was stirred at 80 °C for 3 h. The solution was concentrated under reduced pressure at 50 °C and the residue was purified by preparative HPLC (water, acetonitrile) yielding a white solid (67.5 mg, 107 µmol, 79.6 %).

HR-ESI-MS: calcd. for [**234**+H]$^+$ $C_{27}H_{44}BrFN_5O_6$ m/z= 632.2454, found m/z= 632.2455.

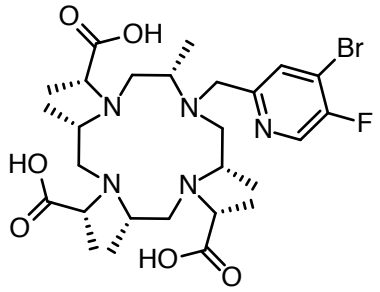

234

TM-M7-FPY-BR-DOTA (**235**).

To a solution of (2*R*,2'*R*,2''*R*)-2,2',2''-((2*S*,5*S*,8*S*,11*S*)-10-((4-((3,5-bis(trifluoromethyl)phenyl)sulfonyl)pyridin-2-yl) methyl)-2,5,8,11-tetramethyl-1,4,7,10-tetraazacyclododecane-1,4,7-triyl) tripropionic acid (**234**) (20.0 mg, 31.6 µmol, 1.0 eq.) in aqueous ammonium acetate (100 mM, 10 mL) was added $Tm(OTf)_3$ (48.7 mg, 79.0 µmol, 2.5 eq.). The mixture was stirred at 80 °C for 18 h before purified by preparative HPLC (water, acetonitrile) yielding a white solid (19.0 mg, 23.8 µmol 75.3 %).

HR-ESI-MS: calcd. for [**235**+H]$^+$ $C_{27}H_{41}BrFN_5O_6Tm$ m/z= 798.1561, found m/z= 798.1571.

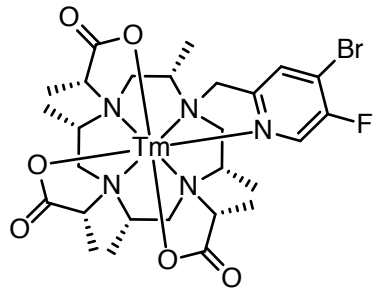

235

TM-M7-FPY-S-BIPHENYL-SSPY-DOTA **224**.

Tm-M7-FPy-SO_2-Phe-DOTA **158** (17.0 mg, 19.8 µmol, 1.0 eq.) and potassium carbonate were suspended in acetonitrile (3.0 mL). 4,4'-Bis(mercaptomethyl)biphenyl (48.8 mg, 198 µmol, 10.0 eq.) was added and the reaction was stirred for 2 h at 20-25 °C. The suspension was filtered and the filtrate was evaporated to dryness. The crude oil was purified by preparative HPLC (water, acetonitrile). The isolated free thiol was immediately dissolved in methanol (5.0 mL) and acetic acid (1.0 mL). 2,2'-Dithiodipyridine (21.8 mg,

99.0 µmol, 5.0 eq.) was added and the reaction mixture was stirred for 2 h at 20-25 °C before directly purified by preparative HPLC (water, acetonitrile) yielding a white solid (5.0 mg, 4.65 µmol, 23.5 %).

HR-ESI-MS: calcd. for [**224**+H]$^+$ $C_{46}H_{56}FN_6O_6S_3Tm$ m/z= 1073.2822, found m/z= 1073.2820.

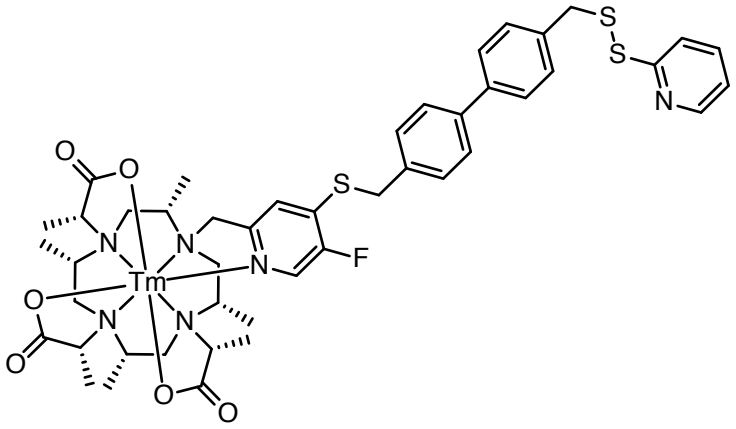

224

2-METHYL-3-NITROPYRIDIN-4-OL (**177**).

2-Methylpyridin-4-ol (877 mg, 8.04 mmol, 1.0 eq.) was dissolved in concentrated sulphuric acid (2.00 mL) at 0-5 °C. Fuming nitric acid (90 %, 2.0 mL) was added. The solution was stirred at 0-5 °C for 3 h and afterwards allowed to slowly warm up to 20-25 °C overnight. The solution was poured on ice (approx. 50 g), the precipitate was filtered off, washed with ice-cold water (20 mL) and dried under vacuum yielding an off white solid (463 mg, 3.01 mmol, 37.0 %).

ESI-MS: calcd. for [**177**+H]$^+$ $C_6H_7N_2O_3$ m/z= 155.05, found m/z= 155.20.

^{1}H-NMR (500.13 MHz, 298 K, DMSO−d_6): δ = 7.74 (d, $^3J_{HH}$ = 7.5 Hz, 1 H, H_6), 6.36 (d, $^3J_{HH}$ = 7.5 Hz, 1 H, H_5), 2.30 (s, 3 H, H_1).

^{13}C{H}-NMR (125.77 MHz, 298 K, DMSO−d_6): δ = 168.01 (1 C, C_4), 143.62 (1 C, $C_{2/3}$), 142.08 (1 C, $C_{3/2}$), 138.06 (1 C, C_6), 117.88 (1 C, C_5), 15.35 (1 C, C_1).

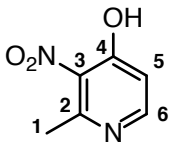

177

4-BROMO-2-METHYL-3-NITROPYRIDINE (**177**).

2-Methyl-3-nitropyridin-4-ol (**177**) (495 mg, 3.21 mmol, 1.0 eq.) was suspended in toluene (20 mL) at 20-25 °C. Phosphorous oxybromide (2.10 g, 7.31 mmol, 2.3 eq.) was added and the suspension was heated to reflux. The reaction mixture was refluxed for 19 h before cooled to 20-25 °C. Aqueous sodium hydroxide (1 M, 30 mL) and ethyl acetate (50 mL) were added. The layers were separated and the organic layer was washed with water (2x 20 mL) and dried over sodium sulphate. The crude brown oil was purified by flash column chromatography (SiO_2, pentane / *tert*-butyl methylether (7:3)) yielding a brownish solid (80.0 mg, 370 µmol, 11.5 %).

^{1}H-NMR (500.13 MHz, 298 K, $CDCl_3$): δ = 8.41 (d, $^3J_{HH}$ = 5.3 Hz, 1 H, H_6), 7.50 (d, $^3J_{HH}$ = 5.3 Hz, 1 H, H_5), 2.60 (s, (3 H, H_1).

^{13}C{H}-NMR (125.77 MHz, 298 K, $CDCl_3$): δ = 151.67 (1 C, $C_{arom.}$), 150.35 (1 C, C_6), 148.42 (1 C, $C_{arom.}$), 126.16 (1 C, C_5), 123.64 (1 C, C_{arom}), 20.76 (1 C, C_1).

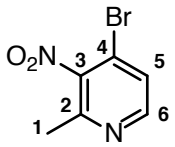

174

2-METHYL-3-NITRO-4-(PHENYLTHIO)PYRIDINE (**178**).

4-Bromo-2-methyl-3-nitropyridine (**174**) (69.0 mg, 318 µmol, 1.0 eq.) was dissolved in dimethylformamide (4.0 mL). Then potassium carbonate (94.0 mg, 680 µmol, 2.1 eq.) and thiophenol (34.3 mg, 312 µmol, 1.0 eq.) were added. The solution was heated to 80 °C for 70 min. Afterwards the solvent was evaporated. The residue was dissolved in ethyl acetate (5.0 mL) and water (5.00 mL). The layers were separated and the aqueous layer was washed with ethyl acetate (2x 20 mL). The combined organic layers were dried over sodium sulphate. The solvent was evaporated yielding a yellow solid (80.0 mg, 324 µmol, quant.) .

ESI-MS: calcd. for [**178**+H]$^+$ $C_{12}H_{11}N_2O_2S$ m/z= 247.06, found m/z= 247.45.

^{1}H-NMR (500.13 MHz, 298 K, $CDCl_3$): δ = 8.21 (d, $^3J_{HH}$ = 5.5 Hz, 1 H, H_6), 7.59 (m, 5 H, H_8, H_9, H_{10}), 6.60 (d, $^3J_{HH}$ = 5.5 Hz, 1 H, H_5), 2.66 (s, 3 H, H_1).

^{13}C{H}-NMR (126.77 MHz, 298 K, $CDCl_3$): δ = 152.24 ($C_{arom.}$), 149.63 (1 C, C_6), 146.27 ($C_{arom.}$), 144.36 ($C_{arom.}$), 135.89 ($C_{arom.}$), 130.75 (1 C, C_{10}),

130.48 ($C_{arom.}$), 128.71 (1 C, C_7), 120.14 (1 C, C_5), 22.19 (1 C, C_1).

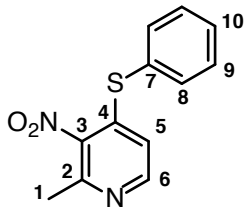

178

2-METHYL-3-NITRO-4-(PHENYLSULFONYL)PYRIDINE (**179**).

2-Methyl-3-nitro-4-(phenylthio)pyridine ([**178**) (77.7 mg, 315 µmol, 1.0 eq.) was dissolved in methanol (5.0 mL). Then sodium tungstate dihydrate (102 mg, 309 µmol, 1.0 eq.) and aqueous hydrogen peroxide (30 %, 298 µL, 3.15 mmol, 10 eq.) were added. The solution was stirred at 20-25 °C for 4 h. More sodium tungstate dihydrate (204 mg, 618 µmol, 2.0 eq.) and aqueous hydrogen peroxide (30 %, 600 µL, 6.30 mmol, 20 eq.) were added. The solution was stirred at 20-25 °C for further 72 h. Afterwards water (5.0 mL) was added and methanol was removed by distillation. The aqueous layer was extracted with ethyl acetate (3x 10 mL). The organic layer was dried over sodium sulphate and the solvent was evaporated. The crude product was purified by preparative HPLC (water, acetonitrile) yielding yellow solid (35.0 mg, 126 µmol, 40.0 %).

HR-ESI-MS: calcd. for [**179**+H]$^+$ $C_{12}H_{11}N_2O_4S$ m/z= 279.05, found m/z= 279.45.

^{1}H-NMR (600.13 MHz, 298 K, $CDCl_3$): δ = 8.84 (d, $^3J_{HH}$ = 5.1 Hz, 1 H, H_6), 7.99-7.94 (m, 2 H, $H_{9/8}$), 7.86 (d, $^3J_{HH}$ = 5.1 Hz, 1 H, H_5), 7.7-7.67 (m, 1 H, H_{10}), 7.6-7.56 (m, 2 H, $H_{9/8}$), 2.59 (s, 3 H, H_1).

^{13}C{H}-NMR (125.77 MHz, 298 K, $CDCl_3$): δ = 152.48 (1 C, $C_{arom.}$), 151.64 (1 C, C_6), 142.71 ($C_{arom.}$), 140.87 ($C_{arom.}$), 129.63 (2 C, $C_{9/8}$), 128.62 (2 C, $C_{9/8}$), 134.92 (1 C, C_{10}), 120.54 (1 C, C_5), 20.11 (1 C, C_1).

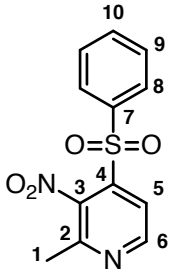

179

2-METHYL-4-(METHYLTHIO)-3-NITROPYRIDINE (**180**).

2-Methyl-3-nitropyridin-4-ol (**177**) (250 mg, 1.62 mmol, 1.0 eq.) was suspended in thionyl chloride (1.5 mL). Dimethylformamide (20.0 µL) was added and the reaction mixture was heated to 70 °C for 18 h. The brownish solution was evaporated to dryness yielding a yellow crude oil which was dissolved in dimethylformamide (2.0 mL). Potassium carbonate (448 mg, 3.24 mmol, 2.0 eq.) and sodium methanthiolate (136 mg, 1.94 mmol, 1.2 eq.) were added and the reaction mixture was stirred for 2 h at 20-25 °C. The solution was evaporated and the crude product was purified by flash column chromatopgraphy (SiO_2, ethyl acetate / cyclohexane (5:5)) yielding a yellow solid (110 mg, 598 µmol, 36.9 %).

^{1}H-NMR (600.13 MHz, 298 K, $CDCl_3$): δ = 8.43 (d, $^3J_{HH}$ = 5.5 Hz, 1 H, H_6), 7.10 (d, $^3J_{HH}$ = 5.5 Hz, 1 H, H_5), 2.62 (s, 3 H, H_1), 2.52 (s, 3 H, H_7).

^{13}C{H}-NMR (150.95 MHz, 298 K, $CDCl_3$): δ = 151.77 (1 C, C_2), 149.57 (1 C, C_6), 145.54 (1 C, C_4), 145.11 (1 C, C_3), 117.83 (1 C, C_5), 21.91 (1 C, C_1), 15.11 (1 C, C_7).

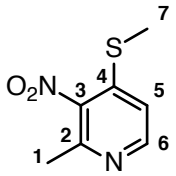

180

2-(BROMOMETHYL)-4-(METHYLTHIO)-3-NITROPYRIDINE (**181**).

2-Methyl-4-(methylthio)-3-nitropyridine (**180**) (30.0 mg, 163 µmol, 1.0 eq.), was dissolved in tetrachloromethane (2.0 mL) and refluxed. To this solution over a period of 5 h NBS (580 mg, 3.26 mmol, 20.0 eq.) and AIBN (10 mg) were added in small portions. After 6 h the mixture was cooled to 20-25 °C, filtered and evaporated to dryness. The crude mixture was purified by flash column chromatography (SiO_2, ethyl acetate / cyclohexane (5:5)) yielding a yellow oil (8.3 mg, 32.0 µmol, 19.4 %).

^{1}H-NMR (250.13 MHz, 298 K, $CDCl_3$): δ = 8.59 (d, $^3J_{HH}$ = 5.5 Hz, 1 H, H_6), 7.49 (d, $^3J_{HH}$ = 5.5 Hz, 1 H, H_5), 4.80 (s, 2 H, H_1), 2.68 (s, 3 H, H_7).

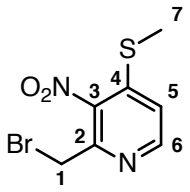

181

5-METHYLTHIAZOLO[5,4-B]PYRIDINE-2-THIOL (**186**).

2-Bromo-6-methylpyridin-3-amine (2.42 g, 12.9 mmol, 1.0 eq.) and potassium ethyl xanthogenate (4.55 g, 28.4 mmol, 2.2 eq.) was dissolved in dimethylformamide (5.0 mL) and heated to 130 °C for 16 h. The resulting suspension was diluted with water (250 mL) yielding a brownish solution. The solution was acidified with hydrochloric acid (4 M, 5.0 mL). The precipitate was filtered and washed with water (50 mL) yielding a brownish solid (2.17 g, 11.9 mmol, 92.3 %).

HR-ESI-MS: calcd. for [**186**+H]$^+$ $C_7H_7N_2S_2$ m/z= 183.0045, found m/z= 183.0044.

^{1}H-NMR (400.13 MHz, 298 K, $CDCl_3$): δ = 11.08 (bs, 1 H, H_8), 7.42 (d, $^3J_{HH}$ = 8.2 Hz, 1 H, H_4), 7.14 (d, $^3J_{HH}$ = 8.2 Hz, 1 H, H_3), 2.59 (s, 3 H, H_1).

^{13}C{H}-NMR (100.6 MHz, 298 K, $CDCl_3$): δ = 190.02 (1 C, C_7), 155.86 (1 C, C_2), 151.68 (1 C, C_6), 132.73 (1 C, C_5), 121.45 (1 C, C_4), 118.55 (1 C, C_3), 23.99 (1 C, C_1).

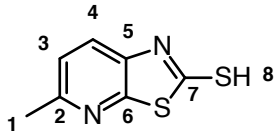

186

5-METHYL-2-(METHYLTHIO)THIAZOLO[5,4-B]PYRIDINE (**187**).

5-Methylthiazolo[5,4-b]pyridine-2-thiol (**186**) (540 mg, 2.96 mmol, 1.0 eq.) was dissolved in acetonitrile (60 mL) and acetone (10 mL). To this solution potassium carbonate (818 mg, 5.92 mmol, 2.0 eq.) and iodomethane (221 µL, 3.55 mmol, 1.2 eq.) were added. The suspension was stirred at 20-25 °C for 2 h. The solids were filtered off and the crude product was obtained by evaporation of the solvent. The crude product was purified by flash column chromatography (SiO_2, ethyl acetate / cyclohexane (3:7)) yielding a off-white solid (450 mg, 2.29 mmol, 77.4 %).

HR-ESI-MS: calcd. for [**187**+H]$^+$ $C_8H_9N_2S_2$ m/z= 197.0202, found m/z= 197.0201.

^{1}H-NMR (400.13 MHz, 298 K, $CDCl_3$): δ = 7.93 (d, $^3J_{HH}$ = 8.3 Hz, 1 H, H_4), 7.18 (d, $^3J_{HH}$ = 8.3 Hz, 1 H, H_3), 2.77 (s, 3 H, H_8), 2.62 (s, 3 H, H_1).

^{13}C{H}-NMR (100.6 MHz, 298 K, $CDCl_3$): δ = 168.05 (1 C, C_7), 158.20 (1 C, C_6), 155.07 (1 C, C_2), 144.60 (1 C, C_5), 128.09 (1 C, C_4), 121.29 (1 C, C_3), 24.31 (1 C, C_1), 15.48 (1 C, C_8).

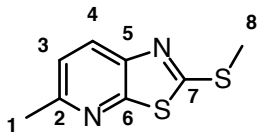

187

5-METHYL-2-(METHYLSULFONYL)THIAZOLO[5,4-B]PYRIDINE (**190**).

5-Methyl-2-(methylthio)thiazolo[5,4-b]pyridine (**187**) (271 mg, 1.38 mmol, 1.0 eq.), were dissolved in dichloromethane (5.0 mL) and cooled to 0-5 °C. 3-Chloroperoxybenzoic acid (680 mg, 3.04 mmol, 2.2 eq.) was added and the reaction mixture was stirred at 0-5 °C for 1 h before it was allowed to warm up to 20-25 °C. The reaction mixture was stirred another 1 h at 20-25 °C. The reaction mixture was extracted with aqueous sodium hydroxide (1 M, 3.0 mL), dried with sodium sulphate and evaporated to dryness. The crude product was purified by flash column chromatography (SiO_2, ethyl acetate / cyclohexane (1:1)) yielding a white solid (211 mg, 925 µmol, 67.0 %).

ESI-MS: calcd. for [**190**+H]$^+$ $C_8H_9N_2O_2S_2$ m/z= 229.00, found m/z= 228.95.

^{1}H-NMR (600.13 MHz, 298 K, $CDCl_3$): δ = 8.31 (d, $^3J_{HH}$ = 8.4 Hz, 1 H, H_4), 7.45 (d, $^3J_{HH}$ = 8.4 Hz, 1 H, H_3), 3.39 (s, 3 H, H_8), 2.75 (s, 3 H, H_1).

^{13}C{H}-NMR (150.9 MHz, 298 K, $CDCl_3$): δ = 166.01 (1 C, C_7), 160.70 (1 C, C_2), 158.07 (1 C, C_6), 143.92 (1 C, C_5), 132.72 (1 C, C_4), 123.41 (1 C, C_3), 42.26 (1 C, C_8), 24.97 (1 C, C_1).

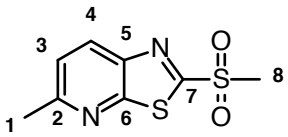

190

5-(BROMOMETHYL)-2-(METHYLSULFONYL)THIAZOLO[5,4-B] PYRIDINE (**182**).

5-Methyl-2-(methylsulfonyl)thiazolo[5,4-b]pyridine (**190**) (130 mg, 569 µmol, 1.0 eq.) was dissolved in carbon tetrachloride (15 mL) and acetonitrile (5.0 mL). The solution was heated to reflux. At reflux over a period of 2.5 h *N*-bromosuccinimide (304 mg, 1.71 mmol, 3.0 eq.) and AIBN (cat. 5.0 mg) were added in small portions. The reaction was refluxed for 5 h, filtered and evaporated to dryness under vacuum at 40 °C. The crude product was purified by flash column chromatography (SiO_2, ethyl acetate / cyclohexane (1:1)) yielding a white solid (75.0 mg, 244 µmol, 42.9 %).

ESI-MS: calcd. for [**182**+H]$^+$ $C_8H_8BrN_2O_2S_2$ m/z= 306.91, found m/z= 306.85.

^{1}H-NMR (500.13 MHz, 298 K, $CDCl_3$): δ = 8.45 (d, $^3J_{HH}$ = 8.5 Hz, 1 H, H_4), 7.74 (d, $^3J_{HH}$ = 8.5 Hz, 1 H, H_3), 4.69 (s, 2 H, H_1), 3.41 (s, 3 H, H_8).

^{13}C{H}-NMR (125.8 MHz, 298 K, $CDCl_3$): δ = 168.77 (1 C, C_7), 158.58 (1 C, C_6), 158.31 (1 C, C_2), 145.14 (1 C, C_5), 133.71 (1 C, C_4), 123.32 (1 C, C_3), 42.19 (1 C, C_8), 32.75 (1 C, C_1).

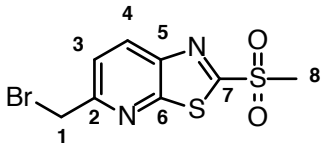

182

5-(BROMOMETHYL)-2-(METHYLTHIO)THIAZOLO[5,4-B]PYRIDINE (**193**).

5-Methyl-2-(methylthio)thiazolo[5,4-b]pyridine (**187**) (210 mg, 1.07 mmol, 1.0 eq.) was dissolved in carbon tetrachloride (10.0 mL). The solution was heated to reflux. At reflux, over a period of 2 h *N*-bromosuccinimide (286 mg, 1.71 mmol, 1.5 eq.) and AIBN (cat.) were added in small portions. The reaction was refluxed for 4 h, filtered and evaporated to dryness under vacuum at 40 °C. The crude product was purified by flash column chromatography (SiO_2, ethyl acetate / cyclohexane (3:7)) yielding a white solid (70.3 mg, 256 µmol, 23.9 %).

ESI-MS: calcd. for [**193**+H]$^+$ $C_8H_8BrN_2S_2$ m/z= 274.9, found m/z= 274.85.

^{1}H-NMR (500.13 MHz, 298 K, $CDCl_3$): δ = 8.03 (d, $^3J_{HH}$ = 8.3 Hz, 1 H, H_4), 7.48 (d, $^3J_{HH}$ = 8.3 Hz, 1 H, H_3), 4.63 (s, 2 H, H_1), 2.80 (s, 3 H, H_1).

$^{13}C\{H\}$-NMR (125.8 MHz, 298 K, $CDCl_3$): δ = 170.07 (1 C, C_7), 158.55 (1 C, C_6), 152.93 (1 C, C_2), 146.07 (1 C, C_5), 128.55 (1 C, C_4), 121.58 (1 C, C_3), 33.63 (1 C, C_1), 15.50 (1 C, C_8).

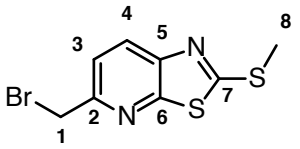

193

TRI-*tert*-BUTYL 2,2′,2″-((2*S*,5*S*,8*S*,11*S*)-2,5,8,11-TETRAMETHYL-10-((2-(METHYLSULFONYL)THIAZOLO[5,4-B]-PYRIDIN-5-YL)METHYL)-1,4,7,10-TETRAAZACYCLODODECANE-1,4,7-TRIYL)(2*R*,2′*R*,2″*R*)-TRIPROPIONATE (**191**).

Tri-*tert*-butyl 2,2',2″-((2*S*,5*S*,8*S*,11*S*)-2,5,8,11-tetramethyl-1,4,7,10-tetraazacyclododecane-1,4,7-triyl)(2*R*,2′*R*,2″*R*)-tripropionate (**129**) (50.0 mg, 81.6 µmol, 1.0 eq.) and potassium carbonate (45.1 mg, 326 µmol, 4.0 eq.) were suspended in acetonitrile (5.0 mL). To this suspension 5-(bromomethyl)-2-(methylsulfonyl)thiazolo[5,4-b]pyridine (**182**) (25.1 mg, 81.6 µmol, 1.0 eq.) was added and the mixture was stirred for 18 h at 20-25 °C. The mixture was filtered and evaporated to dryness. The residue was purified by preparative HPLC (water, acetonitrile) yielding a white solid (55.0 mg, 65.5 µmol, 80.3 %).

HR-ESI-MS: calcd. for [**191**+H]$^+$ $C_{41}H_{71}N_6O_8S_2$ m/z= 839.4769, found m/z= 839.4771.

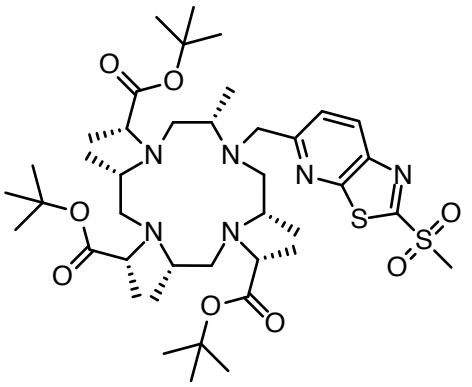

191

(2R,2′R,2″R)-2,2′,2″-((2S,5S,8S,11S)-2,5,8,11-TETRAMETHYL-10-((2-(METHYLSULFONYL)THIAZOLO[5,4-B]PYRIDIN-5-YL)METHYL)-1,4,7,10-TETRAAZACYCLODODECANE-1,4,7-TRIYL)TRIPROPIONIC ACID (**192**).

Tri-*tert*-butyl 2,2′,2″-((2S,5S,8S,11S)-2,5,8,11-tetramethyl-10-((2-(methylsulfonyl)thiazolo [5,4-b]pyridin-5-yl)methyl)-1,4,7,10-tetraazacyclododecane-1,4,7-triyl)(2*R*,2′*R*,2″*R*)-tripropionate (**191**) (55.0 mg, 65.5 µmol, 1.0 eq.) was dissolved in acetonitrile (2.0 mL) and aqueous hydrochloric acid (1 M, 5.0 mL). The solution was heated to 80 °C for 7 h. The solution was concentrated under reduced pressure at 50 °C and the residue was purified by preparative HPLC (water, acetonitrile) yielding a white solid (18.0 mg, 26.8 µmol, 41.0 %).

HR-ESI-MS: calcd. for [**192**+H]$^+$ $C_{29}H_{47}N_6O_8S_2$ m/z= 671.2891, found m/z= 671.2895.

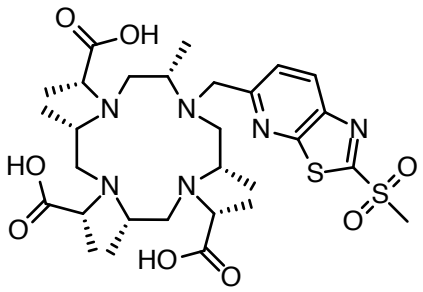

192

LU-M7PYTHIAZOL-SO$_2$ME-DOTA **188**.

To a solution of (2R,2′R,2″R)-2,2′,2″-((2S,5S,8S,11S)-2,5,8,11-tetramethyl-10-((2-(methylsulfonyl)thiazolo[5,4-b]pyridin-5-yl)methyl)-1,4,7,10-tetraazacyclododecane-1,4,7-triyl)tripropionic acid (**192**) (18.0 mg, 26.8 µmol, 1.0 eq.) in aqueous ammonium acetate (100 mM, 10 mL) was added Lu(OTf)$_3$ (33.3 mg, 53.6 µmol , 2.0 eq.). The mixture was stirred at 80 °C for 18 h before purified by preparative HPLC (water, acetonitrile) yielding a white solid (12.3 mg, 14.6 µmol, 54.5 %).

HR-ESI-MS: calcd. for [**188**+H]$^+$ $C_{29}H_{44}LuN_6O_8S_2$ m/z= 843.2064, found m/z= 843.2067.

^{1}H-NMR (600.13 MHz, 298 K, D_2O): δ = 8.76 (d, $^3J_{HH}$ = 8.7 Hz, 1 H, H_{25}), 7.83 (d, $^3J_{HH}$ = 8.7 Hz, 1 H, H_{24}), 4.78 (d, $^2J_{HH}$ = 18.1 Hz, 1 H, H_{22a}), 4.65 (d, $^2J_{HH}$ = 18.1 Hz, 1 H, H_{22b}), 3.88 (q, $^3J_{HH}$ = 7.4 Hz, 1 H, H_{20}), 3.84 (q, $^3J_{HH}$ = 7.4 Hz, 1 H, H_{17}), 3.58 (s, 3 H, H_{29}), 3.53 (dd, $^2J_{HH}$ = 14.8 Hz, $^3J_{HH}$ = 13.3 Hz, 1 H, H_{1ax}), 3.28-3.21 (m, 1 H, H_{11}), 3.20-3.13 (m, 1 H, H_8), 3.18-3.10 (m, 1 H, H_{10ax}), 3.12-3.07 (m, 1 H, H_{4ax}), 3.09-3.04 (m, 1

H, H_{7ax}), 3.05-2.99 (m, 1 H, H_5), 2.98-2.93 (m, 1 H, H_2), 2.93-2.85 (m, 1 H, H_{10eq}), 2.89 (q, $^3J_{HH}$ = 7.2 Hz, 1 H, H_{14}), 2.77 (dd, $^2J_{HH}$ = 15.3 Hz, $^3J_{HH}$ = 1.6 Hz, 1 H, H_{7eq}), 2.73 (dd, $^2J_{HH}$ = 14.8 Hz, $^3J_{HH}$ = 2.8 Hz, 1 H, H_{1eq}), 2.69 (d, $^2J_{HH}$ = 14.2 Hz, 1 H, H_{4eq}), 1.52 (d, $^3J_{HH}$ = 7.3 Hz, 3 H, H_{16}), 1.50 (d, $^3J_{HH}$ = 7.4 Hz, 3 H, H_{19}), 1.27 (d, $^3J_{HH}$ = 6.7 Hz, 3 H, H_{12}), 1.24 (d, $^3J_{HH}$ = 5.6 Hz, 3 H, H_{13}), 1.23 (d, $^3J_{HH}$ = 5.4 Hz, 3 H, H_9), 1.22 (d, $^3J_{HH}$ = 6.5 Hz, 3 H, H_6), 1.09 (d, $^3J_{HH}$ = 6.5 Hz, 3 H, H_3).

^{13}C{H}-NMR (150.92 MHz, 298 K, D_2O): δ = 183.37 (1 C, C_{21}), 183.03 (1 C, C_{18}), 182.71 (1 C, C_{15}), 167.90 (1 C, C_{28}), 161.98 (1 C, C_{23}), 156.30 (1 C, C_{27}), 146.96 (1 C, C_{26}), 136.76 (1 C, C_{25}), 122.48 (1 C, C_{24}), 67.63 (1 C, C_{17}), 67.36 (1 C, C_{20}), 66.72 (1 C, C_{14}), 65.72 (1 C, C_{22}), 61.61 (1 C, C_{11}), 60.74 (1 C, C_8), 60.58 (1 C, C_5), 60.47 (1 C, C_2), 55.60 (1 C, C_1), 46.30 (1 C, C_7), 45.80 (1 C, C_4), 45.21 (1 C, C_{10}), 42.09 (1 C, C_{29}), 13.51 (1 C, C_{19}), 13.27 (1 C, C_{16}), 13.21 (1 C, C_6), 12.77 (2 C, C_3, C_9), 12.59 (1 C, C_{13}), 10.17 (1 C, C_{12}).

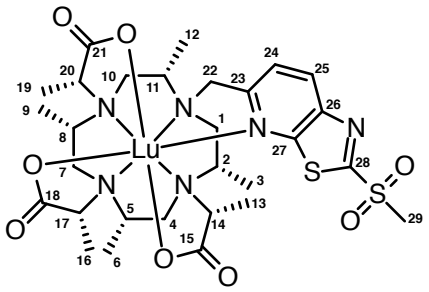

188

TM-M7PYTHIAZOL-SO_2ME-DOTA **189**.

To a solution of (2R,2′R,2″R)-2,2′,2″-((2S,5S,8S,11S)-2,5,8,11-tetramethyl-10-((2-(methylsulfonyl)thiazolo[5,4-b]pyridin-5-yl)methyl)-1,4,7,10-tetraazacyclododecane-1,4,7-triyl)tripropionic acid (**192**) (18.0 mg, 26.8 µmol, 1.0 eq.) in aqueous ammonium acetate (100 mM, 10 mL) was added $Tm(OTf)_3$ (33.0 mg, 53.6 µmol, 2.0 eq.). The mixture was stirred at 80 °C for 18 h before purified by preparative HPLC (water, acetonitrile) yielding a yellowish solid (4.1 mg, 4.77 µmol, 17.8 %).

HR-ESI-MS: calcd. for [**189**+H]$^+$ $C_{29}H_{44}N_6O_8S_2Tm$ m/z= 837.1999, found m/z= 837.2003.

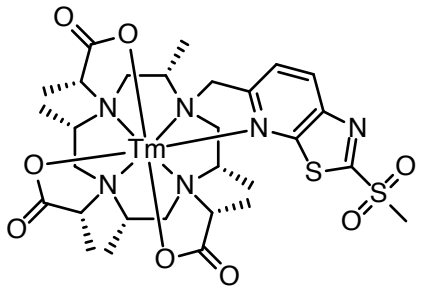

189

TRI-TERT-BUTYL 2,2′,2′′-((2*S*,5*S*,8*S*,11*S*)-2,5,8,11-TETRAMETHYL-10-((2-(METHYLTHIO)THIAZOLO[5,4-B]PYRIDIN-5-YL)METHYL)-1,4,7,10-TETRAAZACYCLODODECANE-1,4,7-TRIYL)(2*R*,2′*R*,2′′*R*)-TRIPROPIONATE (**194**).

Tri-*tert*-butyl 2,2',2′′-((2(*S*),5(*S*),8S,11(*S*))-2,5,8,11-tetramethyl-1,4,7,10-tetraazacyclododecane-1,4,7-triyl)(2*R*,2′*R*,2′′*R*)-tri|propion|ate (**129**) (50.0 mg, 81.6 µmol, 1.0 eq.) and potassium carbonate (45.1 mg, 326 µmol, 4.0 eq.) were suspended in acetonitrile (5.0 mL). To this suspension 5-(bromomethyl)-2-(methylthio)thiazolo[5,4-b]pyridine (**193**) (29.2 mg, 106 µmol, 1.3 eq.) was added and the mixture was stirred for 18 h at 20-25 °C. The mixture was filtered and evaporated to dryness. The residue was purified by preparative HPLC (water, acetonitrile) yielding a white solid (54.3 mg, 67.2 µmol, 82.4 %).

HR-ESI-MS: calcd. for [**194**+H]$^+$ $C_{41}H_{71}N_6O_6S_2$ m/z= 807.4871, found m/z= 807.4870.

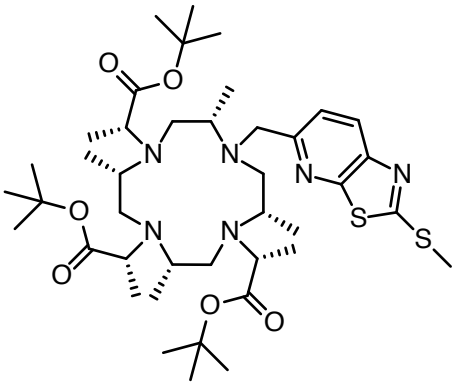

194

(2*R*,2′*R*,2″*R*)-2,2′,2″-((2*S*,5*S*,8*S*,11*S*)-2,5,8,11-TETRAMETHYL-10-((2-(METHYLTHIO)THIAZOLO[5,4-B]PYRIDIN-5-YL)METHYL)-1,4,7,10-TETRAAZACYCLODODECANE-1,4,7-TRIYL)-TRIPROPIONIC ACID (**195**).

Tri-*tert*-butyl 2,2′,2″-((2*S*,5*S*,8*S*,11*S*)-2,5,8,11-tetramethyl-10-((2-(methylthio)thiazolo[5,4-b]pyridin-5-yl)methyl)-1,4,7,10-tetraazacyclododecane-1,4,7-triyl)(2(*R*),2′(*R*),2″(*R*))-tripropionate (**194**) (52.3 mg, 64.8 µmol, 1.0 eq.) was dissolved in dichloromethane (2.0 mL) and trifluoroacetic acid (2.0 mL) and stirred at 20-25 °C for 36 h. The solvent was removed and the residue was purified by preparative HPLC (water, acetonitrile) yielding a white solid (35.6 mg mg, 55.7 µmol, 86.0 %).

HR-ESI-MS: calcd. for [**195**+H]$^+$ $C_{29}H_{47}N_6O_6S_2$ m/z= 639.2993, found m/z= 639.3002.

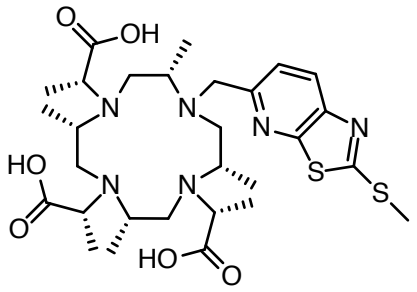

195

TB-M7PYTHIAZOL-SME-DOTA (**196**).

To a solution of (2*R*,2′*R*,2″*R*)-2,2′,2″-((2*S*,5*S*,8*S*,11*S*)-2,5,8,11-tetramethyl-10-((2-(methylthio)thiazolo[5,4-b]pyridin-5-yl)methyl)-1,4,7,10-tetraazacyclododecane-1,4,7-triyl)tripropionic acid (**195**) (12.0 mg, 18.8 µmol, 1.0 eq.) in aqueous ammonium acetate (100 mM, 10 mL) was added $Tb(Cl)_3$ (14.0 mg, 37.6 µmol, 2.0 eq.). The mixture was stirred at 80 °C for 18 h before purified by preparative HPLC (water, acetonitrile) yielding a white solid (8.9 mg, 11.2 µmol, 59.6 %).

ESI-MS: calcd. for [**196**+H]$^+$ $C_{29}H_{44}N_6O_8S_2Tb$ m/z= 795.19, found m/z= 795.25.

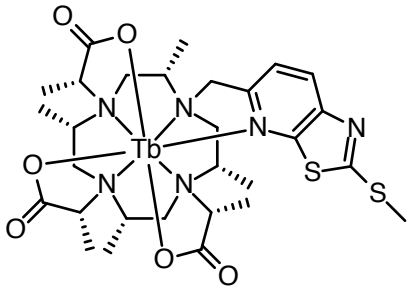

196

DY-M7PYTHIAZOL-SME-DOTA (**197**).

To a solution of (2*R*,2′*R*,2″*R*)-2,2′,2″-((2*S*,5*S*,8*S*,11*S*)-2,5,8,11-tetramethyl-10-((2-(methylthio)thiazolo[5,4-b]pyridin-5-yl)methyl)-1,4,7,10-tetraazacyclododecane-1,4,7-triyl)tripropionic acid (**195**) (12.0 mg, 18.8 µmol, 1.0 eq.) in aqueous ammonium acetate (100 mM, 10 mL) was added $Dy(OTf)_3$ (22.9 mg, 37.6 µmol, 2.0 eq.). The mixture was stirred at 80 °C for 18 h before purified by preparative HPLC (water, acetonitrile) yielding a white solid (9.8 mg, 12.3 µmol, 65.3 %).

ESI-MS: calcd. for [**197**+H]$^+$ $C_{29}H_{44}DyN_6O_8S_2$ m/z= 800.20, found m/z= 800.20.

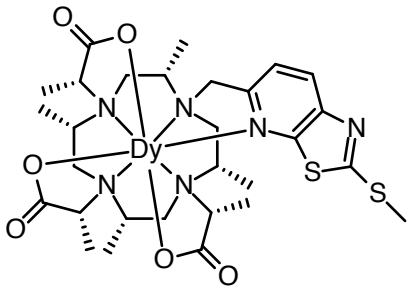

197

SM-M7PYTHIAZOL-SME-DOTA (**198**).

To a solution of (2*R*,2′*R*,2″*R*)-2,2′,2″-((2*S*,5*S*,8*S*,11*S*)-2,5,8,11-tetramethyl-10-((2-(methylthio)thiazolo[5,4-b]pyridin-5-yl)methyl)-1,4,7,10-tetraazacyclododecane-1,4,7-triyl)tripropionic acid (**195**) (30.0 mg, 47.0 µmol, 1.0 eq.) in aqueous ammonium acetate (100 mM, 10 mL) was added $SmCl_3 \cdot {}_6H_2O$ (34.3 mg, 94.0 µmol, 2.0 eq.). The mixture was stirred at 80 °C for 18 h before purified by preparative HPLC (water, acetonitrile) yielding a white solid (29.0 mg, 36.8 µmol, 78.4 %).

ESI-MS: calcd. for [**198**+H]$^+$ $C_{29}H_{44}N_6O_6S_2Sm$ m/z= 788.20, found m/z= 788.20.

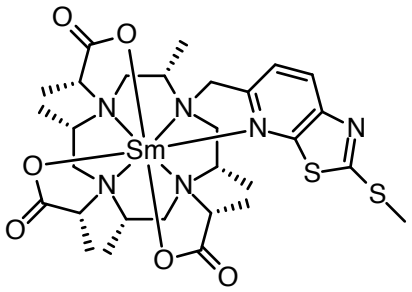

198

TB-M7PYTHIAZOL-SO2ME-DOTA **199**.

To a solution of Tb-M7PyThiazol-SMe-DOTA **196** (8.0 mg, 10.1 µmol, 1.0 eq.) in dichloromethane (5.0 mL) was added 3-chloroperoxybenzoic acid (>77 %, 11.3 mg, 50.5 µmol, 5.0 eq.). The mixture was stirred at 20-25 °C for 18 h. The solvent was removed and the residue was purified by preparative HPLC (water, acetonitrile) yielding a white solid (6.3 mg, 7.62 µmol, 75.4 %).

HR-ESI-MS: calcd. for [**199**+H]$^+$ $C_{29}H_{44}N_6O_8S_2Tb$ m/z= 827.1914, found m/z= 827.1910.

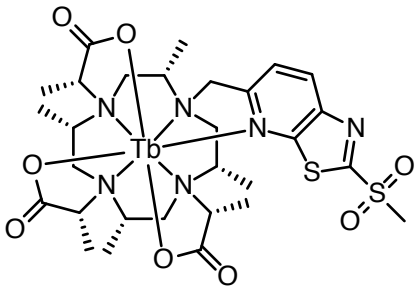

199

DY-M7PYTHIAZOL-SO2ME-DOTA **200**.

To a solution of Dy-M7PyThiazol-SMe-DOTA **197** (9.2 mg, 11.5 µmol, 1.0 eq.) in dichloromethane (5.0 mL) was added 3-chloroperoxybenzoic acid (>77 %, 25.8 mg, 115 µmol, 10.0 eq.). The mixture was stirred at 20-25 °C for 18 h. The solvent was removed and the residue was purified by preparative HPLC (water, acetonitrile) yielding a white solid (7.3 mg, 8.79 µmol, 76.4 %).

HR-ESI-MS: calcd. for [**200**+H]$^+$ $C_{29}H_{44}DyN_6O_8S_2$ m/z= 832.1951, found m/z= 832.1955.

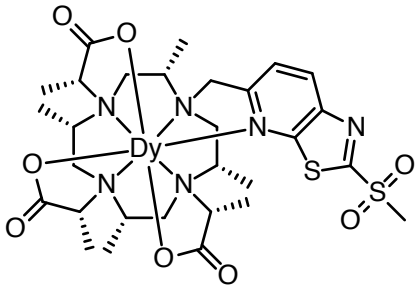

200

SM-M7PYTHIAZOL-SO2ME-DOTA **201**.

To a solution of Sm-M7PyThiazol-SMe-DOTA **198** (29.0 mg, 36.8 mmol, 1.0 eq.) in dichloromethane (10.0 mL) was added 3-chloroperoxybenzoic acid (>77 %, 82.5 mg, 368 µmol, 10.0 eq.). The mixture was stirred at 20-25 °C for 18 h. The solvent was removed and the residue was purified by preparative HPLC (water, acetonitrile) yielding a white solid (23.1 mg, 28.2 µmol, 76.6 %).

HR-ESI-MS: calcd. for [**201**+H]$^+$ $C_{29}H_{44}N_6O_8S_2Sm$ m/z= 820.1852, found m/z= 820.1852.

^{1}H-NMR (600.13 MHz, 298 K, D_2O): δ = 8.41 (d, $^3J_{HH}$ = 8.7 Hz, 1 H, H_{25}), 7.97 (d, $^3J_{HH}$ = 8.7 Hz, 1 H, H_{24}), 7.91 (bs, 1 H, H_{11}), 7.49 (d, $^2J_{HH}$ = 15.9 Hz, 1 H, H_{22a}), 7.02 (q, $^3J_{HH}$ = 6.9 Hz, 1 H, H_{20}), 6.53 (q, $^3J_{HH}$ = 6.8 Hz, 1 H, H_{14}), 6.10 (q, $^3J_{HH}$ = 7.3 Hz, 1 H, H_{17}), 5.56 (d, $^2J_{HH}$ = 15.9 Hz, 1 H, H_{22b}), 4.71 (bs, 1 H, H_5), 4.54 (bs, 1 H, H_2), 3.33 (s, 3 H, H_{29}), 2.76 (d, $^3J_{HH}$ = 6.9 Hz, 3 H, H_{19}), 2.58 (d, $^2J_{HH}$ = 14.2 Hz, 1 H, H_{1eq}), 2.45 (d, $^3J_{HH}$ = 6.8 Hz, 3 H, H_{13}), 2.28 (d, $^2J_{HH}$ = 14.9 Hz, 1 H, H_{10eq}), 1.86 (bs, 1 H, H_8), 1.83 (d, $^2J_{HH}$ = 14.8 Hz, 1 H, H_{4eq}), 1.68 (d, $^3J_{HH}$ = 7.3 Hz, 3 H, H_{16}), 1.59 (d, $^3J_{HH}$ = 6.2 Hz, 3 H, H_{12}), 1.05 (d, $^3J_{HH}$ = 6.7 Hz, 3 H, H_3), 0.94 (dd, $^2J_{HH}$ = 14.2 Hz, $^3J_{HH}$ = 13.3 Hz, 1 H, H_{1ax}), 0.16 (d, $^3J_{HH}$ = 5.9 Hz, 3 H, H_9), 0.13 (d, $^3J_{HH}$ = 6.3 Hz, 3 H, H_6), –0.73 (d, $^2J_{HH}$ = 15.4 Hz, 1 H, H_{7eq}), –1.78 (dd, $^2J_{HH}$ = 14.9 Hz, $^3J_{HH}$ = 11.4 Hz, 1 H, H_{10ax}), –2.46 (dd, $^2J_{HH}$ = 14.8 Hz, $^3J_{HH}$ = 11.03 Hz, 1 H, H_{4ax}), –3.96 (dd, $^2J_{HH}$ = 15.4 Hz, $^3J_{HH}$ = 13.4 Hz, 1 H, H_{7ax}).

^{13}C{H}-NMR (150.92 MHz, 298 K, D_2O): δ = 195.38 (1 C, C_{21}), 194.95 (1 C, C_{15}), 187.76 (1 C, C_{18}), 167.05 (1 C, C_{28}), 163.41 (1 C, C_{23}), 154.83 (1 C, C_{27}), 145.01 (1 C, C_{26}), 136.28 (1 C, C_{25}), 122.25 (1 C, C_{24}), 73.48 (1 C, C_{14}), 72.24 (1 C, C_{20}), 70.15 (1 C, C_{22}), 67.05 (1 C, C_{17}), 64.98 (1 C, C_{11}), 63.69 (1 C, C_2), 59.24 (1 C, C_5), 57.84 (1 C, C_8), 57.30 (1 C, C_1), 47.78 (1 C, C_{29}), 45.72 (1 C, C_{10}), 45.85 (1 C, C_4), 40.52 (1 C, C_7), 14.77 (1 C, C_{19}), 14.09 (1 C, C_{13}), 12.09 (1 C, C_3), 11.79 (1 C, C_6), 11.68 (1 C, C_{16}), 10.76 (1 C, C_9), 9.37 (1 C, C_{12}).

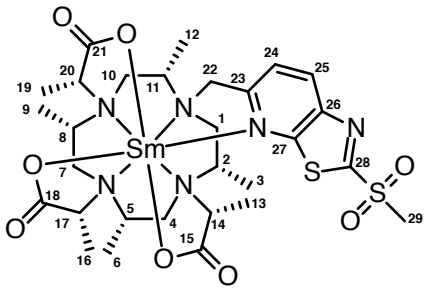

201

2-(4-(METHOXYCARBONYL)PHENOXY)-6-METHYLNICOTINIC ACID (**214**).

Sodium methoxide (490 mg, 9.00 mmol, 1.5 eq.) was dissolved in dry methanol (5.00 mL), followed by the addition of methyl-4-hydroxybenzoate (4.56 g, 30.0 mmol, 5.0 eq.) and 6-methyl-2-chloronicotinic acid (1.03 g, 6.00 mmol, 1.0 eq.). Methanol was removed under reduced pressure and the reaction was heated for 24 h at 125 °C in a Kugelrohr oven. To the oil residue water (20 mL) and methyl *tert*-butyl ether (20.0 mL) were added. The layers were separated, and the aqueous layer was extracted with methyl *tert*-butyl ether (2x 20 mL). The combined organic layers were extracted with aqueous saturated sodium hydrogen carbonate (30 mL). The combined aqueous layers were acidified with aqueous hydrochloric acid (37 %). The resulting suspension was filtered and washed with cold water (20 mL) yielding an off-white solid (1.41 g, 4.91 mmol, 81.8 %).

HR-ESI-MS: calcd. for [**214**+H]$^+$ $C_{15}H_{14}NO_5$ m/z= 288.0866, found m/z= 288.0868.

^{1}H-NMR (500.13 MHz, 298 K, $CDCl_3$): δ = 8.41 (d, $^3J_{HH}$ = 7.8 Hz, 1 H, H_4), 8.15-8.11 (m, 2 H, H_{11}), 7.26-7.23 (m, 2 H, H_{10}), 7.08 (d, $^3J_{HH}$ = 7.8 Hz, 1 H, H_3), 3.93 (s, 3 H, H_{14}), 2.41 (s, 3 H, H_1).

^{13}C{H}-NMR (125.77 MHz, 298 K, $CDCl_3$): δ = 166.58 (1 C, C_{13}), 165.47 (1 C, C_7), 163.35 (1 C, C_2), 160.11 (1 C, C_6), 156.63 (1 C, C_9), 143.71 (1 C, C_4), 131.48 (2 C, C_{11}), 127.32 (1 C, C_{12}), 121.49 (2 C, C_{10}), 119.79 (1 C, C_3), 110.75 (1 C, C_5), 52.37 (1 C, C_{14}), 24.49 (1 C, C_1).

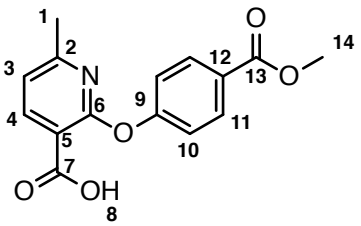

214

METHYL 2-METHYL-5-OXO-5H-CHROMENO[2,3-B]PYRIDINE-7-CARBOXYLATE (**210**).

Polyphosphoric acid (70.0 g) was added to 2-(4-methoxycarbonylphenoxy)--6-methylnicotinic acid (**214**) (1.00 g, 3.48 mmol, 1.0 eq.) and the reaction mixture was stirred at 120 °C for 18 h under argon. The resulting brown liquid was cooled and methanol (50.0 mL) was carefully added. The mixture was stirred until a homogeneous solution was formed. The solution was carefully adjusted to an apparent pH of approximately 7 by the addition of aqueous potassium hydroxide (10 %, 1.20 L). The mixture was extracted with dichloromethane (3x 200 mL) and the solvent was removed yielding a yellow solid. The crude product was crystallized from ethyl acetate / dichloromethane yielding a yellowish solid (530 mg, 1.97 mmol, 56.6 %).

HR-ESI-MS: calcd. for [**210**+H]$^+$ $C_{15}H_{12}NO_4$ m/z= 270.0761, found m/z= 270.0759.

^{1}H-NMR (500.13 MHz, 298 K, $CDCl_3$): δ = 8.99 (d, $^4J_{HH}$ = 2.2 Hz, 1 H, H_{13}), 8.61 (d, $^3J_{HH}$ = 7.8 Hz, 1 H, H_4), 8.41 (dd, $^3J_{HH}$ = 8.8 Hz, $^4J_{HH}$ = 2.2 Hz, 1 H, H_{11}), 7.65 (d, $^3J_{HH}$ = 8.8 Hz, 1 H, H_{10}), 7.34 (d, $^3J_{HH}$ = 7.8 Hz, 1 H, H_3), 3.98 (s, 3 H, H_{15}), 2.73 (s, 3 H, H_1).

^{13}C{H}-NMR (125.77 MHz, 298 K, $CDCl_3$): δ = 177.04 (1 C, C_7), 165.72 (1 C, C_{14}), 165.68 (1 C, C_2), 159.88 (1 C, C_6), 158.22 (1 C, C_9), 137.64 (1 C, C_4), 136.13 (1 C, C_{11}), 129.30 (1 C, C_{13}), 129.07 (1 C, C_{10}), 126.74 (1 C, C_{12}), 121.88 (1 C, C_3), 121.41 (1 C, C_8), 114.36 (1 C, C_5), 52.68 (1 C, C_{15}), 25.30 (1 C, C_1).

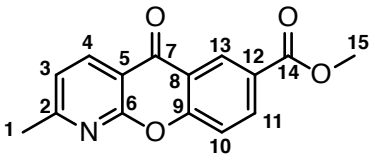

210

METHYL 2-(BROMOMETHYL)-5-OXO-5H-CHROMENO[2,3-B]-PYRIDINE-7-CARBOXYLATE (**213**).

Methyl 2-methyl-5-oxo-5H-chromeno[2,3-b]pyridine-7-carboxylate (**210**) (1.00 g, 3.71 mmol, 1.0 eq.) was suspended in tetrachloromethane (100 mL) and degased with argon. The degassed suspension was heated to reflux under an argon atmosphere. At reflux, acetonitrile (15.0 mL) was added until a solution was formed. *N*-bromosuccinimide (660 mg, 3.71 mmol, 1.0 eq.) and AIBN (1.0 mg) were added and a UV lamp was placed in front of the flask. The reaction was refluxed for 4 d and 5 portions of *N*-bromosuccinimide (660 mg, 3.71 mmol, 1.0 eq.) and AIBN (1.0 mg) were added in portions

ever 12-16 h. The reaction was stopped when the NMR showed a conversion of about 70 %. The crude reaction mixture was cooled to 0-5 °C and the participate was filtered off. The filtrate was evaporated to dryness and the crude product was purified by flash chromatography (SiO_2, dichloromethane / pentane (9 :1)) yielding a white solid (490 mg , 1.41 mmol, 37.9 %).

HR-ESI-MS: calcd. for [**213**+H]$^+$ $C_{15}H_{11}BrNO_4$ m/z= 347.9866, found m/z= 347.9866.

^{1}H-NMR (600.13 MHz, 298 K, $CDCl_3$): δ = 8.99 (d, $^4J_{HH}$ = 2.2 Hz, 1 H, H_{13}), 8.72 (d, $^3J_{HH}$ = 7.9 Hz, 1 H, H_4), 8.43 (dd, $^3J_{HH}$ = 8.8 Hz, $^4J_{HH}$ = 2.2 Hz, 1 H, H_{11}), 7.67 (d, $^3J_{HH}$ = 8.8 Hz, 1 H, H_{10}), 7.62 (d, $^3J_{HH}$ = 7.9 Hz, 1 H, H_3), 4.61 (s, 2 H, H_1), 3.98 (s, 3 H, H_{15}).

^{13}C{H}-NMR (150.92 MHz, 298 K, $CDCl_3$): δ = 176.59 (1 C, C_7), 165.68 (1 C, C_{14}), 162.64 (1 C, C_2), 159.77 (1 C, C_6), 158.35 (1 C, C_9), 138.97 (1 C, C_4), 136.47 (1 C, C_{11}), 129.35 (1 C, C_{13}), 127.22 (1 C, C_{12}), 121.48 (1 C, C_8), 121.46 (1 C, C_3), 119.10 (1 C, C_{10}), 116.13 (1 C, C_5), 52.70 (1 C, C_{15}), 32.14 (1 C, C_1).

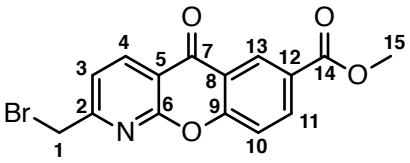

213

TETRA-*tert*-BUTYL 2,2′,2″,2‴-((2*S*,5*S*,8*S*,11*S*)-2,5,8,11-TETRAMETHYL-1,4,7,10-TETRAAZACYCLODODECANE-1,4,7,10-TETRAYL)(2*R*,2′*R*,2″*R*,2‴*R*)-TETRAPROPIONATE (**207**).

(2*S*,5*S*,8*S*,11*S*)-2,5,8,11-tetramethyl-1,4,7,10-tetraazacyclododecane (**22**) (100 mg, 43.8 µmol, 1.0 eq.) and potassium carbonate (363 mg, 2.63 mmol, 6.0 eq.) were suspended in acetonitrile (3.00 mL). tert-Butyl (S)-2-(((trifluoromethyl)sulfonyl)oxy)propanoate (731 mg, 2.63 mmol, 6.0 eq.) was dissolved in acetonitrile (4.0 mL). This solution was added to the reaction and the mixture was stirred for 6 h. The suspension was filtered and evaporated to dryness. The crude product was purified by preparative HPLC (water, acetonitrile) yielding a white solid (220 mg, 297 µmol, 67.8 %).

ESI-MS: calcd. for [**207**+H]$^+$ $C_{40}H_{77}N_4O_8$ m/z= 741.57, found m/z= 741.60.

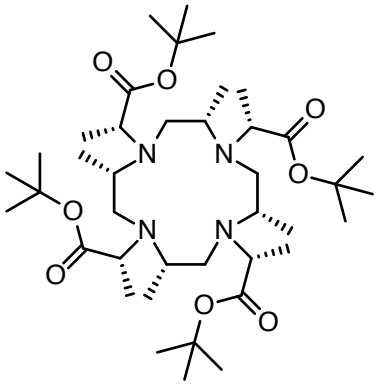

207

(2*R*,2′*R*,2″*R*,2‴*R*)-2,2′,2″,2‴-((2*S*,5*S*,8*S*,11*S*)-2,5,8,11-TETRAMETHYL-1,4,7,10-TETRAAZACYCLODODECANE-1,4,7,10-TETRAYL)TETRAPROPIONIC ACID (**208**).

Tetra-*tert*-butyl 2,2′,2″,2‴-((2*S*,5*S*,8*S*,11*S*)-2,5,8,11-tetramethyl-1,4,7,10-tetraazacyclododecane-1,4,7,10-tetrayl)(2*R*,2′*R*,2″*R*,2‴*R*)-tetrapropionate (**207**) (40.0 mg, 54.0 µmol, 1 eq.) was dissolved in water (15 mL) and trifluoroacetic acid (500 µL) was added. The solution was heated in the microwave to 120 °C and stirred for 30 min. After cooling to 20-25 °C the solution was evaporated to dryness and the crude product was purified by preparative HPLC (water / acetonitrile) yielding a white solid (19.8 mg, 38.0 µmol, 71.0 %).

HR-ESI-MS: calcd. for [**208**+H]$^+$ $C_{24}H_{45}N_4O_8$ m/z= 517.32, found m/z= 517.30.

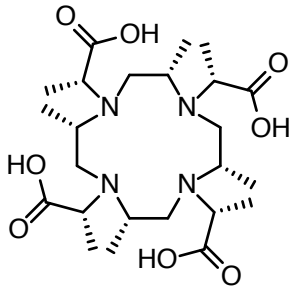

208

METHYL 5-OXO-2-(((2*S*,5*S*,8*S*,11*S*)-2,5,8,11-TETRAMETHYL-1,4,7,10-TETRAAZACYCLODODECAN-1-YL)METHYL)-5H-CHROMENO[2,3-B]PYRIDINE-7-CARBOXYLATE (**236**).

(2*S*,5*S*,8*S*,11*S*)-2,5,8,11-tetramethyl-1,4,7,10-tetraazacyclododecane (**22**) (295 mg, 1.29 mmol, 3.0 eq.) and methyl 2-(bromomethyl)-5-oxo-5H-chromeno[2,3-b]pyridine-7-carboxylate (150 mg, 43.1 µmol, 1.0 eq.) were

suspended in dichloromethane (15 mL) and stirred at 20-25 °C for 18 h. The solvent was removed and the crude product was purified by preparative HPLC (water, acetonitrile) yielding a white solid (120 mg, 242 µmol, 56.2 %).

HR-ESI-MS: calcd. for [**236**+H]$^+$ $C_{27}H_{38}N_5O_4$ m/z= 496.2918, found m/z= 496.2922.

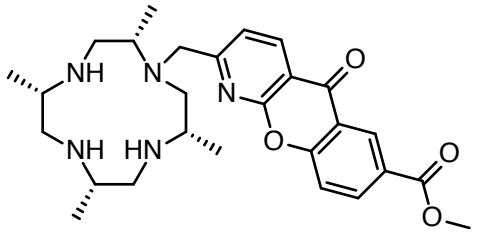

236

TRI-*tert*-BUTYL 2,2′,2″-((2*S*,5*S*,8*S*,11*S*)-10-((7-(METHOXYCARBONYL)-5-OXO-5H-CHROMENO[2,3-B]PYRIDIN-2-YL)METHYL)-2,5,8,11-TETRAMETHYL-1,4,7,10-TETRAAZACYCLODODECANE-1,4,7-TRIYL)(2*R*,2′*R*,2″*R*)-TRIPROPIONATE (**215**).

Method A

Methyl 5-oxo-2-(((2*S*,5*S*,8*S*,11*S*)-2,5,8,11-tetramethyl-1,4,7,10-tetraazacyclododecan-1-yl)methyl)-5H-chromeno[2,3-b]pyridine-7-carboxylate (**236**) (40.0 mg, 80.7 µmol, 1.0 eq.) and potassium carbonate (66.9 mg, 484 µmol, 6.0 eq.) were suspended in acetonitrile (2.0 mL). *tert*-Butyl (*S*)-2-(((trifluoromethyl)sulfonyl)oxy)propanoate (135 mg, 484 µmol, 6.0 eq.) was dissolved in acetonitrile (2.00 mL) and added to the reaction mixture. The reaction was stirred for 4 h. The solids were filtered off and the filtrate was evaporated to dryness. The crude product was purified by preparative HPLC (water, acetonitrile) yielding a white solid (68.2 mg, 77.4 µmol, 88.4 %).

Method B

Tri-*tert*-butyl 2,2′,2″-((2*S*,5*S*,8*S*,11*S*)-2,5,8,11-tetramethyl-1,4,7,10-tetraazacyclododecane-1,4,7-triyl)(2*R*,2′*R*,2″*R*)-tripropionate (**129**) (90.0 mg, 147 µmol, 1.0 eq.), methyl 2-(bromomethyl)-5-oxo-5H-chromeno[2,3-b]pyridine-7-carboxylate (**213**) (56.2 mg, 162 µmol, 1.1 eq.) and potassium carbonate (60.9 mg, 441 µmol, 3.0 eq.) were suspended in acetonitrile (7.0 mL) and stirred at 20-25 °C for 18 h. The suspension was filtered and the filtrate was evaporated to dryness. The crude product was purified by preparative HPLC (water, acetonitrile) yielding a white solid (88.0 mg,

100 µmol, 68.1 %).

ESI-MS: calcd. for [**215**+H]$^+$ $C_{48}H_{74}N_5O_{10}$ m/z= 880.54, found m/z= 880.90.

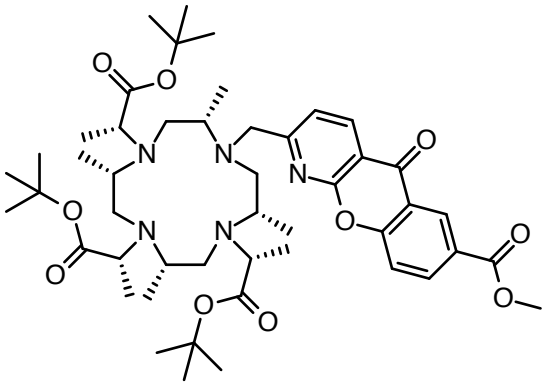

215

(2*R*,2′*R*,2″*R*)-2,2′,2″-((2*S*,5*S*,8*S*,11*S*)-10-((7-(METHOXYCARBONYL)-5-OXO-5H-CHROMENO[2,3-B]PYRIDIN-2-YL)METHYL)-2,5,8,11-TETRAMETHYL-1,4,7,10-TETRAAZACYCLODODECANE-1,4,7-TRIYL)TRIPROPIONIC ACID (**216**).

Tri-*tert*-butyl 2,2′,2″-((2*S*,5*S*,8*S*,11*S*)-10-((7-(methoxycarbonyl)-5-oxo-5H-chromeno[2,3-b]pyridin-2-yl)methyl)-2,5,8,11-tetramethyl-1,4,7,10-tetraazacyclododecane-1,4,7-triyl)(2*R*,2′*R*,2″*R*)-tripropionate (**215**) (30.0 mg, 34.0 µmol, 1.0 eq.) was dissolved in a mixture of trifluoroacetic acid / thioanisol / water 92:6:2 (4.0 mL) and stirred at 20-25 °C for 7 h. The solution was evaporated to dryness and the crude product was purified by preparative HPLC (water / acetonitrile) yielding a white solid (22.1 mg, 31.0 µmol, 91.1 %).

ESI-MS: calcd. for [**216**+H]$^+$ $C_{36}H_{50}N_5O_{10}$ m/z= 712.35, found m/z= 712.60.

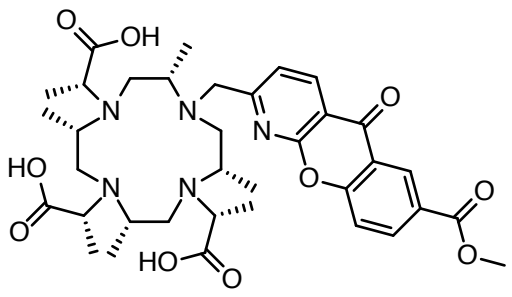

216

EU-DOTA-M7-AZAXANTHON **209**.

(2*R*,2′*R*,2″*R*)-2,2′,2″-((2*S*,5*S*,8*S*,11*S*)-10-((7-(methoxycarbonyl)-5-oxo-5H-chromeno[2,3-b]pyridin-2-yl)methyl)-2,5,8,11-tetramethyl-1,4,7,10-tetraazacyclododecane-1,4,7-triyl)tripropionic acid (**216**) (20.8 mg, 29.2 µmol, 1.0 eq.) and $Eu(OTf)_3$ (64.8 mg, 108 µmol, 4.0 eq.) were dissolved in aqueous ammonium acetate (100 mM, 5.0 mL) and stirred at 75 °C for 18 h. The reaction mixture was directly purified by preparative HPLC (water, acetonitrile) yielding a white solid (12.9 mg, 15.0 µmol, 55.4 %).

HR-ESI-MS: calcd. for [**209**+H]$^+$ $C_{36}H_{47}EuN_5O_{10}$ m/z= 862.25, found m/z= 862.60.

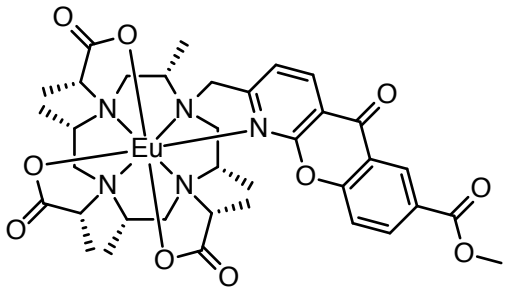

209

EU-DOTA-M8 **202**.

Tetra-*tert*-butyl 2,2′,2″,2‴-((2*S*,5*S*,8*S*,11*S*)-2,5,8,11-tetramethyl-1,4,7,10-tetraazacyclododecane-1,4,7,10-tetrayl)(2*R*,2′*R*,2″*R*,2‴*R*)-tetrapropionate (**207**) (40.0 mg, 77.4 µmol, 1.0 eq.) and $Eu(OTf)_3$ (57.5 mg, 96.0 µmol, 1.2 eq.) were dissolved in aqueous ammonium acetate (100 mM, 5.0 mL). The solution was stirred at 70 °C for 16 h. The reaction mixture was cooled to 20-25 °C and directly purified by preparative HPLC (water, acetonitrile) yielding a white solid (22.4 mg, 34.0 µmol, 43.5 %).

HR-ESI-MS: calcd. for [**202**+2Na]$^+$ $C_{24}H_{40}EuN_4Na_2O_8$ m/z= 711.1850, found m/z= 711.1834.

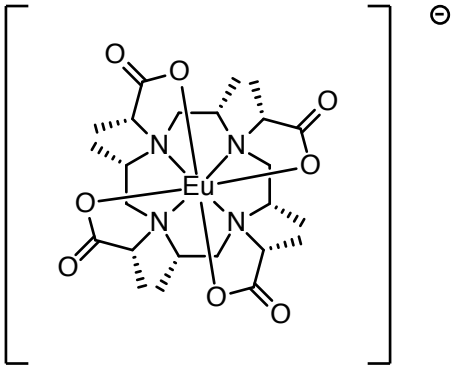

202

EU-DOTA-M4 **203**.

(2R,2′R,2″R,2‴R)-2,2′,2″,2‴-(1,4,7,10-tetraazacyclododecane-1,4,7,10-tetrayl)tetrapropionic acid (20.0 mg, 36.5 µmol, 1.0 eq.) was dissolved in aqueous ammonium acetate (100 mM, 4.00 mL) and stirred at 70 °C for 17 h. The reaction mixture was cooled to 20-25 °C and directly purified by preparative HPLC (water, acetonitrile) yielding a white solid (24.1 mg, quant.).

ESI-MS: calcd. for [**203**]$^-$ m/z= 609.14, found m/z= 609.40.

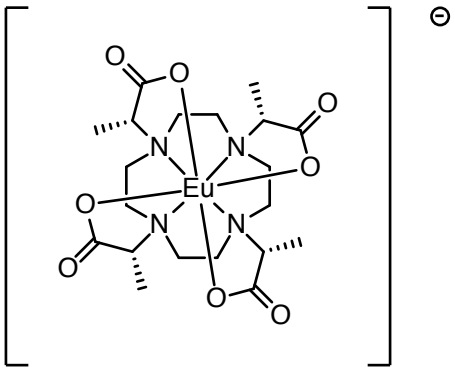

203

EU-DOTA **204**.

2,2′,2″,2‴-(1,4,7,10-tetraazacyclododecane-1,4,7,10-tetrayl)tetraacetic acid (10.0 mg, 24.0 µmol, 1.0 eq.) was dissolved in aqueous ammonium acetate (100 mM, 4.00 mL) and stirred at 70 °C for 17 h. The reaction mixture was cooled to 20-25 °C and directly purified by preparative HPLC (water, acetonitrile) yielding a white solid (13.6 mg, quant.).

HR-ESI-MS: calcd. for [**204**]$^-$ $C_{16}H_{24}EuN_4O_8$ m/z= 553.08, found m/z= 553.30.

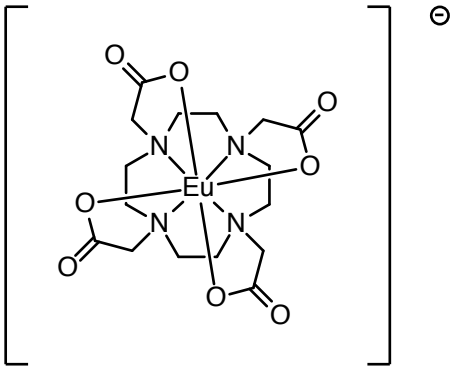

204

(2*R*,2′*R*,2′′*R*)-2,2′,2′′-((2*S*,5*S*,8*S*,11*S*)-10-((*R*)-1-((6-((2-(4--(DIMETHYLAMINO)PHENYL)BENZO[D]THIAZOL-6-YL)OXY)HEXYL)AMINO)-1-OXOPROPAN-2-YL)-2,5,8,11-TETRAMETHYL-1,4,7,10-TETRAAZACYCLODODECANE-1,4,7-TRIYL)TRIPROPIONIC ACID (**237**).

4-(6-((6-aminohexyl)oxy)benzo[d]thiazol-2-yl)-N,N-dimethylaniline (50.0 mg, 135 µmol, 1.0 eq.) was dissolved in dimethylformamide (10.0 mL). *N*-Diisopropylamine (134 µL, 810 µmol, 6.0 eq.) and HATU (61.6 mg, 162 mmol, 1.2 eq.) were added. The solution was stirred at 20-25 °C for 1 h. The reaction mixture was evaporated to dryness yielding a yellow crude product. The crude product was purified by flash column chromatography (SiO_2, ethyl acetate). The fractions containing the product were evaporated to dryness and the residue was dissolved in hydrobromic acid solution (5 % in acetic acid, 2.0 mL) and stirred at 40 °C for 20 min. The solution was evaporated to dryness and the residue was purified by preparative HPLC (water, acetonitrile) yielding a yellow solid (72.0 mg, 82.9 µmol, 61.4 %).

ESI-MS: calcd. for [**237**+2H]$^{2+}$ $C_{45}H_{72}N_7O_8S$ m/z= 434.75, found m/z= 434.64.

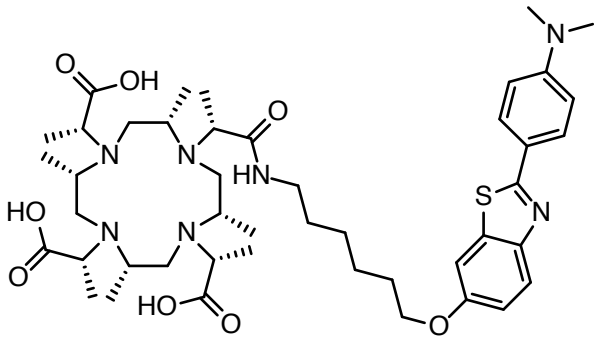

237

GD-M8-PITSC6-DOTA **238**.

(2*R*,2′*R*,2″*R*)-2,2′,2″-((2*S*,5*S*,8*S*,11*S*)-10-((*R*)-1-((6-((2-(4-(dimethylamino)-phenyl)benzo[d]thiazol-6-yl)oxy)hexyl)amino)-1-oxopropan-2-yl)-2,5,8,11-tetramethyl-1,4,7,10-tetraazacyclododecane-1,4,7-triyl)tripropionic acid (**237**) (72.0 mg, 82.9 µmol, 1.0 eq.) was dissolved in dimethylformamide (5.0 mL) and $Gd(OTf)_3$ (326 mg, 540 µmol, 6.5 eq.) was added. The solution was heated to 80 °C for 16 h. The solvent was evaporated and the crude product was purified by preparative HPLC (water, acetonitrile) yielding a yellow solid (60.0 mg, 58.7 µmol, 70.8 %).

ESI-MS: calcd. for [**238**+2H]$^{2+}$ $C_{45}H_{66}GdN_7O_8S$ m/z= 512.20, found m/z= 512.09.

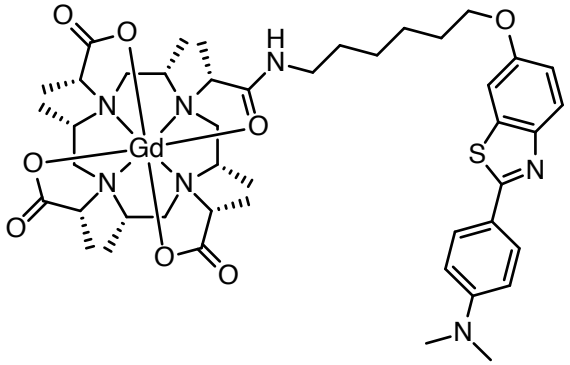

238

A

APPENDIX

Table A.1: *In-vitro* ^{1}H-^{15}N HSQC peak assignment in ppm of GB1 E19C tagged with Lu, Tb and Tm loaded M7Py-DOTA at 298 K.

Residue	**Lu**		**Tm**		**Tb**	
	HN	N	HN	N	HN	N
M1	-	-	-	-	-	-
Q2	-	-	-	-	-	-
Y3	124.2	9.10	-	-	-	-
K4	122.9	9.26	-	-	-	-
L5	126.8	8.75	126.3	7.49	125.8	7.83
I6	126.6	9.27	126.0	8.84	126.1	8.82
L7	126.0	8.86	125.4	8.00	125.7	8.74
N8	126.8	9.08	126.4	8.72	126.6	8.87
G9	110.0	8.09	109.7	7.68	109.7	7.96
K10	121.5	9.69	121.3	9.46	121.3	9.53
T11	108.8	8.98	108.6	8.71	108.6	8.84
L12	125.9	7.53	125.6	7.17	125.7	7.42
K13	124.2	8.28	123.6	7.69	124.0	8.23
G14	109.7	8.60	108.9	7.76	109.6	8.58
E15	119.1	8.58	117.6	7.03	119.0	8.70
T16	116.0	8.91	113.9	6.97	115.6	8.54
T17	112.0	8.24	-	-	-	-
T18	114.3	9.11	-	-	-	-
E19	-	-	-	-	-	-
A20	126.4	9.35	-	-	-	-
V21	116.2	8.72	-	-	-	-
D22	115.7	7.49	-	-	111.0	3.56

Continued on next page

Table A.1 – continued from previous page

Residue	Lu		Tm		Tb	
	HN	N	HN	N	HN	N
A23	121.9	8.47	-	-	-	-
A24	120.9	8.22	125.1	12.77	118.7	6.00
T25	116.7	8.44	-	-	115.0	6.60
A26	124.1	7.34	-	-	-	-
E27	117.1	8.48	119.7	11.69	115.2	6.51
K28	117.0	7.10	118.5	8.94	115.7	5.91
V29	121.0	7.49	121.9	8.76	119.9	6.34
F30	121.1	8.66	121.6	9.62	120.0	7.44
K31	123.3	9.25	123.7	9.94	122.5	8.42
Q32	120.0	7.59	120.1	7.93	119.3	7.04
Y33	121.4	8.40	121.1	8.25	120.8	8.00
A34	122.9	9.35	122.7	9.21	122.5	8.93
N35	118.0	8.42	117.9	8.38	117.6	8.08
D36	121.8	9.10	121.6	8.90	121.5	8.89
N37	115.8	7.55	115.5	7.21	115.6	7.35
G38	108.4	7.96	108.2	7.74	108.2	7.74
V39	121.4	8.26	121.2	8.08	121.1	8.00
D40	128.2	8.77	128.1	8.71	127.7	8.49
G41	107.5	7.90	107.6	8.00	107.1	7.56
E42	121.2	8.33	121.3	8.41	120.9	8.01
W43	128.8	9.50	129.3	9.86	128.3	9.02
T44	115.1	9.45	115.6	9.91	114.4	8.86
Y45	121.0	8.72	122.0	9.60	120.0	7.95
D46	128.8	7.79	129.9	9.02	127.7	6.73
D47	125.3	8.72	127.0	10.20	123.9	7.58
A48	120.2	8.48	121.4	9.41	119.0	7.58
T49	103.6	7.15	103.9	7.66	103.0	6.53
K50	123.5	8.01	125.9	10.24	121.8	6.40
T51	111.5	7.53	113.3	9.14	110.1	6.27
F52	131.3	10.52	132.4	11.45	130.0	9.31
T53	117.6	9.28	117.9	9.73	116.8	8.61
V54	123.7	8.32	123.8	8.19	123.1	7.93
T55	124.2	8.51	124.2	8.52	123.8	8.17

Continued on next page

Table A.1 – continued from previous page

Residue	Lu		Tm		Tb	
	HN	N	HN	N	HN	N
E56	134.4	7.96	134.4	7.80	101.2	7.74

Table A.2: *In-vitro* ^{1}H-^{15}N HSQC peak assignment in ppm of GB1 E42C tagged with Lu, Tb and Tm loaded M7Py-DOTA at 298 K.

Residue	Lu		Tm		Tb	
	HN	N	HN	N	HN	N
Q2	123.8	8.42	124.0	8.70	123.6	8.32
Y3	125.0	9.27	125.1	9.45	124.7	8.95
K4	122.7	9.25	122.8	9.40	122.3	8.96
L5	126.8	8.76	126.8	8.79	126.1	8.18
I6	126.6	9.26	126.5	8.99	125.5	8.38
L7	126.1	8.87	125.9	8.76	124.8	7.67
N8	126.8	9.05	126.0	7.73	125.1	7.40
G9	110.1	8.11	109.0	7.30	109.0	7.04
K10	121.5	9.66	120.1	7.98	121.1	9.45
T11	108.8	8.99	108.1	8.04	108.5	8.74
L12	125.8	7.52	125.3	6.78	125.3	7.09
K13	124.1	8.28	123.9	8.15	123.2	7.55
G14	109.7	8.61	109.7	8.64	108.6	7.50
E15	119.1	8.57	119.2	8.66	118.2	7.81
T16	116.1	8.90	116.1	8.91	115.4	8.22
T17	112.2	8.23	112.2	8.25	111.6	7.79
T18	115.1	9.14	115.1	9.25	114.6	8.77
E19	126.4	8.10	126.5	8.19	126.1	7.79
A20	127.8	9.49	128.0	9.69	127.6	9.20
V21	116.1	8.64	116.4	8.89	115.8	8.34
D22	115.6	7.49	115.9	7.87	115.2	7.12
A23	121.8	8.44	122.5	9.17	121.3	8.02
A24	120.9	8.21	121.9	9.18	120.1	7.55
T25	116.7	8.43	117.3	9.06	116.1	7.88
A26	124.0	7.30	124.5	7.84	123.5	6.78
E27	117.0	8.50	117.7	9.31	116.2	7.73

Continued on next page

Table A.2 – continued from previous page

Residue	Lu		Tm		Tb	
	HN	N	HN	N	HN	N
K28	116.9	7.10	117.4	7.64	116.2	6.42
V29	121.0	7.45	121.1	7.62	120.6	6.98
F30	121.0	8.67	121.0	8.76	120.5	8.13
K31	123.3	9.25	123.0	9.19	122.8	8.70
Q32	119.9	7.57	119.3	7.14	-	-
Y33	121.3	8.38	120.7	7.89	121.0	8.12
A34	123.0	9.36	122.1	8.54	122.7	9.11
N35	118.1	8.45	116.8	7.23	118.2	8.55
D36	121.9	9.08	120.9	8.16	122.0	9.14
N37	115.8	7.55	115.0	6.60	115.8	7.52
G38	108.5	7.97	107.3	6.78	108.5	8.12
V39	121.3	8.26	119.5	6.61	121.4	8.40
D40	127.8	8.70	124.4	5.42	128.2	9.25
G41	106.7	8.06	100.3	1.99	107.4	9.02
E42	119.9	8.65	-	-	-	-
W43	132.6	9.75	129.2	3.76	-	-
T44	114.9	9.50	-	-	-	-
Y45	120.9	8.75	-	-	119.6	7.33
D46	128.8	7.75	128.0	7.16	131.0	9.33
D47	125.3	8.75	125.1	8.52	126.7	10.55
A48	120.3	8.50	120.1	8.07	121.2	9.93
T49	103.6	7.16	103.4	6.86	104.1	8.10
K50	123.6	8.01	123.6	8.00	123.9	8.51
T51	111.4	7.53	111.3	7.43	111.6	8.04
F52	131.5	10.54	131.4	10.50	131.4	10.27
T53	117.9	9.34	116.6	7.86	-	-
V54	123.6	8.35	121.2	6.52	122.2	6.95
T55	123.8	8.52	117.6	0.78	-	-
E56	134.8	8.03	-	-	101.4	7.25

Table A.3: *In-vitro* ^{1}H-^{15}N HSQC peak assignment in ppm of GB1 K28C tagged with Lu, Tb and Tm loaded M7Py-DOTA at 298 K.

Residue	**Lu**		**Tm**		**Tb**	
	HN	N	HN	N	HN	N
M1	-	-	-	-	-	-
Q2	123.9	8.52	124.4	8.88	122.86	7.73
Y3	124.9	9.27	125.6	10.18	123.37	7.63
K4	122.7	9.26	123.4	9.82	-	-
L5	126.8	8.77	127.3	9.36	126.01	8.02
I6	126.6	9.27	126.8	9.45	-	-
L7	126.0	8.87	126.1	8.98	125.55	8.38
N8	126.9	9.08	126.7	8.88	126.71	9.04
G9	110.0	8.08	109.8	7.99	109.82	7.93
K10	121.5	9.69	121.3	9.49	121.35	9.68
T11	108.9	8.97	108.9	8.95	-	-
L12	125.9	7.54	126.0	7.57	-	-
K13	124.2	8.27	124.3	8.35	123.70	7.94
G14	109.7	8.59	109.8	8.68	109.19	8.19
E15	119.1	8.57	119.4	8.80	118.36	7.95
T16	116.2	8.91	116.6	9.38	115.04	7.87
T17	112.2	8.23	113.0	9.03	110.53	6.70
T18	115.0	9.14	116.5	10.38	-	-
E19	126.4	8.11	128.1	10.03	125.52	7.50
A20	127.8	9.47	128.8	10.33	-	-
V21	116.3	8.69	117.5	9.11	-	-
D22	115.7	7.49	-	-	-	-
A23	121.7	8.44	122.3	9.05	-	-
A24	121.2	8.23	121.9	8.99	-	-
T25	117.2	8.49	118.2	9.37	-	-
A26	124.1	7.34	125.1	7.94	-	-
E27	117.2	8.58	-	-	-	-
K28	115.7	7.41	-	-	-	-
V29	121.8	7.74	-	-	-	-
F30	121.0	8.72	-	-	-	-
K31	123.4	9.16	-	-	-	-

Continued on next page

Table A.3 – continued from previous page

Residue	Lu		Tm		Tb	
	HN	N	HN	N	HN	N
Q32	119.7	7.64	122.8	10.88	-	-
Y33	121.5	8.36	-	-	-	-
A34	123.0	9.38	123.5	10.40	-	-
N35	117.9	8.34	-	-	-	-
D36	121.7	9.02	-	-	-	-
N37	115.7	7.53	-	-	-	-
G38	108.5	7.94	109.4	9.17	107.39	6.71
V39	121.4	8.23	-	-	-	-
D40	128.5	8.80	127.8	8.22	128.70	9.06
G41	107.6	7.90	105.7	5.81	109.08	9.91
E42	120.9	8.33	119.2	6.93	122.68	9.74
W43	128.8	9.50	127.1	7.43	131.11	12.39
T44	115.1	9.45	114.5	8.85	116.06	10.31
Y45	120.7	8.74	120.8	8.50	121.20	9.15
D46	128.8	7.79	128.9	7.91	128.47	7.51
D47	125.3	8.73	125.4	8.93	124.85	8.44
A48	120.2	8.49	120.4	8.68	119.74	8.16
T49	103.6	7.16	103.8	7.35	103.11	6.77
K50	123.5	8.02	123.8	8.29	122.84	7.47
T51	111.5	7.53	111.9	7.79	110.76	6.97
F52	131.3	10.53	131.5	10.88	130.59	9.71
T53	117.6	9.28	116.7	8.48	117.40	9.38
V54	123.8	8.32	123.4	8.09	123.90	8.35
T55	124.2	8.52	123.5	7.66	124.72	9.38
E56	134.3	7.96	133.6	7.45	-	-

Table A.4: *In-cell* ^{1}H-^{15}N HSQC peak assignment in ppm of GB1 E19C tagged with Lu and Tm loaded M7Py-DOTA at 298 K.

Residue	Lu		Tm	
	HN	N	HN	N
M1	-	-	-	
Q2	-	-	-	-

Continued on next page

Table A.4 – continued from previous page

Residue	Lu		Tm	
	HN	N	HN	N
Y3	-	-	-	-
K4	124.1	9.08	-	-
L5	122.9	9.24	-	-
I6	126.8	8.75	126.2	7.50
L7	126.6	9.26	125.9	8.81
N8	126.0	8.86	125.3	7.95
G9	126.8	9.07	126.3	8.66
K10	110.0	8.08	109.6	7.61
T11	121.5	9.68	121.2	9.38
L12	108.8	8.97	108.5	8.64
K13	125.8	7.51	125.5	7.10
G14	124.1	8.26	-	-
E15	109.7	8.58	108.8	7.71
T16	119.1	8.57	117.6	7.00
T17	116.1	8.90	113.8	7.00
T18	112.0	8.24	-	-
E19	114.2	9.10	-	-
A20	126.0	9.27	-	-
V21	116.3	8.73	-	-
D22	115.7	7.48	-	-
A23	121.9	8.48	-	-
A24	120.9	8.22	-	-
T25	116.8	8.43	-	-
A26	124.1	7.34	-	-
E27	117.0	8.46	-	-
K28	117.0	7.09	-	-
V29	121.0	7.49	121.7	8.68
F30	121.0	8.66	121.5	9.53
K31	122.9	9.24	-	
Q32	119.9	7.59	120.1	7.86
Y33	121.3	8.38	121.0	8.16
A34	122.9	9.34	122.6	9.14
N35	118.0	8.41	117.8	8.31

Continued on next page

Table A.4 – continued from previous page

Residue	Lu		Tm	
	HN	N	HN	N
D36	121.8	9.09	121.6	8.81
N37	115.8	7.53	-	-
G38	108.4	7.95	108.0	7.68
V39	121.3	8.25	121.1	8.01
D40	128.2	8.78	128.1	8.65
G41	107.5	7.89	107.5	7.93
E42	121.2	8.33	121.2	8.34
W43	128.8	9.49	129.2	9.79
T44	115.0	9.44	115.5	9.83
Y45	121.0	8.70	121.9	9.51
D46	128.8	7.78	129.8	8.93
D47	125.2	8.72	126.9	10.13
A48	120.2	8.47	121.3	9.33
T49	103.5	7.15	103.8	7.58
K50	123.4	8.00	-	-
T51	111.5	7.52	113.1	9.02
F52	131.3	10.51	132.3	11.40
T53	117.6	9.27	117.9	9.66
V54	123.7	8.31	123.8	8.12
T55	124.2	8.50	124.1	8.46
E56	134.3	7.96	134.3	7.73

Table A.5: *In-cell* ^{1}H-^{15}N HSQC peak assignment in ppm of GB1 E42C tagged with Lu and Tm loaded M7Py-DOTA at 298 K.

Residue	Lu		Tm	
	HN	N	HN	N
M1	-	-	-	-
Q2	123.8	8.41	124.0	8.69
Y3	124.9	9.26	125.1	9.42
K4	122.7	9.24	122.8	9.37
L5	126.8	8.76	126.8	8.77
I6	126.6	9.25	126.5	8.97

Continued on next page

Table A.5 – continued from previous page

Residue	Lu		Tm	
	HN	N	HN	N
L7	126.1	8.87	125.9	8.76
N8	126.8	9.04	126.0	7.72
G9	110.1	8.10	109.0	7.30
K10	121.5	9.65	120.1	7.96
T11	108.8	8.99	108.1	8.04
L12	125.8	7.51	125.2	6.77
K13	124.1	8.28	123.9	8.15
G14	109.7	8.60	109.7	8.65
E15	119.1	8.56	119.2	8.66
T16	116.1	8.90	116.1	8.90
T17	112.2	8.23	112.2	8.25
T18	115.0	9.13	115.0	9.24
E19	126.4	8.10	126.5	8.18
A20	127.8	9.48	128.0	9.67
V21	116.1	8.64	116.3	8.88
D22	115.6	7.48	115.9	7.85
A23	121.8	8.45	122.8	9.15
A24	120.9	8.21	121.8	9.15
T25	116.8	8.43	117.3	9.03
A26	124.0	7.30	124.5	7.81
E27	117.0	8.48	117.7	9.27
K28	116.9	7.09	117.3	7.61
V29	121.0	7.45	121.0	7.60
F30	121.0	8.66	121.0	8.73
K31	123.2	9.25	122.8	9.15
Q32	119.9	7.57	119.3	7.13
Y33	121.3	8.37	120.7	7.88
A34	123.0	9.35	122.1	8.53
N35	118.1	8.45	116.8	7.23
D36	121.9	9.07	120.9	8.15
N37	115.7	7.53	115.0	6.59
G38	108.5	7.96	107.3	6.79
V39	121.3	8.25	119.5	6.61

Continued on next page

Table A.5 – continued from previous page

Residue	Lu		Tm	
	HN	N	HN	N
D40	127.8	8.70	-	-
G41	106.7	8.05	100.3	2.03
E42	119.9	8.64	-	-
W43	132.6	9.74	-	-
T44	114.9	9.49	-	-
Y45	120.9	8.74	-	-
D46	128.8	7.73	127.9	7.08
D47	125.3	8.74	125.1	8.45
A48	120.2	8.49	120.1	8.03
T49	103.5	7.15	103.3	6.82
K50	123.6	8.00	123.5	7.97
T51	111.4	7.52	111.3	7.38
F52	131.5	10.53	131.4	10.45
T53	117.9	9.32	116.5	7.75
V54	123.7	8.35	121.1	6.47
T55	123.8	8.52	-	-
E56	134.7	8.03	-	-

Table A.6: *In-cell* ^{1}H-^{15}N HSQC peak assignment in ppm of GB1 K28C tagged with Lu and Tm loaded M7Py-DOTA at 298 K.

Residue	Lu		Tm	
	HN	N	HN	N
M1	-	-	-	-
Q2	123.9	8.51	124.4	8.89
Y3	124.8	9.26	125.6	10.19
K4	122.8	9.26	123.4	9.84
L5	126.8	8.77	127.3	9.36
I6	126.6	9.27	126.9	9.45
L7	126.1	8.87	126.1	8.98
N8	126.8	9.08	126.7	8.87
G9	110.0	8.08	109.8	7.98
K10	121.5	9.68	121.3	9.49

Continued on next page

Table A.6 – continued from previous page

Residue	Lu		Tm	
	HN	N	HN	N
T11	108.8	8.97	108.8	8.96
L12	125.9	7.53	125.9	7.56
K13	124.0	8.26	124.2	8.35
G14	109.7	8.59	109.8	8.67
E15	119.1	8.57	119.4	8.80
T16	116.2	8.91	116.6	9.39
T17	112.2	8.23	113.1	9.04
T18	115.0	9.14	116.5	10.38
E19	126.4	8.11	128.1	10.05
A20	127.7	9.47	128.8	10.32
V21	116.2	8.69	117.5	9.11
D22	115.7	7.48	-	-
A23	121.7	8.44	122.3	9.06
A24	121.1	8.22	121.9	8.98
T25	117.2	8.49	118.2	9.35
A26	124.1	7.34	125.1	7.94
E27	117.2	8.57	-	-
K28	115.7	7.40	-	-
V29	121.7	7.75	-	-
F30	121.0	8.72	-	-
K31	123.3	9.15	-	-
Q32	119.7	7.64	-	-
Y33	121.4	8.35	-	-
A34	123.0	9.38	123.5	10.36
N35	117.9	8.34	-	-
D36	121.6	9.01	-	-
N37	115.7	7.53	-	-
G38	108.4	7.94	109.4	9.16
V39	121.4	8.22	-	-
D40	128.5	8.81	127.8	8.21
G41	107.6	7.89	105.8	5.79
E42	121.0	8.33	119.2	6.93
W43	128.8	9.50	127.1	7.44

Continued on next page

Table A.6 – continued from previous page

Residue	Lu		Tm	
	HN	N	HN	N
T44	115.1	9.44	114.4	8.84
Y45	120.7	8.74	120.8	8.51
D46	128.8	7.79	128.9	7.91
D47	125.3	8.73	125.4	8.93
A48	120.2	8.49	120.4	8.68
T49	103.6	7.16	103.7	7.35
K50	123.5	8.01	124.0	8.29
T51	111.5	7.53	111.9	7.79
F52	131.3	10.52	131.5	10.88
T53	117.6	9.27	116.7	8.47
V54	123.9	8.32	123.4	8.08
T55	124.2	8.51	123.5	7.66
E56	134.3	7.96	133.6	7.46

Table A.7: *In-vitro* and *in-cell* ^{1}H-^{15}N backbone amide RDC in Hz of GB1 mutants tagged with Tm (paramagnetic) and Lu (diamagnetic reference) loaded M7Py-DOTA at 293 K and 600 MHz.

Residue	*in-vitro*			*in-cell*		
	E19C	E42C	K28C	E19C	E42C	K28C
1	-	-	-	-	-	-
2	-	-3.9	4.9	-	1.0	5.4
3	-	-10.6	1.8	-	-14.5	-6.6
4	-	-7.2	6.1	-	-2.4	-
5	12.8	1.1	-2.3	23.5	1.6	1.8
6	14.0	2.6	4.3	11.6	0.7	7.2
7	22.0	7.1	-2.8	20.3	7.8	-1.9
8	14.2	5.4	3.7	23.8	5.0	3.5
9	15.5	5.4	-7.0	16.3	5.2	-4.9
10	7.1	1.3	-1.0	-	0.7	-
11	2.4	1.5	-0.3	3.8	2.2	-0.8
12	15.8	3.3	-1.1	15.1	6.0	-3.8
13	9.4	1.1	5.3	-	2.5	5.0

Continued on next page

Table A.7 – continued from previous page

Residue	*in-vitro*			*in-cell*		
	E19C	E42C	K28C	E19C	E42C	K28C
14	11.4	0.4	1.5	14.5	1.3	-0.9
15	8.8	-1.0	1.8	-	-0.5	0.0
16	5.4	-8.0	2.4	-	-2.1	1.9
17	-	-11.0	0.2	-	-6.1	3.3
18	-	-11.4	16.7	-	-9.2	5.1
19	-	-11.1	0.7	-	-8.1	5.1
20	-	-8.1	0.1	-	-7.8	2.3
21	-	-11.7	-	-	-8.1	-
22	-	-7.4	-	-	-4.0	-
23	-	-12.0	16.1	-	-4.3	12.1
24	-7.8	6.4	5.0	-	2.2	9.3
25	-	-0.1	13.3	-	0.3	10.4
26	-	-4.0	-	-	-3.6	11.4
27	-5.2	-0.9	-	-	0.2	-
28	-9.9	5.4	-	-	2.9	-
29	-8.9	-1.5	-	-	-1.3	-
30	-6.1	-2.6	-	-	-0.9	-
31	-6.1	-6.0	-	-	3.0	-
32	-7.8	5.2	-	-4.0	3.6	-
33	-8.5	-0.9	-	-16.5	-0.3	-
34	-4.4	-0.2	-	-6.8	1.1	-
35	-7.5	-0.4	-	-7.9	3.3	-
36	-8.5	3.1	-	-15.0	2.0	-
37	-4.9	-1.9	-	-	-1.4	4.2
38	-6.4	0.8	2.4	-	0.1	-2.9
39	-9.4	-2.7	-	-18.7	1.9	-7.7
40	-7.8	-	-1.2	-0.8	-	-1.5
41	-6.1	-	0.6	-1.0	2.1	-4.0
42	2.1	-	3.4	2.1	-	-0.4
43	19.6	-	-	17.5	6.4	3.7
44	13.7		2.9	12.9	-	1.6
45	7.8	-	1.8	10.5	-	-0.8
46	3.1	-3.2	7.4	-3.8	-3.6	1.9

Continued on next page

Table A.7 – continued from previous page

Residue	***in-vitro***			***in-cell***		
	E19C	E42C	K28C	E19C	E42C	K28C
47	11.6	-0.8	-8.8	12.5	1.2	-6.8
48	-0.4	2.1	-10.3	-1.8	3.2	-47.6
49	9.6	13.1	-12.8	-	6.4	-6.1
50	6.1	-3.3	-	-	-1.9	2.9
51	-3.3	-7.1	4.1	2.1	-7.5	2.6
52	7.5	-0.5	-9.7	2.3	-1.2	-3.5
53	16.5	10.8	-3.7	17.0	3.2	2.9
54	20.6	8.8	1.1	16.7	5.2	-0.8
55	15.8	-	2.6	16.2	4.5	3.2
56	21.2	-	-2.1	19.0	-	-1.7

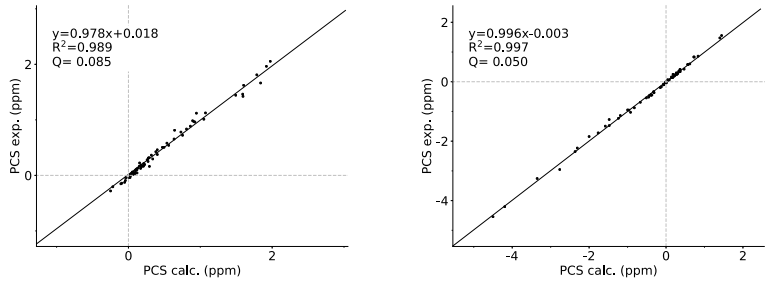

(a) E19C Tb

(b) E19C Tm

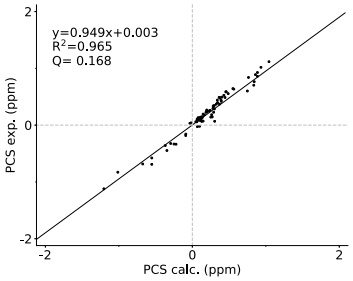

(c) E42C Tb

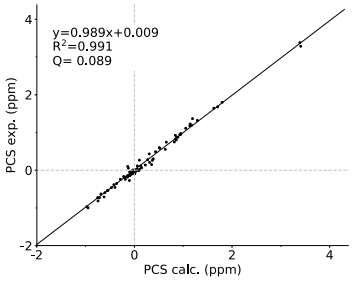

(d) E42C Tm

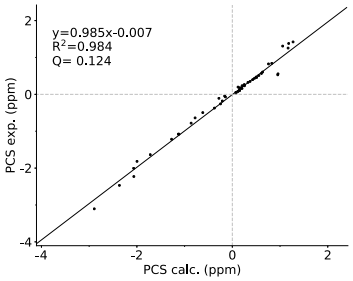

(e) K28C Tb

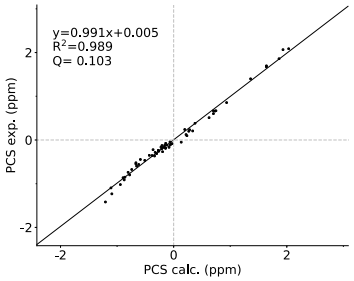

(f) K28C Tm

Figure A.1: Correlation graphs between PCSs calculated from the X-ray structure 2QMT and the experimental *in-vitro* PCSs.

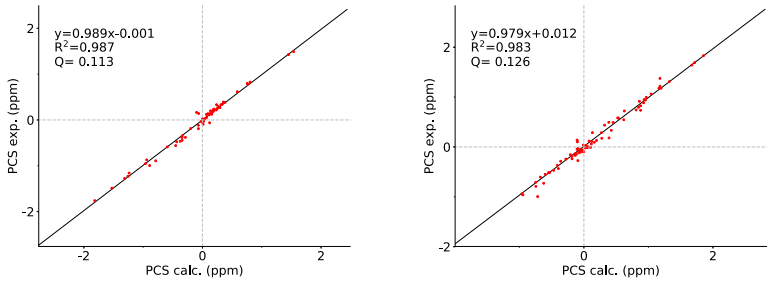

(a) E19C Tm (b) E42C Tm

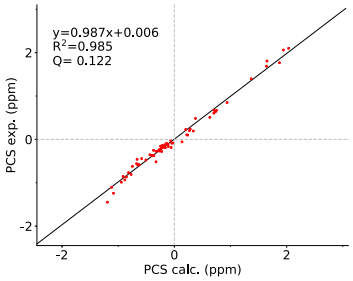

(c) K28C Tm

Figure A.2: Correlation graphs between PCSs calculated from the X-ray structure 2QMT and the experimental *in-cell* PCSs.

Table A.8: *In-vitro* ^{1}H-^{15}N HSQC peak assignment in ppm of ubiqutin S57C tagged with Lu and Tm loaded M7FPy-DOTA at 298 K.

Residue	**Lu**		**Tm**	
	HN	N	HN	N
M1	-	-	-	-
Q2	8.87	123.2	8.64	122.9
I3	8.23	115.3	7.69	114.7
F4	8.53	118.6	7.79	117.9
V5	9.20	121.2	8.71	120.7
K6	8.86	128.0	8.33	127.5
T7	8.67	115.6	8.35	115.3
L8	9.05	121.3	8.76	121.1
T9	7.55	105.9	7.33	105.7
G10	7.74	109.3	7.52	109.1
K11	7.17	122.0	6.96	121.8
T12	8.56	120.7	8.34	120.5

Continued on next page

Table A.8 – continued from previous page

Residue	Lu		Tm	
	HN	N	HN	N
I13	9.46	127.7	9.11	127.4
T14	8.66	121.6	8.40	121.3
L15	8.68	125.3	8.26	125.0
E16	8.03	122.6	7.85	122.4
V17	8.85	117.5	8.81	117.5
E18	8.59	119.9	8.95	120.6
P19	-	-	-	-
S20	7.04	103.9	8.19	107.4
D21	7.93	123.5	7.19	122.4
T22	7.84	108.9	6.20	106.8
I23	8.42	121.3	5.81	119.0
E24	10.03	121.3	8.55	119.9
N25	7.87	121.5	6.68	120.5
V26	7.98	122.1	6.78	121.1
K27	8.45	118.9	7.51	118.0
A28	7.92	123.6	7.28	123.0
K29	7.77	120.3	7.26	119.8
I30	8.18	121.4	7.68	121.0
Q31	8.47	123.6	8.07	123.2
D32	7.92	119.8	7.65	119.5
K33	7.33	115.5	7.08	115.2
E34	8.64	114.5	8.39	114.2
G35	8.42	109.0	8.20	108.7
I36	6.06	120.3	5.79	120.1
P37	-	-	-	-
P38	-	-	-	-
D39	8.44	113.7	8.09	113.3
Q40	7.74	116.9	7.39	116.6
Q41	7.40	118.2	6.96	117.8
R42	8.41	123.2	7.92	122.7
L43	8.76	124.6	7.94	123.8
I44	9.03	122.3	8.22	121.5
F45	8.78	125.1	7.74	124.1

Continued on next page

Table A.8 – continued from previous page

Residue	Lu		Tm	
	HN	N	HN	N
A46	8.90	100.2	8.12	132.3
G47	8.01	102.5	7.48	102.0
K48	7.89	122.1	7.20	121.5
Q49	8.56	123.2	7.98	122.5
L50	8.48	125.8	7.39	124.6
E51	8.27	123.1	6.63	121.7
D52	8.09	120.5	7.02	119.2
G53	-	-	-	-
R54	7.38	119.3	-	-
T55	8.92	109.1	1.42	102.7
L56	8.20	117.8	2.79	111.3
S57	8.26	117.0	-	-
D58	7.93	121.9	-	-
Y59	7.06	115.4	-3.00	106.1
N60	7.96	116.3	-2.76	104.4
I61	7.14	118.8	-1.04	112.3
Q62	7.52	124.8	-	-
K63	8.47	120.8	6.72	119.1
E64	9.24	114.7	8.51	114.0
S65	7.58	115.0	6.51	114.2
T66	8.64	117.5	7.86	116.7
L67	9.33	127.8	8.49	126.9
H68	9.14	119.5	8.35	118.8
L69	8.19	123.9	7.69	123.4
V70	9.09	126.5	8.60	126.1
L71	8.02	123.0	7.71	122.7
R72	8.50	123.9	8.19	123.6
L73	8.28	124.7	8.04	124.5
R74	8.37	122.1	8.18	121.9
G75	8.41	111.2	8.25	111.1
G76	7.86	115.1	7.71	115.0

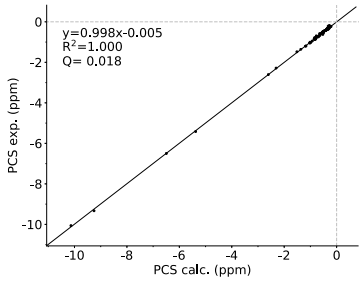

Figure A.3: Correlation graphs between PCSs calculated from the X-ray structure 1UBI and the experimental *in-vitro* PCSs obtained for Tm loaded M7FPy-DOTA

Table A.9: *In-vitro* ^{1}H-^{15}N HSQC peak assignment in ppm of ubiquitin S57C tagged with Lu, Tm, Tb and Dy loaded M7Pythiazol-DOTA at 298 K.

Residue	**Lu**		**Tm**		**Tb**		**Dy**	
	HN	N	HN	N	HN	N	HN	N
M1	-	-	-	-	-	-	-	-
Q2	8.95	123.0	8.88	123.4	7.77	121.7	-	-
I3	8.31	115.2	9.69	116.7	6.82	113.7	5.69	112.5
F4	8.62	118.6	10.08	120.0	7.31	117.3	6.46	116.5
V5	9.29	121.3	10.31	122.4	8.37	120.3	7.84	119.7
K6	8.95	128.0	9.99	128.9	8.08	127.2	7.67	126.8
T7	8.75	115.6	9.36	116.3	8.24	115.1	7.97	114.8
L8	9.13	121.3	9.69	121.9	8.65	120.9	8.43	120.7
T9	7.64	106.0	8.07	106.4	7.27	105.6	7.10	105.5
G10	7.83	109.3	8.25	109.7	7.49	109.0	7.33	108.9
K11	7.27	122.0	7.67	122.4	6.92	121.6	6.74	121.5
T12	8.64	120.7	9.02	121.2	8.30	120.3	8.09	120.1
I13	9.55	127.7	10.24	128.3	8.91	127.1	8.54	126.8
T14	8.74	121.7	9.25	122.3	8.15	120.9	7.75	120.5
L15	8.75	125.3	9.78	126.2	7.66	124.3	6.91	123.6
E16	8.12	122.5	9.05	123.6	7.12	121.4	6.31	120.7
V17	8.94	117.6	10.56	119.3	6.98	115.7	-	-
E18	8.66	119.5	13.10	123.8	-	-	-	-
P19	-	-	-	-	-	-	-	-
S20	7.02	103.7	-	-	-	-	-	-
D21	8.06	123.7	-	-	-	-	-	-
T22	7.84	108.8	11.82	114.2	-	-	-	-

Continued on next page

Table A.9 – continued from previous page

Residue	Lu		Tm		Tb		Dy	
	HN	N	HN	N	HN	N	HN	N
I23	8.53	121.3	13.15	125.6	-	-	-	-
E24	-	-	-	-	-	-	-	-
N25	7.92	121.5	10.19	123.4	6.10	119.9	-	-
V26	8.10	122.2	10.93	124.6	5.92	120.3	-	-
K27	8.57	119.0	10.54	120.8	6.89	117.5	6.08	116.7
A28	7.98	123.6	9.21	124.7	6.84	122.5	6.26	121.9
K29	7.85	120.3	8.99	121.2	6.77	119.4	6.20	118.8
I30	8.29	121.4	9.42	122.4	7.23	120.4	6.68	119.9
Q31	8.56	123.7	9.34	124.4	7.79	122.9	7.39	122.5
D32	8.01	119.8	8.53	120.2	7.41	119.2	7.08	118.9
K33	7.42	115.5	7.93	115.9	6.85	115.0	6.52	114.7
E34	8.73	114.5	9.23	114.9	8.20	114.0	7.90	113.7
G35	8.50	109.0	8.91	109.4	8.05	108.5	7.80	108.2
I36	6.15	120.4	6.64	120.8	5.64	119.8	-	-
P37	-	-	-	-	-	-	-	-
P38	-	-	-	-	-	-	-	-
D39	8.53	113.7	9.08	114.3	7.95	113.1	7.65	112.8
Q40	7.82	117.0	8.42	117.6	7.23	116.4	6.94	116.1
Q41	7.49	118.2	8.27	118.9	6.75	117.5	6.40	117.2
R42	8.50	123.2	9.47	124.2	7.64	122.2	7.27	121.9
L43	8.83	124.5	10.44	126.0	7.43	123.1	7.06	122.7
I44	9.11	122.4	10.76	124.1	7.71	120.8	7.15	120.2
F45	8.85	125.1	10.99	127.2	7.00	123.3	6.41	122.7
A46	8.98	132.9	10.58	101.7	7.80	131.7	7.51	131.4
G47	8.09	102.5	9.34	103.7	7.18	101.6	7.00	101.5
K48	7.98	122.2	9.62	123.6	6.64	121.0	6.40	120.6
Q49	8.64	123.2	10.08	124.8	7.42	121.9	7.07	121.5
L50	8.56	125.8	10.71	128.1	6.60	123.7	5.89	123.0
E51	8.41	123.2	11.26	125.7				
D52	8.16	120.4	9.78	122.3	6.49	118.5	5.73	117.6
G53	-	-	-	-	-	-	-	-
R54	7.46	119.4	10.66	122.7	-	-	-	-
T55	8.95	109.2	-	-	-	-	-	-

Continued on next page

Table A.9 – continued from previous page

Residue	Lu		Tm		Tb		Dy	
	HN	N	HN	N	HN	N	HN	N
L56	8.18	118.0	-	-	-	-	-	-
S57	8.53	117.3	-	-	-	-	-	-
D58	8.12	123.0	-	-	-	-	-	-
Y59	7.19	115.5	-	-	-	-	-	-
N60	8.18	116.6	-	-	-	-	-	-
I61	7.27	119.0	-	-	-	-	-	-
Q62	7.56	124.7	12.13	130.5	-	-	-	-
K63	8.59	120.8	-	-	-	-	-	-
E64	9.33	114.7	10.05	115.2	8.23	114.2	6.87	113.0
S65	7.64	115.0	9.13	116.2	6.26	114.0	-	-
T66	8.72	117.5	10.03	118.9	7.82	116.5	7.38	115.9
L67	9.41	127.9	11.08	129.6	8.03	126.5	7.34	125.8
H68	9.22	119.6	10.82	121.0	7.92	118.4	7.40	117.9
L69	8.27	123.9	9.28	125.0	7.39	123.2	6.84	122.6
V70	9.18	126.6	10.17	127.5	8.33	125.8	7.98	125.5
L71	8.10	123.0	8.70	123.7	7.58	122.5	7.36	122.4
R72	8.59	123.9	9.19	124.5	8.06	123.4	7.82	123.2
L73	8.35	124.7	8.81	125.1	7.96	124.3	7.79	124.1
R74	8.45	122.1	8.80	122.5	8.14	121.8	8.00	121.7
G75	8.49	111.2	8.80	111.5	8.22	111.0	8.09	110.8
G76	7.94	115.2	8.23	115.4	7.69	114.9	7.58	114.8

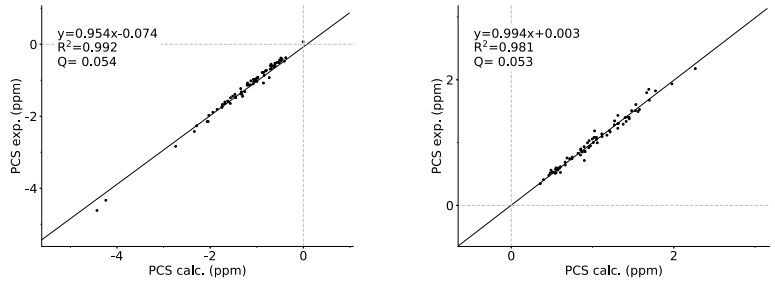

(a) S57C Tm (b) S57C Tb

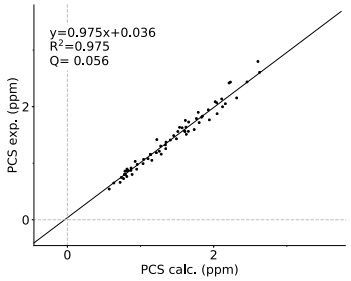

(c) S57C Dy

Figure A.4: Correlation graphs between PCSs calculated from the X-ray structure 1UBI and the experimental *in-vitro* PCSs.

Table A.10: *In-vitro* ^{1}H-^{15}N HSQC peak assignment in ppm of ubiquitin K48C tagged with Lu, Tm, Tb and Dy loaded M7Pythiazol-DOTA at 298 K.

Residue	**Lu**		**Tm**		**Tb**		**Dy**	
	HN	N	HN	N	HN	N	HN	N
M1	-	-	-	-	-	-	-	-
Q2	8.95	122.9	8.37	122.2	8.26	122.2	8.74	122.7
I3	8.31	115.2	7.91	114.7	7.49	114.4	8.01	115.0
F4	8.62	118.6	8.72	118.8	7.09	117.6	7.87	118.3
V5	9.30	121.3	9.68	121.8	8.38	120.2	8.79	120.8
K6	8.96	128.0	10.17	129.1	7.47	126.7	7.99	127.3
T7	8.75	115.6	9.60	116.5	7.95	114.7	8.17	115.0
L8	9.13	121.3	10.14	122.4	8.59	120.7	8.66	120.8
T9	7.64	105.9	8.42	106.8	7.16	105.3	7.20	105.5
G10	7.83	109.3	8.66	110.1	7.13	108.6	7.27	108.8
K11	7.27	122.0	7.90	122.6	6.69	121.4	6.82	121.6
T12	8.64	120.7	9.06	121.2	8.06	120.0	8.31	120.1

Continued on next page

Table A.10 – continued from previous page

Residue	Lu		Tm		Dy		Tb	
	HN	N	HN	N	HN	N	HN	N
I13	9.55	127.7	9.97	128.0	8.89	127.2	9.14	127.5
T14	8.74	121.7	8.79	121.8	8.33	121.4	8.52	121.7
L15	8.74	125.2	8.55	125.0	8.15	125.0	8.52	125.3
E16	8.12	122.5	7.71	122.1	7.87	122.4	8.07	122.6
V17	8.94	117.6	8.20	116.8	8.42	117.2	8.84	117.6
E18	8.66	119.4	7.49	118.2	8.30	119.2	8.72	119.6
P19	-	-	-	-	-	-	-	-
S20	7.03	103.5	5.49	101.6	6.08	102.4	6.79	103.3
D21	8.04	124.0	6.14	122.0	7.56	123.8	8.15	124.3
T22	7.88	109.0	5.81	106.6	8.98	110.3	8.75	110.1
I23	8.52	121.4			13.12	125.1	11.75	124.1
E24	-	-	-	-	-	-	-	-
N25	7.92	121.6	6.01	120.0	10.14	123.8	9.43	123.2
V26	8.09	122.2	6.48	120.9	9.71	123.5	9.31	123.2
K27	8.55	119.0	7.36	118.2	10.42	120.5	9.81	120.1
A28	7.98	123.6	7.07	122.8	9.43	124.9	8.93	124.5
K29	7.86	120.3	7.18	119.8	8.64	121.0	8.41	120.8
I30	8.29	121.4	7.88	121.2	8.90	121.8	8.72	121.8
Q31	8.56	123.7	8.24	123.5	9.28	124.3	9.02	124.1
D32	8.01	119.8	7.70	119.5	8.51	120.3	8.24	120.3
K33	7.43	115.5	7.26	115.4	7.68	115.7	7.58	115.7
E34	8.73	114.5	8.69	114.5	9.00	114.6	8.88	114.5
G35	8.51	109.0	8.44	109.0	8.85	109.4	8.69	109.2
I36	6.16	120.4	6.16	120.3	6.64	120.9	6.40	120.7
P37	-	-	-	-	-	-	-	-
P38	-	-	-	-	-	-	-	-
D39	8.53	113.7	8.03	113.2	10.32	115.8	9.58	115.0
Q40	7.82	117.0	7.60	116.7	9.45	118.7	8.74	118.0
Q41	7.49	118.2	7.44	118.3	9.38	119.8	8.59	119.1
R42	8.51	123.2	9.42	123.9	9.71	124.8	9.15	123.9
L43	8.86	124.5	10.25	126.2	11.70	126.1	10.44	125.3
I44	9.12	122.2	12.77	126.7	7.39	120.9	7.84	121.3
F45	8.79	124.7	-	-	-	-	-	-

Continued on next page

Table A.10 – continued from previous page

Residue	Lu		Tm		Dy		Tb	
	HN	N	HN	N	HN	N	HN	N
A46	9.20	102.0	-	-	-	-	-	-
G47	8.11	102.6	-	-	-	-	-	-
K48	-	-	-	-	-	-	-	-
Q49	-	-	-	-	-	-	-	-
L50	8.58	126.3	-	-	-	-	-	-
E51	8.35	123.2	-	-	-	-	-	-
D52	8.15	120.7	3.14	115.1	-	-	-	-
G53	-	-	-	-	-	-	-	-
R54	7.48	119.2	-	-	-	-	-	-
T55	8.73	108.7	0.90	101.7	-	-	-	-
L56	8.13	118.1	-	-	7.79	117.5	8.80	119.0
S57	8.44	113.3	3.93	109.5	5.93	110.0	8.07	112.9
D58	8.28	120.7	-0.47	111.3	-	-	-	-
Y59	7.05	114.7	-	-	-	-	-	-
N60	8.12	115.5	-	-	-	-	6.88	114.1
I61	7.22	118.9	1.17	113.8	-	-	-	-
Q62	7.64	125.1	-	-	-	-	6.82	124.2
K63	8.50	120.7	7.06	119.4	7.32	119.3	8.28	120.4
E64	9.33	114.7	8.72	114.0	8.15	113.2	8.89	114.0
S65	7.67	115.1	7.08	114.7	5.80	113.0	6.89	114.1
T66	8.74	117.5	9.65	118.3	5.66	115.0	7.03	116.2
L67	9.43	128.0	10.52	129.4	7.11	125.0	8.11	126.3
H68	9.27	119.5	12.50	122.2	6.07	116.8	7.18	117.9
L69	8.28	123.9	9.93	125.8	7.09	122.8	7.42	123.1
V70	9.19	126.7	10.93	128.6	9.15	126.5	8.94	126.5
L71	8.10	123.1	9.44	124.0	8.26	123.4	8.00	123.1
R72	8.61	123.9	-	-	9.79	124.7	9.14	124.4
L73	8.36	124.6	8.59	125.0	9.32	125.6	8.50	125.3
R74	8.45	122.1	-	-	9.44	123.0	8.73	122.7
G75	8.49	111.2	-	-	-	-	-	-
G76	7.95	115.2	-	-	-	-	-	-

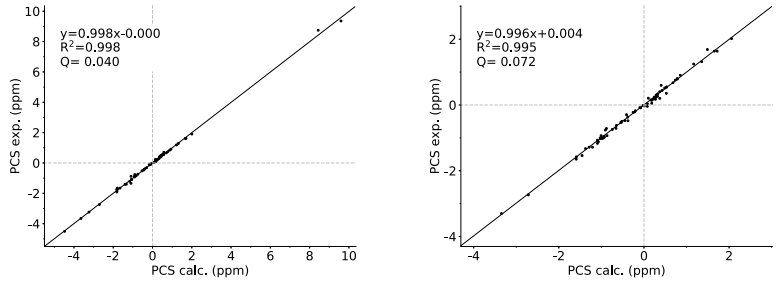

(a) K48C Tm (b) K48C Tb

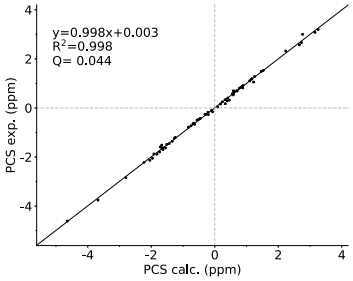

(c) K48C Dy

Figure A.5: Correlation graphs between PCSs calculated from the X-ray structure 1UBI and the experimental *in-vitro* PCSs.

Table A.11: *In-vitro* ^{1}H-^{15}N backbone amide RDC in Hz of ubiquitin mutants tagged with Tm, Tb and Dy (paramagnetic) and Lu (diamagnetic reference) loaded M7PyThiazol-DOTA at 298 K and 600 MHz.

Residue	**K48C**			**S57C**		
	Tm	Dy	Tb	Tm	Dy	Tb
M1	-	-	-	-	-	-
Q2	-14.9	-	18.1	-2.7	-4.8	-
I3	-14.3	-	16.4	-7.3	-0.4	1.0
F4	-10.5	15.2	11.5	-6.7	-0.2	-1.5
V5	-5.9		1.8	-5.4	3.1	4.9
K6	0.3	-3.5	-0.9	-5.5	0.0	-1.2
T7	-2.2	-12.9	-4.6	-4.8	2.5	3.8
L8	-2.3	-	-2.0	-8.1	7.6	8.5
T9	5.4	-	-	-0.8	4.6	8.8
G10	-	-	-	-2.4	4.8	6.7
K11	-11.1	9.9	8.2	-0.5	-1.9	-5.7

Continued on next page

Table A.11 – continued from previous page

Residue	K48C			S57C		
	Tm	Dy	Tb	Tm	Dy	Tb
T12	1.9	-	-1.4	-7.5	4.2	0.4
I13	-6.4	-5.2	0.4	-5.2	3.1	4.0
T14	-4.7	-	6.3	-4.7	-1.8	-3.7
L15	-13.5	23.4	-	-6.8	2.6	1.4
E16	-14.9	32.6	19.5	-1.0	-3.1	-2.2
V17	-15.2	21.7	13.3	-7.0	1.8	-
E18	-15.7	-	14.8	1.3	-	-
P19	-	-	-	-	-	-
S20	-	-6.4	0.7	-	-	-
D21	-5.7	0.2	0.5	-	-	-
T22	-	-	-	-6.4	-	-
I23	-	-	-	-3.6	-	-
E24	-	-	-	-	-	-
N25	5.5	10.6	6.7	0.0	-6.9	-
V26	-0.2	-2.4	0.5	-5.3	-0.5	-
K27	11.4	-17.5	-8.5	-3.3	-0.1	-0.4
A28	16.0	-6.5	-5.0	3.5	-6.1	-11.9
K29	-0.3	-	5.9	-3.9	-4.3	-7.3
I30	6.3	-8.2	-5.7	-4.8	-1.7	-1.4
Q31	18.4	-14.5	-10.5	2.2	-2.3	-6.9
D32	12.4	-	-5.1	2.7	-7.7	-13.8
K33	0.3	1.8	2.6	-3.1	-2.5	-4.8
E34	14.3	-19.1	-9.1	-0.7	-1.6	-5.0
G35	15.7	-8.3	-7.0	13.7	-5.5	-6.8
I36	-9.6	21.5	-	4.9	-6.9	-
P37	-	-	-	-	-	-
P38	-	-	-	-	-	-
D39	-12.2	17.7	11.5	-7.9	3.6	-
Q40	-10.0	0.4	-1.6	0.4	5.5	3.2
Q41	-14.5	-24.8	-	-3.2	8.2	9.4
R42	25.2	-7.7	-18.9	-9.0	1.6	15.9
L43	15.1	-	-17.8	-4.7	1.6	8.0
I44	-	-	-	-4.8	0.9	4.8

Continued on next page

Table A.11 – continued from previous page

Residue	K48C			S57C		
	Tm	Dy	Tb	Tm	Dy	Tb
F45	-	-	-	-6.1	0.9	0.0
A46	-	-	-	-7.8	-	5.0
G47	-	-	-	-4.4	-	-
K48	-83.9	-	-	4.4	-1.5	-6.8
Q49	-	-	-	-2.5	2.7	4.5
L50	-	-	-	0.1	-3.3	-4.1
E51	-	-	-	4.4	-	-
D52	1.5	-	-	12.2	-6.1	-12.9
G53	-	-	-	-	-	-
R54	-	-	-	10.3	-	-
T55	-	-	-	-	-	-
L56	-	-	7.0	-	-	-
S57	-	1.3	-	-	-	-
D58	-	-	-	-	-	-
Y59	-	-	-	-	-	-
N60	-	-	-18.5	-	-	-
I61	1.8	-	-	-	-	-
Q62	-	-	-13.2	2.1	-	-
K63	15.8	0.3	-2.9	-	-	-
E64	-12.5	-	8.6	-8.5	6.2	8.8
S65	18.6	-23.9	-18.0	1.0	6.3	-
T66	-14.7	20.7	11.8	-8.0	1.7	3.0
L67	-8.7	0.7	2.3	-5.6	3.8	8.3
H68	6.9	-11.0	-5.9	-4.8	-0.4	-1.9
L69	9.0	-20.8	-13.9	-4.3	3.8	8.9
V70	24.0	-28.2	-20.7	0.6	2.6	4.5
L71	22.1	-	-15.8	-0.7	5.6	13.9
R72	-	-26.3	-6.5	1.4	5.5	10.3
L73	-15.1	-	12.7	-3.0	2.2	2.7
R74	-	-	20.9	-1.9	0.5	0.5
G75	-	-	-	-0.2	0.1	-0.3
G76	-	-	-	0.3	0.3	0.7

Table A.12: *In-vitro* RDC tensor parameters for ubiqutin S57C fitted against the ubiqutin X-ray structure (PDB code: 1UBI).

	Tm, 37 RDC	Dy, 33 RDC	Tb, 36 RDC
$\Delta\chi_{ax}$ / $10^{-32}m^3$	25.5	-36.0	-18.6
$\Delta\chi_{rh}$ / $10^{-32}m^3$	3.6	-19.7	-8.2
x / Å	20.5	20.5	20.5
y / Å	15.1	15.1	15.1
z / Å	6.3	6.3	6.3
α / °	169.2	20.0	23.6
β / °	43.8	58.0	60.2
γ / °	70.5	35.3	37.0
Q-factor	0.38	0.43	0.41

Tensor parameters were calculated in FANTEN from the indicated number of selected RDC.[138] All tensors are represented in the unique tensor representation UTR.[74] Only amino acids residing in a stable secondary structure (2-7, 12-16, 23-34, 38-40, 41-45, 48-49, 56-59 and 66-71) were used if present in the spectra.

Table A.13: *In-vitro* RDC tensor parameters for ubiqutin K48C fitted against the ubiqutin X-ray structure (PDB code: 1UBI).

	Tm, 32 RDC	Dy, 25 RDC	Tb, 31 RDC
$\Delta\chi_{ax}$ / $10^{-32}m^3$	45.5	62.5	-39.6
$\Delta\chi_{rh}$ / $10^{-32}m^3$	12.2	35.0	-24.1
x / Å	19.0	19.0	19.0
y / Å	18.6	18.6	18.6
z / Å	22.8	22.8	22.8
α / °	4.0	4.8	161.8
β / °	83.4	67.8	83.2
γ / °	83.3	8.5	97.4
Q-factor	0.31	0.29	0.21

Tensor parameters were calculated in FANTEN from the indicated number of selected RDC.[138] All tensors are represented in the unique tensor representation UTR.[74] Only amino acids residing in a stable secondary structure (2-7, 12-16, 23-34, 38-40, 41-45, 48-49, 56-59 and 66-71) were used if present in the spectra.

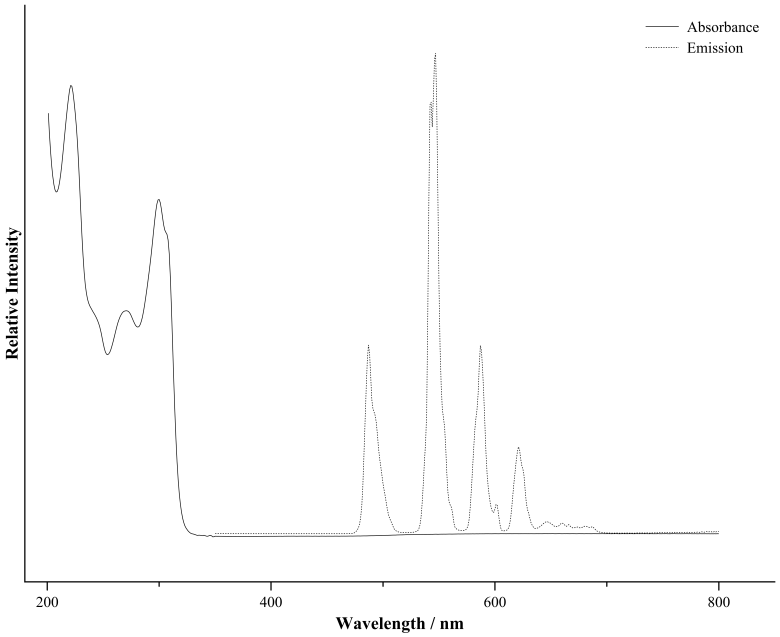

Figure A.6: UV/Vis absorption and emission spectrum of Tb-M7PyThiazol-DOTA **199** measured in acetonitrile at 20-25 °C. λ_{ex}=300 nm.

REFERENCES

(*1*) Campbell, I. D. (2002). The march of structural biology. *Nature Reviews Molecular Cell Biology 3*, 377–381.

(*2*) Edman, P., Högfeldt, E., Sillén, L. G. and Kinell, P.-O. Method for Determination of the Amino Acid Sequence in Peptides., 1950.

(*3*) Liko, I., Allison, T. M., Hopper, J. T. and Robinson, C. V. (2016). Mass spectrometry guided structural biology. *Current Opinion in Structural Biology 40*, 136–144.

(*4*) Some, D. (2013). Light-scattering-based analysis of biomolecular interactions. *Biophysical Reviews 5*, 147–158.

(*5*) Kendrew, J. C., Bodo, G., Dintzis, H. M., Parrish, R. G., Wyckoff, H. and Phillips, D. C. (1958). A three-dimensional model of the myoglobin molecule obtained by x-ray analysis. *Nature 181*, 662–666.

(*6*) Rabi, I. I., Zacharias, J. R., Millman, S. and Kusch, P. (1938). A New Method of Measuring Nuclear Magnetic Moment. *Physical Review 53*, 318–318.

(*7*) Wüthrich, K., Wider, G., Wagner, G. and Braun, W. (1982). Sequential resonance assignments as a basis for determination of spatial protein structures by high resolution proton nuclear magnetic resonance. *Journal of Molecular Biology 155*, 311–319.

(*8*) Overhauser, A. W. (1953). Polarization of nuclei in metals. *Physical Review 92*, 411–415.

(*9*) Palmer, A. G. and Patel, D. J. (2002). Kurt Wüthrich and NMR of biological macromolecules. *Structure 10*, 1603–1604.

(*10*) De Rosier, D. J. and Klug, A. (1968). Reconstruction of three dimensional structures from electron micrographs. *Nature 217*, 130–134.

(*11*) Amos, L. A. and Klug, A. (1975). Three-dimensional image reconstructions of the contractile tail of T4 bacteriophage. *Journal of Molecular Biology 99*, 51–64.

(*12*) Henderson, R. and Unwin, P. N. (1975). Three-dimensional model of purple membrane obtained by electron microscopy. *Nature 257*, 28–32.

(*13*) Shoemaker, S. C. and Ando, N. (2018). X-rays in the Cryo-Electron Microscopy Era: Structural Biology's Dynamic Future. *Biochemistry 57*, 277–285.

(*14*) Balksjö Nannini, J. (2014). The Nobel Prize in Chemistry 2014. *The Royal Swedish Academy of Science 47*, http://www.nobelprize.org/nobel_prizes/chemistry/l.

(*15*) Khoshouei, M., Radjainia, M., Baumeister, W. and Danev, R. (2017). Cryo-EM structure of haemoglobin at 3.2 Å determined with the Volta phase plate. *Nature Communications 8*, 1–6.

(*16*) Shi, Y. (2014). A glimpse of structural biology through X-ray crystallography. *Cell 159*, 995–1014.

(*17*) Murata, K. and Wolf, M. (2018). Cryo-electron microscopy for structural analysis of dynamic biological macromolecules. *Biochimica et Biophysica Acta - General Subjects 1862*, 324–334.

(*18*) Markwick, P. R. L., Malliavin, T. and Nilges, M. (2008). Structural Biology by NMR: Structure, Dynamics, and Interactions. *PLoS Computational Biology 4*, e1000168.

(*19*) Marion, D. (2013). An Introduction to Biological NMR Spectroscopy. *Molecular & Cellular Proteomics 12*, 3006–3025.

(*20*) Jiang, Y. and Kalodimos, C. G. (2017). NMR Studies of Large Proteins. *Journal of Molecular Biology 429*, 2667–2676.

(*21*) Hänsel, R., Luh, L. M., Corbeski, I., Trantirek, L. and Dötsch, V. (2014). In-cell NMR and EPR spectroscopy of biomacromolecules. *Angewandte Chemie (International ed. in English) 53*, 10300–10314.

(*22*) Freedberg, D. I. and Selenko, P. (2014). Live Cell NMR. *Annual Review of Biophysics 43*, 171–192.

(*23*) Forster, T. (1946). Energiewanderung und Fluoreszenz. *Die Naturwissenschaften 33*, 166–175.

(*24*) Sekar, R. B. and Periasamy, A. (2003). Fluorescence resonance energy transfer (FRET) microscopy imaging of live cell protein localizations. *Journal of Cell Biology 160*, 629–633.

(*25*) Jeschke, G. (2018). The contribution of modern EPR to structural biology. *Emerging Topics in Life Sciences 0*, ETLS20170143.

(*26*) Wüthrich, K. (2001). The way to NMR structures of proteins. *Nature Structural Biology 8*, 923–925.

(*27*) Wüthrich, K. (2003). NMR studies of structure and function of biological macromolecules (Nobel Lecture). *Angewandte Chemie - International Edition 42*, 3340–3363.

(*28*) Kazimierczuk, K., Misiak, M. and Zawadzka, A. (2007). Progress in structural studies of proteins by NMR spectroscopy. *Polimery 52*, 736–744.

(*29*) Edwards, a. J. and Reid, D. (2001). Introduction to NMR of proteins. *Current protocols in protein science / editorial board, John E. Coligan ... [et al.] Chapter 17*, Unit 17.5.

(*30*) Wang, G., Zhang, Z.-T., Jiang, B., Zhang, X., Li, C. and Liu, M. (2014). Recent advances in protein NMR spectroscopy and their implications in protein therapeutics research. *Analytical and Bioanalytical Chemistry 406*, 2279–2288.

(*31*) Sattler, M. and Fesik, S. W. (1996). Use of deuterium labeling in NMR: Overcoming a sizeable problem. *Structure 4*, 1245–1249.

(*32*) Pervushin, K., Riek, R., Wider, G. and Wuthrich, K. (1997). Attenuated T2 relaxation by mutual cancellation of dipole-dipole coupling and chemical shift anisotropy indicates an avenue to NMR structures of very large biological macromolecules in solution. *Proceedings of the National Academy of Sciences 94*, 12366–12371.

(*33*) Riek, R., Wider, G., Pervushin, K. and Wuthrich, K. (1999). Polarization transfer by cross-correlated relaxation in solution NMR with very large molecules. *Proceedings of the National Academy of Sciences 96*, 4918–4923.

(*34*) Campbell, I. D. (2013). The evolution of protein NMR. *Biomedical Spectroscopy and Imaging 2*, 245–264.

(*35*) Fiaux, J., Bertelsen, E. B., Horwich, A. L. and Wüthrich, K. (2002). NMR analysis of a 900K GroEL GroES complex. *Nature 418*, 207–211.

(*36*) Wishart, D. (2005). NMR Spectroscopy and Protein Structure Determination: Applications to Drug Discovery and Development. *Current Pharmaceutical Biotechnology 6*, 105–120.

(*37*) Sugiki, T., Furuita, K., Fujiwara, T. and Kojima, C. (2018). Current NMR techniques for structure-based drug discovery. *Molecules 23*, 1–27.

(*38*) Sugiki, T., Kobayashi, N. and Fujiwara, T. (2017). Modern Technologies of Solution Nuclear Magnetic Resonance Spectroscopy for Three-dimensional Structure Determination of Proteins Open Avenues for Life Scientists. *Computational and Structural Biotechnology Journal 15*, 328–339.

(*39*) Baran, M. C., Huang, Y. J., Moseley, H. N. B. and Montelione, G. T. (2004). Automated analysis of protein NMR assignments and structures. *Chemical reviews 104*, 3541–3556.

(*40*) Williamson, M. P., *Chapter 3 Applications of the NOE in Molecular Biology*, 1st ed.; 08; Elsevier Ltd: 2009; Vol. 65, pp 77–109.

(*41*) Herrmann, T. (2010). Protein Structure Calculation and Automated NOE Restraints. *Encyclopedia of Magnetic Resonance*.

(*42*) Vögeli, B., Orts, J., Strotz, D., Güntert, P. and Riek, R. (2012). Discrete three-dimensional representation of macromolecular motion from eNOE-based ensemble calculation. *Chimia 66*, 787–790.

(*43*) Sugiki, T., Kobayashi, N. and Fujiwara, T. (2017). Modern Technologies of Solution Nuclear Magnetic Resonance Spectroscopy for Three-dimensional Structure Determination of Proteins Open Avenues for Life Scientists. *Computational and Structural Biotechnology Journal 15*, 328–339.

(*44*) Karplus, M. (1963). Vicinal Proton Coupling in Nuclear Magnetic Resonance. *Journal of the American Chemical Society 85*, 2870–2871.

(*45*) Neal, S., Berjanskii, M., Zhang, H. and Wishart, D. S. (2006). Accurate prediction of protein torsion angles using chemical shifts and sequence homology. *Magnetic Resonance in Chemistry 44*, 158–167.

(*46*) Shen, Y., Delaglio, F., Cornilescu, G. and Bax, A. (2009). TALOS+: A hybrid method for predicting protein backbone torsion angles from NMR chemical shifts. *Journal of Biomolecular NMR 44*, 213–223.

(*47*) Brunner, E. (2001). Residual Dipolar Couplings in Protein NMR. *Concepts in Magnetic Resonance 13*, 238–259.

(*48*) Downing, A. K., *Protein NMR Techniques*, 2004; Vol. 278, pp 353–78.

(*49*) Chen, K. and Tjandra, N. (2012). The use of residual dipolar coupling in studying proteins by NMR. *Topics in Current Chemistry 326*, 47–67.

(*50*) Rohl, C. A., Strauss, C. E. M., Misura, K. M. S. and Baker, D. (2004). Protein Structure Prediction Using Rosetta. *Methods in Enzymology 383*, 66–93.

(*51*) Kaufmann, K. W., Lemmon, G. H., Deluca, S. L., Sheehan, J. H. and Meiler, J. (2010). Practically useful: What the Rosetta protein modeling suite can do for you. *Biochemistry 49*, 2987–2998.

(*52*) Dorn, M., E Silva, M. B., Buriol, L. S. and Lamb, L. C. (2014). Three-dimensional protein structure prediction: Methods and computational strategies. *Computational Biology and Chemistry 53*, 251–276.

(*53*) Shen, Y. *et al*. (2008). Consistent blind protein structure generation from NMR chemical shift data. *Proceedings of the National Academy of Sciences 105*, 4685–4690.

(*54*) Schmitz, C., Vernon, R., Otting, G., Baker, D. and Huber, T. (2012). Protein structure determination from pseudocontact shifts using ROSETTA. *Journal of Molecular Biology 416*, 668–677.

(*55*) Yagi, H., Pilla, K. B., Maleckis, A., Graham, B., Huber, T. and Otting, G. (2013). Three-dimensional protein fold determination from backbone amide pseudocontact shifts generated by lanthanide tags at multiple sites. *Structure 21*, 883–890.

(*56*) Selenko, P. and Wagner, G. (2007). Looking into live cells with in-cell NMR spectroscopy. *Journal of Structural Biology 158*, 244–253.

(*57*) Serber, Z., Keatinge-Clay, A. T., Ledwidge, R., Kelly, A. E., Miller, S. M. and Dötsch, V. (2001). High-resolution macromolecular NMR spectroscopy inside living cells. *Journal of the American Chemical Society 123*, 2446–2447.

(*58*) Luchinat, E. and Banci, L. (2016). A unique tool for cellular structural biology: In-cell NMR. *Journal of Biological Chemistry 291*, 3776–3784.

(*59*) Guidotti, G., Brambilla, L. and Rossi, D. (2017). Cell-Penetrating Peptides: From Basic Research to Clinics. *Trends in Pharmacological Sciences 38*, 406–424.

(*60*) Pintacuda, G., Kaikkonen, A. and Otting, G. (2004). Modulation of the distance dependence of paramagnetic relaxation enhancements by CSA×DSA cross-correlation. *Journal of Magnetic Resonance 171*, 233–243.

(*61*) Chiliveri, S. C. and Deshmukh, M. V. (2016). Recent excitements in protein NMR: Large proteins and biologically relevant dynamics. *Journal of Biosciences 41*, 787–803.

(*62*) Clore, G. M., *Practical Aspects of Paramagnetic Relaxation Enhancement in Biological Macromolecules*, 1st ed.; Elsevier Inc.: 2015; Vol. 564, pp 485–497.

(*63*) Marius Clore, G. and Iwahara, J. (2009). Theory, practice, and applications of paramagnetic relaxation enhancement for the characterization of transient low-population states of biological macromolecules and their complexes. *Chemical Reviews 109*, 4108–4139.

(*64*) Otting, G. (2010). Protein NMR Using Paramagnetic Ions. *Annual Review of Biophysics 39*, 387–405.

(*65*) Saupe, A. and Englert, G. (1963). High-resolution nuclear magnetic resonance spectra of orientated molecules. *Physical Review Letters 11*, 462–464.

(*66*) Sanders, C. R., Hare, B. J., Howard, K. P. and Prestegard, J. H. (1994). Magnetically-oriented phospholipid micelles as a tool for the study of membrane-associated molecules. *Progress in Nuclear Magnetic Resonance Spectroscopy 26*, 421–444.

(*67*) Hansen, M. R., Mueller, L. and Pardi, A. (1998). Tunable alignment of macromolecules by filamentous phage yields dipolar coupling interactions. *Nature Structural Biology 5*, 1065–1074.

(*68*) Sass, H. J., Musco, G., J. Stahl, S., T. Wingfield, P. and Grzesiek, S. (2000). Solution NMR of proteins within polyacrylamide gels: Diffusional properties and residual alignment by mechanical stress or embedding of oriented purple membranes. *Journal of Biomolecular NMR 18*, 303–309.

(*69*) Lipsitz, R. S. and Tjandra, N. (2004). Residual Dipolar Couplings in NMR Structure Analysis. *Annual Review of Biophysics and Biomolecular Structure 33*, 387–413.

(*70*) Madl, T. and Sattler, M. In *NMR of Biomolecules*, 2012, pp 173–194.

(*71*) Bertini, I., Luchinat, C. and Parigi, G. (2002). Paramagnetic constraints: An aid for quick solution structure determination of paramagnetic metalloproteins. *Concepts in Magnetic Resonance Part A: Bridging Education and Research 14*, 259–286.

(*72*) Nitsche, C. and Otting, G. (2017). Pseudocontact shifts in biomolecular NMR using paramagnetic metal tags. *Progress in Nuclear Magnetic Resonance Spectroscopy 98-99*, 20–49.

(*73*) Liu, W. M., Overhand, M. and Ubbink, M. (2014). The application of paramagnetic lanthanoid ions in NMR spectroscopy on proteins. *Coordination Chemistry Reviews 273-274*, 2–12.

(*74*) Schmitz, C., Stanton-Cook, M. J., Su, X. C., Otting, G. and Huber, T. (2008). Numbat: An interactive software tool for fitting $\delta\chi$-tensors to molecular coordinates using pseudocontact shifts. *Journal of Biomolecular NMR 41*, 179–189.

(*75*) Bertini, I., Janik, M. B., Lee, Y. M., Luchinat, C. and Rosato, A. (2001). Magnetic susceptibility tensor anisotropies for a lanthanide ion series in a fixed protein matrix. *J Am Chem Soc 123*, 4181–4188.

(*76*) Harding, M. M., Nowicki, M. W. and Walkinshaw, M. D. (2010). Metals in protein structures: A review of their principal features. *Crystallography Reviews 16*, 247–302.

(*77*) Pintacuda, G., John, M., Su, X.-C. and Otting, G. (2007). NMR Structure Determination of Protein-Ligand Complexes by Lanthanide Labeling. *Accounts of Chemical Research 40*, 206–212.

(*78*) Su, X. C., Huber, T., Dixon, N. E. and Otting, G. (2006). Site-specific labelling of proteins with a rigid lanthanide-binding tag. *ChemBioChem 7*, 1599–1604.

(*79*) Su, X. C., McAndrew, K., Huber, T. and Otting, G. (2008). Lanthanide-binding peptides for NMR measurements of residual dipolar couplings and paramagnetic effects from multiple angles. *Journal of the American Chemical Society 130*, 1681–1687.

(*80*) Koniev, O. and Wagner, A. (2015). Developments and recent advancements in the field of endogenous amino acid selective bond forming reactions for bioconjugation. *Chem. Soc. Rev. 44*, 5495–5551.

(*81*) Li, Q.-F., Yang, Y., Maleckis, A., Otting, G. and Su, X.-C. (2012). Thiol–ene reaction: a versatile tool in site-specific labelling of proteins with chemically inert tags for paramagnetic NMR. *Chemical Communications 48*, 2704.

(*82*) Yang, Y., Li, Q. F., Cao, C., Huang, F. and Su, X. C. (2013). Site-specific labeling of proteins with a chemically stable, high-affinity tag for protein study. *Chemistry - A European Journal 19*, 1097–1103.

(*83*) Müntener, T., Häussinger, D., Selenko, P. and Theillet, F.-X. (2016). In-Cell Protein Structures from 2D NMR Experiments. *The Journal of Physical Chemistry Letters 7*, 2821–2825.

(*84*) Yang, Y., Wang, J.-T., Pei, Y.-Y. and Su, X.-C. (2015). Site-specific tagging proteins via a rigid, stable and short thiolether tether for paramagnetic spectroscopic analysis. *Chem. Commun. 51*, 2824–2827.

(*85*) Chen, J. L., Wang, X., Yang, F., Cao, C., Otting, G. and Su, X. C. (2016). 3D Structure Determination of an Unstable Transient Enzyme Intermediate by Paramagnetic NMR Spectroscopy. *Angewandte Chemie - International Edition 55*, 13744–13748.

(*86*) Liu, W.-M., Skinner, S. P., Timmer, M., Blok, A., Hass, M. A. S., Filippov, D. V., Overhand, M. and Ubbink, M. (2014). A Two-Armed Lanthanoid-Chelating Paramagnetic NMR Probe Linked to Proteins via Thioether Linkages. *Chemistry - A European Journal 20*, 6256–6258.

(*87*) Hikone, Y., Hirai, G., Mishima, M., Inomata, K., Ikeya, T., Arai, S., Shirakawa, M., Sodeoka, M. and Ito, Y. (2016). A new carbamidemethyl-linked lanthanoid chelating tag for PCS NMR spectroscopy of proteins in living HeLa cells. *Journal of Biomolecular NMR 66*, 99–110.

(*88*) Loh, C. T., Graham, B., Abdelkader, E. H., Tuck, K. L. and Otting, G. (2015). Generation of Pseudocontact Shifts in Proteins with Lanthanides Using Small "clickable" Nitrilotriacetic Acid and Iminodiacetic Acid Tags. *Chemistry - A European Journal 21*, 5084–5092.

(*89*) Ikegami, T., Verdier, L., Sakhaii, P., Grimme, S., Pescatore, B., Saxena, K., Fiebig, K. M. and Griesinger, C. (2004). Novel techniques for weak alignment of proteins in solution using chemical tags coordinating lanthanide ions. *Journal of Biomolecular NMR 29*, 339–349.

(*90*) Prudêncio, M., Rohovec, J., Peters, J. A., Tocheva, E., Boulanger, M. J., Murphy, M. E., Hupkes, H. J., Kosters, W., Impagliazzo, A. and Ubbink, M. (2004). A caged lanthanide complex as a paramagnetic shift agent for protein NMR. *Chemistry - A European Journal 10*, 3252–3260.

(*91*) Peters, F., Maestre-Martinez, M., Leonov, A., Kovačič, L., Becker, S., Boelens, R. and Griesinger, C. (2011). Cys-Ph-TAHA: A lanthanide binding tag for RDC and PCS enhanced protein NMR. *Journal of Biomolecular NMR 51*, 329–337.

(*92*) Port, M., Idée, J. M., Medina, C., Robic, C., Sabatou, M. and Corot, C. (2008). Efficiency, thermodynamic and kinetic stability of marketed gadolinium chelates and their possible clinical consequences: A critical review. *BioMetals 21*, 469–490.

(*93*) Todd, D. J. and Kay, J. (2016). Gadolinium-Induced Fibrosis. *Annual Review of Medicine 67*, 273–291.

(*94*) Barbieri, S., Schroeder, C., Froehlich, J. M., Pasch, A. and Thoeny, H. C. (2016). High signal intensity in dentate nucleus and globus pallidus on unenhanced T1-weighted MR images in three patients with impaired renal function and vascular calcification. *Contrast Media and Molecular Imaging 11*, 245–250.

(*95*) Opina, A. C. L., Strickland, M., Lee, Y.-S., Tjandra, N., Byrd, R. A., Swenson, R. E. and Vasalatiy, O. (2016). Analysis of the isomer ratios of polymethylated-DOTA complexes and the implications on protein structural studies. *Dalton Trans. 45*, 4673–4687.

(*96*) Häussinger, D. and Grzesiek, S. In *In Book of Abstracts; First European Conference on Chemistry for Life Sciences, Rimini, Italy*, 2005.

(*97*) Vlasie, M. D., Comuzzi, C., Van Den Nieuwendijk, A. M., Prudêncio, M., Overhand, M. and Ubbink, M. (2007). Long-range-distance NMR effects in a protein labeled with a lanthanide-DOTA chelate. *Chemistry - A European Journal 13*, 1715–1723.

(*98*) Keizers, P. H., Saragliadis, A., Hiruma, Y., Overhand, M. and Ubbink, M. (2008). Design, synthesis, and evaluation of a lanthanide chelating protein probe: CLaNP-5 yields predictable paramagnetic effects independent of environment. *Journal of the American Chemical Society 130*, 14802–14812.

(*99*) Liu, W. M., Keizers, P. H. J., Hass, M. A. S., Blok, A., Timmer, M., Sarris, A. J. C., Overhand, M. and Ubbink, M. (2012). A pH-sensitive, colorful, lanthanide-chelating paramagnetic NMR probe. *Journal of the American Chemical Society 134*, 17306–17313.

(*100*) Keizers, P. H., Desreux, J. F., Overhand, M. and Ubbink, M. (2007). Increased paramagnetic effect of a lanthanide protein probe by two-point attachment. *Journal of the American Chemical Society 129*, 9292–9293.

(*101*) Lee, M. D., Dennis, M. L., Swarbrick, J. D. and Graham, B. (2016). Enantiomeric two-armed lanthanide-binding tags for complementary effects in paramagnetic NMR spectroscopy. *Chemical Communications 52*, 7954–7957.

(*102*) Häussinger, D., Huang, J. R. and Grzesiek, S. (2009). DOTA-M8: An extremely rigid, high-affinity lanthanide chelating tag for PCS NMR spectroscopy. *Journal of the American Chemical Society 131*, 14761–14767.

(*103*) Graham, B. *et al*. (2011). DOTA-amide lanthanide tag for reliable generation of pseudocontact shifts in protein NMR spectra. *Bioconjugate Chemistry 22*, 2118–2125.

(*104*) Yang, F., Wang, X., Pan, B. B. and Su, X. C. (2016). Single-armed phenylsulfonated pyridine derivative of DOTA is rigid and stable paramagnetic tag in protein analysis. *Chemical Communications 52*, 11535–11538.

(*105*) Loh, C. T., Ozawa, K., Tuck, K. L., Barlow, N., Huber, T., Otting, G. and Graham, B. (2013). Lanthanide tags for site-specific ligation to an unnatural amino acid and generation of pseudocontact shifts in proteins. *Bioconjugate Chemistry 24*, 260–268.

(*106*) Ranganathan, R. S., Pillai, R. K., Raju, N., Fan, H., Nguyen, H., Tweedle, M. F., Desreux, J. F. and Jacques, V. (2002). Polymethylated DOTA ligands. 1. Synthesis of rigidified ligands and studies on the effects of alkyl substitution on acid-base properties and conformational mobility. *Inorganic Chemistry 41*, 6846–6855.

(*107*) Lambert, J. N., Mitchell, J. P. and Roberts, K. D. (2001). The synthesis of cyclic peptides. *Journal of the Chemical Society, Perkin Transactions 1*, 471–484.

(*108*) Glenn, M. P., Kelso, M. J., Tyndall, J. D. and Fairlie, D. P. (2003). Conformationally homogeneous cyclic tetrapeptides: Useful new three-dimensional scaffolds. *Journal of the American Chemical Society 125*, 640–641.

(*109*) Bock, V. D., Perciaccante, R., Jansen, T. P., Hiemstra, H. and Van Maarseveen, J. H. (2006). Click chemistry as a route to cyclic tetrapeptide analogues: Synthesis of cyclo-[Pro-Val-ψ(triazole)-Pro-Tyr]. *Organic Letters 8*, 919–922.

(*110*) Tai, D.-F. and Lin, Y.-F. (2008). Molecularly imprinted cavities template the macrocyclization of tetrapeptides. *Chemical Communications*, 5598.

(*111*) Lüttin, F. Synthesis and Characterisation of Cyclo-Tetra- Alanine as Precursor for Lanthanide Chelating Tags suitable for PCS-NMR Spectroscopy., Basel, 2014.

(*112*) Chen, M. H., Iakovleva, E., Kesten, S., Magano, J., Rodriguez, D., Sexton, K. E., Zhang, J. and Lee, H. T. (2002). A convenient reduction of highly functionalized aromatic carboxylic acids to alcohols with borane-THF and boron trifluoride-etherate. *Organic Preparations and Procedures International 34*, 665–670.

(*113*) Titlestad, K. Cyclic Tetra- and Octapeptides of Sarcosine in Combination with Alanine or Glycine. Synthesis and Conformation., 1977.

(*114*) More, J. D. and Finney, N. S. (2002). A simple and advantageous protocol for the oxidation of alcohols with o-iodoxybenzoic acid (IBX). *Organic Letters 4*, 3001–3003.

(*115*) Heidelberg, T. and Martin, O. R. (2004). Synthesis of the Glycopeptidolipid of Mycobacterium avium Serovar 4: First Example of a Fully Synthetic C-Mycoside GPL. *Journal of Organic Chemistry 69*, 2290–2301.

(*116*) Vogel, R. Synthesis of a Carbon-13 labelled Lanthanide Chelating Tag for PCS NMR Spectroscopy and Study of the $\Delta\chi$-Tensors., Basel, 2018.

(*117*) Kanai, M., Yasumoto, M., Kuriyama, Y., Inomiya, K., Katsuhara, Y., Higashiyama, K. and Ishii, A. (2004). Practical Synthesis of Optically Active Fluorine-substituted α-Phenylethylamines by Retardation of Hydrogenolytic Cleavage at Benzylic Position. *Chemistry Letters 33*, 1424–1425.

(*118*) Thommen, F. New Lanthanide Chelating Tags based on decorated Cyclen for Pseudocontact Shift NMR Spectroscopy., Basel, 2016.

(*119*) Myers, A. G., Zhong, B., Movassaghi, M., Kung, D. W., Lanman, B. A. and Kwon, S. (2000). Synthesis of highly epimerizable N-protected α-amino aldehydes of high enantiomeric excess. *Tetrahedron Letters 41*, 1359–1362.

(*120*) Gsellinger, H. Combining NMR spectroscopy and organic synthesis: From small building blocks to large biomolecules., Ph.D. Thesis, 2014.

(*121*) Selenko, P., Serber, Z., Gadea, B., Ruderman, J. and Wagner, G. (2006). Quantitative NMR analysis of the protein G B1 domain in Xenopus laevis egg extracts and intact oocytes. *Proceedings of the National Academy of Sciences 103*, 11904–11909.

(*122*) Schlosser, M. and Ruzziconi, R. (2010). Nucleophilic substitutions of nitroarenes and pyridines: New insight and new applications. *Synthesis*, 2111–2123.

(*123*) Sass, J., Cordier, F., Hoffmann, A., Rogowski, M., Cousin, A., Omichinski, J. G., Löwen, H. and Grzesiek, S. (1999). Purple membrane induced alignment of biological macromolecules in the magnetic field. *Journal of the American Chemical Society 121*, 2047–2055.

(*124*) Hart, T. W., Vine, M. B. and Walden, N. R. (1985). Thiolsulphonate derivatives of amino acids. *Tetrahedron Letters 26*, 3879–3882.

(*125*) Fielding, A. J., Concilio, M. G., Heaven, G. and Hollas, M. A. (2014). New developments in spin labels for pulsed dipolar EPR. *Molecules 19*, 16998–17025.

(*126*) Graham, S. L. and Scholz, T. H. (1986). The Reaction of Sulfinic Acid Salts with Hydroxylamine- O -sulfonic Acid. A Useful Synthesis of Primary Sulfonamides. *Synthesis 1986*, 1031–1032.

(*127*) Toda, N., Asano, S. and Barbas, C. F. (2013). Rapid, stable, chemoselective labeling of thiols with Julia- Kocienski-like reagents: A serum-stable alternative to maleimide-based protein conjugation. *Angewandte Chemie - International Edition 52*, 12592–12596.

(*128*) Geißler, D. and Hildebrandt, N. (2011). Lanthanide Complexes in FRET Applications. *Current Inorganic Chemistry 1*, 17–35.

(*129*) Geißler, D., Linden, S., Liermann, K., Wegner, K. D., Charbonnière, L. J. and Hildebrandt, N. (2014). Lanthanides and quantum dots as Förster resonance energy transfer agents for diagnostics and cellular imaging. *Inorganic Chemistry 53*, 1824–1838.

(*130*) Atkinson, P. *et al*. (2006). Azaxanthones and azathioxanthones are effective sensitisers for europium and terbium luminescence. *Organic & Biomolecular Chemistry 4*, 1707.

(*131*) Kielar, F., Law, G.-L., New, E. J. and Parker, D. (2008). The nature of the sensitiser substituent determines quenching sensitivity and protein affinity and influences the design of emissive lanthanide complexes as optical probes for intracellular use. *Organic & Biomolecular Chemistry 6*, 2256.

(*132*) Klunk, W. E. *et al*. (2004). Imaging Brain Amyloid in Alzheimer's Disease with Pittsburgh Compound-B. *Annals of Neurology 55*, 306–319.

(*133*) Diner, I., Dooyema, J., Gearing, M., Walker, L. C. and Seyfried, N. T. (2017). Generation of Clickable Pittsburgh Compound B for the Detection and Capture of β-Amyloid in Alzheimer's Disease Brain. *Bioconjugate Chemistry 28*, 2627–2637.

(*134*) Wu, Z., Lee, M. D., Carruthers, T. J., Szabo, M., Dennis, M. L., Swarbrick, J. D., Graham, B. and Otting, G. (2017). New Lanthanide Tag for the Generation of Pseudocontact Shifts in DNA by Site-Specific Ligation to a Phosphorothioate Group. *Bioconjugate Chemistry 28*, 1741–1748.

(*135*) Neese, F. (2012). The ORCA program system. *Wiley Interdisciplinary Reviews: Computational Molecular Science 2*, 73–78.

(*136*) Neese, F. (2018). Software update: the ORCA program system, version 4.0. *Wiley Interdisciplinary Reviews: Computational Molecular Science 8*, 4–9.

(*137*) Aravena, D., Neese, F. and Pantazis, D. A. (2016). Improved Segmented All-Electron Relativistically Contracted Basis Sets for the Lanthanides. *Journal of Chemical Theory and Computation 12*, 1148–1156.

(*138*) Rinaldelli, M., Carlon, A., Ravera, E., Parigi, G. and Luchinat, C. (2015). FANTEN: A new web-based interface for the analysis of magnetic anisotropy-induced NMR data. *Journal of Biomolecular NMR 61*, 21–34.